The extracellular mannoprotein Cig1 functions in iron acquisition from heme in the fungal pathogen *Cryptococcus neoformans*

by

Brigitte Cadieux

B.Sc., University of Ottawa, 1998
M.Sc., McGill University, 2001

A THESIS SUBMITTED IN PARTIAL FULFILLMENT OF THE REQUIREMENTS FOR THE DEGREE OF

DOCTOR OF PHILOSOPHY

in

THE FACULTY OF GRADUATE STUDIES

(Microbiology and Immunology)

THE UNIVERSITY OF BRITISH COLUMBIA
(Vancouver)

April, 2013

Abstract

Cryptococcus neoformans is an encapsulated fungal pathogen that causes cryptococcosis, a life-threatening disease which affects an estimated 1 million people worldwide annually. Iron acquisition is an important but poorly understood aspect of the pathogenesis of *C. neoformans*. In particular, no heme uptake system has thus far been characterized in this fungus, although it has been shown to utilize heme as an iron source. A previous study identified the transcript for the extracellular mannoprotein *CIG1* as the most abundant message in iron-starved cells with marked down-regulation by iron repletion, thus suggesting a possible iron-related role for Cig1. In the current study, it was found that deletion of *CIG1* resulted in an extended lag phase in low iron medium with heme added as the sole iron source. Additionally, the *cig1Δ* mutant was more resistant to toxic heme analogs than the wild-type or complemented strains implying a role for Cig1 in heme uptake. Western blot analysis and immunofluorescence microscopy identified Cig1 at the cell surface and in association with extracellular vesicles. A heme pull-down experiment, absorbance spectroscopy and isothermal calorimetry also demonstrated that Cig1 is a potential heme-binding protein. Importantly, deletion of *CIG1* led to attenuated virulence in a mouse infection model in absence of the high-affinity iron uptake system. More detailed studies on Cig1 revealed that the length of the lag phase of a *cig1Δ* mutant in low iron medium supplemented with heme was dependent on the inoculum size in support of a cell density-dependent heme acquisition system. Similarly, growth at acidic pH rescued the heme defect of a *cig1Δ* mutant indicating the presence of a Cig1-independent pathway at low pH. The transcription factor Rim101 may function in this pathway. Finally, expression of a Cig1 truncated polypeptide established a role for Cig1 in secretion and cell wall integrity. In this context, a strain overexpressing *CIG1* produced an enlarged capsule and secreted more extracellular vesicles than the wild-type strain. Overall, the data presented in this thesis have

contributed to a better understanding of heme uptake and secretion in *C. neoformans* and the results may facilitate the development of new strategies to treat cryptococcosis.

Preface

Relative contributions of all collaborators:

Some of the work presented in this thesis resulted from collaborative efforts. The people who have contributed to the different experiments have been identified in each of the respective sections of the Materials and Methods. The details of their contributions are as follows:

Most of the work presented in Chapter 2 and a portion of the work from Chapter 3 have been published in the manuscript entitled "**The mannoprotein Cig1 supports iron acquisition from heme and virulence in the pathogenic fungus *Cryptococcus neoformans***" in the Journal of Infectious Diseases on January 15th, 2013. Tian Lian and Carmelo Biondo contributed to this study by preparing some of the strains as indicated. Dr. Guanggan Hu constructed the *E. coli* strain expressing *Cig1::GST* and purified the recombinant fusion protein. Joyce Wang performed the virulence assay and determined the fungal loads in mouse tissue, while Dr. A. Louise Creagh did the isothermal titration calorimetry experiments. Victor Liu provided some technical assistance and Dr. Michael E. Murphy suggested the idea to test the toxicity of non-iron metalloporphyrins as an indicator for heme uptake. I was responsible for all the remaining experiments and data collection. The manuscript was written by myself and my supervisor, Dr. James W. Kronstad, except for some details about the collaborative work included in the Materials and Methods, which were written by Dr. Guanggan Hu, Joyce Wang and Dr. A. Louise Creagh, respectively.

Another publication with the preliminary title **"The fungal pathogen *Cryptococcus neoformans* casts a heme binding net"**, is in preparation for publication of the rest of the work

included in Chapter 3. Tian Lian, Carmelo Biondo and Dr. Emma J. Griffiths prepared some of the strains used in the study, as indicated, while Dr. A. Louise Creagh performed the isothermal titration calorimetry experiments. I was responsible for all the remaining experiments and data collection. The manuscript will be written by myself and my supervisor, Dr. James W. Kronstad.

Finally, a portion of the work presented in Chapter 4 was previously started by Tian Lian. Specifically, Tian had constructed some of the strains, as indicated, and tested the susceptibility of these strains to secretion inhibitors and agents that challenge the cell wall. All the other data included in this chapter resulted from my work.

Publications arising from graduate work:

-Cadieux B, Lian T, Hu G, Wang J, Biondo C, Teti G, Liu V, Murphy ME, Creagh AL, Kronstad JW. (2013). The mannoprotein Cig1 supports iron acquisition from heme and virulence in the pathogenic fungus *Cryptococcus neoformans.* J Infect Dis. (Epub ahead of print).

-Hu G, Caza M, **Cadieux B**, Chan V, Liu V, Kronstad J. (2013). *Cryptococcus neoformans* Requires the ESCRT Protein Vps23 for Iron Acquisition from Heme, for Capsule Formation, and for Virulence. Infect Immun. *81*, 292-302.

-Kim J, Cho YJ, Do E, Choi J, Hu G, **Cadieux B**, Chun J, Lee Y, Kronstad JW, Jung WH. (2012). A defect in iron uptake enhances the susceptibility of *Cryptococcus neoformans* to azole antifungal drugs. Fungal Genet Biol. *49*, 955-66.

-Kronstad J, Saikia S, Nielson ED, Kretschmer M, Jung W, Hu G, Geddes JM, Griffiths EJ, Choi J, **Cadieux B**, Caza M, Attarian R. (2012). Adaptation of *Cryptococcus neoformans* to mammalian hosts: integrated regulation of metabolism and virulence. Eukaryot Cell. *11*, 109-18.

-Kronstad JW, Attarian R, **Cadieux B**, Choi J, D'Souza CA, Griffiths EJ, Geddes JM, Hu G, Jung WH, Kretschmer M, Saikia S, Wang J. (2011). Expanding fungal pathogenesis: *Cryptococcus* breaks out of the opportunistic box. Nat Rev Microbiol. *9*, 193-203.

University of British Columbia Ethics Board approval:

The protocol for the virulence assays was approved by the University of British Columbia Committee on Animal Care (Certificate Number: A08-0586).

Table of contents

List of tables

List of figures

List of abbreviations

3HAA	3-hydroxyanthranilic acid
AAs	amino acids
ABC transporters	ATP-binding cassette transporter
AIDS	acquired immune deficiency syndrome
ATP	adenosine triphosphate
BFA	brefeldin A
BLAST	basic local alignment search tool
BSA	bovine serum albumin
cDNA	complementary deoxyribonucleic acid
CFEM	eight cysteine-containing domain
Cfo1	*Cryptococcus* ferroxidase 1
Cft1	*C. neoformans* iron permease 1
CFU	colony forming units
CIG1	cytokine-inducing glycoprotein 1
Cir1	*Cryptococcus* iron regulator 1
CM	conditioned media
Ct	cycle threshold
C-terminal	carboxyl-terminal
Da	Dalton
DNA	deoxyribonucleic acid
DOMON	dopamine β-monooxygenase N-terminal
DTT	dithiothreitol
EDTA	ethylenediaminetetraacetic acid
ER	endoplasmic reticulum
ESCRT	endosomal sorting complex required for transport
Fre	ferric iron reductases
Fur	ferric uptake repressor
GalXM	galactoxylomannan
Ga-PPIX	gallium protoporphyrin
GFP	green fluorescent protein
GPI	glycosylphosphatidylinositol
GST	glutathione S-transferase
GXM	glucuronoxylomannan
HA	hemagglutinin
HEPES	4-(2-hydroxyethyl)-1-piperazineethanesulfonic acid
HIS	histidine
HIV	human immunodeficiency virus
HYG	hygromycin
IgG	immunoglobulin G
IL-10	interleukin-10
IPTG	isopropyl beta-D-1-thiogalactopyranoside
ITC	isothermal titration calorimetry
K_d	dissociation constant
L-DOPA	L-3,4-dihydroxyphenylalanine

LIM	low iron medium
LI-YNB	low iron yeast nitrogen base
Mn-PPIX	manganese protoporphyrin
MPs	metalloporphyrins
mRNA	messenger ribonucleic acid
MS	mass spectrometry
n	number of replicates
NAT	nourseothricin
NC	North Carolina
NEAT	near iron transporter
NEM	N-ethyl maleimide
NEO	neomycin
NMR	nuclear magnetic resonance
N-terminal	amino-terminal
NY	New York
PBS	phosphate-buffered saline
PCR	polymerase chain reaction
Plb1	phospholipase B
PSMs	peptide spectrum match
QS	quorum sensing
Qsp1	quorum sensing peptide 1
RNA	ribonucleic acid
RNA-seq	ribonucleic acid sequencing
rRNA	ribosomal ribonucleic acid
RT-PCR	real time polymerase chain reaction
SD	standard deviation
SDS	sodium dodecyl sulfate
SDS-PAGE	sodium dodecyl sulfate polyacrylamide gel electrophoresis
Ser/Thr	serine/threonine
Sit1	siderophore iron transporter
Sod1	superoxide dismutase
sp.	species
TBS	tris-buffered saline
TGF-β	transforming growth factor beta
TLC	thin layer chromatography
TNF-α	tumor necrosis factor-alpha
TTC	2,3,5-triphenyltetrazolium chloride
U.S.A.	United States of America
UV	ultraviolet
var.	variety
WT	wild-type
YNB	yeast nitrogen base
YPD	yeast extract peptone dextrose
YPG	yeast extract peptone galactose

Acknowledgements

I would like to thank all the current and past members of the Kronstad lab, including Anita Sham, Iris Liu, Po-Yan Cheng, Melanie Scofield, Won Hee Jung, Guanggan Hu, Emma Griffiths, Sanjay Saikia, Joyce Wang, Matthias Kretschmer, Jennifer Geddes, Rodgoun Attarian, Horacio Bach, Jaehuyk Choi, Melissa Caza, Erik Nielson, Scott Lambie, Cletus D'Souza, and Debora de Oliveira. You guys have been my colleagues and my friends, but most importantly, I consider you all to be part of my Vancouver family. You were by my side to celebrate the best of times and you were there to support me through the worst of times. I will forever be grateful to all of you. The times we shared together, inside and outside the lab, will always bring back fond memories. I will miss you dearly.

Special thanks to Guanggan Hu for being so helpful, and for providing me with excellent advice and encouragement. Thank you for being patient with me over the past several years and for answering my many questions.

I would like to extend my utmost appreciation to my supervisor Dr. Jim Kronstad for giving me the opportunity to work on such an exciting project. The continuous support and advice that you have offered me over the years have been instrumental in my scientific development.

I would also like to acknowledge the members of my supervisory committee, Dr. Rachel Fernandez, Dr. John Smit, and Dr. Christopher Loewen for challenging me and providing helpful suggestions.

I offer my gratitude to Tian Lian for starting some of the work presented in this thesis, as well as Catherine Gaudin, Sarah Thackray, Louise Creagh, Victor Liu, Lakshmi Miller-Vedam,

Chun Mei Li, Joyce Wang, and Nikolay Stoynov for technical assistance. I would also like to thank Dr. Michael Murphy for his expertise and his insight on the work involving heme binding.

Thanks to Jan Schwerdtner for driving me to work so many times late at night or on the weekend to measure the growth of my cells.

Last but not least, I would like to thank my family and friends from back home who always believed in me. You guys have been by my side every step of the way. You have encouraged me to push harder and aim higher. You will never know how much your love and support was appreciated throughout this journey. I am very lucky to be surrounded by such amazing people.

To my parents who have inspired me in more than one way.

À mes parents qui m’ont inspirée à plusieurs niveaux.

Chapter 1. Introduction

1.1. *Cryptococcus neoformans*

1.1.1. Cryptococcosis

C. neoformans is an encapsulated fungal pathogen which causes cryptococcosis. The yeast cells and spores of *C. neoformans* are ubiquitous in the environment and are often associated with soil, vegetative debris or avian guano (Buchanan and Murphy, 1998; Govender *et al.*, 2011). Cryptococcosis, a life-threatening disease, is acquired by inhaling *C. neoformans* spores which then cause an initial infection of the lungs that manifests itself as pneumonia (Williams *et al.*, 2011). The infection can be cleared by the host's immune system or alternatively can become a latent infection. If the host's immunity is compromised, the dormant cells can become active and proliferate. Eventually, the cells cross the blood-brain barrier and progress to the central nervous system and brain resulting in meningoencephalitis (Dromer and Levitz, 2011). *C. neoformans* is the most common cause of fungal meningoencephalitis (Perfect and Casadevall, 2011). Although the pathogen can cause disease in immunocompetent individuals, it has a propensity to attack immunocompromised individuals, and cryptococcal meningitis is one of the most frequent causes of death among persons with AIDS (Warkentien and Crum-Cianflone, 2010; Park *et al.*, 2011). The incidence of cryptococcosis exploded globally with the AIDS epidemic and as a consequence of organ transplantation and the use of corticosteroids. The highest incidence is found in sub-Saharan regions of Africa, which also have the greatest burden of HIV on a global scale (Park *et al.*, 2011). The worldwide burden of cryptococcosis is estimated at 1 million cases per year with approximately 625,000 deaths, although fatality rates of cryptococcal meningitis can approach 100% in some areas (Park *et al.*, 2009).

Antifungal drugs, such as amphotericin B and fluconazole, suppress but do not necessarily cure cryptococcosis and can be toxic to the human host (Jarvis *et al.*, 2011). Combination antifungal therapy is a more successful approach in the treatment of cryptococcosis; however, access to the drugs is often limited, especially in many parts of the developing world.

C. neoformans is classified into three different varieties, named variety *grubii* (serotype A), var. *gattii* (serotypes B and C), and var. *neoformans* (serotype D), based on antigenic differences of the polysaccharide capsule and distinct DNA fingerprinting patterns (Bhattacharjee *et al.*, 1984; Janbon and Doering, 2011; Kwon-Chung *et al.*, 2011). *C. neoformans* var. *grubii* represents the major clinical serotype, while *C. neoformans* var. *gattii* is emerging as a new and distinct pathogenic species. Since 1999, an outbreak of cryptococcosis has been ongoing on Vancouver Island infecting predominantly immunocompetent individuals (Stephen *et al.*, 2002). The outbreak has also been spreading to the mainland and the Pacific Northwest area of the U.S.A. (Kidd *et al.*, 2004; MacDougall *et al.*, 2007; Bartlett *et al.*, 2008). In British Columbia alone, 281 infections were reported from 1999-2010 and 19 individuals died from the disease (Bartlett *et al.*, 2012). In the U.S.A., 60 cases were reported between 2004 and 2010 resulting in 20 deaths (Centers for Disease Control and Prevention, 2010). In this context, a detailed understanding of the virulence mechanisms for *C. neoformans* is needed to underpin new strategies to treat cryptococcosis.

1.1.2. Virulence traits

The identification of virulence factors associated with *C. neoformans* and the corresponding genes which encode the virulence factors is a very complex task. It is likely that many subtle virulence traits are required for the pathogen's ability to cause disease. So far, three

major virulence traits, as well as several secreted sugars and enzymes, have been identified to play a role in pathogenesis.

1.1.2.1. Polysaccharide capsule

The key virulence trait of *C. neoformans* is its polysaccharide capsule which attaches to and extends from the cell wall. The capsule is composed primarily of two polysaccharides, glucuronoxylomannan (GXM) and galactoxylomannan (GalXM), as well as mannoproteins, described in section 1.1.3.2 (Reiss *et al.*, 1985; Murphy *et al.*, 1988; Bose *et al.*, 2003; Zaragoza *et al.*, 2009). GXM, which makes up 90% of the capsule mass, is a long, unbranched polymer (1,700-7,000 kDa) composed of alpha-1,3-linked mannose residues which are O-acetylated and decorated with xylose and glucuronic acid (McFadden *et al.*, 2006; Zaragoza *et al.*, 2009). GalXM is smaller than GXM (275,000 Da) and has an alpha-1,6-galactan backbone with xylosylated side chains of mannose and galactose (Cherniak *et al.*, 1980; Zaragoza *et al.*, 2009). The capsule of *C. neoformans* is a highly dynamic structure: physiological conditions (i.e., low iron, 5% CO_2) induce capsule synthesis and the cell can modulate capsule thickness in response to the host tissue environment, i.e., the capsule is larger on fungal cells in the brain (Granger *et al.*, 1985; Vartivarian *et al.*, 1993; Zaragoza *et al.*, 2003). It has also been shown that acapsular strains are avirulent in a mouse model of cryptococcosis (Kwon-Chung and Rhodes, 1986; Chang and Kwon-Chung, 1994; 1998; 1999; Chang *et al.*, 1996). The capsule is extremely important for evasion of the host immune system. For example, the capsule can protect the cells from phagocytosis (Garcia-Rodas and Zaragoza, 2012). Interestingly, large amounts of capsular polysaccharides are also shed from the fungal cell into the extracellular environment and can thereby deplete the complement proteins of the host (Bose *et al.*, 2003; Zaragoza *et al.*, 2009). In

fact, GXM is the major cryptococcal component in body fluids of infected patients and can be a measure of the severity of the disease (Vecchiarelli, 2000). Additionally, the capsule interferes with the host immune response by altering antigen presentation, inhibiting leukocyte migration to infected tissues, and modulating cytokine production (Vecchiarelli, 2000; Zaragoza *et al.*, 2009; Vecchiarelli *et al.*, 2011). The capsule can also scavenge reactive oxygen intermediates and confer resistance to the cells against oxidative stress (Zaragoza *et al.*, 2008). Therefore, if fungal cells are engulfed, the capsule allows *C. neoformans* to survive intracellularly and replicate (Tucker and Casadevall, 2002). Although there has been steady progress in understanding the mechanisms of capsule biosynthesis in the past decade, important questions remain unanswered, including where and how is the capsule synthesized.

1.1.2.2. Melanin

Another virulence trait identified for *C. neoformans* is its ability to synthesize melanin. The enzyme laccase, which is localized in the cell wall, converts diphenolic compounds to melanin, a dark brown or black pigmented polymer, through a series of reactions and in combination with auto-oxidation (Polacheck *et al.*, 1982; 1988; 1991; Zhu *et al.*, 2001; Waterman *et al.*, 2007; Eisenman and Casadevall, 2012). The detailed chemical structure of melanin is not known but it has been shown to have a granular structure, and melanin granules are deposited in the inner layer of the *C. neoformans* cell wall (Eisenman *et al.*, 2005; Eisenman and Casadevall, 2012). Melanin production in this organism necessitates the availability of exogenous diphenolic substrates (e.g., catecholamines) and is regulated by glucose, iron and copper levels, as well as by temperature and the available nitrogen source (Nurudeen and Ahearn, 1979). Interestingly, large amounts of natural catecholamines are found in the brain,

which may explain the neurotropism of *C. neoformans* (Polacheck *et al.*, 1982; Nosanchuk *et al.*, 2000). Laccase expression and melanin synthesis have been correlated with virulence in numerous studies (Kwon-Chung *et al.*, 1982; Rhodes *et al.*, 1982; Polacheck and Kwon-Chung, 1988; Salas *et al*, 1996; Zhu and Williamson, 2004; Trofa *et al.*, 2011). Specifically, it has been shown that the enzyme laccase is required for dissemination of *C. neoformans* from the lungs to other organs, and cells which are unable to synthesize melanin are generally attenuated for virulence (Kwon-Chung *et al.*, 1982; Salas *et al.*, 1996; Gomez and Nosanchuk, 2003; Noverr *et al.*, 2004). Additionally, melanin inhibits phagocytosis of fungal cells and interferes with the normal function of phagocytic cells (Wang *et al.*, 1995). For example, the host immune cells kill foreign cells by exposing them to free radicals, which will react with DNA and proteins leading to death of the cells. Melanin protects *C. neoformans* from oxidative and nitrosative challenges by macrophages by reacting with free radicals to neutralize them (Wang *et al.*, 1995). Melanin also provides an increased negative charge to the cryptococcal cells which may explain, at least in part, the role of melanin in phagocytosis inhibition (Blasi *et al.*, 1995; Wang *et al.*, 1995; Nosanchuk and Casadevall, 1997). Furthermore, melanin modulates the immune system by altering cytokine levels and activating the complement system (Rosas *et al.*, 2002; Mednick *et al.*, 2005; Trofa *et al.*, 2011).

1.1.2.3. Growth at 37ºC

To cause infection in humans and animals, *C. neoformans* must be able to proliferate at 37ºC. While it may seem obvious, growth at 37ºC is an important virulence trait for *C. neoformans* as most fungi do not grow optimally above 30ºC. Several functions have been shown to influence growth at elevated temperature, including components of signaling pathways.

For example, Odom *et al.* (1997) showed that an intact calcineurin pathway is essential for thermotolerance. Specifically, a copy of the gene encoding the catalytic A subunit of calcineurin is required for growth at 37ºC (Odom *et al.*, 1997). The *CNB1* gene encoding the calcineurin regulatory subunit is also required for thermotolerance (Fox *et al.*, 2001). Calcineurin is a Ca^{2+}/calmodulin-activated serine/threonine-specific phosphatase involved in stress response and is structurally and functionally conserved from yeast to humans (Hemenway and Heitman, 1999). Perfect (2006) listed 19 additional genes that have been validated to be necessary for high-temperature growth and pathogenesis of *C. neoformans*. Two themes emerged from this list: the apparent protective properties of the sugar, trehalose, and the requirement for antioxidant protection for growth at human body temperature. Both trehalose-6-phosphate synthase (Tps1) and trehalose-6-phosphate phosphatase (Tps2) were found to be required for growth at 37ºC and for virulence of *C. neoformans* (Petzold *et al.*, 2006). Based on studies in *Saccharomyces cerevisiae*, it is thought that accumulation of trehalose can help prevent denaturation of proteins and aid heat-shock protein chaperones in renaturation by preventing aggregation of denatured proteins (Crowe, 2007). Additionally, the superoxide dismutase (Sod2) and the thiol-specific antioxidant (Tsa1) are both required for resistance to oxidative and nitrosative stresses and are necessary for high-temperature growth of *C. neoformans* (Giles *et al.*, 2005; Missall *et al.*, 2004).

1.1.2.4. Other virulence traits

Other possible virulence traits include production of mannitol, superoxide dismutase, protease, phospholipase B, urease and acid phosphatase. However, these virulence traits have not been characterized to the same extent as capsule and melanin production.

It is thought that production of large amounts of mannitol by the enzyme mannitol dehydrogenase increases the osmolality of *C. neoformans*' extracellular environment which may prevent oxidative damage to the fungal cells while inside the host (Perfect *et al.*, 1996; Karkowska-Kuleta et al, 2009). Additionally, large amounts of mannitol may lead to brain edema and facilitate development of meningoencephalitis. Production of mannitol may also help cells resist other environmental stresses including heat stress and osmotic stress (Chaturvedi et al, 1996). *C. neoformans* also secretes multiple extracellular enzymes thought to play a role in virulence, including a role in nutrition of the fungal cell and damage to the host tissue.

Secreted proteases have been demonstrated to degrade host tissues and destroy immunologically important proteins produced by the host in other bacterial and fungal pathogens (Loomes *et al.*, 1993; Jansen *et al.*, 1995; Kaminishi *et al.*, 1995). In *C. neoformans*, extracellular proteinase activity has been detected and it was shown that the fungal pathogen could degrade immunologically important proteins, including immunoglobulin G and complement factor 5 (Chen *et al.*, 1996).

Phospholipase B is involved in fungal invasion by disrupting mammalian cell membranes to allow *C. neoformans* to penetrate host tissues (Djordjevic, 2010). For example, purified phospholipase B (Plb1) hydrolyses lung surfactant and facilitates adherence of *C. neoformans* to lung epithelial cells (Santangelo *et al.*, 1999; Ganendren *et al.*, 2006). Plb1 also facilitates the entry of *C. neoformans* into lung interstitial macrophages. Additionally, Plb1 is essential for dissemination of *C. neoformans* from the lung to the brain via the blood, and may also be required for cryptococcal cells to exit macrophages and thereby avoid killing by the macrophage's immune defense mechanisms (Cox *et al.*, 2001; Noverr *et al.*, 2003; Santangelo *et al.*, 2004; Djordjevic, 2010). Cox *et al.* (2001) demonstrated that disruption of the gene

encoding phospholipase B resulted in attenuation of virulence in mouse and rabbit models of infection, and the mutant exhibited a growth defect in a macrophage-like cell line.

Superoxide dismutase is thought to protect the cells against oxidative stress and allow survival within the phagocytes. Specifically, deletion of *SOD1*, a gene encoding the enzyme superoxide dismutase, resulted in reduction in the expression of a number of virulence traits (e.g., laccase, urease, and phospholipase) (Narasipura *et al.*, 2003). Additionally, the *sod1Δ* mutant showed a marked attenuation of virulence in a mouse model and was significantly susceptible to *in vitro* killing by human neutrophils (Narasipura *et al.*, 2003).

Urease production is also important for pathogenesis as demonstrated by the fact that disruption of the urease gene, *URE1*, resulted in mutants attenuated for virulence in a mouse model of cryptococcosis (Cox *et al.*, 2000). Urease is thought to facilitate yeast sequestration within microcapillaries and disruption of endothelial cells (Olszewski *et al.*, 2004). Thus, urease plays a role in allowing the fungal cells to cross the blood-brain barrier. Finally, acid phosphatase is thought to contribute to pathogenesis by playing a role in adhesion of fungal cells to host epithelial cells (Collopy-Junior *et al.*, 2006).

1.1.3. Secretion in *C. neoformans*

As mentioned above, the ability of *C. neoformans* to influence the intracellular environment of macrophages during fungal proliferation, expulsion and transfer between cells is likely dependent to a great extent on exported fungal factors. Secretion is clearly necessary for cell surface delivery of known virulence traits such as the polysaccharide capsule, the enzyme laccase and the enzymes phospholipase B and urease. Although the molecular details of secretion in *C. neoformans* largely remain a mystery, it has been shown that many of these

factors are delivered, at least in part, by membrane-bound, extracellular vesicles that have been observed to traverse the cell wall (Eisenman *et al.*, 2009; Rodrigues *et al.*, 2007; 2008a). These vesicles are described in more detail in the following section.

1.1.3.1. Extracellular vesicles

Recently, it has been shown that *C. neoformans* produces vesicles which vary in size between 30 and 400 nm, are surrounded by lipid bilayer membranes and somehow cross the cell wall to reach the extracellular environment (Rodrigues *et al.*, 2007; 2008a; Yoneda and Doering, 2006; Eisenman *et al.*, 2009). Newly synthesized capsular polysaccharides were shown to be trafficked within these vesicles and secreted via exocytosis (Yoneda and Doering, 2006). Rodrigues *et al.* (2007) went on to demonstrate that the extracellular vesicles also contain lipids that may contribute to virulence and serve as structural components (e.g., glucosylceramide and sterols). Finally, a proteomic analysis was performed to identify the proteins present in these vesicles (Rodrigues *et al.* 2008a). They identified 76 proteins including several proteins related to virulence (e.g., laccase, urease, acid phosphatase and enzymes linked to capsule synthesis) and protection against oxidative stress (e.g., heat shock proteins, superoxide dismutase).

Furthermore, these extracellular vesicles have different enzymatic activities including laccase, urease and acid phosphatase activity, all known to play a role in virulence (Rodrigues *et al.*, 2008a). The biological activity of the vesicles was confirmed by showing that they were capable of melanization when incubated with the melanin precursor L-3,4-dihydroxyphenylalanine (L-DOPA) (Eisenman *et al.*, 2009). Interestingly, four main groups of extracellular vesicles were observed in *C. neoformans* based on their morphology and electron density (Rodrigues *et al.*, 2008a). It is conceivable that the different types of vesicles contain

different proteins and virulence traits, some of which may be essential for pathogenesis while others may be required for other activities such as cell maintenance. In fact, only a portion of the vesicle population carried capsular polysaccharides (Wolf *et al.*, 2012). This indicates that *C. neoformans* may use the vesicles as part of a general secretion mechanism for trans-cell wall transport and delivery of virulence traits and other cargo (e.g., enzymes) to the extracellular environment. Rodrigues et al (2008a) have thereby termed these vesicles "virulence-factor-delivery bags".

The exact mechanism by which the extracellular vesicles are formed, how they cross the cell wall and how the virulence traits and other cargo are released from the vesicles remains unclear, although different models have been suggested (Figure 1.1). It was proposed that these vesicles are formed by a similar mechanism as described for exosomes (Nosanchuk *et al.,* 2008; Rodrigues *et al.,* 2008a; 2008b). Exosomes are found in maturing reticulocytes of different species (Johnstone, 2005). Their vesicular contents are released when the exosomes fuse with the plasma membrane suggesting that they could serve as a mechanism for shedding surface proteins (Harding *et al.*, 1984; Pan *et al.,* 1985). It is possible that *C. neoformans* utilizes a similar mechanism where multivesicular bodies fuse with the plasma membrane releasing the extracellular vesicles (Rodrigues *et al.*, 2008a; 2008b). Alternatively, the virulence traits could be packaged in the vesicles, along with other cytosolic proteins, at the plasma membrane in a blebbing process (Doering, 2009). Finally, the virulence traits may be secreted via exocytosis. In an attempt to explain vesicular transport across the cell wall, Nosanchuck *et al.* (2008) and Rodrigues *et al.* (2008b) proposed the existence of pores in the *C. neoformans* cell wall which are large enough to allow the shuttling of the vesicles. It is also possible that the lipid bilayers of the vesicles are compressible to smaller diameters allowing transport through smaller pores.

Additionally, some motor proteins are most likely needed for efficient vesicular transport across the cell wall (Nosanchuck *et al.*, 2008; Rodrigues *et al.*, 2008b).

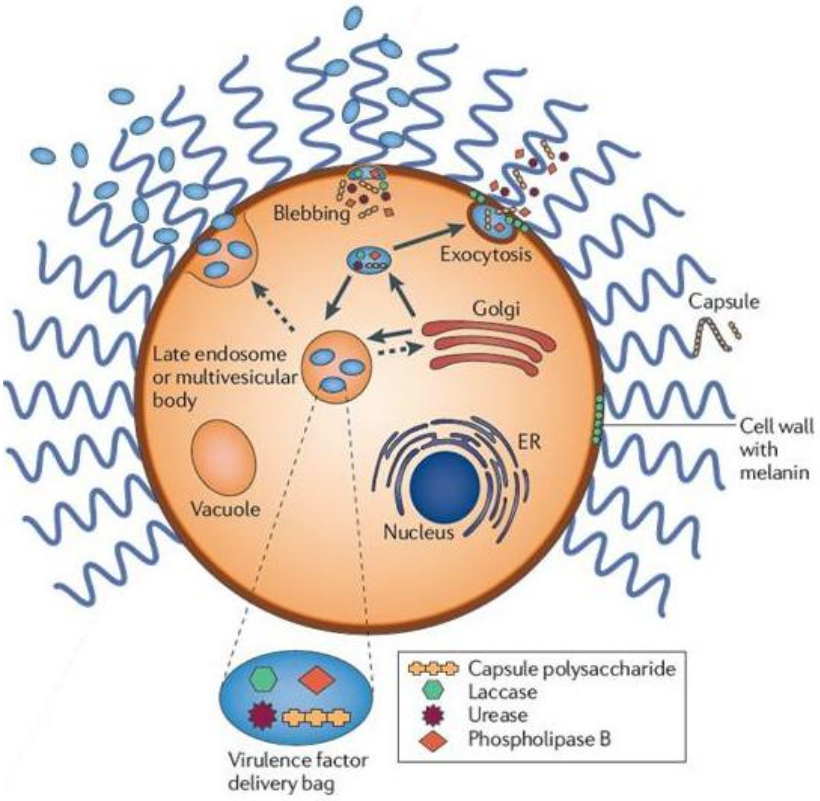

Figure 1.1 Secretion of virulence traits via extracellular vesicles in *C. neoformans*. The exact mechanism of trans-cell wall trafficking has not been identified although different models have been proposed, including fusion of the multivesicular bodies with the plasma membrane, blebbing from the plasma membrane, and exocytosis as illustrated. Figure prepared by B. Cadieux and Dr. J. Choi, and reproduced from Kronstad *et al.* (2011).

There are multiple potential advantages for *C. neoformans* to secrete proteins, lipids, enzymes and virulence traits in extracellular vesicles (Rodrigues *et al.*, 2008a; 2008b). Primarily, this mechanism may be important for survival of the fungal cell in the host, and perhaps particularly inside phagocytic cells. More specifically, packaging virulence traits within vesicles may allow delivery of a concentrated toxic payload which would be far more damaging

to the host than if each virulence trait was secreted individually and had to reach the target cells by diffusion. Additionally, packaging fungal compounds in extracellular vesicles may increase the uptake efficiency by the host cells. It is also possible that packaging antioxidant proteins in the extracellular vesicles may help protect the fungal cell from the host immune response.

The extracellular vesicles produced by *C. neoformans* have been shown to be important for pathogenesis and to influence the host immune response during infection. For example, the extracellular vesicles were produced by *C. neoformans* during infection of mouse macrophages, and the vesicle-associated proteins reacted with sera from cryptococcosis patients (Rodrigues *et al.*, 2007; 2008a). The extracellular vesicles were internalized by mouse macrophages and stimulated phagocytic and microbicidal activities (Oliveira *et al.*, 2010). The secreted vesicles also modulated the nitric oxide and cytokine production by macrophages (e.g., TNF-α, IL-10, and TGF-β). Finally, incubation of the extracellular vesicles with macrophages resulted in rapid disruption of the vesicles, enabling release of their cargo (Wolf *et al.*, 2012).

Similar outer membrane vesicles have been described in Gram-negative and Gram-positive bacteria as a delivery mechanism for virulence factors or as a way to modulate the host defense response (Wai *et al.*, 2003; Kuehn and Kesty, 2005; Lee *et al.*, 2009). Additionally, other fungal species, including the human pathogen *Histoplasma capsulatum*, also secrete extracellular vesicles (Albuquerque *et al.*, 2008).

1.1.3.2. Secreted mannoproteins

Mannoproteins are a group of cell surface proteins and represent the majority of proteins secreted by *C. neoformans* (Mansour *et al.*, 2002; Biondo *et al.*, 2006; Eigenheer *et al.*, 2007). Many mannoproteins share common structural features, such as an N-terminal signal sequence,

Ser/Thr rich regions, O-glycosylation and N-glycosylation sites, and a C-terminal glycosylphosphatidylinositol (GPI) anchor (Mansour and Levitz, 2003). This GPI anchor serves to attach these mannoproteins to the cell membrane or to the β-1,6-glucans in the cell wall, however, cleavage of the GPI anchor results in secretion of the protein to the extracellular space (Djordjevic *et al.*, 2005). Some mannoproteins are known to be regulated by iron, such as the *FIT* mannoproteins in *S. cerevisiae* (Protchenko *et al*, 2001). Several mannoproteins are also immunodominant cryptococcal antigens which play an important role in cell-mediated immunity against *C. neoformans* (Murphy, 1988; Zaragoza *et al.*, 2009). For example, many mannoproteins are recognized by serum from patients with cryptococcosis (Biondo *et al.*, 2005). Mannoproteins are also responsible for stimulating T-cell responses and can mediate partial protection in mice against *C. neoformans* (Levitz *et al.*, 2001; Biondo *et al.*, 2002; Huang *et al.*, 2002). Finally, various studies have demonstrated that glycosylation of mannoproteins is critical for T-cell responses, enabling the mannose receptors on host cells to bind and internalize the cryptococcal mannoproteins (Mansour *et al.*, 2002; Levitz and Specht, 2006; Specht *et al.*, 2007).

1.2. Iron and microbial pathogenesis

Iron is required by most organisms for growth and proliferation. Iron serves as a catalyst for many oxidative enzymes and is important in the synthesis of DNA as well as energy metabolism. It also serves as an essential co-factor in various cellular enzymes, oxygen carriers and electron transfer systems. The metal is particularly important in *C. neoformans* because its availability influences growth, capsule production and size, laccase expression and consequently pathogenesis (Jung *et al.*, 2006). Specifically, capsule enlargement occurs in mammalian tissue, in part, due to the extremely low availability of iron (Zaragoza *et al.*, 2009). Additionally, studies have shown that iron overload exacerbated virulence in a mouse model, facilitated colonization of the brain, as well as delayed and/or prevented a local cytokine response (Barluzzi *et al.*, 2002). The iron-responsive regulator, Cir1, links iron sensing to virulence and iron uptake mechanisms (Jung *et al.*, 2006; Jung and Kronstad, 2008). This link between iron uptake and virulence has been well established in bacteria. For example, *Corynebacterium diphtheriae* evolved a system where the expression of the diphtheria toxin, encoded by the *tox* gene, is induced at low iron levels (Tai *et al.*, 1990). An iron-dependent negative-regulatory protein, DtxR, represses the diphtheria toxin gene, as well as siderophores and other components of the high-affinity iron uptake system, from being transcribed under high-iron conditions (Lee *et al.*, 1997).

1.2.1. Iron uptake in bacteria

Considering the fact that iron is essential for growth and proliferation of most organisms, the mammalian host protects itself from invading micro-organisms by sequestering most of its iron with iron-binding proteins (e.g., hemoglobin, transferrin, ferritin, lactoferrin), resulting in an

extremely limited level of free iron. The concentration of free iron in the mammalian host has been reported to be approximately 10^{-18} M (Bullen *et al.*, 1978). This mechanism of sequestering free iron has a dual purpose, it also protects the host from the toxicity of free iron. Free iron is toxic to biological cells as it forms reactive oxygen species that rapidly destroy membranes, nucleic acids and proteins. In order to colonize and proliferate inside the host, pathogens must develop mechanisms to overcome the problem of iron unavailability. Gram-negative bacteria differ from Gram-positive bacteria based on their cell wall and membrane structures. Gram-negative bacteria have a cytoplasmic membrane and an outer membrane and the two membranes are separated by the periplasmic space. Gram-positive bacteria differ in that they do not have an outer membrane. Instead, they have a thick peptidoglycan layer. Bacteria must therefore develop different uptake systems to allow passage of iron across these different cell wall and membrane structures. Most of these systems rely on cell surface receptors and transporters.

1.2.1.1. Gram-negative bacteria

Important iron sources in the host include transferrin and lactoferrin. Transferrin is found in serum, while lactoferrin is present in lymph and mucosal secretions. Siderophores are small molecules which are produced and secreted by bacteria and fungi to chelate ferric iron. Siderophores have an extremely high affinity and can therefore steal iron from the host's iron-binding proteins (i.e., transferrin and lactoferrin). To allow transport of iron inside the Gram-negative cell, bacteria possess highly specific outer membrane receptors (Braun *et al.*, 2000). The receptors also serve as transporters and can translocate the iron across the outer membrane into the periplasmic space. Once the iron enters the periplasmic space, it is bound by iron-binding proteins, which protects the cell from the toxicity of free iron. In the final step, iron

transverses the cytoplasmic membrane via ATP-binding cassette (ABC) transporters in an energy-dependent manner. ABC transporters typically consist of one or two integral membrane proteins that act as permeases, coupled with two copies of one or two ATPases which provide the required energy. One example of a well characterized iron uptake system is the transport of the siderophore, ferrichrome, in *Escherichia coli* (Ferguson *et al.*, 1998; 2000; Locher *et al.*, 1998; Braun *et al.*, 2000; Clarke *et al.*, 2000). The system depends on the outer membrane receptor FhuA which also acts as the transporter (Ferguson *et al.*, 1998; Locher *et al.*, 1998). It is thought that the energy required for this process is provided by the protein complex, TonB, ExbB and ExbD, localized at the cytoplasmic membrane (Braun and Endriss, 2007). Once the ferrichrome reaches the periplasmic space, it is chelated by the periplasmic protein FhuD (Clarke *et al.*, 2000). FhuD directly delivers the ferrichrome to the cytoplasmic membrane transport protein FhuB (Rohrbach *et al.*, 1995). Ferrichrome is then transported across the cytoplasmic membrane via FhuB which acts as the permease, while the energy required for transport is provided by the ATPase, FhuC. Interestingly, outer membrane receptors are highly specific and usually different receptors are required for transportation of different iron sources. In contrast, the cytoplasmic transporters allow transport of different iron sources (Braun *et al.*, 2000). For example, the outer membrane receptor FhuE transports the siderophore, coprogen, while IutA transports iron bound to the siderophore, aerobactin. However, both iron sources are transported across the cytoplasmic membrane via the FhuCDB transporter, the same transporter that is required for transport of ferrichrome.

E. coli can also transport ferrous iron via the FeoABC iron transport system (Kammler *et al.*, 1993). FeoA is a small protein thought to be localized in the cytosol. FeoB has been identified as a protein located at the cytoplasmic membrane that likely functions as the permease,

while FeoC may function as an iron-sulfur-dependent transcriptional repressor (Cartron *et al.*, 2006). These proteins are also found in *Salmonella enterica*, *Helicobacter pylori*, and *Vibrio cholera* (Tsolis *et al.*, 1995; Velayudhan *et al.*, 2000; Wyckoff *et al.*, 2006; Mey *et al.*, 2008).

1.2.1.2. Gram-positive bacteria

Gram-positive bacteria possess similar iron uptake systems as Gram-negative bacteria but have developed a different approach to circumvent the differences in their cell wall. In Gram-positive bacteria, iron transport is mediated by an iron-binding protein anchored to the cytoplasmic membrane by lipids, and by ABC transporters (Schneider and Hantke, 1993; Braun, 2001). The iron-binding protein acts as a receptor and delivers the iron to the associated ABC transporter which will allow transport of iron across the cytoplasmic membrane. However, the exact mechanism for transport across the cell wall remains unclear.

Transport of siderophore-bound iron is a major iron uptake mechanism in Gram-positive bacteria. The transport of siderophore-bound iron has been characterized in different bacteria including *Staphylococcus aureus*, *Listeria monocytogenes*, and *Bacillus anthracis* (Hammer and Skaar, 2011; Honsa and Maresso, 2011; Klebba *et al.*, 2012). Specifically, *S. aureus* synthesizes at least two different siderophores, staphyloferrin A and staphyloferrin B. Both siderophores can scavenge iron from the host's transferrin and lactoferrin. Once the iron is coupled to the siderophore, it is transported across the cell wall to the specific ABC transporter on the cytoplasmic membrane. The lipoprotein HtsA serves as the receptor for staphyloferrin A and is coupled with the membrane permease HtsBC (Beasley *et al.*, 2009; Grigg *et al.*, 2010). Staphyloferrin B-bound iron is acquired in a similar fashion although the lipoprotein SirA acts as the receptor and the membrane permease consists of SirBC (Dale *et al.*, 2004; Grigg *et al.*,

2010). Finally, *S. aureus* is also able to take up iron bound to siderophores produced by other organisms. The lipoprotein receptors FhuD1 and FhuD2 and the permease FhuBG are involved in the transport of these xenosiderophores (Sebulsky *et al.*, 2000; 2003; 2004). The energy required for transport of iron bound to all these different siderophores is thought to be generated by the ATPase, FhuC (Beasley *et al.*, 2009; Speziali *et al.*, 2006). Other bacteria, such as *L. monocytogenes*, are unable to synthesize siderophores and rely exclusively on uptake of iron bound to siderophores produced by other organisms (Klebba *et al.*, 2012).

Alternatively, Gram-positive bacteria can also extract iron from mammalian iron-binding proteins, including transferrin. For example, a Tpn transferrin-binding protein has been identified in *S. aureus* and *Staphylococcus epidermidis*. The Tpn protein is a glyceraldehyde-3-phosphate dehydrogenase that is localized at the cell wall and that binds transferrin to facilitate iron release. The released iron can then be transported into the cytoplasm via the ABC transporters (Modun *et al.*, 1998). Some bacteria, such as *Bacillus cereus*, have also been shown to utilize ferritin (Daou *et al.*, 2009).

1.2.1.3. Heme acquisition in bacteria

Heme is a prosthetic group that contains iron and is commonly found as a component of hemoglobin or other hemoproteins (e.g., myoglobin, cytochrome). Heme comprises the largest iron pool in the mammalian body, and therefore, can serve as an important iron source for many bacterial pathogens (Tong and Guo, 2009; Nobles and Maresso, 2011). Heme refers to the molecule in which the prosthetic group contains iron in the ferrous state (Fe^{2+}), while hemin is used when the prosthetic group contains oxidized iron (Fe^{3+}). The two terms are often used interchangeably and, for the sake of simplicity, heme will be used throughout the remainder of

this thesis. Bacteria employ specific heme transporters and receptors, and some bacteria also secrete heme-binding proteins known as hemophores (Tong and Guo, 2009; Nobles and Maresso, 2011; Wandersman and Delepelaire, 2012). Similarly to the uptake of other iron sources, the heme transport systems in Gram-negative bacteria are also composed of an outer membrane transport protein, a periplasmic heme-binding protein and an ABC transporter localized at the cytoplasmic membrane to allow transport of heme into the cell (Braun, 2001; Tong and Guo, 2009). For example, in *Pseudomonas aeruginosa*, PhuR acts as the single outer membrane heme receptor, while PhuT binds heme in the periplasm and delivers it to the ABC transporter which is composed of PhuUVW (Ochsner *et al.*, 2000; Tong and Guo, 2009). Some bacteria, including *Serratia marcescens*, *P. aeruginosa*, *Yersinia pestis*, and *Haemophilus influenzae*, also secrete hemophores into the extracellular space to release the heme from hemoglobin and deliver it to the outer membrane receptor (Hanson *et al.*, 1992; Letoffe *et al.*, 1994; 1998; 1999; 2000; Jarosik *et al.*, 1995; Cope *et al.*, 1998; Arnoux *et al.*, 1999; 2000; Wandersman and Stojiljkovic, 2000; Rossi *et al.*, 2001; Tong and Guo, 2009).

In Gram-positive bacteria, heme uptake relies on multiple cell surface proteins that form a relay system across the cell wall to ultimately deliver heme to an ABC transporter at the cytoplasmic membrane. One of the best described systems is the one present in *S. aureus* (Hammer and Skaar, 2011; Nobles and Maresso, 2011). A multi-gene operon, termed the iron-regulated surface determinants (Isd) locus, encodes seven heme binding proteins (IsdA, IsdB, IsdC, IsdD, IsdE, IsdG, and IsdI). The operon also encodes sortases (SrtA, SrtB) which anchor the Isd proteins, specifically IsdA, IsdB, and IsdC, to the cell wall. IsdB is the most surface exposed protein, followed by IsdA and then by IsdC. Heme is passed along these proteins to finally be directed to the ABC transporter (IsdDEF), which receives the heme from IsdC. IsdD

functions as the permease, IsdE is a lipoprotein receptor, and IsdF is the ATPase. Finally, IsdH is also surface exposed and was shown to bind hemoglobin and haptoglobin. Interestingly, many Isd proteins (IsdA, IsdB, IsdC, and IsdH) contain near iron transporter (NEAT) domains and it has been demonstrated that heme binding occurs via the NEAT domains (Andrade *et al.*, 2002; Grigg, *et al.*, 2007; Hammer and Skaar, 2011; Nobles and Maresso, 2011). In the past few years, Gram-positive bacteria, including *B. anthracis* and *L. monocytogenes*, have also been found to secrete hemophores (Maresso *et al.*, 2008; Wandersman and Delepelaire, 2012; Klebba *et al.*, 2012; Honsa and Maresso, 2011). Specifically, *B. anthracis* possesses a heme uptake system similar to the Isd system in *S. aureus*, but also contains two additional secreted proteins, IsdX1 and IsdX2, which have been shown to both contain NEAT domains and to bind heme (Maresso *et al.*, 2008). These hemophores acquire heme from hemoglobin and transfer the heme to IsdC. Hemophores have also been recently described in *Mycobacterium tuberculosis* (Tullius *et al.*, 2011).

Once inside the cell, the iron must be released from the heme porphyrin through oxidative degradation by the heme oxygenase which cleaves heme to produce biliverdin XI, carbon monoxide, and iron (Nobles and Maresso, 2011). The free iron can then be used directly by the cell in cellular functions or can be recycled. One of the first heme oxygenases characterized was the one found in *C. diphtheriae* (Schmitt, 1997), however, they have now been identified in many Gram-negative and Gram-positive bacteria. In fact, heme oxygenases are highly conserved among prokaryotes, fungi and higher eukaryotes (Wilks, 2002; Skaar *et al.*, 2004; 2006; Wu *et al.*, 2005). Not surprisingly, the expression of heme oxygenases in pathogenic bacteria is usually up-regulated in low-iron conditions and in the presence of heme (Schmitt, 1997; Reniere *et al.*, 2010).

1.2.2. Iron uptake in *C. neoformans* and other fungi

C. neoformans has also evolved multiple strategies to acquire iron while in the host, including a reductive high-affinity iron uptake pathway, a low-affinity iron uptake pathway, transport and use of siderophore-bound iron, and acquisition of iron from heme. These mechanisms will be described in detail in the following sections.

1.2.2.1. The reductive high-affinity iron uptake pathway

The reductive high-affinity iron uptake pathway mediates iron utilization from inorganic iron sources and transferrin, which is an important iron source for *C. neoformans* during infection (Jung and Kronstad, 2008). Components of this pathway are induced upon iron limitation (Lian *et al.*, 2005). In this pathway, iron must first be reduced, either by cell surface ferric iron reductases (Fre) or other reductants such as melanin and 3-hydroxyanthranilic acid (3HAA), and then be transported inside the cell by the iron permease/ferroxidase complex localized at the plasma membrane (Jacobson *et al.*, 1997; Jung *et al.*, 2008; 2009). Jung *et al.* (2008) demonstrated that *C. neoformans* possesses two high-affinity iron permeases, Cft1 and Cft2. They showed that deletion of *CFT1* resulted in reduced growth and iron uptake in presence of low concentrations of ferric chloride and transferrin as sole iron sources. Additionally, the *cft1Δ* mutant was attenuated for virulence in a mouse model and resulted in a lower fungal burden in the brain when compared to infection with the wild-type strain. Interestingly, Cft2 played no apparent role in iron acquisition but was involved in virulence. Two multicopper ferroxidases were also found in *C. neoformans*, Cfo1 and Cfo2 (Jung *et al.*, 2009). Similarly, Cfo1 was essential for growth in presence of low concentrations of ferric chloride and transferrin

as sole iron sources and resulted in attenuated virulence in a mouse model, while no phenotypes were associated with deletion of *CFO2* (Jung *et al.*, 2009).

The reductive high-affinity iron uptake pathway was first described in *S. cerevisiae* (Lesuisse *et al.*, 1987; Askwith *et al.*, 1994; Stearman *et al.*, 1996; Philpott, 2006). In this organism, the pathway also involves reduction of iron by extracellular ferric reductases (i.e., Fre1 and Fre2) and transport within the cell via the permease/multicopper ferroxidase complex, Ftr1/Fet3 (Askwith *et al.*, 1994; Stearman *et al.*, 1996). It was established that prior to being transported into the cell via Ftr1, the iron must first be oxidized by Fet3 (De Silva *et al.*, 1995; 1997; Hassett *et al.*, 1998; Wang *et al.*, 2003). The reductive high-affinity iron uptake pathway has now been described in most pathogenic fungi (Kornitzer, 2009). In *Candida albicans*, two iron permeases are present, CaFtr1 and CaFtr2, although only CaFtr1 is required for growth in low-iron conditions and virulence in a mouse model (Ramanan and Wang, 2000). Additionally, a multicopper ferroxidase, CaFet3, is also required for growth in low iron environments, but is not essential for virulence (Eck *et al.*, 1999). Similarly, the permease/multicopper ferroxidase complex (FetC and FtrA) is also found in *Aspergillus fumigatus* (Schrettl *et al.*, 2004). However, deletion of *FTRA* does not result in any growth defect or attenuation in virulence.

1.2.2.2. Low-affinity iron uptake pathway

When in abundance, iron can be taken up by the cell via the low-affinity iron uptake pathway in *C. neoformans* (Jacobson *et al.*, 1998). This system relies on reduction of iron by reductants, including melanin, 3HAA or other secreted reductants, and eventual transport inside the cell via transporters, which have not been identified as of yet (Jacobson *et al.*, 1997). The details and mechanism of this iron uptake pathway are still currently unknown.

A low-affinity iron uptake pathway has also been relatively well described in *S. cerevisiae* (Philpott, 2006; Sutak *et al.*, 2008). A non-ATP-dependent trans-membrane transporter, Fet4, is the main component of the pathway (Dix *et al.*, 1994). Similarly to *C. neoformans*, ferric iron must first be reduced to ferrous iron before being transported into the cell. The permeases involved in low-affinity iron uptake are not specific to iron but can also take up copper and zinc (Kaplan and Kaplan, 2009). For example, Fet4 has been implicated in transport of ferrous iron, zinc, copper and cadmium (Dix *et al.*, 1994; 1997; Hassett *et al.*, 2000). Other metal transporters described in *S. cerevisiae* are Smf1, Smf2, and Smf3 (Culotta *et al.*, 2005). Smf1 and Smf2 are primarily manganese transporters although Smf1 can also transport ferrous iron (Cohen *et al.*, 2000; Portnoy *et al.*, 2000). Smf3 is involved in transfer of iron from the vacuolar stores to the cytosol (Portnoy *et al.*, 2000). A similar low-affinity iron uptake system has not yet been characterized in *C. albicans* or *A. fumigatus*.

1.2.2.3. Transport of siderophore-bound iron

C. neoformans does not produce siderophores, however, it can utilize iron bound to xenosiderophores. *C. neoformans* possesses siderophore iron transporters, one of which (Sit1) has been characterized by Tangen *et al.* (2007). They demonstrated that Sit1 is required for use of siderophore-bound iron and for growth in a low-iron environment. Deletion of *SIT1* also resulted in altered melanin deposition and laccase activity, and changes in cell wall density. However, the importance of the siderophore in iron uptake during disease is not yet clear. Sit1 did not play a role in virulence, possibly because other iron uptake pathways were functional in the mutant and allowed acquisition of other iron sources *in vivo*, masking the role of the siderophore iron uptake pathway.

The siderophore non-reductive iron uptake pathway is very common among the different species of fungi. It was first described in *S. cerevisiae* but has now been characterized in several fungal species. The siderophore-iron chelates are transported into the cell via Arn/Sit transporters, which likely function as proton symporters energized by the membrane potential (Lesuisse *et al.*, 1998). *S. cerevisiae* possesses four siderophore transporters (Kosman, 2003), each transporting a specific type of siderophore. In *C. albicans*, only one siderophore transporter, CaSit1/CaArn1, has been well characterized to date (Almeida *et al.*, 2009). It is not specific to only one type of siderophore as it can transport a range of siderophores from other organisms as well as other iron complexes (Ardon *et al.*, 2001; Heymann *et al.*, 2002; Lesuisse *et al.*, 2002; Bernier *et al.*, 2005). Interestingly, transport of siderophores via CaSit1/CaArn1 has been linked to an endocytic pathway (Hu *et al.*, 2002, Weissman *et al.*, 2008). Although the CaSit1/CaArn1 siderophore transporter was not required for virulence in a mouse model, it appeared to be essential for epithelial invasion in a human cell model (Heymann *et al.*, 2002; Hu *et al.*, 2002). In *A. fumigatus*, uptake of iron by siderophore transporters appears to be the major iron uptake pathway (Haas, 2012). Ten putative *SIT* genes have been reported in this organism, although only two (MirA and MirB) have been characterized so far (Haas *et al.*, 2003; 2008). *A. fumigatus* is also capable of synthesizing its own siderophores and biosynthesis has been linked to virulence. Specifically, deletion of the ornithine monooxygenase (SidA), an enzyme involved in siderophore biosynthesis results in loss of virulence in a mouse model (Schrettl *et al.*, 2004; Hissen *et al.*, 2005).

1.2.2.4. Acquisition of iron from heme

Many pathogenic fungi can utilize heme as an iron source (Foster, 2002; Santos *et al.*, 2003; Jung *et al.*, 2008). However, very little is known about the mechanism involved in heme uptake in fungi. For example, *H. capsulatum* can grow on heme and it has been speculated that heme uptake is mediated by unidentified cell surface receptors (Foster, 2002). *C. albicans* can also grow on heme and the heme uptake mechanism relies on hemolytic factors to release the hemoglobin from the erythrocytes, and cell surface receptors (Manns *et al.*, 1994; Pendrak *et al.*, 2000). So far, two heme-binding proteins, Rbt5 and Rbt51, have been characterized as cell surface receptors for heme and hemoglobin utilization (Weissman and Kornitzer, 2004). Rbt5 and Rbt51 are both cell surface mannoproteins and carry a CFEM domain characterized by a set of eight conserved cysteine residues (Weissman and Kornitzer, 2004; Kulkarni *et al.*, 2003). CFEM domains are common to many fungal surface proteins, however, their function is still unknown (Kulkarni *et al.*, 2003). The expression of *RBT5* was strongly induced in low-iron conditions and deletion of the gene resulted in growth defects in presence of heme or hemoglobin (Weissman and Kornitzer, 2004). Additionally, expression of CaRbt51 in *S. cerevisiae* enabled the cells to utilize hemoglobin as an iron source (Weissman and Kronitzer, 2004). Furthermore, Weissman *et al.* (2008) demonstrated that Rbt5 facilitates the rapid endocytosis of hemoglobin into the vacuole in *C. albicans*, and the pathway depends on the lumen acidification of late secretory vesicles and on the endosomal sorting complex required for transport (ESCRT). ESCRT proteins are required to sort proteins to the lysosome for degradation and they also participate in the formation of multivesicular bodies (Hurley, 2010). Interestingly, deletion of *RBT5* did not result in attenuation of virulence in either a mouse or rabbit model of infection, possibly because other iron uptake pathways compensated for the loss

of the heme uptake pathway (Braun *et al.*, 2000). Jung *et al.* (2008) have shown that *C. neoformans* can also utilize iron from heme, although the heme uptake system has not yet been characterized. Given that the majority of iron in mammals is present in heme, this source may be particularly important for *C. neoformans.* In the past year, work in our laboratory has shown that the ESCRT protein Vps23 plays a role in heme acquisition. Deletion of *VPS23* resulted in a growth defect on heme, a capsule defect and attenuation of virulence in a mouse model (Hu *et al.*, 2013). This study demonstrated that in *C. neoformans*, like in *C. albicans*, the ESCRT pathway may be involved in heme uptake. Finally, *C. neoformans* has a putative heme oxygenase, however, it has not yet been demonstrated to play a role in heme acquisition.

1.2.3. Regulation of iron uptake

The uptake and utilization of iron need to be tightly regulated because of the highly toxic nature of iron. In *C. neoformans,* as in other fungi and bacteria, genes involved in the uptake, storage and utilization of iron are more highly expressed in iron deprived environments to allow the cell to survive and proliferate in such conditions (Yamaguchi-Iwai *et al.*, 1995; 1996; Braun 2001; Jung *et al.*, 2006; Nobles and Maresso, 2011). Iron regulation in pathogenic fungi appears to depend on the GATA-binding and CCAAT-binding classes of transcription factors (Kornitzer, 2009). For example, the GATA-binding transcription factor, *Cryptococcus* iron regulator (Cir1), was identified as the iron master regulator in *C. neoformans* (Jung *et al.*, 2006) and was shown to integrate iron sensing with the expression of virulence traits. Specifically, microarray analysis revealed that Cir1 controls the expression of genes involved in iron acquisition, iron transport and iron homeostasis, and functions both as an activator or repressor (Jung *et al.*, 2006). Cir1 also controls the expression of the genes encoding known virulence traits, including the capsule,

melanin synthesis and the ability to grow at 37°C. Upon deletion of the *CIR1* gene, the mutant was defective in capsule formation and growth at 37°C but had increased laccase activity. Furthermore, the *cir1Δ* mutant was avirulent in a mouse model indicating a role for Cir1 in iron acquisition in the host (Jung *et al.*, 2006). In *C. albicans*, the GATA-binding transcription factor Sfu1 was identified as the master iron regulator, regulating the expression of at least 149 genes, while SreA was identified to regulate the expression of at least 49 genes in *A. fumigatus* (Lan *et al.*, 2004; Schrettl *et al.*, 2008). The CCAAT-binding transcription factors in both *C. albicans* and *A. fumigatus* were also found to affect iron regulation (Kornitzer, 2009).

Similarly, the expression of genes involved in iron uptake in many Gram-negative and Gram-positive bacteria, including *E. coli* and *S. aureus*, are regulated by the ferric uptake repressor (Fur) (Xiong *et al.*, 2000; Hantke, 2001; Nobles and Maresso, 2011). The Fur transcription factor forms a dimer and binds to a palindromic DNA sequence known as a Fur box. When iron is present, it binds to Fur and results in the protein binding to the Fur box in the promoters of target genes, thus preventing the transcription of these genes. In low iron conditions, Fur dissociates from the box, permitting the RNA polymerase to initiate transcription of the target genes.

HapX is another transcription factor involved in the regulation of iron acquisition in *C. neoformans*. For example, HapX plays a positive regulatory role in siderophore transporter expression as well as in expression of the Cir1 transcription factor (Jung *et al.*, 2010). Deletion of *HAPX* resulted in a slight attenuation of virulence indicating that HapX plays a minimal role during infection of mammalian hosts (Jung *et al.*, 2010). It is suggested that HapX may be more important as a regulator of environmental iron uptake functions. Interestingly, HapX is highly

conserved among most fungal species and orthologs have been identified in *C. albicans* and in *A. fumigatus* (Hortschansky *et al.*, 2007; Baek *et al.*, 2008).

Rim101 is another highly conserved transcription factor among fungal species and is responsible for regulating gene expression in response to pH, thereby allowing the cells to adapt to changes in the environmental pH. However, Rim101 also regulates genes involved in iron acquisition in both *C. neoformans* and *C. albicans* (Bensen *et al.*, 2004; Thewes *et al.*, 2007; Baek *et al.*, 2008; Nobile *et al.*, 2008; Liang *et al.*, 2009; O'Meara *et al.*, 2010). Specifically, a microarray analysis in *C. neoformans* revealed a role for Rim101 in metal homeostasis and many proteins involved in iron transport were differentially regulated between the wild-type and *rim101Δ* strains (O'Meara *et al.*, 2010). Phenotypically, the *rim101Δ* mutant had a capsule attachment defect, displayed a growth defect at alkaline pH or in presence of high salt, and had slower growth in low-iron conditions. Interestingly, the *rim101Δ* mutant proved to be hypervirulent in a mouse model, which could possibly be explained by the fact that the mutant survives better than the wild-type strain within macrophages.

1.3. Cytokine-inducing glycoprotein (*CIG1*)

Previous work to identify iron uptake systems in *C. neoformans* characterized the transcriptome upon growth at different iron concentrations and in different iron sources (Lian *et al.*, 2005; Jung *et al.*, 2006; 2010). In addition to the reductive and siderophore uptake systems, these studies revealed that the *CIG1* gene was the most abundant transcript in iron-starved cells of the C. *neoformans* var. *neoformans* strain B3501A. *CIG1* was differentially expressed in response to iron and its expression was decreased by 10 fold when the cells were grown in iron-replete medium (Lian *et al.*, 2005). The *CIG1* gene encodes a predicted mannoprotein with a signal peptide which presumably allows the protein to be secreted to the cell surface (Levitz and Specht, 2006). It has been suggested that Cig1 is a cytokine-inducing glycoprotein as it was detected in a cell fraction containing several extracellular proteins that reacted with serum antibodies from AIDS patients infected with *C. neoformans* and it triggered cytokine production in cultured immune cells (Biondo *et al.*, 2005; 2006; Murphy *et al.*, 1993). Thus, Cig1 may represent one of the mannoproteins involved in modulating the immune response to *C. neoformans*.

Disruption of the *CIG1* gene in a *C. neoformans* var. *neoformans* causes a growth defect in low iron medium (LIM) and the loss of iron suppression of capsule size (Lian *et al.*, 2005). Biondo *et al.* (2006) also identified Cig1 as one of 13 major secreted proteins. Additionally, *CIG1* was recently identified to be regulated by the pH-responsive transcription factor Rim101 (O'Meara *et al.*, 2010). The microarray analysis revealed that *CIG1* was the most significantly differentially expressed transcript and was repressed over 470 fold in the *rim101Δ* mutant compared to wild-type strain.

1.4. Rationale and aims of study

Iron acquisition and processing is essential for the pathogenesis of *C. neoformans*. As mentioned above, heme is the most abundant iron source in the mammalian host and *C. neoformans* has been shown to utilize heme as an iron source. However, the heme uptake pathway has not yet been characterized. Understanding the key players in the acquisition of this iron source could prove invaluable in identifying additional drug targets for more efficient therapy against cryptococcosis.

1.4.1. Hypotheses

Given that the expression of *CIG1* is strongly regulated by iron and that the protein is predicted to be localized extracellularly, the primary hypothesis for this study was that Cig1 functions in iron acquisition in *C. neoformans.* Additionally, iron is an essential component of pathogenesis leading to the second hypothesis that Cig1 plays a role in virulence. The analysis revealed that deletion of *CIG1* resulted in delayed growth of *C. neoformans* in LIM supplemented with heme, however, the *cig1Δ* mutant was eventually able to grow, leading to the third hypothesis that an alternative pathway for heme acquisition must exist in *C. neoformans*. Finally, previous findings that disruption of *CIG1* resulted in the loss of iron suppression of capsule size led to the fourth hypothesis that Cig1 may be involved in the regulation of capsule elaboration, possibly via secretion.

1.4.2. Research objectives

The general objective of this study was to characterize the role of the *CIG1* gene in both *C. neoformans* var. *grubii* and var. *neoformans*. The objective in Chapter 2 was to examine

whether Cig1 plays a key role in iron uptake. The specific goals were: 1) to determine if Cig1 is required for growth in different iron sources, 2) to establish the role of Cig1 in heme uptake, 3) to confirm the extracellular localization of Cig1, 4) to evaluate the ability of Cig1 to bind to heme, and 5) to test whether Cig1 contributes to virulence.

For Chapter 3, the objective was to focus in more detail on establishing and elucidating alternative heme acquisition systems for *C. neoformans*. The specific goal was to examine the contribution of different factors which may be involved in Cig1-independent heme acquisition, including: 1) pH, 2) the pH master regulator Rim101, and 3) cell density.

Finally, the goal in chapter 4 was to assess the link between Cig1 and the elaboration of the capsule. Specifically, the role of Cig1 in secretion and in maintaining cell wall integrity was evaluated.

Chapter 2. Role of Cig1 in heme acquisition in *C. neoformans* var. *grubii*

2.1. Introduction

Iron is an essential nutrient for most organisms. As part of the immune defense system, the mammalian host protects itself against invading microorganisms by using iron-binding proteins to restrict the level of free iron. In order to survive and proliferate, *C. neoformans* has evolved multiple strategies to acquire iron while inside the host (Jacobson *et al.*, 1997; 1998; Tangen *et al.*, 2007; Jung *et al.*, 2008; 2009; Jung and Kronstad, 2008). Iron availability is a particularly important aspect of cryptococcal disease because the metal influences the *C. neoformans* in mice (Jung *et al.*, 2008; 2009)

C. neoformans has also been shown to utilize heme as an iron source, however the mechanism for heme uptake is still unknown (Jung *et al.*, 2008). In fact, very little is known about heme uptake in fungi, although heme acquisition systems have been well described in pathogenic bacteria (Weissman and Kornitzer, 2004; Weissman *et al.*, 2008; Nobles and Maresso, 2011; Tong and Guo, 2009; Wandersman and Delepelaire, 2012). In general, heme uptake is mediated by cell surface heme receptors and transporters to traffic the molecule to the intracellular space (Nobles and Maresso, 2011; Tong and Guo, 2009). In addition, some microbes also secrete hemophores, which are high-affinity heme-binding proteins, to sequester heme from the environment and deliver it to the cell surface receptors (Wandersman and Delepelaire, 2012). Given that the majority of iron in mammals is present in heme, this source may be particularly important for *C. neoformans.*

A previous study identified *CIG1* as the most abundant transcript in *C. neoformans* var. *neoformans* cells grown in LIM. The *CIG1* transcript was also found to be differentially expressed when the cells were grown in iron-replete conditions compared to LIM (Lian *et al.*,

2005). The abundance and regulation of *CIG1* led to the hypothesis that Cig1 may play an important role in *C. neoformans* and that it may be involved in iron acquisition. The goal of this study was therefore to characterize the role of Cig1 in iron acquisition.

C. neoformans var. *grubii* represents the most important clinical serotype in individuals with AIDS, while *C. neoformans* var. *neoformans* is less virulent, based on a mouse model of infection, and is less clinically significant (Chaturvedi *et al.*, 2002; Toffaletti *et al.*, 2004; Barchiesi *et al.*, 2005; Lin *et al.*, 2007; Perfect and Casadevall, 2011). In this study, an ortholog of Cig1 was identified in the *C. neoformans* var. *grubii* strain H99, and this strain was chosen to examine the contribution of Cig1 in iron acquisition so that virulence could be assessed.

The effects of deleting the *CIG1* gene in *C. neoformans* and growing the cells in LIM supplemented with different iron sources were studied in order to test the hypothesis that Cig1 may be involved in iron acquisition. The *cig1Δ* mutant resulted in delayed growth in LIM supplemented with heme. The role of Cig1 in heme uptake was examined using toxic heme analogs. The localization of Cig1 was elucidated and the ability of Cig1 to bind to heme was also investigated. Finally, the contribution of Cig1 to virulence was assessed in a mouse model of infection.

2.2. Materials and Methods

2.2.1. Strains and growth conditions

All strains used in this study are listed in Table 2.1. LIM was prepared as described (Vartivarian *et al.*, 1993) and the pH was adjusted to 7.2. The water used for LIM was treated with Chelex-100 resin (Bio-Rad) to chelate iron. Alternatively, yeast nitrogen base (YNB; Difco) was also used. Low iron YNB (LI-YNB) was prepared with chelated water, as above, and 100 µM bathophenanthroline disulfonic acid (Sigma) was added to chelate any residual iron in the medium. Cells for growth assays were pre-grown overnight at 30°C with shaking in yeast extract peptone dextrose broth (YPD; Fisher). The cells were then washed twice with low iron water, inoculated into LIM at 4 x 10^6 cells/mL and grown at 30°C for two days to starve the cells for iron. After starvation, the cells were harvested, washed and inoculated in LIM alone or supplemented with heme (porcine hemin, Sigma), $FeCl_3$ (Sigma), hemoglobin (Sigma), or ferrioxamine (Sigma) to a final concentration of 5 x 10^4 cells/mL. Cultures were incubated at 30°C and growth was monitored by measuring the optical density at 600 nm using a DU530 Life Science UV/Visible spectrophotometer (Beckman Instruments).

Growth was also monitored by three other methods: 1) microscopically counting the number of cells; 2) determining the number of viable cells by colony forming units (CFU) and; 3) measuring the total reductase activity of the cells at each time point. The CFU were determined by diluting the cells in water and plating the dilutions on YPD: 1% agarose (Invitrogen) was added as the solidifying agent. The CFU were counted after incubating the plates for 3 days at 30°C. Total reductase activity was measured as an index of the number of cells based on metabolic viability (Conconi *et al.*, 2000). Briefly, 850 µL of cells from each time point were washed and resuspended in 0.05 M sodium phosphate buffer (pH 7.5), and then 350

μL of a 0.5% 2,3,5-triphenyltetrazolium chloride (TTC) solution were added to the cells. The samples were incubated at room temperature in the dark for 24 hours, and the cells were then washed in water. The formazan formed by the reductase activity was extracted from the cells by bead beating with glass beads in ethanol:acetone (1:1) for 5 minutes at maximum power. The cells were pelleted and the relative quantity of extracted formazan was determined by measuring the absorbance of the supernatant at 485 nm.

To examine growth on solid media, iron-starved cells were diluted to 1 x 10^6 cells/mL in low iron water. Ten-fold serial dilutions were made in low iron water and 5 μL of each dilution was plated on LIM alone or supplemented with heme or $FeCl_3$: 1% agarose was added as the solidifying agent. Plates were incubated for three days at 30°C and then photographed.

Table 2.1. Strains used in this study

Strain	Description	Provided by/ Prepared by
H99	*C. neoformans* wild-type strain	Dr. Joseph Heitman
cig1Δ	*cig1* disruption mutant	Carmelo Biondo
cig1Δ +CIG1	*CIG1* complemented strain	Tian Lian
cig2Δ	*cig2* deletion mutant	Tian Lian
cig2Δ +CIG2	*CIG2* complemented strain	Brigitte Cadieux
cig1Δ cig2Δ	*cig1 cig2* double deletion mutant	Tian Lian
cig1Δ cig2Δ +CIG1	*CIG1* complemented in *cig1Δ cig2Δ* background	Brigitte Cadieux
cig3Δ	*cig3* deletion mutant	Brigitte Cadieux
cig1Δ cig2Δ cig3Δ	*cig1 cig2 cig3* triple deletion mutant	Brigitte Cadieux
cfo1Δ	*cfo1* deletion mutant	Dr. Wonhee Jung
cig1Δ cfo1Δ	*cig1 cfo1* double deletion mutant	Brigitte Cadieux
cig1Δ cfo1Δ +CIG1	*CIG1* complemented in *cig1Δ cfo1Δ* background	Brigitte Cadieux
HA::Cig1	*HA*-tagged Cig1 strain	Tian Lian
Cig1::GST	*E. coli* strain expressing recombinant *GST*-tagged Cig1	Dr. Guanggan Hu

2.2.2. *In silico* protein analysis

The Cig1 amino acid sequence from the *C. neoformans* serotype D strain B3501A was used to search the *C. neoformans* serotype A genome sequence of the H99 strain (http://www.broadinstitute.org/annotation/genome/cryptococcus_neoformans) as well as other serotypes of *C. neoformans* (http://blast.ncbi.nlm.nih.gov/Blast.cgi?PAGE=Proteins) to identify homologs of *CIG1*. Multiple sequence alignments were performed using Clustal W (http://www.ebi.ac.uk/clustalw/). The signal peptide for the Cig1 sequence was predicted using Signal P (http://www.cbs.dtu.dk/services/SignalP). Sites for glycosylation were predicted using NetNGlyc (http://www.cbs.dtu.dk/services/NetNGlyc) and NetOGlyc (http://www.cbs.dtu.dk/services/NetOGlyc) for N- and O- glycosylation, respectively. Big-PI Predictor (http://mendel.imp.ac.at/sat/gpi/gpi_server.html) was used to inspect sequences for the presence of putative GPI cleavage sites, while TMHMM was used to predict transmembrane regions (http://www.cbs.dtu.dk/services/TMHMM). HHpred (http://toolkit.tuebingen.mpg.de/hhpred) was used to search for remote protein homology based on protein structure prediction, while Phyre (www.sbg.bio.ic.ac.uk/phyre) was used to predict protein folds.

2.2.3. Construction of strains

Primers used for construction of all strains are listed in Table 2.2.

Table 2.2. Primers used for strain construction

Allele constructed	Primer identification	Primer sequence
cig1:NAT	cig1-R	TCAGTTACTACTCAGCATACATAG
	cig1-F	ATGCGCGCTTATCACTTGCAGGC
	cig1-up	TGGGTGAGTACATCCTTCGGTAG
	cig1-low	TGGGTATGCCAGAAGATACAGACT
CIG1:NEO	cig1A-int-F	AAACCGGACCACCACAATAA
	cig1A-int-R	CACTTTGGGCTTCTCTGAGG
CIG1:HYG	cig1A-comp1	TCGGCCGACTTAGTTGACAT
	cig1A-comp2	AATTCCAGCACACTGGCGGCCGTTACTAGTGCCA CTGTCCGAGGAAATAA
	cig1A-comp3	AATTCTGCAGATATCCATCACACTGGCGGCAGAT GGTGCGAAGTATATAATAGGG
	cig1A-comp4	TCCACTTGACCAAAAGGTGT
cig2:NEO	TL2081	AAATGGCAGGCCAGCTAAGACCGA
	TL2082	AATTCCAGCACACTGGCGGCCGTTACTAGTAAGT ATAGAGGAAAGACGAGCCAG
	TL2083	AATTCTGCAGATATCCATCACACTGGCGGCGAGA AAGCACACGTTCGCACAGT
	TL2084	CTGCACCCACCCCCGATCATTCA
	TL2085	CCCCATTTGGGAAGCTGAT
	TL2086	CAGCATTCTTCAACACAACAACC
	TL2087	GACTAGGGGTTACCAATGC
	TL2088	CCGTGTTAATACAGATAAACCAA
CIG2:HYG	cig2A-comp1	AAGCGGAGTGTCTTCTGCAT
	cig2A-comp2	AATTCCAGCACACTGGCGGCCGTTACTAGTTTGG CGTCATGTTGTTCAGT
	cig2A-comp3	AATTCTGCAGATATCCATCACACTGGCGGCCCTCT TGTTTTGTACACATATTTCAAC
	cig2A-comp4	CCCCTATGTCTCGACCTCAA
	cig2A-int-F	ACCGTTACCTGCTCCAACAC
	cig2A-int-R	AGGGGTTTTGTGGTCAACAG
cig3:HYG	cig3A-1	AAGGAATGATTGTAGTTTCCCTTTC
	cig3A-3	AATTCTGCAGATATCCATCACACTGGCGGCGAAT GATGATGGGTGAAGATATAGG
	cig3A-4	AATTCCAGCACACTGGCGGCCGTTACTAGTAGAC ACTCACTTTGACGCTTTTAAT
	cig3A-6	AGTAACCCAAATTAACTCTCGCTTT
	cig3A-7	GTTCACGTTAGGAATGATTCTGG
	cig3A-8	GTTGCTTCTTATCTCGAGCACAT
cfo1:NEO	CFO1-KO1	GACGAAATCTCTCCCGAAAACTTTG
	CFO1-KO4	GGGATGTTACAGAACAGCTCTTC
	CFO1-KO5	CAGGGTATTCCCATCGCCTACC
	CFO1-KO6	GGTCGACTTGAAGTACTTGGACTTTTG
	CFO1-KO22	AATTCTGCAGATATCCATCACACTGGCGGCGAAG

Allele constructed	Primer identification	Primer sequence
		CAAAGGGCAATTGACACTAG
HA::Cig1	311	CGTGACTATGTCGACTTTGAGTTGTA
	300	TCAGGAACATCGTATGGGTACTGTGTATCGATGA TCAGTC
	303	ACGTTCCAGATTACGCTGCTGACTTCGACACGAG TCCCG
	312	AAGAATGTTAACATTTGTAGCATCG
	301	GACTGATCATCGATACACAGTACCCATACGATGT TCCTGA
	302	CGGGACTCGTGTCGAAGTCAGCAGCGTAATCTGG AACGT
Cig1::GST	BamH1-Cig1-Not1-5	CTCGTGGGATCCATCAGTGTTCAACGCAGAGCCC AGATC
	BamH1-Cig1-Not1-3	AGTCAGGCGGCCGCTCAGAGACGCTCCTTGGTGG GTATGCCAG
NEO, HYG	TL2001	ACTAGTAACGGCCGCCAGTGTGCTGGAATT
	TL2002	GCCGCCAGTGTGATGGATATCTGCAGAATT
Transformant screen	colPCR-Rev	GCCACTCGAATCCTGCATGCTTATG

2.2.3.1. Construction of the *cig1Δ* mutant and complemented strains

To construct a *cig1:NAT* disruption allele in the serotype A strain H99, a 3.4Kb fragment of the *CIG1* gene was obtained by amplification of genomic H99 DNA using primers cig1-R and cig1-F; this fragment was cloned into the TA vector (Invitrogen). The nourseothricin (*NAT*) resistance cassette was obtained by amplification from the vector pCH233 with the introduction of SnabI and ClaI restriction enzyme sites. The fragment was cloned into the SnabI and ClaI sites in the *CIG1* open reading frame resulting in partial deletion of the gene. The 4.8 Kb *cig1:NAT* disruption allele was introduced into strain H99 by biolistic transformation by the method of Toffaletti *et al.* (1993) and transformants were screened by colony polymerase chain reaction (PCR) using primers cig1 up and cig1 low. Transformants in which the wild-type allele was replaced were confirmed by hybridization to genomic DNA blots with a probe amplified from genomic H99 DNA using primers cig1A-comp3 and cig1A-comp4 (Figure 2.1A). To

complement the disruption mutation, the wild-type *CIG1* gene was reintroduced to one of the mutants on the vector pHYG-kB1 that confers HYG resistance (Hua *et al.*, 2000). Construction of the *cig1Δ* mutant and complemented strains was done by Carmelo Biondo and Tian Lian, respectively.

2.2.3.2. Construction of the *cig2Δ* and *cig1Δ cig2Δ* mutants, and complemented strains

The *cig2:NEO* deletion allele was constructed by overlap PCR using the methods described by Davidson *et al.* (2002) and Yu (2004). In the first round of PCR, the 1,128 bp sequence upstream of the 5' end of the *CIG2* gene was amplified from genomic H99 DNA with primers TL2081 and TL2082, and the 1,080 bp sequence downstream of *CIG2* was amplified with primers TL2083 and TL2084. The 1,970 bp sequence of the neomycin gene *(NEO)* was amplified from plasmid pJAF1 with primers TL2001 and TL2002. The nested primers TL2085 and TL2086 were then used to overlap the three products to yield the 4,096 bp *cig2:NEO* deletion allele. The construct was introduced into *C. neoformans* serotype A strain H99 and into the *cig1Δ* mutant by biolistic transformation to generate the *cig2Δ* and *cig1Δ cig2Δ* mutants, respectively. The resulting transformants were screened by colony PCR using primers TL2087 and TL2088. Transformants in which the wild-type allele was replaced were confirmed by hybridization to genomic DNA blots with a probe amplified from genomic H99 DNA using primers cig2A-comp3 and cig2A-comp4 (Figure 2.1B). Construction of the *cig2Δ* and *cig1Δ cig2Δ* mutant strains was done by Tian Lian.

To complement the *cig2Δ* mutation, the wild-type *CIG2* gene was reintroduced into one of the mutants by biolistic transformation. The *CIG2:HYG* construct was prepared by overlap PCR. The left arm of the construct, including the open reading frame of the *CIG2* gene, 696 bp

upstream of the start codon and 275 bp downstream of the stop codon, was amplified from strain H99 genomic DNA with primers cig2A-comp1 and cig2A-comp2. The right arm was amplified with primers cig2A-comp3 and cig2A-comp4 and included 725 bp downstream of the *CIG2* gene. The 2,201bp sequence of the *HYG* marker was amplified from plasmid pJAF15 (kindly provided by Dr. J. Heitman, Duke University, Durham, NC, U.S.A.) with primers TL2001 and TL2002. Primers cig2A-comp1 and cig2A-comp4 were then used to overlap the three products to yield the 5,092 bp *CIG2:HYG* construct. Transformants were screened by colony PCR using primers cig2A-int-F and cig2A-int-R.

A construct containing the *CIG1* gene and the *HYG* resistance cassette was generated by overlap PCR to complement *cig1Δ* in the *cig1Δ cig2Δ* double mutant. In the first round of PCR, the wild-type *CIG1* gene was amplified from genomic DNA of strain H99 using primers cig1A-comp1 and cig1A-comp2 and the construct included 687 bp upstream of the gene and 167 bp downstream of the gene. The *HYG* gene was amplified as described above. The third fragment of the construct included a 692 bp sequence downstream of the *CIG1* gene and was amplified with primers cig1A-comp3 and cig1A-comp4. Primers cig1A-comp1 and cig1A-comp4 were then used to overlap the three products to yield the 4,751 bp *CIG1:HYG* construct which was then introduced into the *cig1Δ cig2Δ* mutant by biolistic transformation. Transformants were screened by colony PCR using primers cig1A-int-F and cig1A-int-R.

2.2.3.3. Construction of the *cig3Δ* and *cig1Δ cig2Δ cig3Δ* mutants

The *cig3:HYG* deletion allele was constructed by overlap PCR. In the first round, the 855 bp sequence upstream of the 5' end of the *CIG3* gene was amplified from genomic H99 DNA with primers cig3A-1 and cig3A-3, and the 963 bp sequence downstream of *CIG3* was

amplified with primers cig3A-4 and cig3A-6. The 2,201 bp sequence of the *HYG* gene was amplified as described above. The nested primers cig3A-7 and cig3A-8 were then used to overlap the three products to yield the 3,904 bp *cig3:HYG* deletion allele. The construct was introduced into the *C. neoformans* serotype A strain H99 and into the *cig1Δ cig2Δ* mutant by biolistic transformation to generate the *cig3Δ* mutant and the *cig1Δ cig2Δ cig3Δ* triple mutant, respectively. Transformants were screened by colony PCR using primers cig3A-1 and colPCR-Rev. Transformants in which the wild-type allele was replaced were confirmed by hybridization to genomic DNA blots with a probe amplified from genomic H99 DNA using primers cig3A-4 and cig3A-6 (Figure 2.1C).

2.2.3.4. Construction of the *cig1Δ cfo1Δ* mutant and the *cig1Δ cfo1Δ CIG1* complemented strain

The *cfo1:NEO* construct was amplified using primers CFO1-KO5 and CFO1-KO6 from genomic DNA from the *cfo1Δ cfo2Δ* mutant kindly provided by Dr. W. Jung (Jung *et al.*, 2009). The 3,874 bp *cfo1:NEO* construct was introduced into the *cig1Δ* mutant by biolistic transformation to yield the *cig1Δ cfo1Δ*. The resulting transformants were screened by colony PCR using primers CFO1-KO4 and colPCR-Rev. Transformants in which the wild-type allele was replaced were confirmed by hybridization to genomic DNA blots with a probe amplified from genomic H99 DNA using primers CFO1-KO1 and CFO1-KO22 (Figure 2.1D).

To complement the *cig1Δ* deletion mutation in the *cig1Δ cfo1Δ* strain, the *CIG1:HYG* construct described in Section 2.2.3.2 was introduced into the *cig1Δ cfo1Δ* double mutant by biolistic transformation. Reintroduction of the wild-type allele was confirmed by PCR using primers cig1A-int-F and cig1A-int-R.

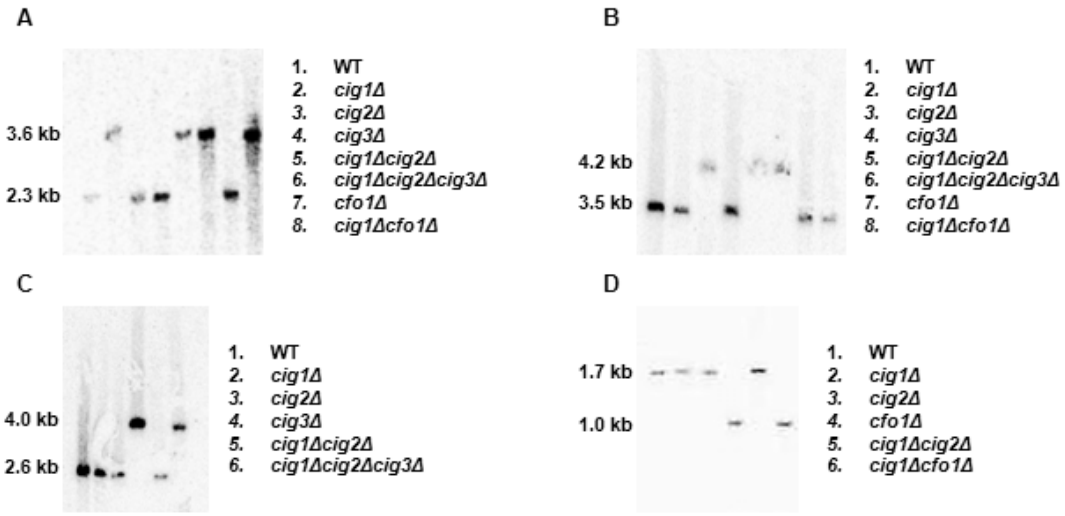

Figure 2.1 Confirmation of mutants. Southern blot analyses were performed to confirm deletion of the *CIG1* (A), *CIG2* (B), *CIG3* (C) and *CFO1* (D) genes. In panel A, genomic DNA of the indicated strains was digested with NcoI and hybridized with the downstream arm of the *CIG1:HYG* construct. In panel B, genomic DNA from the indicated strains was digested with ScaI and hybridized with the downstream arm of the *CIG2:HYG* construct. In panel C, genomic DNA from the indicated strains was digested with SpeI and hybridized with the upstream arm of the *cig3:HYG* construct. In panel D, genomic DNA from the indicated strains was digested with EcoRV and SalI and hybridized with the downstream arm of the *cfo1:HYG* construct.

2.2.3.5. Construction of an *HA::Cig1* fusion allele

The *HA::Cig1* strain, which expresses a triple copy of the *HA* epitope inserted at the 30th amino acid position of *CIG1* (just downstream of the signal peptide) was constructed by overlap PCR. In the first round, the 5' end of the *CIG1* gene was amplified with primers 311 and 300, the 3' end was amplified with primers 303 and 312, and the *HA* epitope was amplified with primers 301 and 302. The *HA* sequence was amplified from the plasmid pIS027-3xHA. Primers 311 and 312 were then used to overlap the three products to yield the 800 bp *HA::Cig1* allele. The fragment from the overlapping PCR was cloned into the SalI and HpaI sites of the pJAF15 plasmid which confers HYG resistance. The plasmid was transformed into the *cig1Δ* mutant thereby potentially complementing the *cig1Δ* mutation. Integration of the HA epitope-tagged

allele was confirmed by PCR and expression was confirmed by Western blot analysis. Construction of the *HA::Cig1* strain was done by Tian Lian.

2.2.3.6. Construction of an *E. coli* strain expressing *Cig1::GST*

Total RNA was extracted using the RNeasy mini kit (Quiagen) from H99 cells cultured in LIM. The RNA was then reverse transcribed into cDNA using SuperScript II reverse transcriptase (Invitrogen). A *CIG1* cDNA fragment (without the signal peptide) of 789 bp was amplified using primers BamH1-Cig1-Not1-5 and BamH1-Cig1-Not1-3, and the product was digested with BamHI and NotI, and cloned into BamHI/NotI digested pGEX-6P-3 (GE Healthcare, USA) to generate plasmid pCig1c. The plasmid pCig1c was then transformed into *E. coli* strain BL21 for protein expression. Construction of the *E. coli* strain expressing *Cig1::GST* was done by Dr. Guanggan Hu.

2.2.4. Purification of the recombinant *Cig1::GST* fusion protein

Expression of the recombinant *GST*-tagged Cig1 fusion protein was induced by the addition of 0.5 mM IPTG to a culture in Luria-Bertania medium (LB; 1% tryptone, 1% sodium chloride, 0.5% yeast extract) followed by overnight growth at room temperature. The extraction and purification of the recombinant *Cig1::GST* protein was performed using a glutathione affinity resin kit (Qiagen), following the manufacturer's recommendations. The concentration of purified *Cig1::GST* protein was determined by absorption at 280 nm using a calculated extinction coefficient for Cig1 (72770 $M^{-1}cm^{-1}$). Purification of the recombinant *Cig1::GST* fusion protein was performed by Dr. Guanggan Hu.

2.2.5. Quantitative real time PCR

Quantitative real time (RT) PCR was used to examine gene expression. The cells were grown in LIM alone or LIM supplemented with $FeCl_3$ or heme for 6 hours at 30°C with shaking. Total RNA was extracted using the RNeasy kit (Qiagen), treated with DNase (Qiagen) and cDNA was synthesized using the SuperScript First Strand System (Invitrogen) following the manufacturers' recommendations. PCR reactions were monitored using the 7500 system (Applied Biosystems) as described previously (Tangen *et al.*, 2007), while the primers used were designed using Primer Express software 3.0 (Applied Biosystems) and are listed in Table 2.3. The relative gene expression was quantified using the SDS software 1.3.1 (Applied Biosystems), based on the $2^{-\Delta\Delta CT}$ method (Livak and Schmittgen, 2001). The average cycle threshold value (Ct) of 18S rRNA was used for normalization.

Table 2.3. Primers used for quantitative RT-PCR

Primer identification	Primer sequence	Target Gene
CIG1A-RT-F	GGTGGTCCGGTTTCCTTCA	*CIG1*
CIG1A-RT-R	GACTCGTGGTCGTGCATAACA	*CIG1*
CIG2A-RT-F	GCCGTCTTCGGCTTTGC	*CIG2*
CIG2A-RT-R	GGAGGGCATTACGGGAGAA	*CIG2*
CIG3A-RT-F	CGCTACTATTGTTGCCTTCATCTC	*CIG3*
CIG3A-RT-R	TGCCATTACTGGTAGTGTTGAAGTC	*CIG3*
18S-RT-F	AACAGGTCTGTGATGCCCTTAGA	18S rRNA
18S-RT-R	ACTCGCTGGCTCAGTCAGTGT	18S rRNA

2.2.6. Protein extraction and Western blot analysis

Three types of *C. neoformans* protein fractions, whole-cell, cytosolic and membrane, were employed to examine the localization of Cig1 (Chen *et al*, 1999). Briefly, cells expressing *HA::Cig1* fusion protein were grown for 24 hours at 30°C in 50 mL LI-YNB. The cells were washed twice with ice-cold, sterile distilled water and lyophilized overnight. Glass beads (a 0.5

mL volume of 4 mm diameter beads) were added to the pellets and the cells were disrupted by vortexing to generate a fine powder. The cell powder was suspended in ice cold lysis buffer containing phosphate-buffered saline (PBS; Gibco), 1 mM DTT (BioChemika), 1 mM ethylenediaminetetraacetic acid (EDTA; Sigma), 1% Triton X-100 (Sigma), and complete protease inhibitor cocktail (Roche). The disrupted cells were incubated at 37°C for one hour and approximately 90% of cells were confirmed to be broken by microscopic observation. Cell debris was removed by centrifugation (3,000 × *g*, 2 minutes, 4°C), and the supernatants, representing the total cell extracts, were placed in tubes. For the separation of cytosol and membrane fractions, these extracts were centrifuged in a Beckman Optima Ultracentrifuge with the TLA100.3 rotor (Beckman Instruments Inc.) at 100,000 × *g* for one hour at 4°C. The supernatant consisted of the cytosolic protein fraction. The membranes were resuspended in wash buffer containing PBS, 1 mM EDTA and protease inhibitors, and collected by centrifugation (100,000 × *g*, 30 minutes, 4°C). Membrane proteins were extracted in PBS containing 1 mM EDTA, 1% sodium dodecyl sulfate (SDS), and protease inhibitors by heating the mixture to 65°C for 20 minutes, and removing the cell debris by centrifugation (12,000 × *g*, 15 minutes, 4°C). Protein concentrations were determined by using the Bio-Rad Protein Assay (Bio-Rad).

SDS-polyacrylamide gel electrophoresis (SDS-PAGE) was performed in the Bio-Rad Mini-Protean 3 system at 125 V in 25 mM Tris-HCl, 192 mM glycine, 0.1% SDS running buffer according to the method of Laemmli (1970). Transfer to nitrocellulose membranes was carried out using the Transblot SD semi dry transfer system (Bio-Rad) at 25 volts for 20 minutes with a buffer composed of 25 mM Tris-HCl, 192 mM glycine, 0.05% SDS, and 20% methanol. Membranes were blocked with 2% milk in Tris-buffered saline (TBS; 50 mM Tris, 150 mM

NaCl [pH 7.4]) for one hour at room temperature. Membranes were incubated with rabbit anti-*HA* antibody (Sigma) diluted in TBS buffer with 1% milk to detect *HA::Cig1*. Alternatively, rabbit anti-Cig1 antibodies prepared against the recombinant *Cig1::GST* fusion protein (Pro-Sci Inc.) or anti-*GST* monoclonal antibodies produced in mice (GenScript) were used to detect wild-type Cig1 and *Cig1::GST*, respectively. After primary antibody incubation, membranes were washed three times with TBS and then incubated with horseradish peroxidase-conjugated goat antibody to rabbit IgG (Cedarlane) or peroxidase-conjugated goat antibody to mouse IgG (Bio-Rad) at a dilution of 1:2,000 in TBS buffer with 1% milk. Membranes were washed again as described and the bands were visualized with Super Signal West Pico chemiluminescence substrate (Thermo Scientific). All antibody incubations were performed for one hour at room temperature.

2.2.7. Vesicle preparation

Cells expressing *HA::Cig1* fusion protein were grown in one liter of LI-YNB with or without 100 µM $FeCl_3$ for four days at 30°C with shaking. The extracellular vesicles were isolated from the culture supernatant as described by Rodrigues *et al.*, (2007). Briefly, the culture supernatant was harvested by centrifugation, concentrated 10 times using the stirred ultrafiltration cell with a 100,000 molecular weight cut-off membrane (Amicon). The concentrated supernatant was then ultracentrifuged and the pellet was resuspended in 1 mL of PBS. The concentration of proteins within the vesicle preparations was determined by using the Bio-Rad Protein Assay (Bio-Rad) and normalized. The proteins were then separated using SDS-PAGE and the *HA::Cig1* protein was detected by Western blot analysis, as described above.

2.2.8. Fluorescence microscopy

The fluorescence of cells expressing *HA::Cig1* fusion protein was examined after overnight growth at 30°C with shaking in 25 mL of LI-YNB. The cells were harvested by centrifugation, fixed with 3% paraformaldehyde in PBS for 30 minutes, and permeabilized with 1% Triton-X-100 in PBS for 10 minutes. The cells were incubated with rabbit anti-*HA* antibody diluted 1:50 in PBS with 1% Bovine Serum Albumin (BSA). The cells were then washed with 1% BSA-PBS and incubated with fluorescence-conjugated goat antibodies to rabbit IgG (Alexa 488, Molecular Probes) diluted 1:100 in 1% BSA-PBS. The cells were finally washed in 1% BSA-PBS and viewed on a Zeiss 510 Meta laser scanning confocal microscopy for fluorescence with the appropriate fluorescence filter. For visualizing the capsule, a monoclonal mouse anti-GXM antibody diluted 1:100 was used in combination with a fluorescence-conjugated antibodies to mouse IgG (Alexa 568, Molecular Probes). The monoclonal mouse antibody was kindly provided by Dr. A. Casadevall (Albert Einstein College of Medicine, Bronx, NY, U.S.A.). The extracellular vesicles were also visualized by immuno-fluorescence microscopy using anti-*HA* antibody and fluorescence-conjugated secondary antibody, as described above. A ceramide dye (Bodipy TR ceramide complexed to BSA, Molecular Probes) was added at 1:100 with the primary and secondary antibodies as a marker for the vesicles. The vesicles were incubated with the dye and antibodies for 30 min at 4°C and one hour at room temperature. The washes were performed with PBS filtered through a 0.22 μm filter and the vesicles were collected from the washes by ultracentrifugation at 100,000 × *g*, for 1 hour at 4°C.

2.2.9. Uptake of metalloporphyrins

To test for metalloporphyrin uptake, cells were grown overnight in YPD but not starved for iron. The cells were washed and 10-fold serial dilutions were prepared in low iron water. YPD or LIM plates with or without 10 µM heme or 100 µM $FeCl_3$ were spread with 200 µl of 10 µM Ga-protoporphyrin (Ga-PPIX; Frontier Scientific), 100 µM Mn-protoporphyrin (Mn-PPIX; Frontier Scientific) or 10 µM $GaCl_3$ (Sigma) prior to spotting 5 µl of the diluted cells. The plates were incubated for two days at 30°C.

To determine whether Ga-PPIX had fungicidal or fungistatic activity, LIM alone or LIM supplemented with 100 µM $FeCl_3$, or 10 µM heme and 100 µM Ga-PPIX was inoculated with 5 x 10^7 cells/mL. The cultures were incubated at 30°C for 24 hours. Following this incubation period, the cells were harvested by centrifugation (15,000 x g for 1 minute) using an Eppendorf centrifuge 5424, washed twice with water to remove any residual Ga-PPIX, diluted and plated on YPD agar plates to determine the number of viable cells. The plates were incubated at 30°C for 48 hours before counting the CFU.

2.2.10. Heme binding assays

Heme binding to Cig1 was determined by batch adsorption to heme-agarose beads (bovine hemin-agarose beads; Sigma), as described by Tsutsui and Mueller (1982a) with some minor modifications. Briefly, 10 µg of an extracellular vesicle preparation derived from cells expressing *HA::Cig1* fusion protein or 0.3 µg of the purified *Cig1::GST* fusion protein were incubated with 100 µl heme-agarose beads for one hour at 37°C. After three washes with 0.5 M NaCl, 10 mM sodium phosphate, pH 7.5, the proteins bound to the beads were eluted with 100 µl protein electrophoresis sample buffer and heated at 95°C for two minutes. Sepharose 4B

(Sigma) agarose beads without the heme conjugate were used as a negative control to verify for non-specific binding to the agarose beads. Following adsorption to the beads, the proteins from different fractions were separated by SDS-PAGE and *HA::Cig1* was detected by Western blot analysis using anti-*HA* antibodies as described above. Alternatively, recombinant *Cig1::GST* was detected using anti-*GST* antibodies.

2.2.11. Mass spectrometry

Cells from the wild-type strain were grown in LI-YNB with or without 100 µM $FeCl_3$ at 30°C with shaking. After 4 days, the culture supernatant was harvested by centrifugation (15, 000 × g, 15 minutes, 4°C) and concentrated 10 times using the stirred ultrafiltration cell with a 3,000 molecular weight cut-off membrane (Amicon). A batch adsorption experiment was performed using 20 mL of concentrated culture supernatant and 300 µl heme-agarose beads as described above (Tsutsui and Mueller, 1982a). Proteins were allowed to bind for 1.5 hours at 37°C and eluted with 150 µl protein electrophoresis sample buffer for 30 minutes at 37°C before electrophoretic separation on an SDS-PAGE gel. After electrophoresis, the gel was fixed with 40% ethanol; 10% acetic acid overnight, stained for 2 hours with a modified Coomassie Blue G-250 stain (Candiano *et al.*, 2004), and destained with water. The whole lane representing all the proteins eluted from the heme-agarose beads or from the agarose beads was excised from the gel and the proteins were in-gel digested with trypsin as described by Shevchenko *et al.*, (1996). The trypsinized peptides were purified using the stop and go extraction tips as described by Rappsilber *et al.*, (2003), and analyzed by tandem mass spectrometry (MS; LTQ Orbitrap Velos, Thermo Scientific). The tandem MS spectra were then used to search the *C. neoformans* H99 protein sequence database

(www.broadinstitute.org/annotation/genome/cryptococcus_neoformans). The mass spectrometry analysis (excluding the sample preparation) was performed by Nikolay Stoynov.

2.2.12. Absorption spectrophotometry

Titrations of purified recombinant *Cig1::GST* protein with heme were monitored by absorption spectroscopy in the Soret range as previously described (Gaudin *et al.*, 2011). Briefly, increasing amounts of heme dissolved in 0.1 M NaOH and diluted in 50 mM Tris, 100 mM NaCl buffer (pH 7.5) were added to 1 mL of 5 µM *Cig1::GST* in buffer. The preparation was incubated at room temperature for 5 minutes after adding heme to allow binding before measuring the absorbance spectra. Heme added to buffer without protein served as a reference. Spectra were measured using a Cary 50 Bio UV-visible spectrophotometer (Agilent Technologies) with an optical path length of 1 cm in a quartz cell.

2.2.13. Isothermal titration calorimetry experiments

Isothermal titration calorimetry (ITC) was performed using a MicroCal iTC_{200} (GE Healthcare). Samples were in 50 mM Tris pH 7.5, 0.1 M NaCl or 10 mM phosphate pH 7 or 7.5, 0.5 M NaCl. Titrations were performed by injecting consecutive 2 µL aliquots of heme solution (0.4-0.7 mM) into the calorimeter (volume = 200 µL) containing *Cig1::GST* protein (4-50 µM). All solutions were degassed at room temperature before loading in the ITC. The heat of dilution data were obtained by titrating 2 µL injections of heme solution into Cig1-free buffer. All titrations were performed at 25 °C. ITC experiments were performed by Dr. Louise Creagh.

2.2.14. Virulence assays and determination of fungal loads in mouse tissue

The virulence of each cryptococcal strain was examined using female A/Jcr mice (4 to 6 weeks old) from the Jackson Laboratory (Sacramento, CA). The iron-starved fungal cells were washed twice and resuspended in PBS (Invitrogen, Canada). The A/Jcr mice in groups of 10 were anesthetized intraperitoneally with ketamine (80 mg/kg of body weight) and xylazine (5.5 mg/kg) in PBS and inoculated intranasally with 50 μL of the cell suspensions (5×10^4 cells). The number of viable cells in each inoculum was confirmed by CFU. The health status of the mice was monitored daily post-inoculation. Mice reaching the humane endpoint were euthanized by CO_2 asphyxiation.

Three mice from each group were used at the endpoint to assess fungal loads in the lungs and brains of the animals. Following euthanasia, the brains and the lungs were aseptically removed and immersed in PBS. Organs were homogenized using an automated tissue homogenizer (Retsch, PA, USA). The samples were serially diluted in PBS and plated on YPD supplemented with 35 μg/mL chloramphenicol. After two days of incubation at 30^{o}C, the CFU were counted manually.

The protocol for the virulence assays (protocol A08-0586) was approved by the University of British Columbia Committee on Animal Care. Statistical analysis of survival differences was performed by Kaplan-Meier survival curves and log rank tests. An unpaired, two-tailed t-test was used to determine the differences in mean CFU per organ (i.e., brain and lung) between mice inoculated with different cryptococcal strains. A P-value of 0.05 or less was considered significant. All statistical analyses were carried out using GraphPad Prism version 4 for Windows (GraphPad Software, San Diego, CA). The virulence assay and determination of fungal loads in mouse tissue was performed by Joyce Wang.

2.3. Results

2.3.1. Characterization and expression of the *CIG1* gene in *C. neoformans*

Previous analysis of transcriptome changes upon growth of *C. neoformans* var. *neoformans* in high and low iron concentrations identified the transcript of the *CIG1* gene as the most abundant mRNA in cells grown in LIM, and a strong regulation of the transcript level by iron was also observed (Lian *et al.*, 2005). The amino acid sequence of Cig1 was further examined to potentially give insight into its role. *In silico* analysis of the predicted 282 amino acid polypeptide sequence did not identify any known functional domains but revealed structural characteristics common to mannoproteins, such as a putative signal peptide, four potential sites for N-glycosylation, and a serine/threonine-rich region for potential O-glycosylation as shown in Figure 2.2 (Mansour & Levitz, 2003; Biondo *et al.*, 2005). One trans-membrane region was also predicted near the C-terminus. Additionally, a chitin-binding fold was predicted by remote protein homology and this region shared 22% similarity to the chitin-binding protein found in *S. marcescens.* The predicted chitin-binding fold starts at the 57^{th} amino acid of the Cig1 sequence and extends up to the 148^{th} amino acid. A putative immunoglobulin-like beta-sandwich fold that overlaps the chitin-binding fold was also identified based on structure prediction (11% identity to E set domains of sugar-utilizing enzymes) and this fold extends from the 68^{th} to the 159^{th} amino acid of the Cig1 sequence.

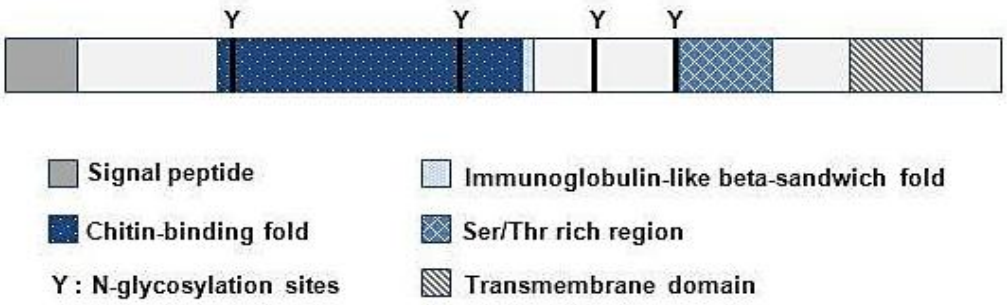

Figure 2.2 Cig1 is an iron-regulated mannoprotein in *C. neoformans.* Diagram of the Cig1 polypeptide illustrating the predicted sites for post-translational modifications, domains and folds.

Orthologs of the *CIG1* gene are present in *C. neoformans* var. *grubii*, the variety responsible for the majority of cases of cryptococcosis in AIDS patients, as well as in *Cryptococcus gattii*, a related species responsible for infections in immunocompetent individuals (Currie and Casadevall, 1994; Franzot *et al.*, 1997; Viviani *et al.*, 2006; Stephen *et al.*, 2002). The amino acid sequences of the *CIG1* orthologs share clear similarities as shown by the multiple sequence alignment (Figure 2.3). A BLASTp search identified a putative homolog of Cig1 in the fungal pathogen *Trichosporon asahii* which shares 35% identity with the *C. neoformans* protein. This protein in *T. asahii* was also annotated as a cytokine-inducing glycoprotein, probably based on its similarity with the *C. neoformans* protein. Finally, potential but distant homologs were found in various other fungal species (e.g., *Gibberella* species, *Penicillium* sp., *Nectria* sp., *Aspergillus* sp., *Glomerella* sp.); however, the predicted homologs were annotated as hypothetical proteins.

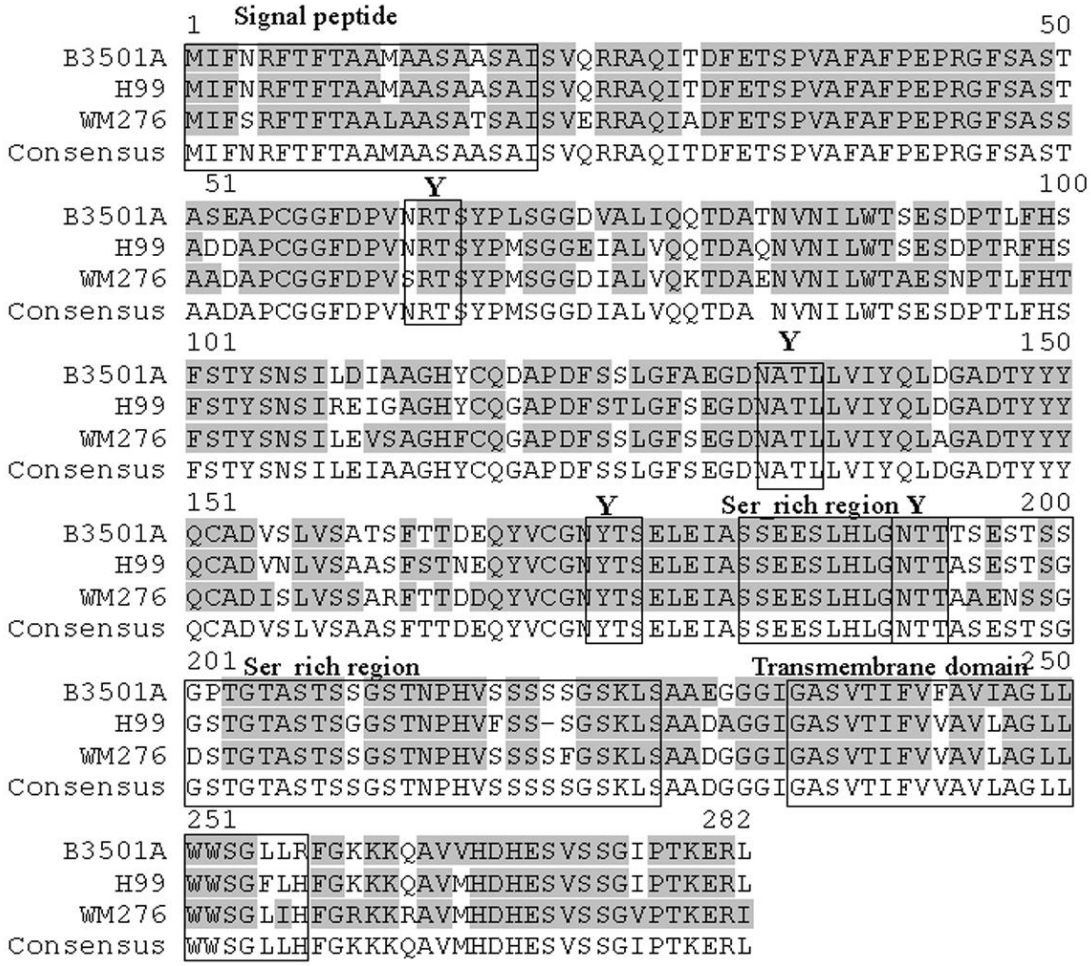

Figure 2.3 Cig1 is conserved in the different varieties of *C. neoformans*. Multiple sequence alignment of the Cig1 amino acid sequence from *C. neoformans* var. *neoformans* (B3501A), *C. neoformans* var. *grubii* (H99) and *C. gattii* (WM276).

Finally, two potential paralogs of *CIG1* were found in *C. neoformans* var. *grubii* based on sequence homology, although the similarity between amino acid sequences was relatively low (27-29%) as seen in Figure 2.4. The abundance of the *CIG1* transcript in cells grown in LIM and the conservation of the gene within different varieties of cryptococci and potentially among multiple fungi suggest that Cig1 plays an important role in *C. neoformans* under low iron conditions, such as those encountered in the mammalian host environment during cryptococcosis. Consequently, the role of Cig1 in virulence was further studied in the H99 strain

of *C. neoformans* var. *grubii*, a strain commonly used to investigate mechanisms of cryptococcal pathogenesis.

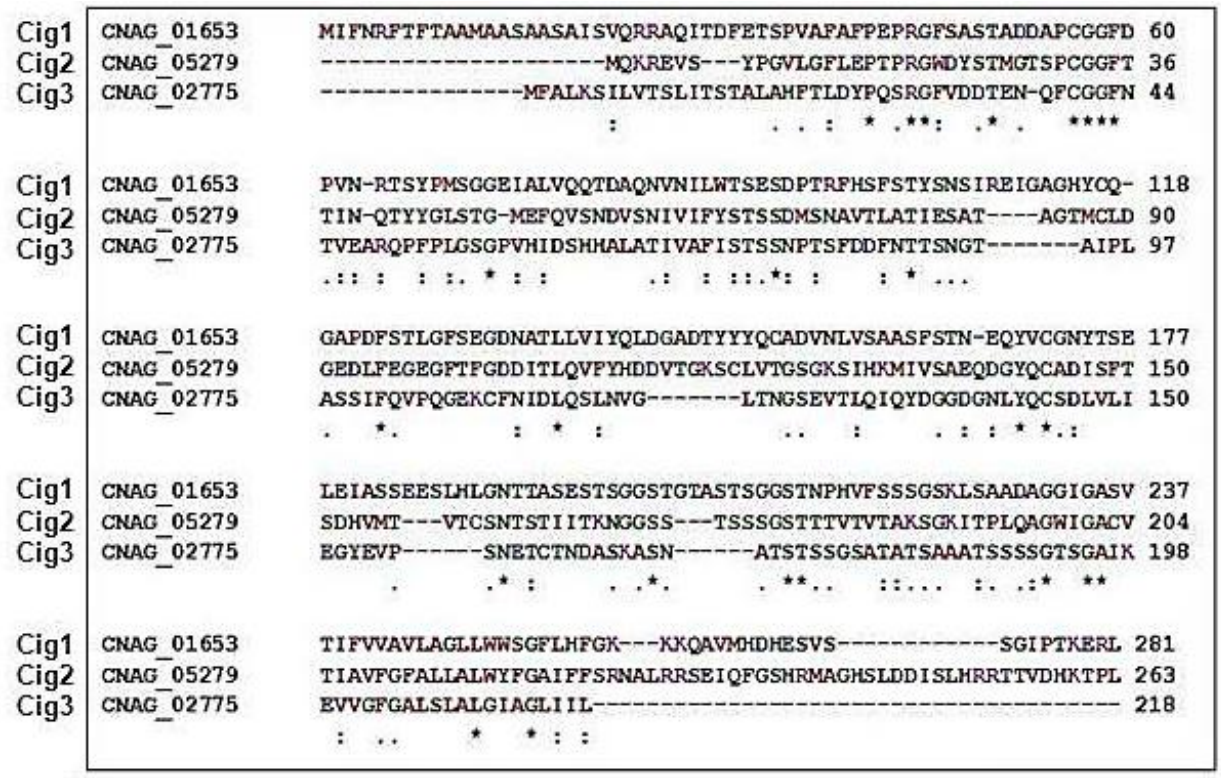

Figure 2.4 *CIG2* and *CIG3* are putative paralogs of *CIG1*. Multiple sequence alignment of the Cig1, Cig2, and Cig3 amino acid sequences from *C. neoformans* var. *grubii* strain H99.

The iron-regulation of *CIG1* observed in var. *neoformans* was also observed in var. *grubii* strain H99 as demonstrated by quantitative PCR (Figure 2.5A). In this strain, *CIG1* transcript levels were reduced more than four-fold in presence of inorganic ($FeCl_3$) or mammalian-host-related (heme) iron sources, compared to the low iron condition. Based on the heme concentrations tested, the regulation of *CIG1* did not vary in response to the amount of heme but rather in response to its absence or presence (Figure 2.5B). Specifically, a lower concentration (10 µM) of heme resulted in the same level of expression of *CIG1* as a higher

concentration (100 µM) of heme. Therefore, *C. neoformans* var. *grubii* responds to iron deprivation in a similar fashion to var. *neoformans* by increasing the expression of *CIG1*.

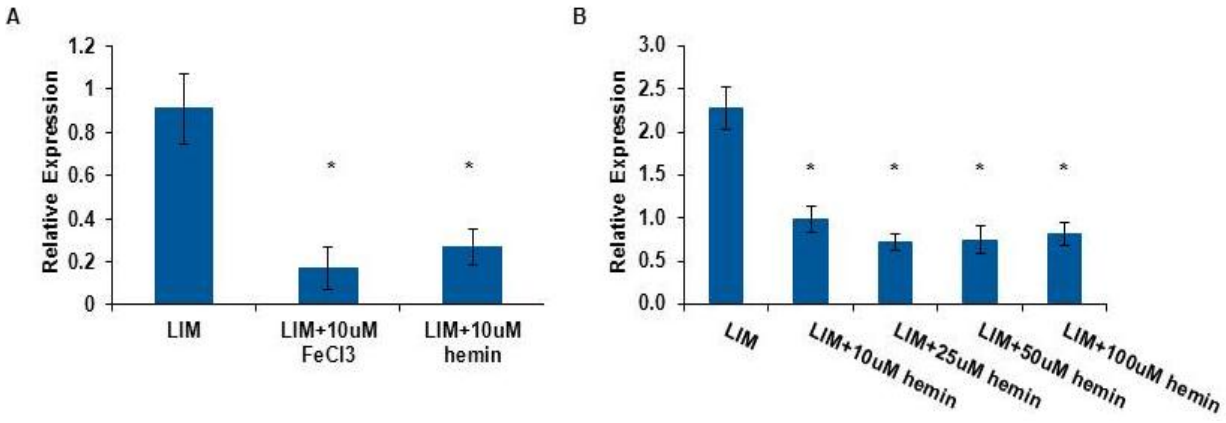

Figure 2.5 Expression of *CIG1*. The wild-type cells were grown in LIM, LIM + 10 µM $FeCl_3$, or LIM + 10 µM heme (A) or in LIM with different concentrations of heme (B). All experiments were repeated three times and the data are plotted as the average ± SD. Statistical analysis was performed by Student's *t* test. The * represents significant differences at $P < 0.05$ relative to LIM alone.

2.3.2. Cig1 is required for heme utilization

The regulation of *CIG1* by iron suggests that the protein plays an iron-related role in *C. neoformans*. Therefore, mutants lacking *CIG1* were constructed for phenotypic analysis. Complemented strains were also created by reintroducing the wild-type copy of *CIG1* into the mutants. The complemented strains were included as controls in all experiments. To examine the role of Cig1 in iron utilization, the *cig1Δ* mutant was grown in LIM with the addition of different iron sources including $FeCl_3$, heme, hemoglobin, and the iron-loaded siderophore, ferrioxamine. Growth of the *cig1Δ* mutant was measured spectrophotometrically and compared to the wild-type and complemented strains (Figure 2.6A-E). As expected, iron-depleted medium did not support growth of any of the strains confirming that iron is necessary for the growth of *C. neoformans*. The *cig1Δ* mutant grew as well as the wild-type and complemented strains in LIM supplemented with $FeCl_3$ and ferrioxamine. However, when grown in LIM with heme added as

a sole iron source, the *cig1Δ* mutant remained in lag phase for significantly longer (60 hours) than the wild-type strain (36 hours). The *cig1Δ* mutant eventually did initiate exponential growth to reach stationary phase at a similar cell density as the wild-type strain. The reintroduction of *CIG1* into the *cig1Δ* mutant restored growth, confirming that the phenotype of the mutant was due to deletion of *CIG1*. Similarly, the *cig1Δ* mutant also had a longer lag phase when grown in hemoglobin as a sole iron source, but at this time, it is not known how *C. neoformans* processes hemoglobin. Preliminary studies from our laboratory did not detect any hemolytic activity by *C. neoformans* on blood agar (Drs. W. Jung and G. Hu, personal communications). It is likely that the hemoglobin preparation used in this study was contaminated with free heme, and further work is therefore needed to investigate the use of hemoglobin. Overall, the data indicate that Cig1 is required for efficient utilization of heme as an iron source under low iron conditions but has no significant role in utilization of $FeCl_3$ or ferrioxamine under the conditions tested. Growth was also tested on solid LIM containing various concentrations of heme (Figure 2.6F). Interestingly, the *cig1Δ* mutant displayed a growth defect at a lower heme concentration (10 µM) but not at higher heme concentrations (50-100 µM) suggesting a possible role for Cig1 in high-affinity heme acquisition. High-affinity uptake systems are usually important in conditions of low substrate concentration while low-affinity uptake systems play a role when the substrate is present in high concentrations.

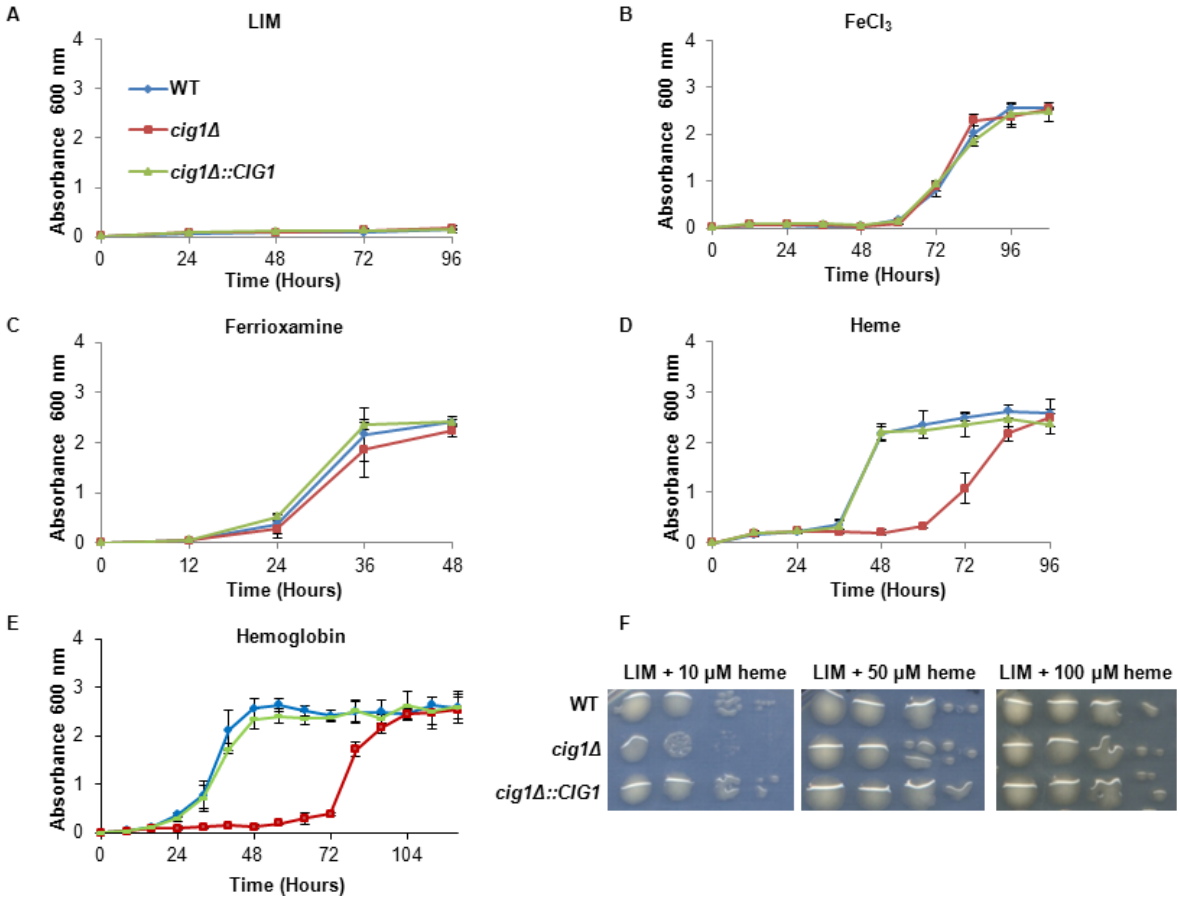

Figure 2.6 Cig1 is required for growth in LIM supplemented with heme. Growth of iron-starved cells in LIM (A), LIM + 10 µM $FeCl_3$ (B), LIM + 10 µM ferrioxamine (C), LIM + 10 µM heme (D), and LIM + 10 µM hemoglobin (E). Growth was monitored by measuring the optical density at 600 nm. All experiments were repeated three times and the data are plotted as the average ± SD. (F) Ten-fold serial dilutions of iron-starved cells spotted onto LIM + 10 µM, 50 µM or 100 µM heme as indicated. The plates were incubated at 30°C for two days and photographed. The experiment was repeated three times and a representative photograph is shown. Figure reproduced and modified from Cadieux *et al.* (2013).

Aggregates of cells were detected during growth in LIM supplemented with heme, and this phenomenon will be discussed further in Chapter 3. However, the formation of these aggregates prompted a further examination of the growth in LIM supplemented with heme to confirm that the extended lag phase observed for the *cig1Δ* mutant was indeed a result of the cells not dividing, and not due to inaccurate measurements of optical density. Therefore, growth was assessed by three additional techniques including microscopically counting the cells,

determining the number of viable cells by plating and counting the CFU, and lastly, measuring metabolic activity by using the formation of formazan as an indicator of total reductase activity. The results from all three of these methods correlated well with the results obtained by measuring the optical density of the cells at different time points (Figure 2.7), thus validating the use of optical density as an indicator of cell growth. Considering that measuring optical density is the simplest and fastest method to determine cell numbers, this method was used throughout the remainder of the growth studies presented in this thesis.

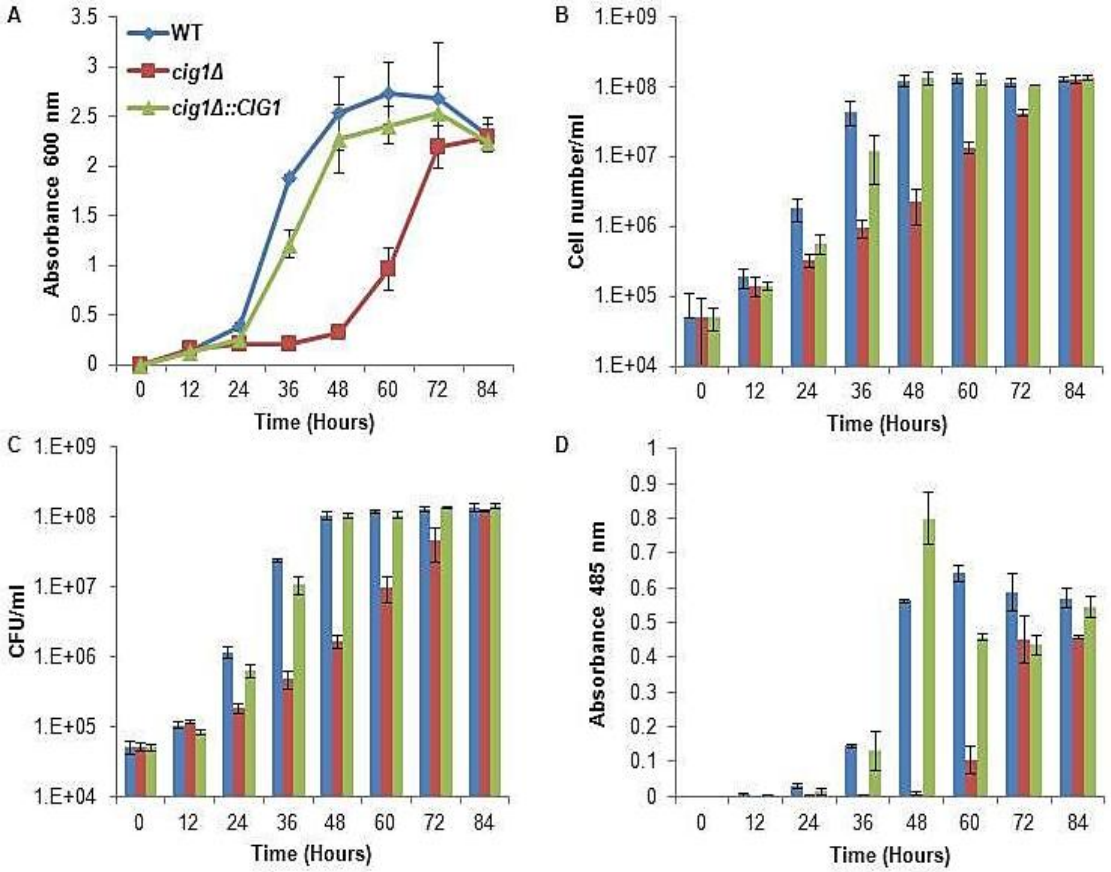

Figure 2.7 Further examination of growth in LIM supplemented with heme. Growth of iron-starved cells in LIM + 10 µM heme as determined by measuring the optical density at 600 nm (A), by counting the cells microscopically (B), by counting CFU on YPD plates (C), and by measuring the total reductase activity of the cells using TTC (D). All experiments were repeated three times and the data are plotted as the average ± SD.

2.3.3. *CIG2* and *CIG3* do not contribute to iron utilization

CIG2 and *CIG3* were identified as potential paralogs of *CIG1*. Although *CIG2* and *CIG3* share a low level of similarity with *CIG1* (27-29% identity), it is possible that they share functional redundancy. The expression of these genes in low iron and iron-replete medium was investigated by quantitative RT-PCR (Figure 2.8A). *CIG2* appeared to be regulated in a similar fashion as *CIG1* (i.e., down-regulated in the presence of $FeCl_3$ and heme) and *CIG3* was also similarly regulated in presence of $FeCl_3$, but it was not differentially expressed in the presence versus absence of heme.

Mutants lacking *CIG2* or *CIG3*, as well as mutants lacking both *CIG1* and *CIG2*, or even all three *CIG* genes were constructed to determine the contribution of each paralog in iron utilization. Complemented strains were also created by reintroducing the wild-type copy of *CIG1* into the mutants. All strains were tested for growth in LIM supplemented with heme (Figure 2.8B). The *cig2Δ* and *cig3Δ* mutants did not exhibit any difference in growth compared to the wild-type or complemented strains in LIM supplemented with heme whereas the *cig1Δ cig2Δ* double mutant and the *cig1Δ cig2Δ cig3Δ* triple mutant showed similar growth defects as the *cig1Δ* single mutant. Based on these results, *CIG2* and *CIG3* do not appear to play an important role in heme utilization and are most likely not functionally redundant with *CIG1*.

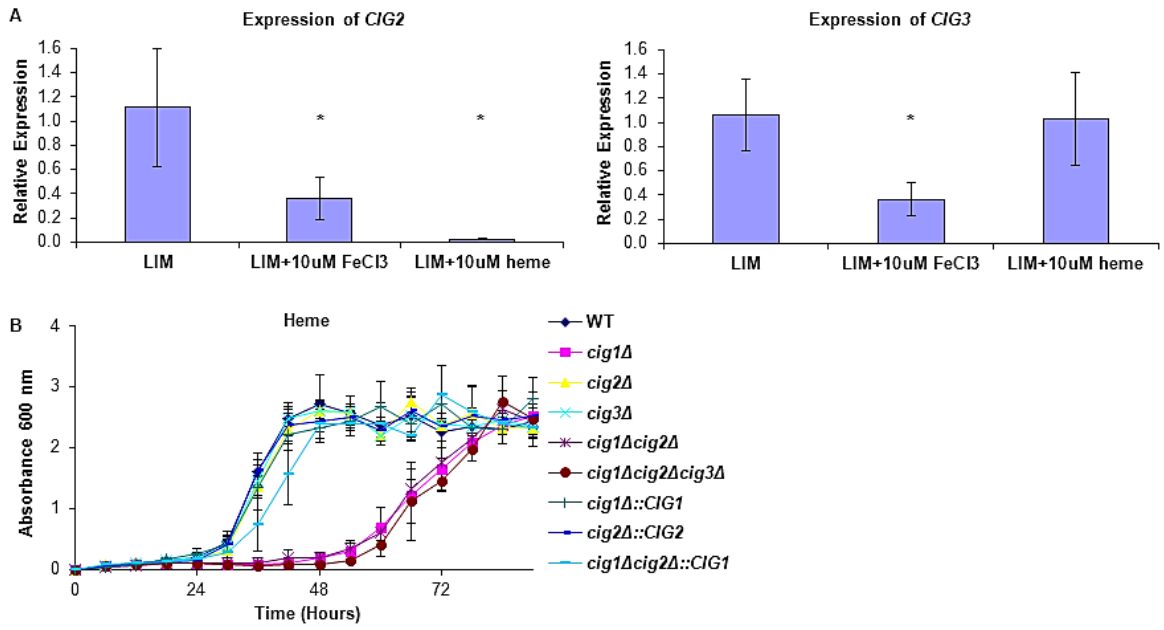

Figure 2.8 Cig2 and Cig3 are not required for growth in LIM supplemented with heme. (A) Expression of *CIG2* and *CIG3* in the wild-type grown in LIM, LIM + 10 µM $FeCl_3$, or LIM + 10 µM heme. All experiments were repeated three times and the data are plotted as the average ± SD. Statistical analysis was performed by Student's *t* test. The * represents significant differences at $P < 0.05$ relative to LIM alone. (B) Growth of iron-starved cells in LIM + 10 µM heme was monitored by measuring the optical density at 600 nm. All experiments were repeated three times and the data are plotted as the average ± SD.

2.3.4. The reductive high-affinity iron uptake system does not contribute to Cig1-mediated heme utilization

The reductive high affinity iron uptake system is required for uptake of inorganic iron and iron from transferrin (Jung *et al.*, 2008; 2009). To determine whether this high-affinity uptake system contributes to the role of Cig1 in utilization of heme, a strain lacking the *CFO1* gene was used. *CFO1* encodes the essential ferroxidase component of the high-affinity uptake system (Jung *et al.*, 2009). The *CFO1* gene was also deleted in the *cig1*Δ mutant. The growth of these strains in LIM, $FeCl_3$, ferrioxamine, and heme as sole iron sources was measured as described above and compared to the wild-type and complemented strains (Figure 2.9). As previously reported, the *cfo1Δ* mutant was unable to grow in LIM supplemented with $FeCl_3$ but

grew as well as the wild-type strain in LIM supplemented with heme, confirming that the reductive high-affinity uptake system is not involved in heme acquisition. Similarly, when *CFO1* was deleted in the *cig1Δ* mutant background, the strain was also unable to grow in LIM supplemented with $FeCl_3$, while the *cig1Δ cfo1Δ* mutant showed a similar growth defect as the *cig1Δ* mutant when grown in LIM with heme. The growth defect for heme was restored when *CIG1* was reintroduced in the *cig1Δ cfo1Δ* mutant confirming that the phenotype is due to the loss of *CIG1* and not the loss of *CFO1*. These results indicate that the role of Cig1 is independent of Cfo1 and that the high-affinity iron uptake pathway does not contribute to Cig1-mediated heme utilization.

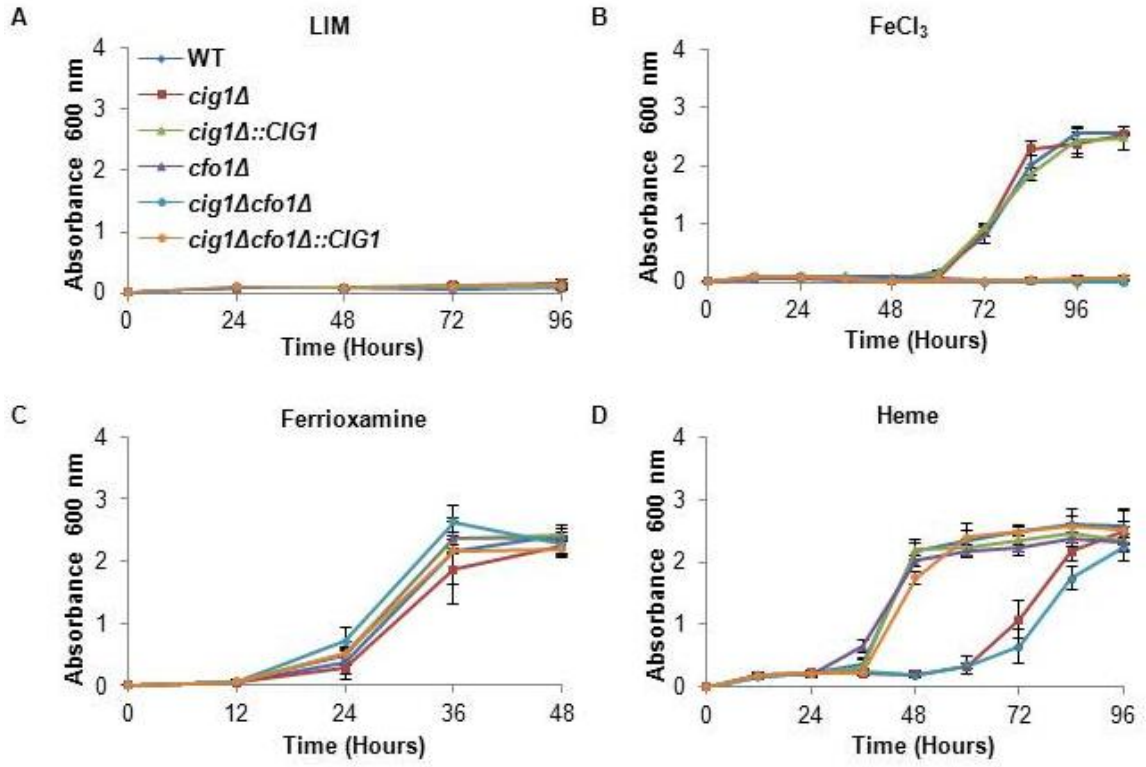

Figure 2.9 Cfo1 is required for growth in LIM supplemented with $FeCl_3$ but not with heme. Growth of iron-starved cells in LIM (A), LIM + 10 µM $FeCl_3$ (B), LIM + ferrioxamine (C), and LIM + 10 µM heme (D). Growth was monitored by measuring the optical density at 600 nm. All experiments were repeated three times and the data are plotted as the average ± SD. Figure reproduced and modified from Cadieux *et al.* (2013).

2.3.5. Cig1 is involved in heme uptake

Non-iron metalloporphyrins (MPs), which are toxic heme analogs, were employed as reagents to indirectly investigate the potential role of Cig1 in heme uptake. Non-iron MPs, such as Ga-PPIX and Mn-PPIX, share structural similarities with heme and, therefore, gain entry into the cell via heme uptake systems, as shown in bacteria (Stojiljkovic *et al.*, 1999). Non-iron MPs may stimulate production of reactive oxygen radicals leading to toxicity and displace heme in essential metabolic functions (Stojiljkovic *et al.*, 1999). Growth of the strains was compared in the presence of Ga-PPIX or Mn-PPIX (Figure 2.10). When grown on YPD or LIM with added $FeCl_3$, the wild-type, *cig1Δ* mutant and complemented strains all grew well in the absence or presence of Ga-PPIX indicating that the heme uptake system was not essential in these conditions (Figure 2.10A). Interestingly, the *cfo1Δ* mutant did not grow on YPD in the presence of Ga-PPIX, while the *cig1Δ cfo1Δ* mutant grew well, presumably because heme uptake systems are up-regulated in absence of the high-affinity iron uptake system. Reintroduction of *CIG1* into the double mutant also resulted in susceptibility to Ga-PPIX although not to the level of the *cfo1Δ* mutant (possibly because of partial complementation). Additionally, the *cfo1Δ* mutants did not grow well in LIM supplemented with $FeCl_3$ whether Ga-PPIX was absent or present. When heme was provided as the iron source, the wild-type, *cfo1Δ* mutant, and the complemented strains were unable to grow in the presence of Ga-PPIX while the *cig1Δ* mutant grew well. The toxicity of Ga-PPIX for the wild-type strain was eliminated by adding excess heme (Figure 2.10B). Interestingly, the *cig1Δ cfo1Δ* mutant had difficulty growing in LIM supplemented with heme plates in the presence or absence of Ga-PPIX; this phenotype is likely due to a contribution of Cfo1 to an additional mechanism of heme use and/or to high-affinity acquisition of any free iron contaminating the heme. Mn-PPIX has also been reported to be toxic for cells with a

functional heme uptake system although Mn-PPIX is less potent than Ga-PPIX in bacteria (Stojiljkovic *et al.*, 1999). Accordingly, growth in the presence of Mn-PPIX also yielded similar results to Ga-PPIX for *C. neoformans*, although a 10-fold higher concentration of Mn-PPIX was required. Finally, all of the strains grew well in the presence or absence of $GaCl_3$ thus supporting the idea that toxicity was due to uptake of Ga-PPIX rather than gallium. These results suggest that Cig1 contributes to the uptake of Ga-PPIX resulting in toxicity for the cells, but in absence of Cig1, the cells do not acquire Ga-PPIX and, consequently, are not affected. Instead, a separate heme uptake system may be present that allows the *cig1Δ* mutant to grow in LIM supplemented with heme as the sole iron source in the presence of Ga-PPIX. In this case, the other system may allow heme utilization in the absence of uptake (e.g., by surface reduction/extraction of the iron from the heme molecule and uptake of the released iron via the high-affinity reductive iron system), and therefore, not promote Ga-PPIX susceptibility.

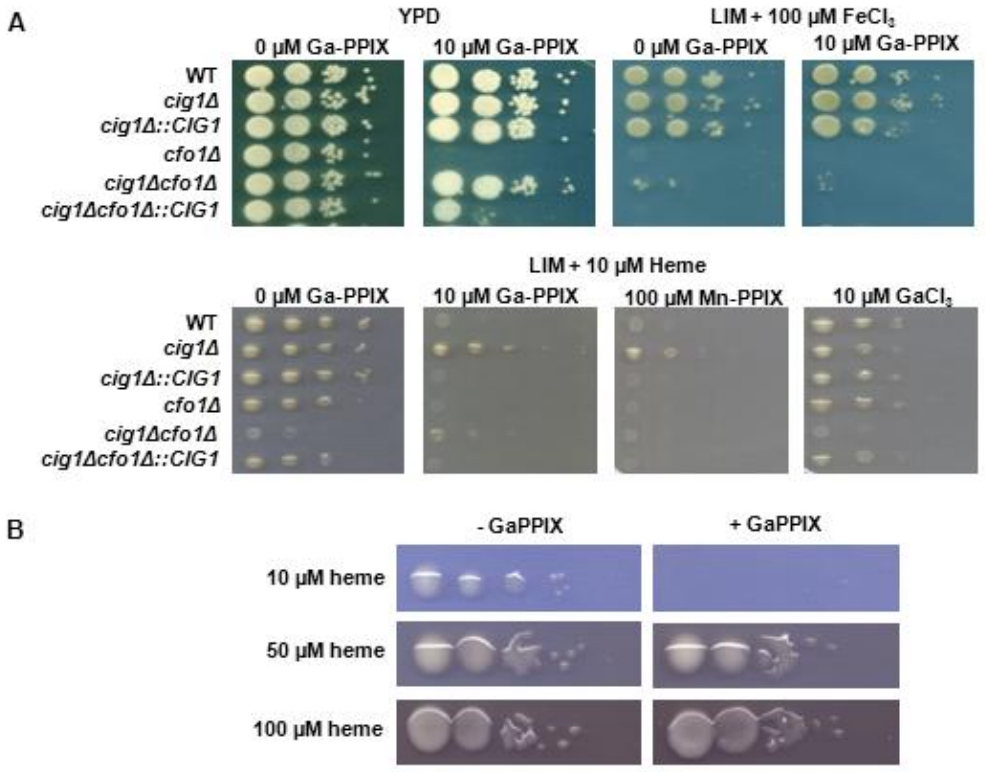

Figure 2.10 Cig1 influences susceptibility to non-iron MPs. Ten-fold serial dilutions of strains grown in YPD were spotted onto YPD, LIM + 100 μM $FeCl_3$ or LIM + 10 μM heme in absence or presence of 10 μM Ga-PPIX, 100 μM Mn-PPIX or 10 μM $GaCl_3$ as indicated (A). Ten-fold serial dilutions of iron-starved wild-type cells were spotted onto LIM + 10 μM, 50 μM, and 100 μM heme in absence or presence of 10 μM Ga-PPIX (B). The plates were incubated at 30°C for two days and photographed. The experiments were repeated three times and a representative photograph is shown. Figure reproduced and modified from Cadieux *et al.* (2013).

To determine whether the toxicity of Ga-PPIX was fungistatic or fungicidal, the cells of the wild-type, *cig1Δ* mutant and complemented strains were exposed to a 10-fold higher concentration of Ga-PPIX than was employed in the experiments shown in Figure 2.10A. The cells were then washed and plated on YPD to count CFU and assess survival (Figure 2.11). The number of cells recovered after exposure was similar for all three strains and was not significantly different from the number of cells prior to exposure. Therefore, the survival rate

was high and equivalent for all three strains, suggesting a fungistatic effect of Ga-PPIX on *C. neoformans*.

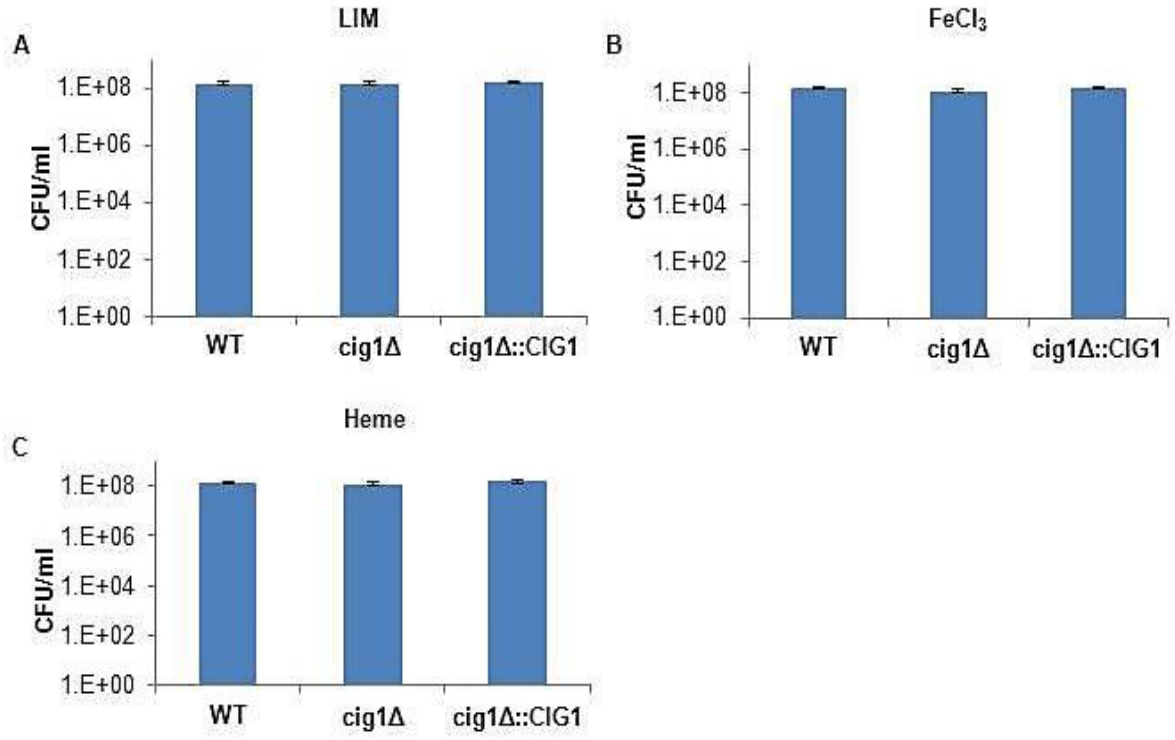

Figure 2.11 Ga-PPIX has fungistatic activity against *C. neoformans*. Survival of iron-starved cells after incubating 5 x 10^7 cells/mL in LIM (A), LIM + 100 µM $FeCl_3$ (B) or LIM + 10 µM heme (C) supplemented with 100 µM Ga-PPIX for 24 hours. The cells were washed prior to plating onto YPD. All experiments were repeated three times and the data are plotted as the average ± SD.

2.3.6. Localization of Cig1

The localization of the Cig1 protein was examined next. The amino acid sequence of Cig1 contains a putative signal peptide, one predicted trans-membrane domain near the C-terminal of the polypeptide, and no GPI anchor, suggesting that Cig1 is a secreted protein. Additionally, Biondo *et al.* (2006) identified Cig1 as a secreted protein in the culture supernatant of *C. neoformans* giving evidence for the expression of *CIG1* and implying an extracellular localization for at least a portion of the protein. Primary antibodies against Cig1 were prepared

using the recombinant *GST::Cig1* fusion protein expressed in *E. coli* to help evaluate the localization of Cig1. The specificity of the antibodies was assessed using different cellular fractions, including cell lysates, cytosolic fractions and cell wall/membrane fractions (Figure 2.12A). Additionally, *C. neoformans* produces extracellular vesicles and, therefore, the specificity of the antibodies was also tested using fractions containing the extracellular vesicles as seen in Figure 2.12B (Rodrigues *et al.*, 2007; 2008a; Yoneda and Doering, 2006). Unfortunately, these antibodies proved to be uninformative, presumably because of the lack of affinity towards native Cig1 and particularly because of a lack of specificity. In fact, it was not possible to clearly identify the Cig1 protein among several protein bands identified on a Western blot containing proteins from the wild-type strain and mutants lacking the *CIG1* gene.

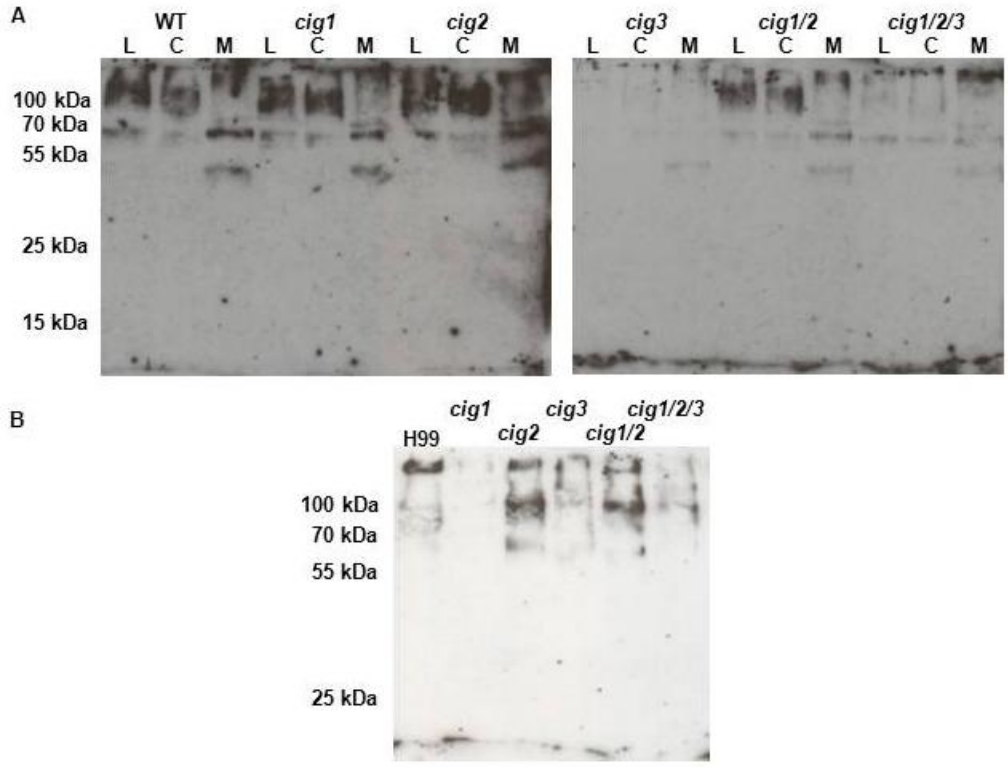

Figure 2.12 Production of anti-Cig1 antibodies. Antibodies against recombinant *Cig1::GST* protein were used to detect Cig1 in different cell fractions from wild-type and mutant strains. (A) Cells from the designated strains were grown in LI-YNB and fractionated into cell lysate (L), cytosol (C) and membrane/cell wall (M). (B) Cells from the designated strains were grown as in (A) and extracellular vesicles were isolated from the culture supernatant. Samples were separated by SDS-PAGE and blotted onto a nitrocellulose membrane. *cig1*: *cig1Δ* mutant; *cig2*: *cig2Δ* mutant; *cig3*: *cig3Δ* mutant; *cig1/2*: *cig1Δ cig2Δ* double mutant; *cig1/2/3*: *cig1Δ cig2Δ cig3Δ* triple mutant.

To further examine the localization of the Cig1 protein, an *HA::Cig1* strain was constructed in which a triple copy of the *HA* epitope was inserted at the 30th amino acid, just downstream of the signal peptide. After growing the *HA::Cig1* cells in LI-YNB, the proteins were isolated from the different cell fractions and analyzed by SDS-PAGE and Western blot, using antibodies specific to the *HA* tag. Cig1 was detected in the membrane/cell wall fraction, but not in the cytosol (Figure 2.13A).

Immuno-fluorescence microscopy was next used to localize Cig1 (Figure 2.13B). After growing the *HA::CIG1* cells in low iron and iron-replete media, the cells were fixed and permeabilized, and Cig1 was detected using antibodies specific to the *HA* tag and fluorescence-conjugated secondary antibodies before viewing by epifluorescence. According to the resulting fluorescence, the Cig1 was localized only at the surface of the cells and in a punctate distribution. As expected, no Cig1 was detected in cells grown in iron-replete conditions. The association of Cig1 with the capsule was also examined. Co-localization of a portion of Cig1 with the capsule was shown using antibodies specific to GXM, the major capsular polysaccharide, while some Cig1 was found outside the capsule in the extracellular space. Overall, these results confirm the reported extracellular localization of Cig1 (Biondo *et al.*, 2006). Unfortunately, insertion of the *HA::Cig1* allele in the *cig1Δ* mutant did not complement for the loss of *CIG1* and a lag phase longer than that of the wild-type and *cig1Δ* strains was observed when the cells were grown in LIM supplemented with heme (Appendix A). However, given that detection of the *HA::Cig1* protein confirmed the reported localization of Cig1, the strain was used to further investigate localization.

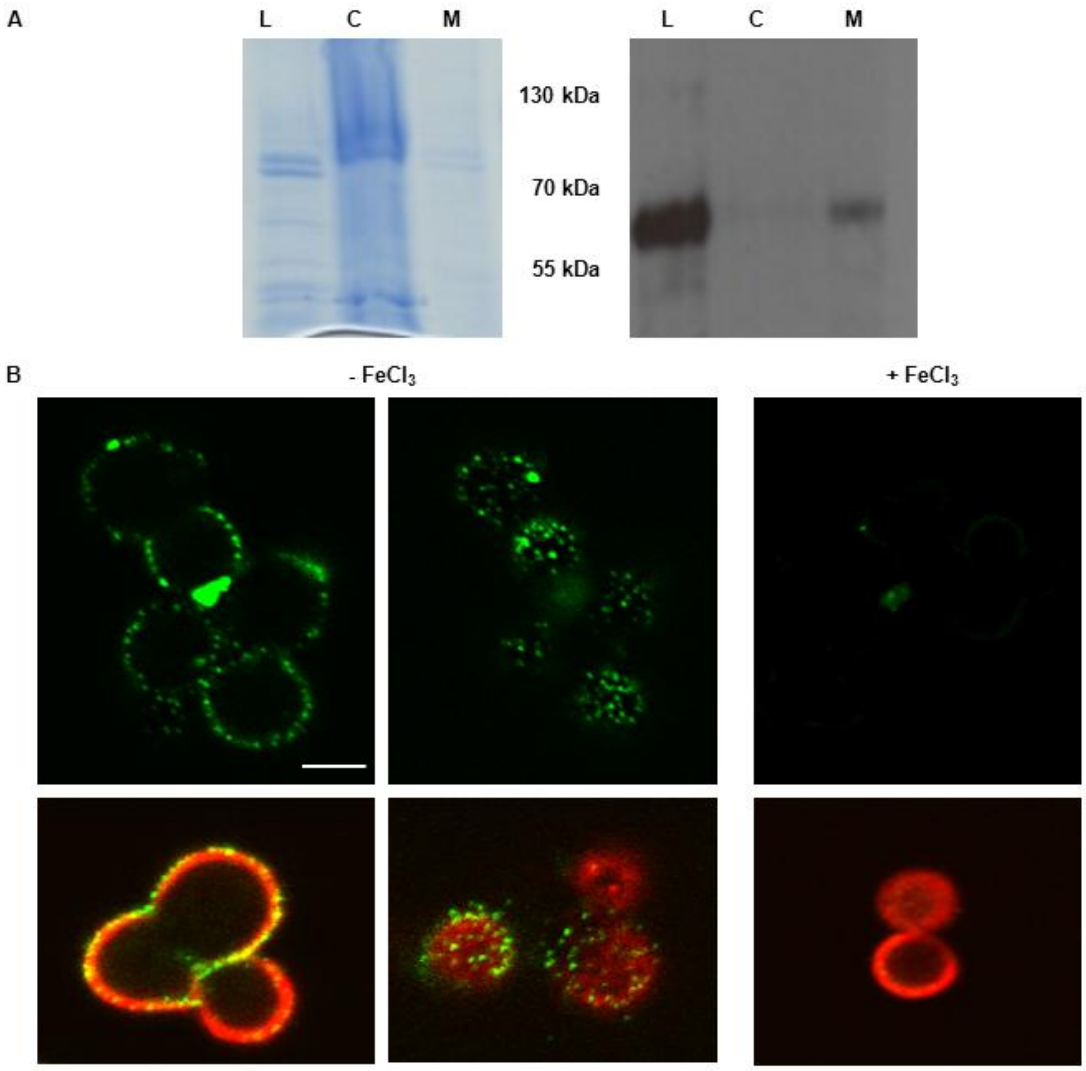

Figure 2.13 Cig1 is found at the cell surface. (A) The *C. neoformans* strain expressing *HA::Cig1* protein was grown in LI-YNB. Cells were fractionated into cell lysate (L), cytosol (C), and membrane/cell wall (M). Samples were separated by SDS-PAGE and blotted onto a nitrocellulose membrane. The *HA::Cig1* protein was detected using antibodies against *HA*. (B) Immunofluorescence microscopy of cells grown in LI-YNB either alone or supplemented with 100 µM $FeCl_3$. Antibodies against *HA* and against the capsular component GXM were used to detect *HA::Cig1* (green) and the capsule (red), respectively. Bar = 5 µm.

As mentioned above, it has been shown that *C. neoformans* produces extracellular vesicles that somehow cross the cell wall to be released in the extracellular environment (Rodrigues *et al.*, 2007; 2008a; Yoneda and Doering, 2006). The extracellular distribution of Cig1 demonstrated in Figure 2.13B suggested that Cig1 might be associated with extracellular

vesicles. To confirm this, *HA::CIG1* cells were grown in low iron and iron-replete media until stationary phase and the extracellular vesicles were isolated from the culture supernatant by a series of centrifugation steps as described by Rodrigues *et al.* (2007). The proteins from the vesicle fractions were analyzed by Western blot, using antibodies specific to the *HA* tag to determine if Cig1 was associated with the extracellular vesicles (Figure 2.14A). Cig1 was detected in the isolated vesicle fraction but only when the cells were grown in LI-YNB and not when the cells were grown in iron-replete conditions. The vesicles were examined more closely using immuno-fluorescence microscopy. For visualization, the isolated vesicles were labeled with a ceramide dye to stain the glucosylceramide in the vesicular membrane and the *HA*-tagged Cig1 protein was detected with antibodies specific for the *HA* tag (Figure 2.14B). Fluorescence from *HA::Cig1* was found to co-localize with the fluorescence from the ceramides in the vesicles. Again, no Cig1 was detected in the vesicles isolated from cells grown in iron-replete media and only fluorescence from the ceramide dye could be observed. Also, a sample of the vesicles isolated from the culture supernatant of cells grown in iron-replete media was spiked with vesicles isolated from the culture supernatant of cells grown in LIM. The sample was prepared as above for visualization of vesicles and *HA*-tagged Cig1 by immuno-fluorescence microscopy. As expected, the majority of the vesicles only emitted fluorescence from the ceramide dye while a fraction of the vesicles emitted fluorescence for both Cig1 and the ceramides in the vesicles; again, co-localization of fluorescence from Cig1 and from the ceramide dye was observed (Figure 2.14B). Taken together, these results demonstrate that Cig1 is localized at the cell surface and is associated, at least partially, with extracellular vesicles.

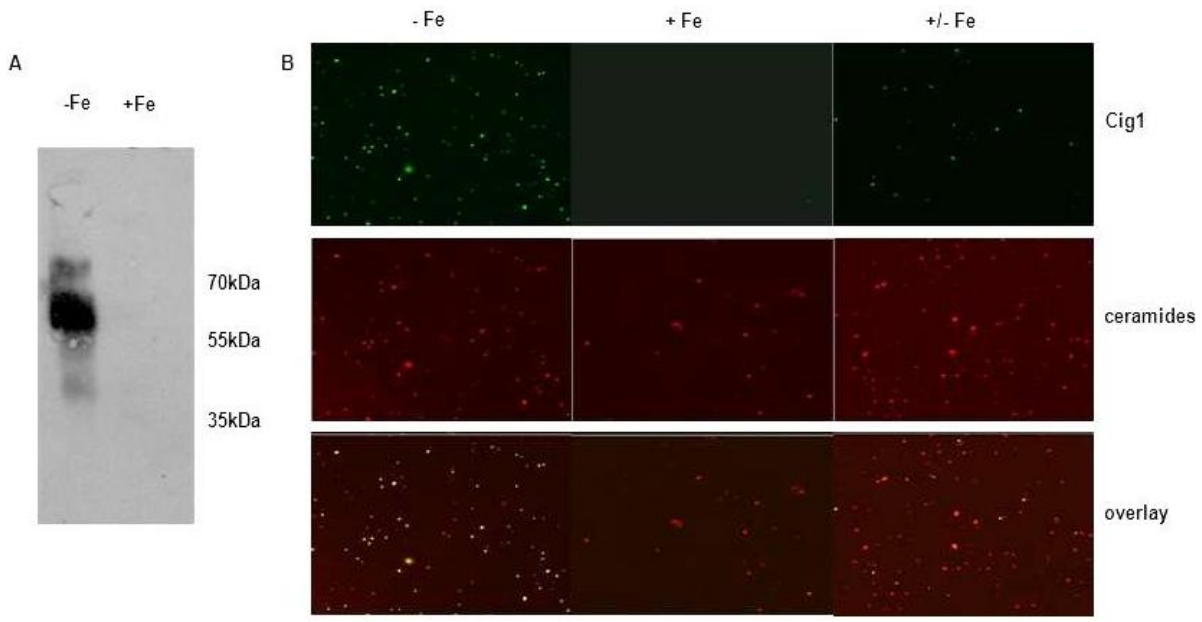

Figure 2.14 Cig1 is associated with extracellular vesicles. (A) Western blot analysis of the proteins found in the extracellular vesicle fraction isolated from cells grown in LI-YNB either alone or supplemented with 100 µM $FeCl_3$. Antibodies against *HA* were used to detect *HA::Cig1*. (B) Immunofluorescence microscopy of the extracellular vesicle fraction. Antibodies against *HA* were used to detect Cig1 (green) and a ceramide dye was used to visualize the vesicular membranes (red).

2.3.7. Analysis of Cig1 binding to heme

The extracellular location of Cig1 and the genetic evidence for a role in iron acquisition from heme suggested that Cig1 could directly interact with heme. To examine the ability of Cig1 to bind heme, extracellular vesicles with associated Cig1 were incubated with heme-agarose beads. Vesicles isolated from the *HA*-tagged Cig1 strain were used to be able to detect Cig1 using antibodies specific to the *HA* tag. The unbound, washed and eluted proteins were separated by gel electrophoresis and analyzed by Western blotting (Figure 2.15A). All of the detectable Cig1 was found in the eluted fraction suggesting an interaction between Cig1 and heme, or between heme and vesicles that contained or were associated with Cig1. The extracellular vesicle fraction was also incubated with agarose beads without the heme ligand and the separated proteins were analyzed by Western blotting to determine if Cig1 was interacting

non-specifically with the agarose beads. Cig1 was only detected in the unbound protein fraction which implies that the interaction is specific for the heme ligand. The same experiment was also performed using a recombinant *Cig1::GST* protein purified from cell lysates of *E. coli*. As above, the *Cig1::GST* protein was only detected in the eluted protein fraction when the protein was incubated with the heme-agarose beads and not upon incubation with agarose beads (Figure 2.15B). Together, these results suggest that Cig1 can bind heme.

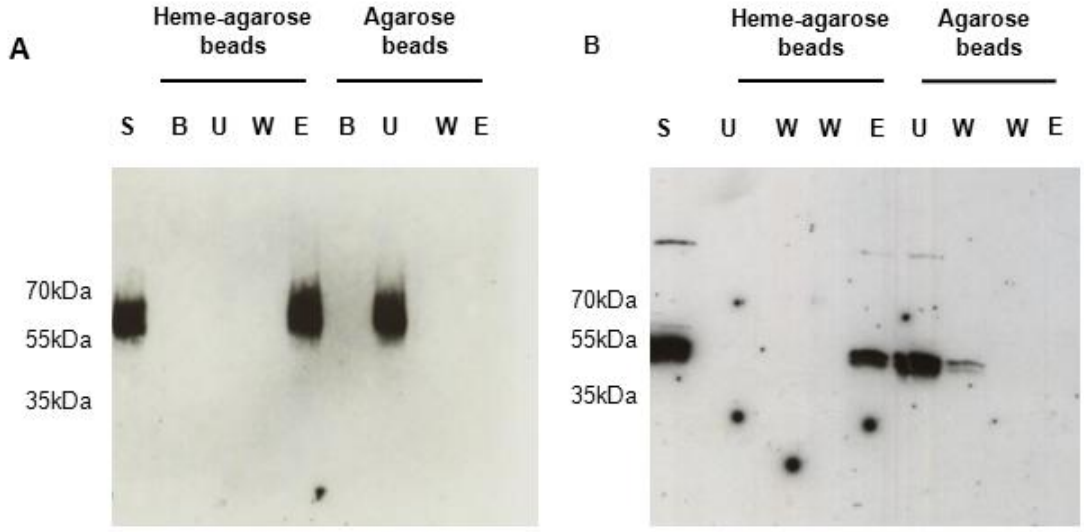

Figure 2.15 Vesicles containing Cig1 and purified recombinant Cig1 bind to heme-agarose beads. The proteins within the extracellular vesicle fraction isolated from cells expressing *HA::Cig1* (A) and purified recombinant *Cig1::GST* expressed in *E. coli* (B) were analyzed by Western blot after batch adsorption to heme-agarose beads or agarose beads. Lanes include the proteins in the start material (S), the unbound proteins (U) the proteins collected during the washes (W) and the eluted proteins (E). The beads (B) with no proteins added were also loaded on the gel as a control. The *HA::Cig1* protein was detected using antibodies against *HA*, while the *Cig1::GST* protein was detected using antibodies against *GST*. Agarose beads were used as a control for non-specific binding as described in the text.

The potential interaction between Cig1 and heme was also investigated further by measuring the absorbance spectra of the purified *Cig1::GST* protein after the addition of increasing amounts of heme. Heme groups have characteristic absorbance bands that depend on

the ligation and conformational state of the chromophore allowing detection of heme-binding proteins by spectrophotometry. Titration of *Cig1::GST* protein with heme revealed a distinct absorption spectrum defined by a maximum Soret peak at 407 nm as well as β- and α- peaks at 570 nm and 600 nm, respectively, indicative of a heme-binding protein (Figure 2.16A). The heme binding curve of Cig1 yielded multiple inflection points but heme binding saturation was not detected for Cig1 even when a 10-fold molar ratio excess of heme was mixed with the protein (Figure 2.16B). Therefore, the complexity of the interaction between Cig1 and heme did not allow a dissociation constant (K_d) to be determined using this method. Although some *Cig1-GST* degradation products were detected after purification, heme binding was not observed with *GST* alone (Figures 2.16C). Another attempt to determine the K_d was carried out using isothermal titration calorimetry (ITC). As with the spectrophotometric approach, weak binding was observed but saturation was not detected when heme was added to *Cig1::GST* protein, thus preventing determination of a K_d (Figure 2.16D). Overall, the data support the conclusion that Cig1 may be a heme-binding protein, although the interaction appears to be weak or transient.

A putative chitin-binding fold was predicted to be present in Cig1 by remote protein homology. The ability of Cig1 to bind various polysaccharides was evaluated, however, preliminary results did not reveal any binding between Cig1 and the polysaccharides under the conditions tested (Appendix B). Further work will be necessary to fully explore the interaction between Cig1 and polysaccharides.

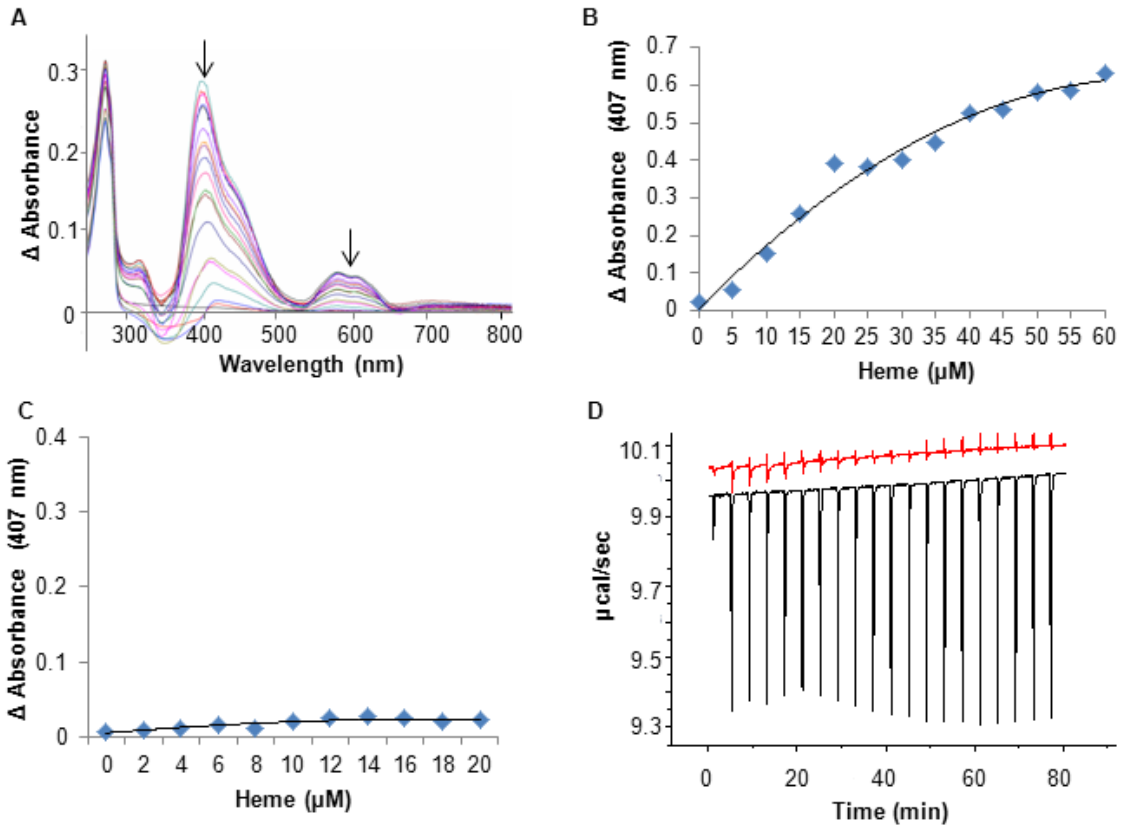

Figure 2.16 Recombinant *Cig1::GST* binds to heme. (A) Absorbance spectra of *Cig1::GST* and heme after addition of increasing amounts of heme (0 to 60 μM) to purified *Cig1::GST* (5 μM). The difference between the absorbance of the Cig1-heme complex and free heme at different heme concentrations is plotted against the measured wavelengths. The arrows represent the Soret peak as well as β- and α-peaks, respectively. (B) Heme binding curve of *Cig1::GST*. The difference between the absorbance of the Cig1-heme complex and free heme at 407 nm is plotted against the increasing concentration of heme. (C) Heme binding curve of *GST*. The difference between the absorbance of the *GST*-heme complex and free heme at 407 nm is plotted against the increasing concentration of heme. (D) Binding of heme to *Cig1::GST*. ITC of heme alone (red) or *Cig1::GST* plus heme (black) over the specified period of time. All assays were repeated three times and representative graphs are shown. Figure reproduced and modified from Cadieux *et al.* (2013).

2.3.8. Identification of other potential heme-binding proteins in *C. neoformans*

The previous experiments described above demonstrated an interaction between Cig1 and heme. However, fusion proteins were used in these experiments and the addition of detectable tags could have modified the conformation of Cig1 and its ability to interact with other molecules, including heme. Therefore, culture supernatants containing the wild-type Cig1

protein were used to further examine the potential for Cig1 to bind heme. Wild-type cells were grown for four days in LI-YNB, alone or supplemented with $FeCl_3$, and a pull-down experiment using heme-agarose beads (as described in Section 2.3.7.) was performed with the concentrated culture supernatants. The eluted proteins were trypsinized and analyzed by tandem MS. A pull-down with agarose beads without the heme ligand was also performed in parallel to identify and eliminate any proteins which interact non-specifically with the beads. The raw data including the list of all proteins detected by MS from two independent replicates are presented in Appendix C. Upon data analysis, any proteins from supernatants of cells grown in either LI-YNB alone or in LI-YNB supplemented with $FeCl_3$, and identified to bind to sepharose beads were removed from the list of potential heme-binding proteins. The thirty most abundant proteins (as determined by the MS score), which were found to bind only to the heme-agarose beads, are listed in Table 2.4.

Cig1 was routinely detected as a heme-binding protein in culture supernatants of cells grown in LI-YNB but not in LI-YNB + $FeCl_3$, which is consistent with the strong iron regulation of Cig1 observed throughout this study with the *HA::Cig1* strain. Additionally, Cig1 did not bind to the sepharose beads indicating that the interaction was specific to heme. The MS data support the conclusion that wild-type Cig1 binds to heme-agarose beads. It also confirms the extracellular localization of Cig1 that was previously determined with the cells expressing the *HA::Cig1* fusion protein. Another interesting putative heme-binding protein listed in Table 2.4 is the predicted transmembrane receptor (CNAG_03524). Although it was not detected at a very high abundance, it could be a receptor involved in heme uptake. Also, like Cig1, it was only detected in supernatants from cells grown in LI-YNB but not in LI-YNB + $FeCl_3$, suggesting that the expression of this protein is iron-regulated. The common regulation of the putative

transmembrane receptor and Cig1 raises the possibility of both proteins being part of the same pathway. Future work will be needed to determine if this candidate transmembrane receptor plays a role in heme utilization.

During the MS analysis, other putative heme-binding proteins were also identified (Table 2.4 and Appendix C). Functions related to polysaccharide and carbohydrate metabolism emerged as common themes among the list of proteins detected. It is possible that the over-representation of these categories is due to the cells having been grown in low carbohydrate concentrations (i.e., 0.5% glucose). In such conditions, the cells could compensate by increasing the expression of genes involved in metabolizing carbohydrates or in breaking down complex carbohydrates/polysaccharides for eventual use. Although the data suggest that these proteins involved in carbohydrate metabolism might also be heme-binding proteins, it does not necessarily indicate a role for these proteins in heme utilization. Further work will be needed to determine if the proteins listed below play a role in heme acquisition and to confirm their interaction with heme.

Lastly, enzymes involved in virulence of *C. neoformans* have also been identified as secreted putative heme-binding proteins, such as laccase, phospholipase B, acid phosphatase, and superoxide dismutase. However, it is unclear whether these proteins directly interact with heme or if they are involved in heme acquisition and, therefore, future work will be required.

Table 2.4. Potential secreted heme-binding proteins

Accession	Description	Score	$FeCl_3$ in medium
CNAG_01239	chitin deacetylase	1004.92	-
CNAG_02030	glyoxal oxidase	773.78	+/- $FeCl_3$
CNAG_00407	glyoxal oxidase	575.23	+/- $FeCl_3$
CNAG_01854	heparinase II/III family protein	574.18	-
CNAG_06501	1,3-beta-glucanosyltransferase	510.53	+/- $FeCl_3$
CNAG_03465	laccase	497.78	-
CNAG_02860	endo-1,3(4)-beta-glucanase	379.03	+/- $FeCl_3$
CNAG_06081	glucose oxidase	315.21	+/- $FeCl_3$
CNAG_04373	alginate lyase	305.52	+/- $FeCl_3$
CNAG_06291	deacetylase	302.52	-
CNAG_01653	cytokine inducing-glycoprotein	298.55	-
CNAG_06835	glucosidase	243.33	-
CNAG_02966	carboxypeptidase D	224.07	-
CNAG_05138	exo-beta-1,3-glucanase	212.26	-
CNAG_03525	trehalase	199.52	+/- $FeCl_3$
CNAG_00799	cellulase	181.56	+/- $FeCl_3$
CNAG_00919	carboxypeptidase D	179.72	-
CNAG_00150	peptidase	178.36	-
CNAG_05799	chitin deacetylase	177.47	+/- $FeCl_3$
CNAG_02189	alpha-amylase	171.95	+/- $FeCl_3$
CNAG_00587	conserved hypothetical protein	152.94	+
CNAG_06085	secreted phospholipase B	120.49	+/- $FeCl_3$
CNAG_04524	zinc metalloprotease	120.28	-
CNAG_00250	conserved hypothetical protein	119.81	-
CNAG_01405	conserved hypothetical protein	108.08	-
CNAG_02850	glucan endo-1,3-alpha-glucosidase agn1	107.75	+/- $FeCl_3$
CNAG_03120	alpha-1,3-glucan synthase	106.72	-
CNAG_05471	alpha-glucosidase	98.04	-
CNAG_03524	transmembrane receptor	90.30	-
CNAG_01562	conserved hypothetical protein	89.51	-

The score reflects how well the observed MS spectra matched to the amino acid sequence of the protein. A higher score indicates a more confident match. The score can also be used as a measure of protein abundance.

2.3.9. Cig1 is required for the full virulence of *C. neoformans*

The virulence of the *cig1Δ* mutant was compared to that of the wild-type and complemented strains using a mouse inhalation model of cryptococcosis. The *cig1Δ* mutant was as virulent as the wild-type and complemented strains, and 100% of the mice exhibited symptoms of cryptococcosis and were euthanized by 23 days post-infection (Figure 2.17). This is likely because the cryptococcal cells are still able to utilize other iron sources besides heme, such as transferrin, which are available within the animal host. In addition, there may be multiple mechanisms of heme utilization. The virulence of the *cfo1Δ* and *cig1Δ cfo1Δ* mutants was also compared to further examine the role of Cig1 during infection. As previously reported, the *cfo1Δ* mutant was attenuated for virulence and the mice survived up to 35 days post-infection (Jung *et al.*, 2009). Interestingly, the *cig1Δ cfo1Δ* mutant was more severely attenuated for virulence than the *cfo1Δ* mutant, with two of the ten mice still not showing symptoms by the end of the experiment (day 60). These results imply that Cig1 plays an important role in iron acquisition and virulence in the host in absence of the high-affinity iron uptake system or possibly when the iron sources acquired by the high-affinity iron uptake system are not available.

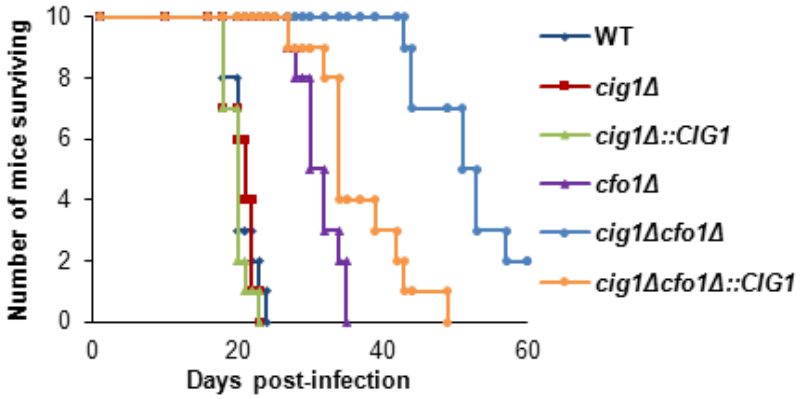

Figure 2.17 *CIG1* is required for virulence in absence of *CFO1*. Ten female A/JCr mice were inoculated intranasally with each of the *C. neoformans* strains indicated. The survival of the mice was monitored daily up to 60 days. Statistical analysis was performed by log rank tests. The difference in survival between the wild-type strain and the *cfo1Δ* or *cig1Δ cfo1Δ* mutants was significant (P<0.0001). Additionally, the difference between the *cfo1Δ* mutant and the *cig1Δ cfo1Δ* mutant was significant (P<0.0001). Figure reproduced and modified from Cadieux *et al.* (2013).

The distribution of fungal cells in different tissues of the infected mice was examined to determine the ability of the *cig1Δ* mutant to colonize host tissue. The lungs and brains of the infected mice were collected when the mice reached the endpoint and the fungal burden was measured by determining the CFU (Figure 2.18). The wild-type, mutant and complemented strains were all equally abundant in the lungs. In addition, the wild-type, *cig1Δ* mutant and complemented strains were all capable of dissemination to the brain and the fungal burden was comparable for all these strains. However, the number of fungal cells in the brain was much lower for the *cfo1Δ* mutant as previously reported (Jung *et al.*, 2009). Additionally, the *cig1Δ cfo1Δ* and *cig1Δ cfo1Δ::CIG1* strains showed similar results to the *cfo1Δ* mutant and no specific contribution of Cig1 in the colonization of these organs was noted. Together, these results suggest that heme may not be the primary source of iron for *C. neoformans* in the mice lungs and brain, and that alternate sources of iron may be preferred in these host tissues.

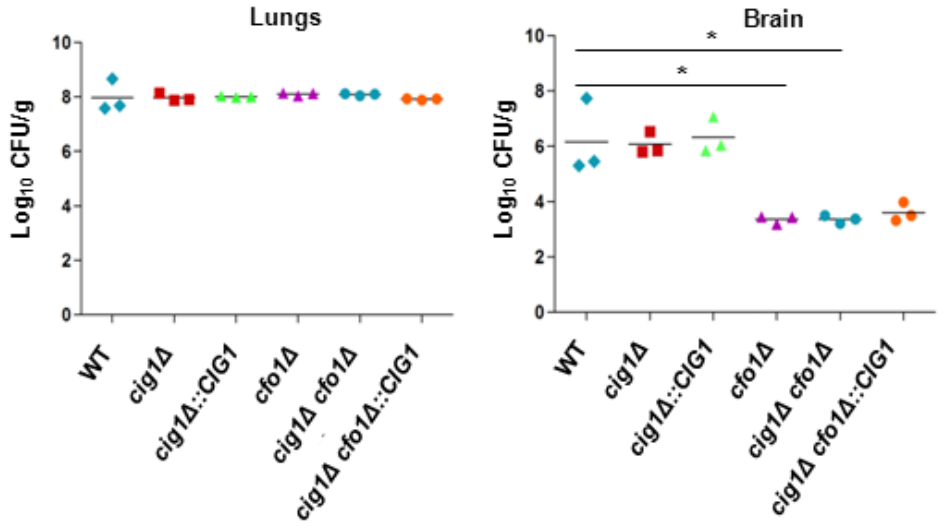

Figure 2.18 Determination of fungal loads in mice tissue. The fungal burden in the lungs and brain of three mice from each group was determined by counting the CFU. The organs were collected at the endpoint, homogenized and the cells were plated onto YPD + 35 µg/mL chloramphenicol. Statistical analysis was performed using an unpaired, two-tailed *t* test. The * represents significant differences with a $P < 0.05$. Figure reproduced and modified from Cadieux *et al.* (2013).

2.4. Discussion

C. neoformans uses heme as a sole iron source although the mechanisms of heme uptake and processing have not been characterized in this pathogen (Jung *et al.*, 2008). In this study, the mannoprotein Cig1, but not Cig2 nor Cig3, was identified as a component of a novel heme uptake mechanism as demonstrated by 1) the extended lag phase of a *cig1Δ* mutant in presence of heme as a sole iron source; 2) the reduced susceptibility to Ga-PPIX and Mn-PPIX that require a heme uptake system for toxicity and; 3) heme binding by a recombinant *Cig1::GST* fusion protein, by an *HA::Cig1* fusion protein associated with extracellular vesicles and by native Cig1 as detected by MS. Heme uptake systems have been well studied in pathogenic bacteria and they generally involve heme-binding cell surface receptors that bind heme with high affinity. Heme is then either transferred between binding domains of multiple surface proteins to a membrane transporter for internalization in the case of Gram-positive bacteria or transferred directly to the membrane transporter in Gram-negative bacteria (Braun, 2001; Nobles and Maresso, 2011). Once inside the cell, heme is degraded and iron is released into the cytoplasm. Some bacteria also secrete heme-binding proteins (hemophores) to the extracellular space to scavenge heme or extract heme from the host heme proteins and return it to the cell surface receptors (Cescau *et al.*, 2007; Wandersman and Delepelaire, 2012). Cig1 was confirmed to be localized at the cell surface, secreted in the extracellular space and associated with extracellular vesicles, and therefore, Cig1 might fulfill a similar role as a hemophore or heme-interacting surface protein for *C. neoformans.*

Other pathogenic fungi, including *C. albicans*, and *H. capsulatum*, are also capable of utilizing heme and/or hemoglobin as an iron source, although little is known about the key players and the mechanisms involved in uptake (Foster, 2002; Santos *et al.*, 2003). For example,

Rbt5 and Rbt51 were identified as receptors for heme and hemoglobin and were localized at the plasma membrane in *C. albicans* (Weissman and Kornitzer, 2004). Rbt5 and Rbt51 are both mannoproteins and the expression of *RBT5* is strongly induced by iron starvation. Similar to the results presented in this study, deletion of *RBT5* significantly reduced the ability of *C. albicans* to use iron from heme. Weissman *et al.* (2008) later identified the ESCRT pathway as a possible endocytic mechanism for hemoglobin uptake in *C. albicans* and they showed that hemoglobin bound to Rbt5 was endocytosed into the vacuole. Presumably, Cig1 may also deliver heme to the cell surface of *C. neoformans* for subsequent internalization.

Deletion of *CIG1* resulted in an extended lag phase but eventual growth to a density comparable to that of the wild-type strain. It is possible that heme contains some contaminating inorganic iron that could be taken up by the high-affinity iron uptake system encoded by the permease Cft1 and the ferroxidase Cfo1 (Jung *et al.* 2008; 2009). This idea is supported by the fact that the double mutant, *cig1Δ cfo1Δ*, grew slightly slower than the *cig1Δ* single mutant, although the difference in growth was not dramatic. An alternative explanation is that one or more additional mechanism(s) for heme use could eventually be activated to compensate for loss of the Cig1 pathway.

Non-iron MPs (e.g., Ga-PPIX and Mn-PPIX) are toxic heme analogs that are taken into bacterial cells via heme uptake pathways (Stojiljkovic *et al.*, 1999). Enzymes that use heme as a co-factor can insert Ga-PPIX in their catalytic centers instead of heme resulting in inactivity because gallium is not able to undergo the same redox reactions as iron. Additionally, non-iron MP may stimulate production of reactive oxygen radicals leading to toxicity (Stojiljkovic *et al.*, 1999). The toxicity of Ga-PPIX and Mn-PPIX for the wild-type strain but not the *cig1Δ* mutant supports a role for Cig1 in heme uptake. This phenotype was only apparent when cells were

forced to use heme as the sole iron source. Interestingly, the *cig1Δ* mutant was able to grow in LIM supplemented with heme as a sole iron source in the presence of Ga-PPIX perhaps because of some residual iron reserves (i.e., the cells were not pre-starved for iron). Moreover, as mentioned earlier, there may be a small amount of free iron contaminating the heme and/or the agarose in the medium to support some growth. The growth defect of the *cig1Δ cfo1Δ* mutant in LIM supplemented with heme partially supports this explanation although a separate mechanism for growth in LIM supplemented with heme may be present. In this case, the additional system may allow heme utilization in the absence of uptake (e.g., by surface reduction and/or extraction of the iron for uptake via the high-affinity system) and therefore not promote non-iron MP susceptibility. The growth defect of the *cig1Δ cfo1Δ* mutant in LIM supplemented with heme supports this hypothesis.

Cig1 was observed to be localized at the cell surface and in association with the extracellular vesicles produced by *C. neoformans*. A strain expressing *HA*-tagged Cig1 protein was used in the experiments performed to study the localization of Cig1. Although the *HA::Cig1* strain was valuable, the results should be interpreted carefully as the expression of *HA::Cig1* did not functionally complement for the loss of *CIG1*. This is most likely due to the presence of the *HA* tag which could prevent proper folding of the *HA::C*ig1 protein, alter its conformation and/or interfere with its function. However, as seen by immunofluorescence microscopy, the *HA::Cig1* is secreted to the cell surface and outside the cell as would be expected for the wild-type Cig1 protein. These observations confirm the findings of Biondo *et al.* (2006), which identified Cig1 as a secreted protein found in the culture supernatant of *C. neoformans*. Additionally, the MS data presented in this study, as well as other MS work done by J. Geddes (personal communications) provide further evidence for the extracellular localization of the wild-type Cig1

protein as it was consistently detected in the culture supernatant of wild-type cells grown in low iron conditions.

A pull-down experiment with heme-agarose beads identified *HA*-tagged Cig1 as a potential heme-binding protein. It is important to note that heme is a hydrophobic molecule and therefore, some of the binding observed could be a result of non-specific interactions rather than heme binding. Specifically, using the extracellular vesicles as starting material could have led to non-specific interactions between the hydrophobic heme ligand and the membranes or lipids in the vesicles. However, binding of Cig1 to the heme-agarose beads was also detected when purified recombinant *Cig1::GST* protein from *E. coli* or wild-type Cig1 protein from concentrated culture supernatants of *C. neoformans* were used as starting material which provides added confidence in the results. Nonetheless, the interaction between Cig1 and heme was investigated further.

Cig1 was demonstrated to bind heme as detected by spectrophotometric titration and ITC using *Cig1::GST* protein from *E. coli*. The absorbance spectra showed the appearance of distinct peaks in the soret, alpha and beta band areas characteristic of a heme-binding protein. Determination of the K_d was not possible because the heme binding curve of Cig1 yielded multiple inflection points and saturation of the binding interaction was not detected, even when more than 10 molar excess of heme was added to protein. Similar cases have been reported in the literature. For example, the heme-binding protein in rabbit has been reported to bind a 25-35 molar excess of heme (Tsutsui and Mueller, 1982b). It has also been reported that the IsdX2 protein isolated from *B. anthracis* required 20 times more heme to protein ratio to reach saturation and that multiple inflection points were detected (Maresso *et al.*, 2008). It is also possible that the lack of saturation is caused by weak binding or even non-specific binding and

that heme could potentially bind to the Cig1 protein at multiple sites on the protein. Alternatively, expressing the *Cig1::GST* protein in *E. coli*, where post-translational modifications such as glycosylation do not occur, could alter the activity of the protein. Glycosylation of proteins plays an important role in their function. For example, glycosylation of a receptor involved in regulating natural killer cell responses has been shown to be required for binding to its ligands (Margraf-Schonfeld *et al.*, 2011). Also, ablation of N-glycosylation of a plant peroxidase by site-directed mutagenesis influenced the folding of the protein, its thermostability and its catalytic ability (Lige *et al.*, 2001). Finally, the presence of the *GST* tag may have altered the conformation of Cig1 or decreased the affinity of the protein for heme. Further work will be needed to fully understand the heme-binding activity of Cig1.

Many heme-binding proteins contain one or multiple conserved heme-binding domains, such as the NEAT domains found in bacteria or possibly the CFEM domains found in the heme receptors from *C. albicans* (Andrade *et al.*, 2002; Grigg *et al.*, 2007; Weissman and Kornitzer, 2004). No conserved heme-binding domains were identified for Cig1 although a chitin-binding fold and a putative immunoglobulin-like β-sandwich fold were detected. It is possible that the chitin-binding fold may be involved in heme binding. For example, the dopamine β-monooxygenase N-terminal (DOMON) domains have been described in several secreted, or cell surface proteins from plants and animals (Aravind, 2001; Ponting, 2001; Lakshminarayan *et al.*, 2007). These DOMON domains are rich in β-strands, adopt a β-sandwich-like fold, and have been shown to be involved in ligand binding, either as heme- or sugar- binding domains (Lakshminarayan *et al.*, 2007). Alternatively, the immunoglobulin-like β-sandwich fold could also participate in heme binding. In fact, one of the two main regions that mediate heme binding, specificity in ligand and transfer functions within the NEAT domains contains an

immunoglobulin-like fold. This fold has been demonstrated to be the platform where the heme molecule sits once it is bound to the NEAT domain (Grigg *et al.*, 2007; Sharp *et al.*, 2007; Watanabe *et al.*, 2008; Honsa and Maresso, 2011; Nobles and Maresso, 2011). The overlapping predicted chitin-binding and immunoglobulin-like folds will be a good starting point to identify the heme-binding domain (s) of Cig1 in future studies.

Interestingly, a general theme of carbohydrate metabolism was revealed during the MS analysis. It is possible that carbohydrate metabolism was over-represented because the cells were grown in low glucose conditions. The proteins (mostly enzymes) identified were found to be secreted in the culture supernatant and to bind to the heme-agarose beads, however, they might not necessarily be involved in heme utilization. The interaction between the proteins and the beads could be non-specific due to the hydrophobic nature of heme, as discussed above. It is also possible that the proteins identified do not bind directly to the heme-agarose beads but bind to other proteins or to secreted polysaccharides that bind to heme. Nonetheless, a link between carbohydrate metabolism and heme uptake may exist. Specifically, the data from this study suggest that Cig1 is a heme-binding protein involved in heme acquisition, and although no known heme-binding domains were found in the Cig1 protein sequence, a fold similar to that of the chitin-binding domain was identified. Another example supporting the link between iron uptake and carbohydrate metabolism was reported in *S. cerevisiae*, where iron limitation resulted in metabolic rearrangement and increased glycerol production (Ansell and Adler, 1999). Finally, kinetic studies of a cellobiose oxidase, an enzyme involved in the break-down of cellobiose, revealed that the protein functions primarily as a ferric reductase in the white-rot fungus *Phanerochaete chrysosporium* (Kremer and Wood, 1992).

Other putative secreted heme-binding proteins identified by the MS analysis involved enzymes that play a role in virulence of *C. neoformans*, including laccase, phospholipase B, acid phosphatase, and superoxide dismutase (Rodrigues *et al.*, 2008a). These proteins have been associated with the extracellular vesicles produced by *C. neoformans* which could explain their presence in the culture supernatants (Rodrigues *et al.* 2008a). It is also possible that the extracellular vesicles, which would remain intact in the concentrated culture supernatants, bind to the heme-agarose beads via Cig1, or another heme-binding protein. Alternatively, the vesicular membranes could bind non-specifically to the hydrophobic heme ligand of the agarose beads. In either case, the vesicles would be found among the eluted proteins, and the cargo proteins transported within the extracellular vesicles would be released upon heating of the samples prior to gel electrophoresis. Overall, future work will be required to determine if the proteins identified by MS analysis play a role in heme acquisition and to further understand their interaction with heme.

The role of Cig1 in virulence reflects a growing appreciation for the multiple mechanisms of iron acquisition by *C. neoformans*. That is, deletion of *CIG1* alone did not attenuate virulence in a mouse model of cryptococcosis but deletion of both *CIG1* and *CFO1* resulted in significant attenuation of virulence beyond that observed with deletion of *CFO1* alone. Thus, the influence of Cig1 is evident only in the absence of the high-affinity iron uptake system (Cft1/Cfo1). Jung *et al.* (2008) reported that transferrin and heme are potential host-derived iron sources for *C. neoformans*, but it is not known whether the fungus preferentially uses one source or the other *in vivo*, and whether there are niche-specific sources and preferences. The results presented here support the conclusion that *C. neoformans* uses both iron sources to proliferate in mammalian hosts. Similar results were found in *C. albicans*, where only deletion of the iron permease,

CaFTR1, of the high-affinity iron uptake system has been shown to play a role in virulence (Ramanan and Wang, 2000). Deletion of the heme receptor Rbt5 did not reveal a role in virulence although a *rbt5Δ* mutation was not tested in the *Caftr1Δ* mutant background (Braun *et al.*, 2000).

In summary, Cig1 was identified as a component of a novel heme uptake system in the fungal pathogen *C. neoformans*, and Cig1 was hypothesized to act as a heme receptor, a transporter at the cell surface or a hemophore that scavenges heme in the extracellular environment. Further investigation will be needed to develop a more detailed understanding of the Cig1-mediated mechanism of heme uptake and to investigate the additional heme uptake mechanism(s) revealed by the characterization of Cig1.

Chapter 3. Further characterization of heme uptake in *C. neoformans*

3.1. Introduction

The work presented in Chapter 2 identified Cig1 as a major player in heme acquisition in *C. neoformans*. However, given enough time, the *cig1Δ* mutant cells were eventually able to grow in LIM supplemented with heme as a sole iron source. This observation led to the hypothesis that *C. neoformans* may have more than one pathway for heme utilization and that a Cig1-independent pathway may be required for heme acquisition in absence of Cig1. The study presented in this chapter focuses on examining various factors that are potentially involved in Cig1-independent heme utilization, including pH, the pH regulator Rim101, and cell density.

The solubility and bioavailability of iron is dependent on pH. For example, at neutral and alkaline pH, iron is mostly found in its ferric state (Fe^{3+}) and is insoluble, making it less available to *C. neoformans* (Wilkins, 1991; Cotton *et al.*, 1999). Transition between ferric iron (Fe^{3+}) and ferrous iron (Fe^{2+}) is pH-dependent, and therefore, iron is more soluble and more readily available at acidic pH. Given the effect of pH on iron bioavailability, changes in pH could contribute to eventual heme utilization by the *cig1Δ* mutant cells.

Rim101 is the master regulator of the pH response and is highly conserved in many fungal species (Tilburn *et al.*, 1995; MacCabe *et al.*, 1996; Ramon *et al.*, 1999; Lamb and Mitchell, 2003). A recent study identified Rim101 as a regulator of iron homeostasis in *C. neoformans* (O'Meara *et al.*, 2010). Specifically, Rim101 was found to regulate the expression of *CIG1* and the *CIG1* transcript was more than 400-fold lower in the *rim101Δ* mutant compared to wild-type cells, implying a probable functional link between Rim101 and Cig1 with regard to heme use. Additionally, Rim101 regulated the expression of the siderophore iron transporter

(*SIT1*), and the ferric permease (*CFT1*) involved in the reductive high-affinity iron uptake pathway. Therefore, it is possible that Rim101 also regulates Cig1-independent heme uptake.

Finally, the long lag phase of the *cig1Δ* mutant when grown in LIM supplemented with heme suggested that cell density and a quorum sensing (QS)-like mechanism could be required for Cig1-independent heme acquisition. Microbial cells often monitor the cell density of the population by releasing and receiving signaling molecules and thereby coordinating the population's behaviour in order to adapt to an array of different and sometimes hostile environments (Bassler, 2002; Joint *et al.*, 2007; Williams, 2007; Albuquerque and Casadevall, 2012). The secreted signals are usually small molecules and their concentration increases with the population size. Once the concentration surpasses a certain threshold, it induces the cells to cooperate in diverse behaviours, including uptake of nutrients, growth, biofilm formation, and elaboration of virulence factors.

To test the hypothesis that *C. neoformans* evolved more than one pathway for heme utilization, this study examined potential factors contributing to Cig1-independent heme uptake. Specifically, the role of pH in heme acquisition and the link between the pH regulator Rim101 and heme utilization were evaluated. The effect of cell density on growth in LIM supplemented with heme was also tested and preliminary identification of a QS-like molecule was attempted.

3.2. Materials and Methods

3.2.1. Strains and growth conditions

All strains used in this study are listed in Table 3.1. LIM was prepared as described (Vartivarian *et al.*, 1993) and the pH was adjusted to 7.2, unless specified otherwise. The water used for LIM was treated with Chelex-100 resin (Bio-Rad) to chelate iron. Cells for growth assays were pre-grown overnight at 30°C with shaking in YPD (Fisher). The cells were then washed twice with low iron water, inoculated into LIM at 4×10^6 cells/mL and grown at 30°C for two days to starve the cells for iron. These cells are designated as pre-starved cells throughout this chapter. After starvation, the cells were harvested, washed and inoculated in LIM alone or supplemented with heme (porcine hemin; Sigma) or $FeCl_3$ (Sigma) to a final concentration of 5×10^4 cells/mL, unless specified otherwise. Cultures were incubated at 30°C and growth was monitored by measuring the optical density at 600 nm using a DU530 Life Science UV/Visible spectrophotometer (Beckman Instruments). The pH of the culture supernatant was measured at specific time points using an Orion 2-star pH meter (Thermo Scientific) and the Orion Ross combination pH electrode (Thermo Scientific). To examine growth on solid media, iron-starved cells were diluted to 1×10^6 cells/mL in low iron water. Ten-fold serial dilutions were made in low iron water and 5 µl of each dilution was plated on LIM alone or supplemented with heme or $FeCl_3$. Agarose (1%, Invitrogen) was added as a solidifying agent. Plates were incubated for three days at 30°C and then photographed.

Table 3.1. Strains used in this study

Strain	Description	Provided by/ Prepared by
H99	*C. neoformans* wild-type strain	Dr. Joseph Heitman
cig1Δ	*cig1* disruption mutant	Carmelo Biondo
cig1Δ +CIG1	*CIG1* complemented strain	Tian Lian
cfo1Δ	*cfo1* deletion mutant	Dr. Wonhee Jung
cig1Δ cfo1Δ	*cig1 cfo1* double deletion mutant	Brigitte Cadieux
cig1Δ cfo1Δ +CIG1	*CIG1* complemented in *cig1Δ cfo1Δ* background	Brigitte Cadieux
rim101Δ	*rim101* deletion mutant	Dr. J. Andrew Alspaugh
rim101Δ +RIM101	*RIM101* complemented strain	Dr. J. Andrew Alspaugh
*GAL7p::CIG1*in *rim101Δ*	Regulated *CIG1* in *rim101* deletion mutant background	Brigitte Cadieux
*GAL7p::CIG1*in H99	Regulated *CIG1* in H99 background	Brigitte Cadieux
cas1Δ	*cas1* deletion mutant	Dr. Emma Griffiths
cap59Δ	*cap59* deletion mutant	Dr. Jennifer Lodge
B3501A	*C. neoformans* var. *neoformans* (serotype D) wild-type strain	Dr. June Kwon-Chung
cqs1Δ	*cqs1* deletion mutant (serotype D)	Dr. June Kwon-Chung

3.2.2. Construction of strains

Primers used for construction of all strains are listed in Table 3.2.

Table 3.2. Primers used for strain construction

Allele constructed	Primer identification	Primer sequence
GAL7p::CIG1	Cig1A-6	ATTCACTGGATCCGTCGGTA
	Gal7-Cig1-LA-R	CTTCCGTGTTAATACAGATAAACCGAGATGAAA ATGTAAAGCTGTCG
	Gal7-Cig1-RA-F2	GCACTCAATTCTCTCCTGAGAATGATTTTTAATC GTTTCACATTC
	Gal7-Cig1-RA-R	TACAGGAGAAGTCATACAAAGCAT
	Gal7-Cig1-F	CGACAGCTTTACATTTTCATCTCGGTTTATCTGT ATTAACACGGAAG
	Gal7-Cig1-R	GAATGTGAAACGATTAAAAATCATGCACTCAAT TCTCTCCTGAGA
	Gal7-Cig1-PO-F	GCCATTATTGTTTCCCGATG
	Gal7-Cig1-PO-R	TCAGGATCTTCATGGCTCCT

3.2.2.1. Construction of the galactose-regulated *CIG1* strains

The *GAL7p::NAT::CIG1* allele was constructed by overlap PCR using the methods described by Davidson *et al.* (2002) and Yu (2004). The sequence upstream of the 5' end of the *CIG1* gene was amplified from genomic DNA from strain H99 with primers Cig1A-6 and Gal7-Cig1-LA-R, and the *CIG1* open reading frame was amplified with primers Gal7-Cig1-RA-F2 and Gal7-Cig1-RA-R. The *NAT::GAL7p* allele was amplified from strain *GAL7p::PKA1* kindly provided by Dr. J. Choi (Choi *et al.*, 2012) with primers Gal7-Cig1-F and Gal7-Cig1-R. The primers Cig1A-6 and Gal7-Cig1-RA-R were then used to overlap the three products to yield the 4.5 kb *GAL7p::NAT::CIG1* allele. The construct was introduced into the *C. neoformans* serotype A strain H99 and the *rim101Δ* strain kindly provided by Dr. J. A. Alspaugh (Duke University, Durham, NC, U.S.A.; O'Meara *et al.*, 2011) by biolistic transformation to generate the *GAL7p::CIG1* regulated strains (Toffaletti *et al.*, 1993). Transformants were screened by colony PCR using primers Gal7-Cig1-PO-F and Gal7-Cig1-PO-R. Transformants in which the wild-type allele was replaced were confirmed by hybridization to genomic DNA blots with a probe amplified from genomic H99 DNA using primers Gal7-Cig1-RA-F2 and Gal7-Cig1-RA-R (Figure 3.1).

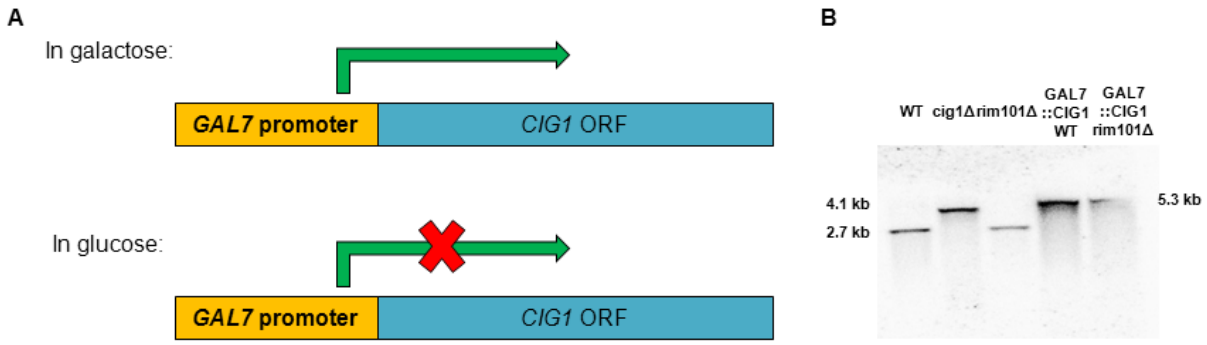

Figure 3.1 Galactose-regulated *CIG1* strains. (A) Diagram of the *GAL7p::NAT::CIG1* construct introduced into the wild-type and *rim101Δ* strains. (B) Southern blot analysis to confirm insertion of the *GAL7* promoter. Genomic DNA of the indicated strains was digested with ScaI and hybridized with the downstream arm of the *GAL7p::NAT::CIG1* construct, which corresponds to the *CIG1* open reading frame.

3.2.3. Quantitative RT-PCR

To examine gene expression, the cells were grown in LIM alone or supplemented with heme for 6 hours at 30°C with shaking. Total RNA was extracted using the RNeasy kit (Qiagen), treated with DNase (Qiagen) and cDNA was synthesized using the SuperScript First Strand System (Invitrogen) following the manufacturers' recommendations. PCR reactions were monitored using the 7500 system (Applied Biosystems) as described previously (Tangen *et al.*, 2007), with primers designed using Primer Express software 3.0 (Applied Biosystems) and are listed in Table 3.3. The relative gene expression was quantified using the SDS software 1.3.1 (Applied Biosystems), based on the $2^{-\Delta\Delta CT}$ method (Livak and Schmittgen, 2001). The average Ct of 18S rRNA was used for normalizing.

Table 3.3. Primers used for quantitative RT-PCR

Primer identification	Primer sequence	Target Gene
CIG1A-RT-F	GGTGGTCCGGTTTCCTTCA	*CIG1*
CIG1A-RT-R	GACTCGTGGTCGTGCATAACA	*CIG1*
18S-RT-F	AACAGGTCTGTGATGCCCTTAGA	18S rRNA
18S-RT-R	ACTCGCTGGCTCAGTCAGTGT	18S rRNA

3.2.4. Aggregate formation

Pre-starved cells were grown in LIM + 10 µM heme and were harvested at the specific time points by centrifugation (13,000 x g for 1 minute). The cells were resuspended in 1/10th volume of LIM, mixed 1:1 in india ink and visualized by negative staining on a Zeiss Axioplan 2 Imaging microscope.

3.2.5. Preparation of conditioned media

Pre-starved cells were inoculated in LIM + 10 µM heme as described above and grown at 30°C with shaking until the cells reached stationary phase. The culture supernatant was harvested by centrifugation (15,000 x g, 15 minutes, 4°C) and filter-sterilized through a 0.45 µm vacuum filter. The conditioned media (CM) was added 1:1 to fresh LIM + 10 µM heme for a final concentration of 50% CM before inoculation for the start of the growth curves.

3.2.6. Isolation of exopolysaccharides

Cells were grown in LIM for seven days at 30°C with shaking. Extracellular polysaccharides were isolated as previously described (Wozniak and Levitz, 2008). Briefly, the culture supernatant was collected by centrifugation (15, 000 x g, 2 minutes, 4°C). The polysaccharides were precipitated by adding 10% sodium acetate and 2.5 volumes of ethanol, and the solution was incubated overnight at room temperature. The supernatant was decanted and the polysaccharides were air dried and dissolved in 1/10th volume of the original culture in low iron water. The polysaccharide concentration was measured by the phenol sulfuric method (Dubois *et al.*, 1951). A fraction of the isolated polysaccharides was treated with 0.1 mg/mL proteinase K (Roche) for 4 hours at 37°C. Another fraction was dialyzed in SnakeSkin dialysis

tubing of 7,000 MWCO (Thermo Scientific) in low iron water at 4°C for 48 hours with two changes of water. All polysaccharide fractions were autoclaved for 10 minutes and 2 mL were added to 20 mL fresh LIM + 10 µM heme prior to inoculating for the start of the growth measurements in liquid cultures.

3.2.7. Absorption Spectrophotometry

Titrations of isolated GXM with heme were monitored by absorption spectroscopy in the Soret range as previously described (Gaudin *et al.*, 2011) to detect heme-binding interactions. Briefly, increasing amounts of heme dissolved in 0.1 M NaOH and diluted in 10 mM phosphate buffer (pH 7.0) were added to 1 mL of 0.2 µM polysaccharides in buffer. The preparation was incubated at room temperature for 5 minutes after adding heme to allow binding before measuring the absorbance spectra. Heme added to buffer without polysaccharides served as a reference. Spectra were measured using a Cary 50 Bio UV-visible spectrophotometer (Agilent Technologies) with an optical path length of 1 cm in a quartz cell. The isolated GXM was kindly provided by Dr. D. de Oliveira and was isolated as described by Nimrichter *et al.*, (2007).

3.2.8. Isothermal titration calorimetry experiments

ITC was performed using a MicroCal iTC_{200} (GE Healthcare). Samples were in 10 mM phosphate buffer (pH 7.0). Titrations were performed by injecting consecutive 2 µL aliquots of heme solution (1-5 mM) into the ITC cell (volume = 200 µL) containing isolated GXM (0.1-0.5 mg/mL). All solutions were degassed at room temperature before loading in the calorimeter. The heat of dilution data were obtained by titrating 2 µL injections of heme solution into

polysaccharide-free buffer. All titrations were performed at 25 °C. ITC experiments were performed by Dr. Louise Creagh.

3.3. Results

3.3.1. Prior adaptation of the *cig1Δ* mutant to growth in LIM supplemented with heme does not alter subsequent growth in presence of this iron source

Over the course of the experiments detailed in Chapter 2, it became increasingly clear that a Cig1-independent heme uptake system existed to allow *C. neoformans* to acquire heme in the absence of Cig1. One possibility is that the *cig1Δ* cells adapt by accumulating compensating mutations or by shifting their metabolism to allow growth in LIM supplemented with heme. Therefore, growth in LIM supplemented with heme was examined after the cells had previously been grown in LIM supplemented with heme to determine if adaptation was the cause of the eventual growth of the *cig1Δ* mutant. The strains were grown in LIM supplemented with heme until the cells reached stationary phase. The cells were then harvested, washed and inoculated in fresh LIM with added heme (Figure 3.2). Interestingly, the growth of the strains did not change whether the cells were previously grown on heme or not. Specifically, the lag phase of the wild-type and complemented strains lasted approximately 24 hours and the strains had reached stationary phase by 48 hours for both cells that were pre-starved for iron and cells that were pre-grown in LIM supplemented with heme. In contrast, the lag phase of the *cig1Δ* mutant lasted approximately 48 hours and the stationary phase was reached by 72 hours. Again, this was the same for the *cig1Δ* cells that had been pre-starved or pre-grown in LIM supplemented with heme. Although these results do not necessarily preclude adaptation of the cells to allow growth in LIM supplemented with heme, they suggest that it is not the major factor involved in heme acquisition via a Cig1-independent pathway.

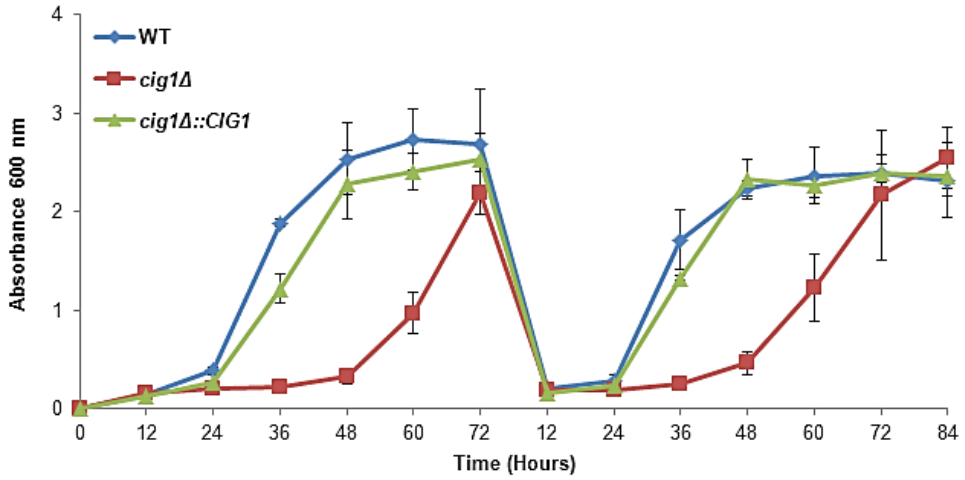

Figure 3.2 Prior adaptation does not rescue the growth defect of the *cig1Δ* mutant in LIM supplemented with heme. Iron-starved cells were grown in LIM + 10 µM heme for 72 hours before being harvested, washed twice in low iron water, and inoculated at 5 x 10^4 cells/mL in fresh LIM + 10 µM heme. Growth was monitored by measuring the optical density at 600 nm. All experiments were repeated three times and the data are plotted as the average ± SD.

3.3.2. The role of Cig1 in heme uptake is pH dependent

In an attempt to characterize the Cig1-independent heme uptake system, the growth of the strains was tested in presence of heme at different pH because pH is known to influence iron availability (Wilkins, 1991; Cotton *et al.*, 1999). Although the *cig1Δ* mutant exhibited a growth defect at pH 7.2, the cells grew as well as the wild-type and complemented strains at pH 5.6 (Figure 3.3A-B). It is possible that the decreased lag phase of the *cig1Δ* mutant at pH 5.6 resulted from iron being released from the heme molecule at this low pH which could thereby be taken up by the cells via an alternate iron uptake pathway, such as the high-affinity iron uptake pathway. A strain lacking *CFO1*, a gene encoding an essential component of the high-affinity iron uptake pathway, was grown in LIM supplemented with heme at both pH levels to test this possibility (Figure 3.3A-B). If iron is released from the heme molecule, one would expect the *cfo1Δ* and/or the *cig1Δ cfo1Δ* mutants to show a growth defect. However, all the cells grew as well as the wild-type strain at pH 5.6 indicating that iron is not released from the heme molecule

in sufficient amounts to influence growth at that pH. As presented in Chapter 2, the *cfo1Δ* mutant grew as well as the wild-type strain at pH 7.2, while the *cig1Δ cfo1Δ* mutant showed a similar growth defect as the *cig1Δ* mutant. Therefore, these results suggest that Cig1 plays an active role in iron acquisition from heme at physiological pH, and that a Cig1-independent system exists to acquire iron from heme at low pH. To examine this hypothesis further, the expression of *CIG1* was tested in cells grown in LIM with and without heme at acidic and physiological pH. The expression of *CIG1* was down-regulated more than five-fold at pH 5.6 compared to pH 7.2, independent of the presence of heme in the culture medium (Figure 3.3C). These results further support a role for Cig1 in heme acquisition at physiological pH, and suggest that another heme utilization system exists to acquire iron from heme in a Cig1-independent manner at low pH.

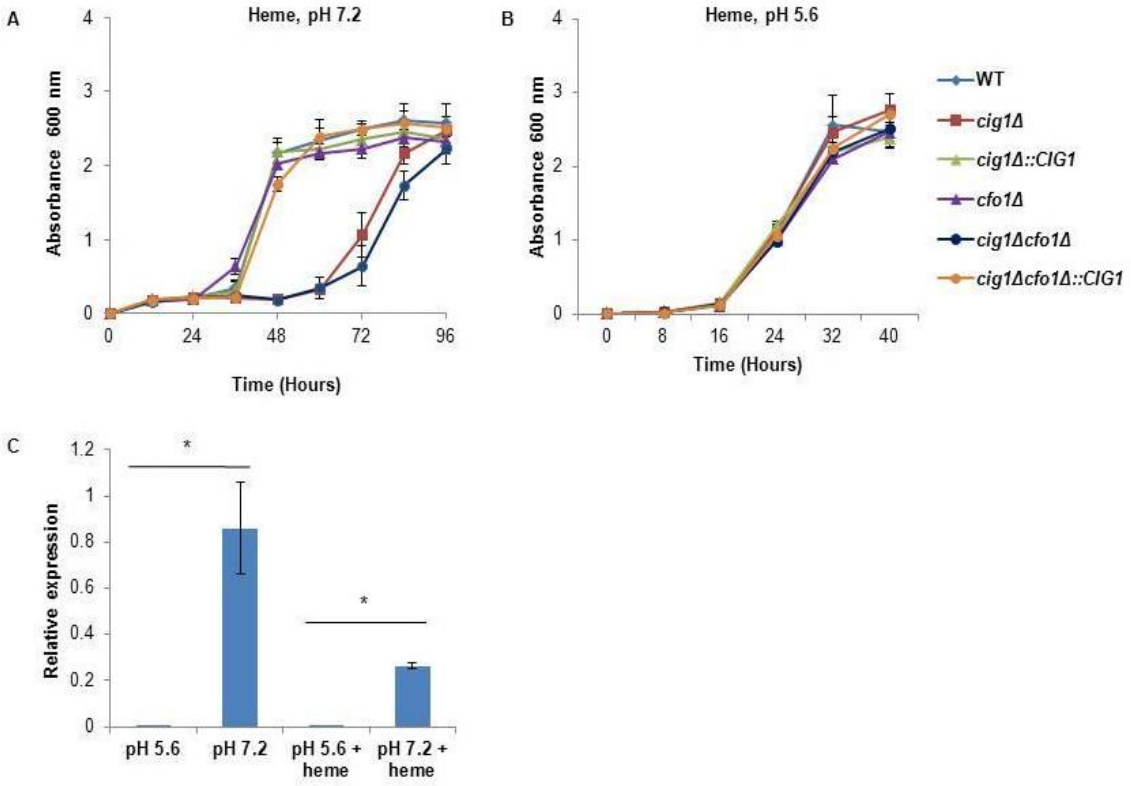

Figure 3.3 Cig1 is not required for growth in LIM supplemented with heme at acidic pH. Growth of iron-starved cells in LIM + 10 µM heme, pH 7.2 (A) and pH 5.6 (B). Growth was monitored by measuring the optical density at 600 nm. (C) Expression of *CIG1* in wild-type cells grown in LIM ± 10 µM heme at pH 5.6 or 7.2. All experiments were repeated three times and the data are plotted as the average ± SD. The * represents significant differences at $P < 0.05$ between pH 7.2 relative to pH 5.6. Figure reproduced and modified from Cadieux *et al.* (2013).

The fact that the *cig1Δ* mutant grew as well as the wild-type strain in LIM supplemented with heme at pH 5.6, suggested that a change in pH might explain the eventual growth of the *cig1Δ* mutant after the extended lag phase at physiological pH. Therefore, the pH of the culture supernatant during growth in LIM supplemented with heme was measured (Figure 3.4A). All the cultures showed a similar trend, that is an increase in pH (up to 8.2-8.3) during the first 24 hours, followed by a decrease in pH (down to 7.5) once the cells reached the exponential growth phase and another increase in pH (up to 7.9-8.3) when the cells reached stationary phase. The *cig1Δ* mutant remained at an elevated pH for a longer period, corresponding to the longer lag

phase of this strain when grown under these conditions. It is unclear whether the change in pH was a cause or a result of the growth of the *cig1Δ* mutant cells. Growth of the cells in LIM supplemented with heme was also monitored upon modification of the buffering conditions of the culture medium (Figure 3.4B-D). The *cig1Δ* mutant exhibited a longer lag phase when no buffer was added to LIM, compared to when 20 mM 4-(2-hydroxyethyl)-1-piperazineethanesulfonic acid (HEPES) was added as buffering agent. The wild-type and complemented strains also grew more slowly in the absence of a buffering agent. It is possible that there may be a more dramatic increase in the pH in the first 24 hours of incubation when no buffer is added to the culture medium, and that the high pH results in decreasing the heme availability. Alternatively, the observed spike in pH could also be inhibitory for growth of the cells when it is not buffered. The *cig1Δ* mutant grew as well as the wild-type cells when the concentration of HEPES was increased five-fold (100 mM) from the original level in the buffer (Figure 3.4D). Increasing the concentration of HEPES in the medium increases its buffering capacity and likely maintains the pH of the culture constant throughout the growth of the cells. Consequently, the pH of the medium would not increase in the first 24 hours, and perhaps that shift in pH contributes to the longer lag phase of the *cig1Δ* mutant. For example, the increase in pH might be the signal which induces the expression of the Cig1-mediated heme uptake pathway. Another explanation could be that the pH influences local activities of the cell surface that are involved in heme processing (e.g., enzymes like ferric reductases, as discussed in Chapter 2). Together, these results suggest that the environmental pH is extremely important for heme uptake and that a Cig1-mediated heme uptake pathway plays a major role at physiological pH while a Cig1-independent acquisition pathway must exist for acquisition of heme at acidic pH.

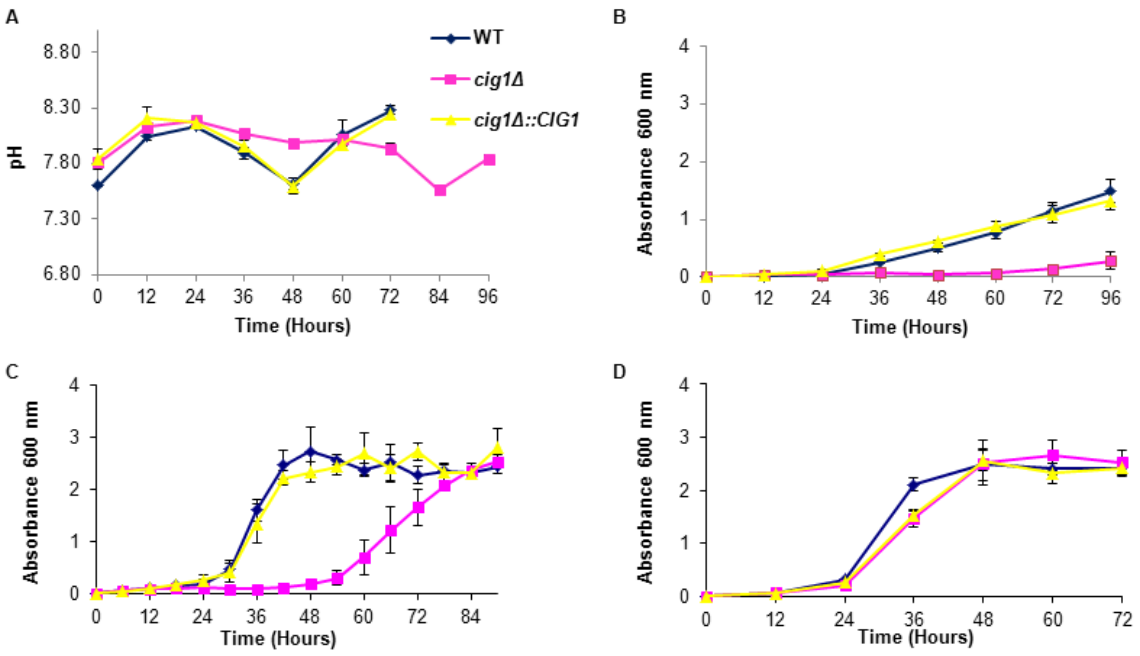

Figure 3.4 The role of Cig1 in heme uptake is highly dependent on pH. pH of the culture medium for iron starved cells grown in LIM + 10 µM heme (A). Growth of iron-starved cells in LIM + 10 µM heme with no added HEPES (B), 20 mM HEPES (C), or 100 mM HEPES (D). Growth was monitored by measuring the optical density at 600 nm. All experiments were repeated three times and the data are plotted as the average ± SD.

3.3.3. Rim101 also contributes to heme acquisition

Given that pH influenced both the expression of *CIG1* and the ability of Cig1 to contribute to heme utilization, the contribution of the pH-regulatory protein Rim101 to growth in LIM supplemented with heme was examined next. Rim101 is a master regulator of the pH response and is highly conserved in many fungal species (Penalva and Arst, 2002; 2004). In addition, Rim101 was shown to positively regulate the expression of *CIG1* and a *C. neoformans rim101Δ* mutant has a growth defect at alkaline pH (O'Meara *et al.*, 2010). Analysis of growth in LIM supplemented with heme revealed that the *rim101Δ* mutant showed an extended lag phase (36 hours) and eventual growth to the wild-type cell density, a phenotype similar to that of the *cig1Δ* mutant (Figure 3.5A). Complementation of the *rim101Δ* mutation restored the wild-

type level of growth in LIM supplemented with heme. These results suggest a role for Rim101 in heme utilization. Next, the expression of *CIG1* was measured in the wild-type and *rim101Δ* strains during growth in LIM supplemented with heme to determine if the regulation of *CIG1* by Rim101 observed by O'Meara *et al.*, (2010) was maintained when the cells were grown in LIM supplemented with heme (Figure 3.5B). As expected, the *CIG1* transcript was down-regulated in the *rim101Δ* mutant compared to the wild-type strain, and this regulation was independent of the growth phase.

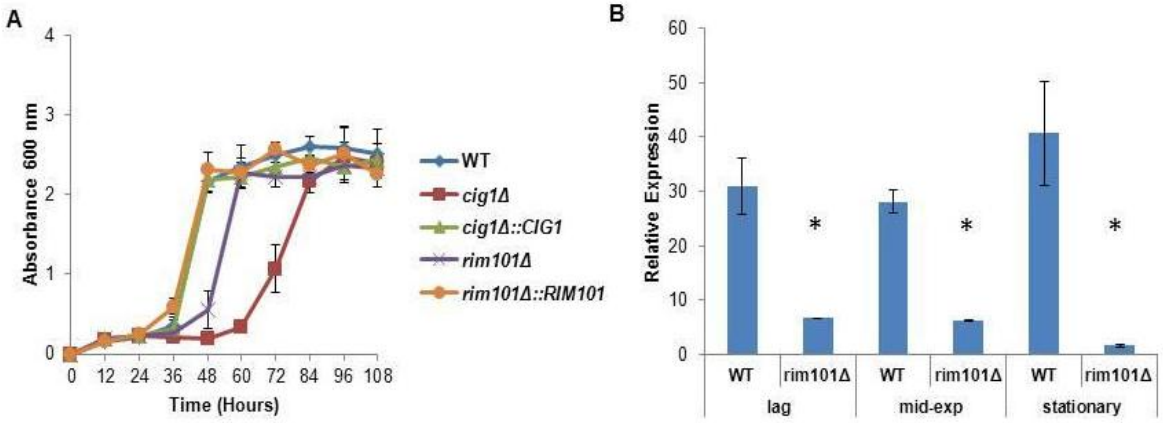

Figure 3.5 Rim101 also contributes to heme utilization. (A) Growth of iron-starved cells in LIM + 10 µM heme was monitored by measuring the optical density at 600 nm. (B) Expression of *CIG1* in the wild-type and *rim101Δ* strains grown in LIM + 10 µM heme. All experiments were repeated three times and the data are plotted as the average ± SD. The * represents significant differences at $P < 0.05$ relative to the wild-type at each stage of growth.

In a separate approach to examine the contribution of Rim101 to growth in LIM supplemented with heme (independent of *CIG1*), the promoter of *CIG1* was replaced with that of the *GAL7* gene, which is galactose inducible and glucose repressible, in the wild-type and *rim101Δ* strains. As expected, *GAL7p::CIG1* in wild-type exhibited a similar growth defect to *cig1Δ* mutant in LIM supplemented with heme in media with glucose (Figure 3.6A), but a wild-type growth pattern on galactose (Figure 3.6B). In contrast, the galactose-inducible *CIG1* strain

in the *rim101Δ* mutant background remained in lag phase significantly longer than either *rim101Δ* or *cig1Δ* when grown in glucose (Figure 3.6A). Although Rim101 regulates the expression of *CIG1* (O'Meara *et al.*, 2010) and may therefore play a role in Cig1-dependent heme utilization, the additive growth defect in the *GAL7p::CIG1 rim101Δ* strain on glucose suggests that Rim101 also plays a role in iron acquisition from heme that is independent of its regulation of *CIG1*. Surprisingly, growth in galactose extended the lag phase of the wild-type and *cig1Δ::CIG1* strains, and particularly exacerbated the growth defect of the *cig1Δ* mutant (Figure 3.6B). The use of galactose as the carbon source also eliminated the growth defect in LIM supplemented with heme for both the *rim101Δ* and *GAL7p::CIG1 rim101Δ* strains relative to wild-type. These results further support the presence of a Cig1-independent mechanism for heme use and suggest an influence of carbon source. That is, galactose may promote the expression of a system to use heme iron that compensates for loss of Rim101. The influence of carbon source on heme acquisition was confirmed by growing the cells in acetate (Figure 3.6C). Utilization of this alternate carbon source resulted in much slower growth for all the strains tested, and the strains that reached stationary phase had a much lower cell density compared to growth of the cells in glucose or galactose. Additionally, the growth defect for the *cig1Δ* and *rim101Δ* mutants, and both *GAL7p::CIG1* strains was severely exacerbated, and the *cig1Δ* and both *GAL7p::CIG1* strains never entered the exponential phase of growth during the course of the experiment. Quantitative RT-PCR analysis of *CIG1* expression confirmed the expected carbon source regulation of the *GAL7p::CIG1* construct and also revealed that growth in galactose reduces expression of *CIG1* relative to growth in glucose (Figure 3.6D). This may explain the extended lag phase in the wild-type and complemented strains on galactose and heme (compare Figures 3.6A and B).

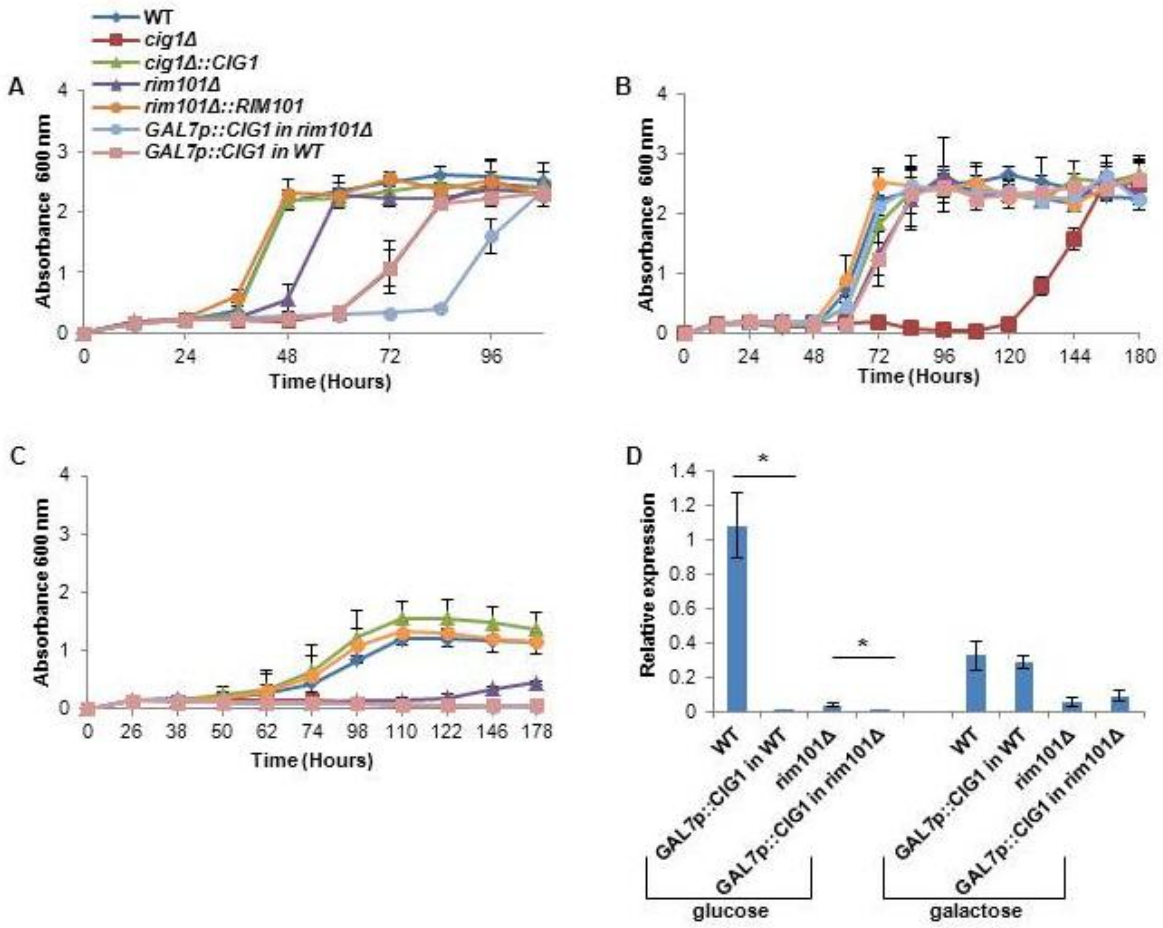

Figure 3.6 Rim101 makes a Cig1-independent contribution to heme uptake. The growth of iron-starved cells in LIM + 10 µM heme is shown for media containing glucose (A), galactose (B), or acetate (C). Growth was monitored by measuring the optical density at 600 nm. (D) Expression of *CIG1* in the wild-type and *rim101Δ* strains and the strains containing a galactose-inducible *CIG1* allele grown in LIM containing glucose or galactose. All experiments were repeated three times and the data are plotted as the average ± SD. The * represents significant differences at $P < 0.05$ in expression of *CIG1* in the *GAL7p::CIG1* strains relative to the parental strain (WT or *rim101Δ*). Figure reproduced and modified from Cadieux *et al.* (2013).

3.3.4. Rim101 plays a role in iron and heme utilization at physiological and alkaline pH

The contribution of Rim101 in heme uptake was further investigated by examining growth in LIM supplemented with heme or $FeCl_3$ at different pH (Figure 3.7). The *cig1Δ* mutant exhibited a growth defect at pH 7.0, but not at lower pH in presence of heme. These results confirm the previous growth assays at pH 5.6 and pH 7.2 (Figure 3.3). In contrast, the *cig1Δ*

mutant grew as well as the wild-type and complemented strains at all pH in LIM supplemented with $FeCl_3$. The *rim101Δ* mutant exhibited a growth defect at pH 7.5 and above in LIM supplemented with heme, but not at lower pH, while the mutant displayed a growth defect only at pH 8.0 when grown in LIM supplemented with $FeCl_3$. The results were confirmed by growing the cells on solid LIM with added heme or $FeCl_3$ at different pH, with similar growth defects being observed (Figure 3.7B). Together, these data support a role for Cig1 in heme acquisition at physiological pH while Rim101 plays a role in both iron and heme acquisition at physiological and alkaline pH. This conclusion is consistent with the role of Rim101 in regulating Cig1 and the heme uptake pathway, as well as components of the high-affinity iron uptake system (e.g., the iron permease gene *CFT1*) (O'Meara *et al.*, 2010). However, as indicated above, Rim101 may also regulate components of another heme utilization pathway.

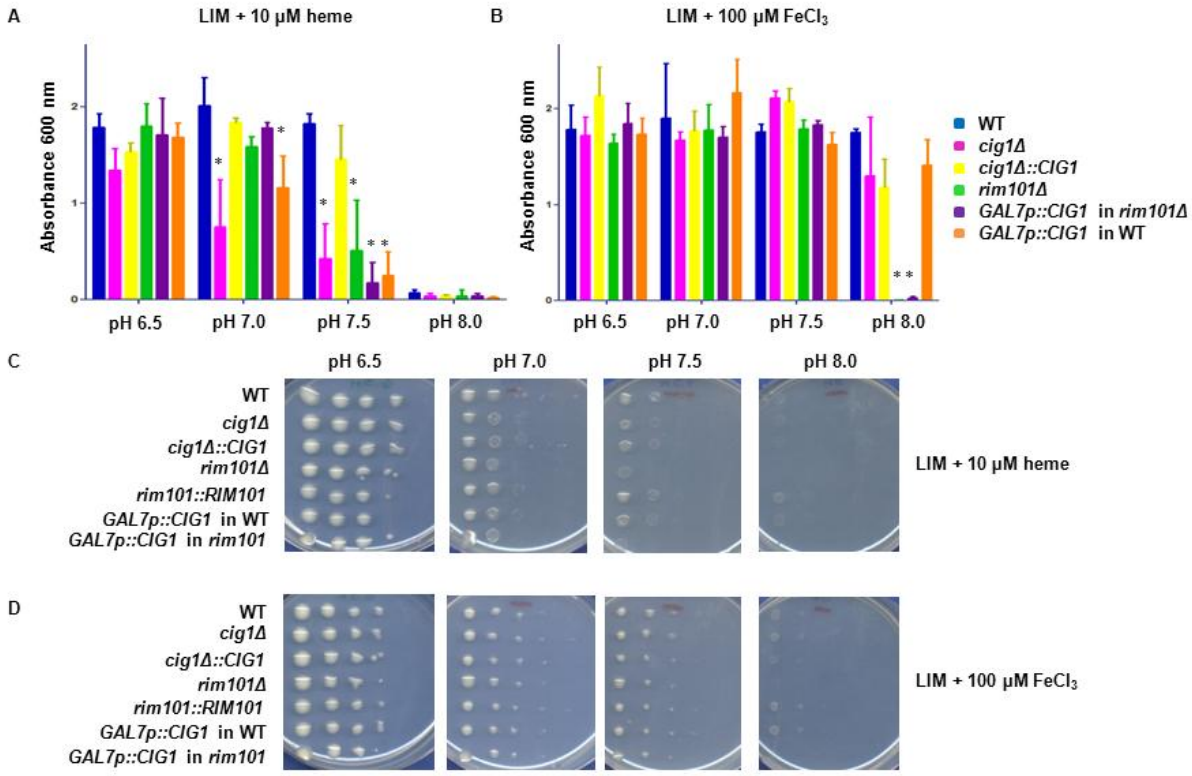

Figure 3.7 Rim101 plays a role in heme uptake at physiological pH and in iron uptake at alkaline pH. Growth of iron-starved cells in LIM + 10 µM heme (A) or LIM + 10 µM $FeCl_3$ (B) after 48 hours at 30C. Growth was monitored by measuring the optical density at 600 nm. All experiments were repeated three times and the data are plotted as the average ± SD. The * represents significant differences at $P < 0.05$ relative to the wild-type strain. Ten-fold serial dilutions of iron-starved cells spotted onto LIM + 10 µM heme (C) or LIM + 10 µM $FeCl_3$ (D) at different pH, as indicated. The plates were incubated at 30°C for three days and photographed. The experiment was repeated three times and a representative photograph is shown.

3.3.5. Cells form aggregates in the early stages of growth in LIM supplemented with heme

While performing the above experiments, the formation of dark brown/black precipitates in the cultures of cells grown in LIM supplemented with heme was observed (Figure 3.8A). The precipitates were present in cultures of all the strains tested, but were more noticeable in cultures of the *cig1Δ* mutant. Microscopy was used to visualize the precipitates and to potentially shed light on their nature. Upon examination, a dark granular substance (probably heme) was found

to surround some of the cells, especially the larger and possibly older cells, but was not directly in contact with the cells (Figure 3.8B). In fact, a halo where the substance appeared to be excluded could be observed surrounding the cells and this was seen for both the wild-type and *cig1Δ* mutant strains, albeit at different times during growth. These observations suggest that heme may physically interact specifically with the capsule of *C. neoformans*. Further examination, using India ink to visualize the capsule, revealed that the aggregates were composed of cells aggregated together with heme (Figure 3.8C-D). As time progressed, the aggregates became larger and encompassed more cells associated with heme, but once the cultures reached late exponential or stationary phase, the majority of aggregates dissociated and the cells returned to their initial single-cell form. The *cig1Δ* cells maintained aggregates for a longer period of time, presumably because the cells required more time to reach late exponential and stationary phases. Also, all cells remained as aggregates for a longer period of time when grown in galactose compared to glucose (Figure 3.8C-D). Again, the slower growth of the cells in galactose may explain this difference, or perhaps changes in capsule composition may occur to influence aggregation. The aggregate formation could possibly be explained by the highly negatively charged nature of the polysaccharide capsule surrounding the cell (Nosanchuk and Casadevall, 1997). Electrostatic interactions between the capsule and the positively charged iron in heme could result in heme binding to the capsular polysaccharides and mediate the formation of aggregates. Alternatively, formation of aggregates could reflect a specific mechanism by which the cells trap heme within the capsular mesh of the aggregates for eventual uptake. Finally, the aggregates could form as a result from the precipitation of heme, forcing the cells to aggregate with the precipitates in order to use the heme. At this point, it is unclear whether the interaction between the capsule and heme or aggregate formation is required for uptake of heme.

Further work will be needed to fully understand the heme-capsule interaction and the link between the observed aggregates and heme acquisition.

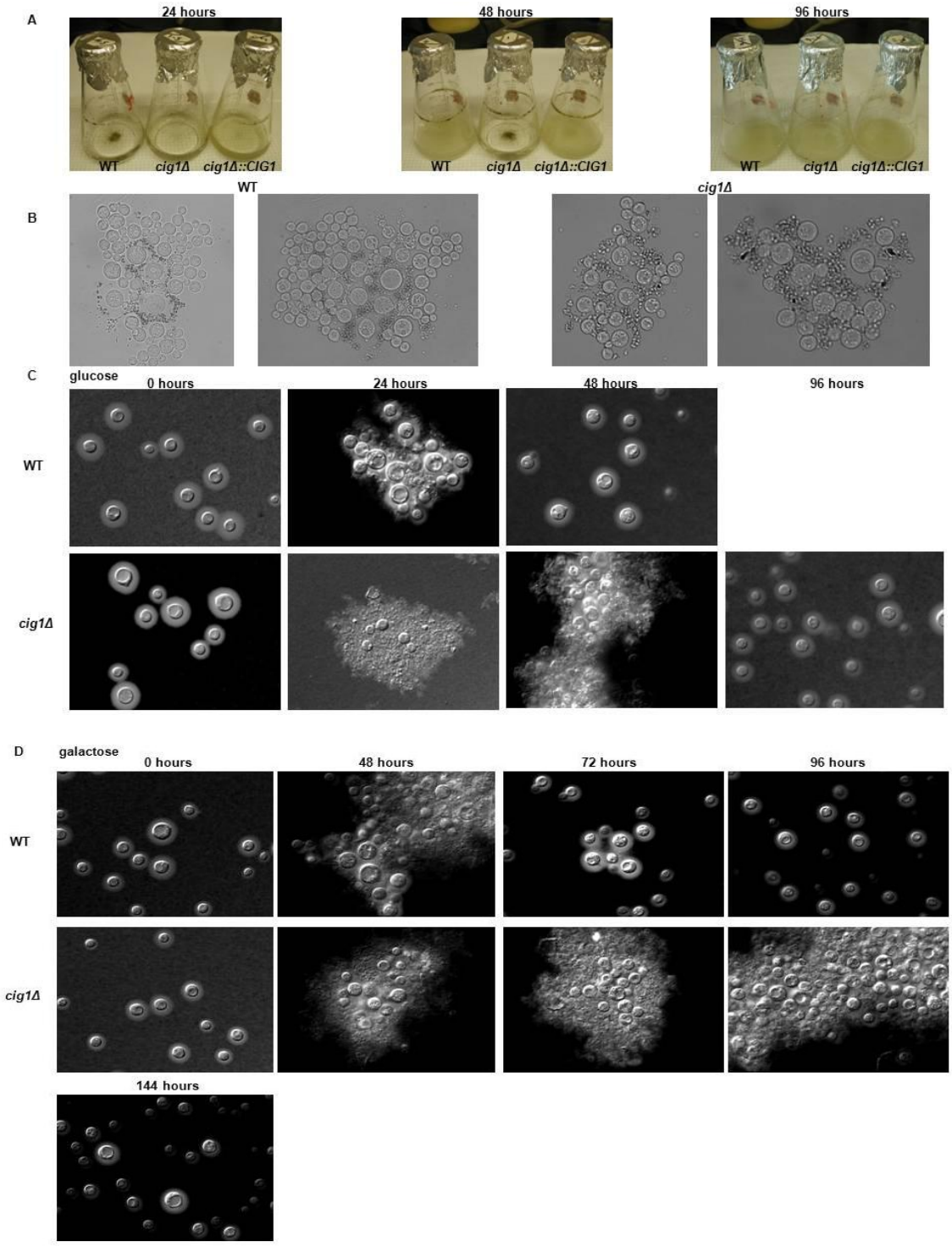

Figure 3.8 The cells and heme form aggregates during growth. Cells were grown in LIM + 10 µM heme in media containing glucose (A-C) or galactose (D). Cells in C and D were harvested and negatively stained with India ink before visualization by differential interference contrast microscopy.

3.3.6. Heme uptake via the Cig1-independent pathway is dependent on cell density

It is possible that the formation of aggregates described above may be essential in heme acquisition as part of a cell density-dependent heme uptake mechanism sharing similarities with the QS phenomenon. QS is a communication system based on the secretion and diffusion of small molecules by microorganisms and relies on the close proximity of the cells to allow for communication between them. The possibility of a QS-like cell density-dependent heme uptake mechanism was investigated by inoculating cultures of the different strains at different cell densities and monitoring the growth in LIM with added heme (Figure 3.9). At low inoculum (10^2 cell/mL), all the cells remained in lag phase for a long period of time before reaching exponential phase. Specifically, the wild-type and complemented strains took 48 hours before starting to grow exponentially, while the *cig1Δ* mutant required 120 hours. Remarkably, the length of the lag phase for all the strains tested decreased as the inoculum size increased. At the highest inoculum (10^6 cells/mL), the lag phase was not detected for any of the strains, and they had all started to grow exponentially by 12 hours. However, the *cig1Δ* mutant grew slightly slower than the wild-type or complemented strains. The cell density-dependent growth of the *cig1Δ* mutant in LIM supplemented with heme was confirmed by plating the iron-starved cells on LIM with added heme. Again, the mutant grew more slowly than the wild-type strain at lower inoculum but grew as well as the wild-type at higher inoculum. These results support a role for cell density as an essential factor involved in the Cig1-independent heme uptake pathway and further suggest a possible link between a QS-like mechanism and heme uptake. For example, as more cells are added initially, more QS-like molecules would be secreted within the first few hours of growth which would induce the Cig1-independent heme uptake system. Alternatively, addition of more cells would also potentially increase the activity of any cell

surface-bound enzymes that process heme, such as the ferric reductases described previously, which could result in increased uptake of iron from heme to allow more rapid growth.

Although growth of the *cig1Δ* mutant in LIM supplemented with heme at acidic pH did not appear to be dependent on cell density (Figure 3.3), further examination of both pathways was required to determine if the two were linked. In order to do so, the strains were grown in LIM supplemented with heme at acidic pH starting with a low inoculum (10^2 cell/mL). As expected, even at a low inoculum, all the strains grew as well as when inoculated at a higher inoculum (compare Figures 3.3 and 3.9). Specifically, the cells remained in lag phase for 12 hours and had reached stationary phase by 48 hours. These data suggest that the two Cig1-independent heme uptake pathways, the pathway for heme acquisition at acidic pH and the cell density-dependent pathway, are distinct. However, this does not preclude possible overlap between the other components involved in each pathway.

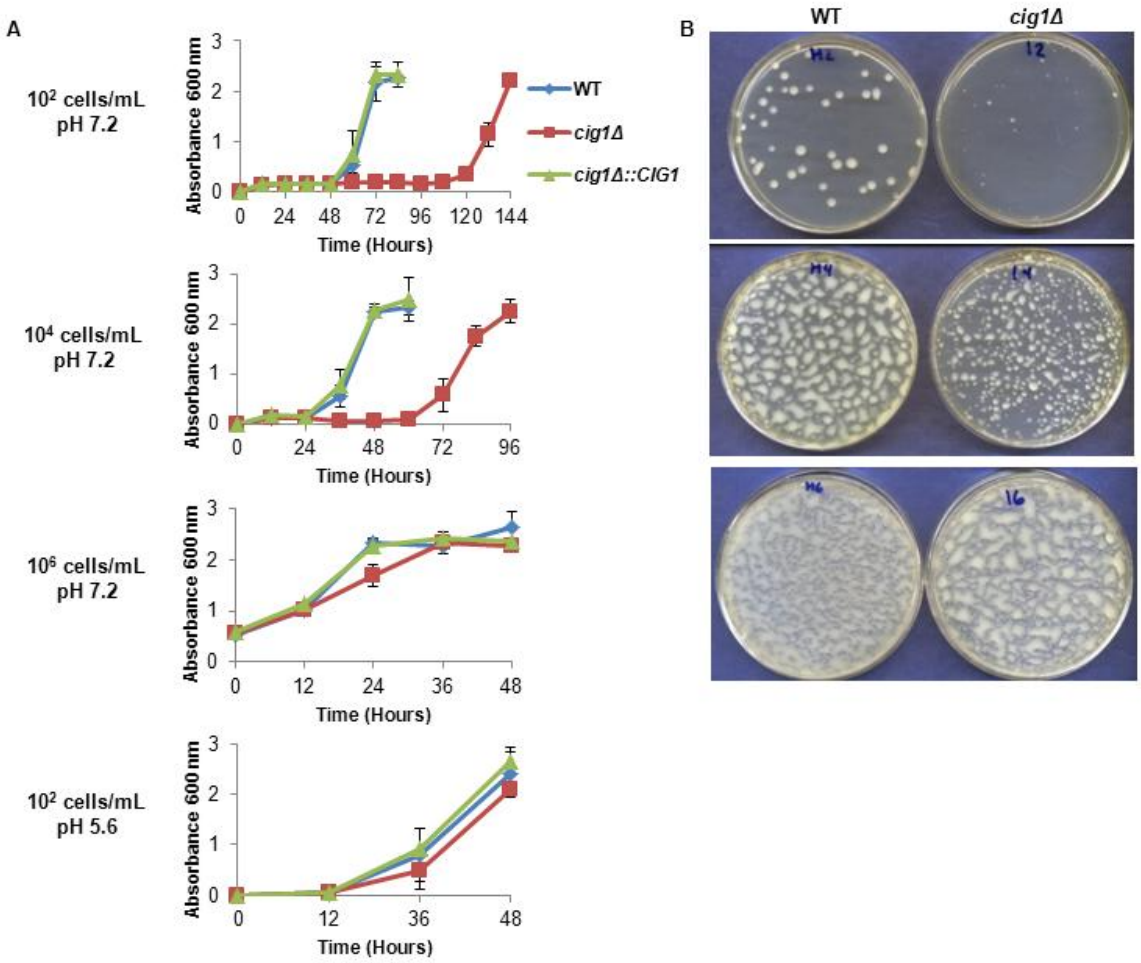

Figure 3.9 Cig1-independent heme uptake is dependent on cell density. (A) Growth of iron-starved cells in LIM + 10 µM heme when inoculated at different cell densities, as indicated. Growth was monitored by measuring the optical density at 600 nm. All experiments were repeated three times and the data are plotted as the average ± SD. (B) Growth of iron-starved cells on LIM + 10 µM heme when plated at different cell densities. The plates were incubated at 30°C for three days and photographed. The experiment was repeated three times and a representative photograph is shown.

3.3.7. Addition of conditioned media allowed the cells to grow faster

QS requires that small signaling molecules be secreted by the cells to coordinate the behaviour of the group, including growth. The concentration of signaling molecules is assumed to be at its peak during stationary phase when the cell density is at its highest. To further investigate the effect of a possible QS-like mechanism on heme acquisition, CM were harvested

from different strains that reached stationary phase. The CM was added to fresh LIM plus heme, and growth of the different strains was compared (Figure 3.10). Addition of CM to fresh medium did not decrease the length of the lag phase for the wild-type and complemented strains, but resulted in more robust growth (based on the higher optical density at 36 hours) compared to growth of the same strains without CM (Figure 3.10A,C). The enhanced growth with the added CM for these strains was consistently observed independently of the origin of the CM. However, the effect of adding CM to cultures of the *cig1Δ* mutant varied depending on the source of the CM. For example, only addition of CM harvested from the *cig1Δ* mutant strain resulted in a shorter lag phase, possibly because the concentration of the QS-like molecule was higher in CM produced by the *cig1Δ* mutant strain (Figure 3.10B). Nevertheless, addition of CM from all the strains tested yielded faster growth of the *cig1Δ* mutant. It is unclear why the *cig1Δ* mutant strain would produce a higher concentration of the QS-like molecule. One possible explanation could be that in absence of a functional Cig1-dependent heme uptake pathway, more QS-like signaling molecules are produced to induce an alternative pathway for heme uptake which appears to be dependent on cell density. Overall, these data suggest that some secreted component found in supernatant of cultures at stationary phase (e.g., polysaccharides, proteins or peptides, lipids, or other small molecules) could act as a QS-like signal that appears to be involved in cell density-dependent heme utilization. Alternatively, the possibility of the CM having more available iron than fresh media because the heme has been processed by cell surface enzymes (e.g., reductases) cannot be discounted and could explain the more robust growth upon addition of CM.

In a preliminary attempt to identify the QS-like molecule, addition of CM harvested from cultures of the *cqs1Δ* mutant were tested to determine if they could allow the cells to grow better

in LIM supplemented with heme (Figure 3.10D). The *cqs1Δ* mutant is defective in secretion of the QS peptide, Qsp1, that is reported to control growth in *C. neoformans* (Lee *et al.*, 2007). This mutant was prepared in the *C. neoformans* var. *neoformans* background, and therefore, the *C. neoformans* var. *neoformans* wild-type strain, B3501A, was used for comparison. Addition of CM from both the wild-type and the *cqs1Δ* mutant resulted in faster growth for all of the strains tested compared to growth without CM implying that the Qsp1 peptide is not the QS-like molecule responsible for the observed phenotype. So far, Qsp1 has been the only identified QS-like molecule produced by *C. neoformans*, however, one can imagine that an array of QS-like molecules are secreted by this fungus in order to adapt to and grow in the many different environments.

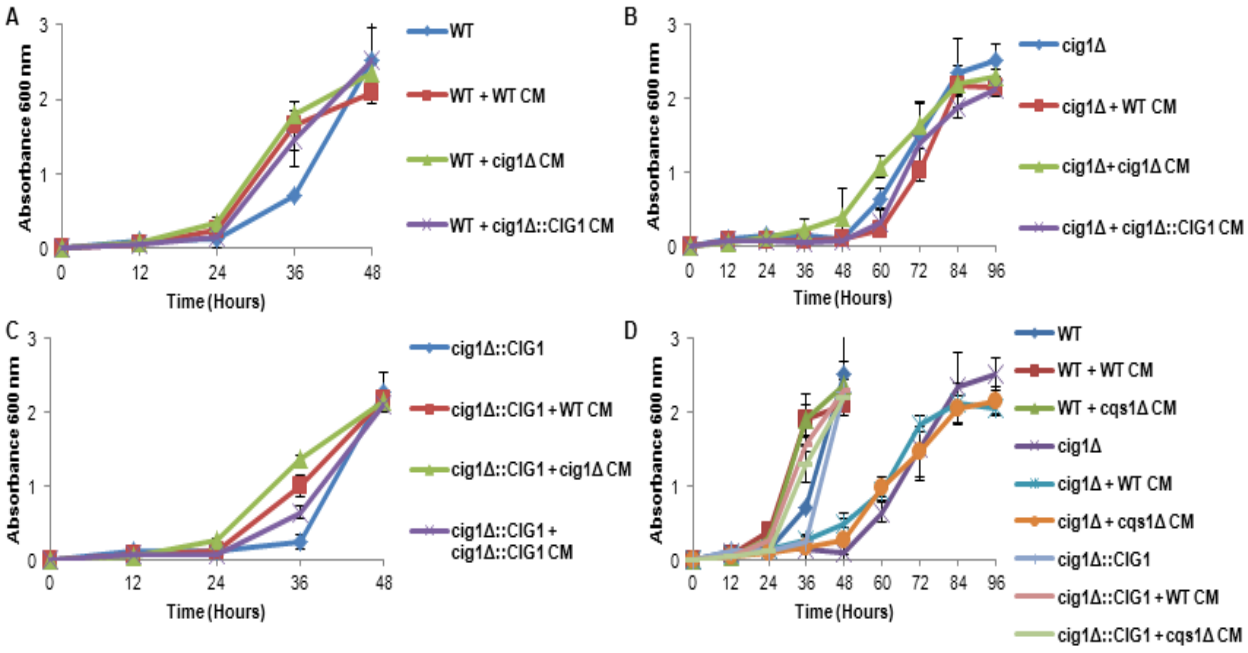

Figure 3.10 Addition of CM allows the cells to grow faster. Growth of iron-starved cells: WT (A), *cig1Δ* (B), and complement (C) in LIM + 10 µM heme with 50% CM from the WT, *cig1Δ*, and complemented strains or (D) from *C. neoformans* var. *neoformans* WT and *cqs1Δ* strains. The CM was harvested by centrifugation once the cells grown in LIM + 10 µM heme had reached stationary phase. Growth was monitored by measuring the optical density at 600 nm. All experiments were repeated three times and the data are plotted as the average ± SD.

3.3.8. Addition of exogenous polysaccharides allowed the cells to grow faster

C. neoformans produces and secretes copious amounts of polysaccharides, some of which are used for capsule biosynthesis, while others, the exopolysaccharides, are soluble and found in culture supernatants (Cherniak, 1988). These exopolysaccharides include GXM, the major capsular polysaccharide, and other minor polysaccharides, such as GalXM. To determine whether exopolysaccharides could act as the QS-like molecule involved in heme acquisition, the CM was fractionated further to isolate the total secreted polysaccharides from the medium. The secreted polysaccharides were then added back to fresh cultures and the growth of the strains in LIM supplemented with heme with and without added exogenous polysaccharides was compared (Figure 3.11A-C). Addition of exogenous polysaccharides did not play a big role in the growth of the wild-type and complemented strains. In contrast, addition of exogenous polysaccharides had a more pronounced effect (although not dramatic) on the growth of *cig1Δ* mutant, resulting in a shorter lag phase (Figure 3.11B). Specifically, addition of exogenous polysaccharides isolated from the wild-type CM reduced the lag phase of the *cig1Δ* mutant by approximately 24 hours, compared to approximately 12 hours when adding polysaccharides isolated from the *cig1Δ* mutant CM. Growth curves obtained after addition of exogenous polysaccharides (Figure 3.11) were very similar to previous experiments with addition of CM described in the previous section (Figure 3.10) suggesting that the QS-like molecule associated with heme utilization is probably also present in the polysaccharide fraction isolated from the CM.

During isolation of the secreted polysaccharides, other proteins or small molecules may have been precipitated along with the exopolysaccharides and could be present in that fraction of the CM. Therefore, the nature of the QS-like molecule was assessed further by treating the isolated polysaccharide fraction with proteinase K to determine if the signaling molecule is a

protein or peptide. Growth of the *cig1Δ* mutant in LIM supplemented with heme with added exogenous polysaccharides was similar whether the isolated polysaccharides had been treated with proteinase K or not, suggesting that the QS-like molecule does not have a proteinaceous nature (Figure 3.11D). In a second attempt to identify the nature of the QS-like molecule, the isolated polysaccharide fraction was dialyzed in dialysis tubing of low molecular weight cut-off to remove any small molecules (i.e., smaller than 7 kDa) that could serve as the QS-like signal. Addition of exogenous polysaccharides after dialysis resulted in similar growth of the *cig1Δ* mutant in LIM supplemented with heme than when non-dialyzed exogenous polysaccharides were added to the culture medium. Together, these results imply that the QS-like molecule is non-proteinaceous and larger than 7 kDa. However, it is important to note that the influence of adding exogenous polysaccharides to the growth medium was not dramatic, and consequently, subtle differences in growth that could have arisen from treating the isolated polysaccharides (i.e., proteinase K, dialysis) may have been difficult to detect.

It is possible that the QS-like molecule involved in the Cig1-independent heme uptake pathway is the GXM polysaccharide. To this end, a *cap59Δ* mutant was used to test the role of GXM in heme acquisition. *CAP59* is a gene necessary for capsule synthesis, and its product is presumably involved in the process of GXM export (Chang *et al.*, 1995; Chang and Kwon-Chung, 1999; Garcia-Rivera *et al.*, 2004). The *cas1Δ* mutant was also used. Cas1 is involved in acetylation of the capsule and the *cas1Δ* mutant has been shown to have increased shedding of GXM in the supernatant (Janbon *et al.*, 2001; Dr. E. Griffiths, personal communications). Growth of the *cap59Δ* and *cas1Δ* mutants in LIM supplemented with heme was compared to that of the wild-type strain and no difference in growth was observed for either strain (Figure 3.11E). Interestingly, growth of the *cas1Δ* mutant in LIM supplemented with $FeCl_3$ resulted in longer lag

phase compared to that of the wild-type strain (Appendix D). Although these observations don't confirm a role for GXM in heme uptake, they don't necessarily rule it out either. If GXM is the QS-like molecule, it is possible that no growth defect is observed under the conditions tested because the Cig1-dependent heme uptake pathway overshadows or compensates for the abnormal GXM shedding in the *cap59Δ* and *cas1Δ* mutants. Also, as mentioned above, addition of exogenous polysaccharides results in subtle differences in growth, and therefore, the contribution of GXM to heme uptake may have been difficult to detect. Finally, addition of exogenous polysaccharides isolated from the culture supernatant of *cap59Δ* and *cas1Δ* mutants also decreased the lag phase of the *cig1Δ* mutant, similar to what was observed with addition of GXM isolated from the wild-type and *cig1Δ* strains (Figure 3.11B, F). Combined, these data suggest that GXM may not be the QS-like molecule, and instead, other exported components within the isolated exopolysaccharide fraction, including GalXM for example, could be the QS-like signal. Future work will be needed to further assess the role of GXM in heme acquisition and to examine the contribution of GalXM in the cell density-dependent heme uptake pathway. Also, if GXM or GalXM are not the QS-like molecule, the isolated exopolysaccharide fraction might need to be separated further to identify other putative QS-like molecules.

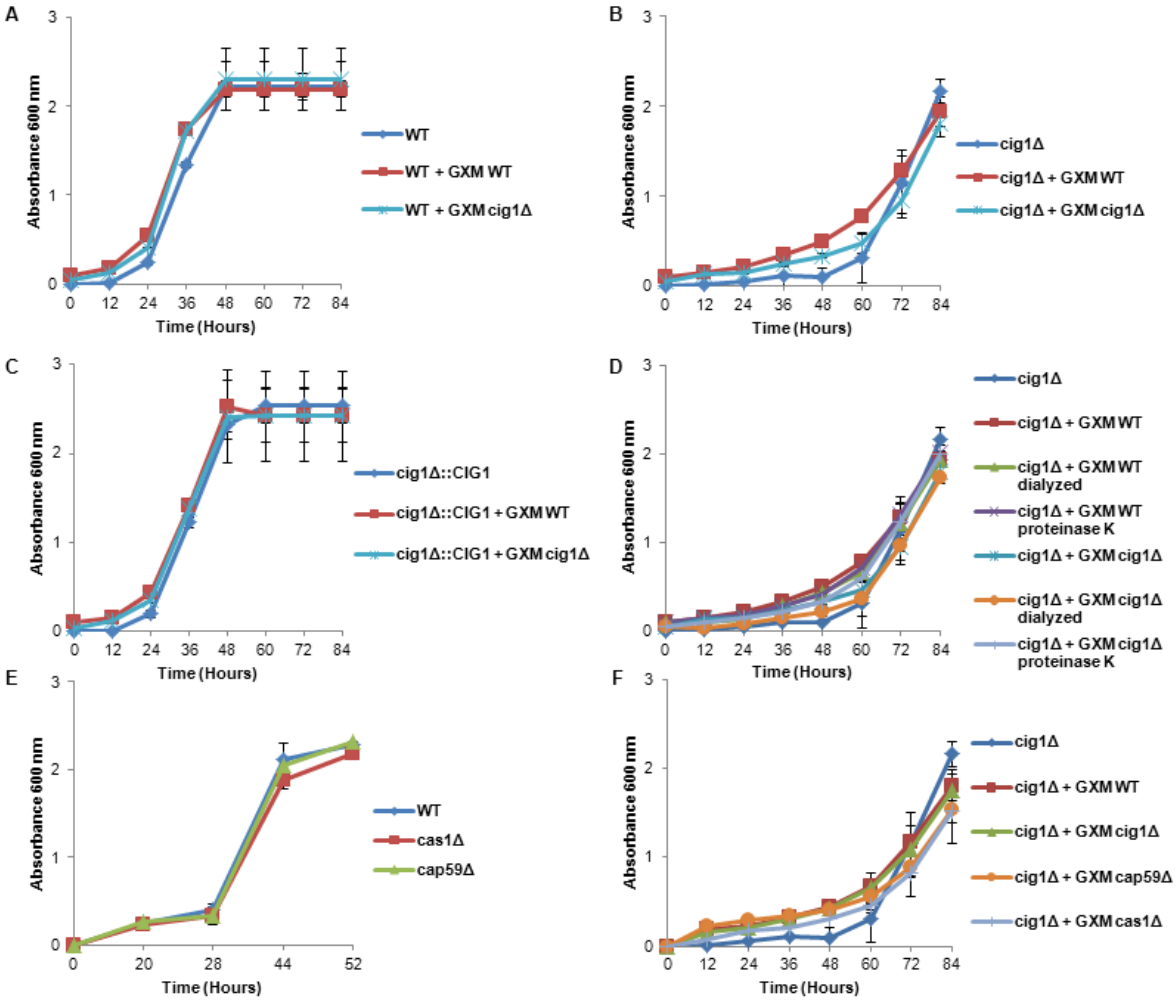

Figure 3.11 Addition of exogenous polysaccharides allows the cells to grow faster. Growth of iron-starved cells in LIM + 10 µM heme with added exogenous polysaccharides isolated from CM. Growth was monitored by measuring the optical density at 600 nm. All experiments were repeated three times and the data are plotted as the average ± SD.

3.3.9. Binding of GXM to heme

The examination of the aggregates formed during growth in LIM supplemented with heme suggested a possible interaction between the capsule and heme. The capsule is composed mainly of GXM, but also contains GalXM and mannoproteins (Reiss *et al.*, 1985; Murphy *et al.*, 1988; Bose *et al.*, 2003; Zaragoza *et al.*, 2009). Consequently, the interaction between the capsule and heme was further investigated by measuring the absorbance spectra of the isolated

GXM after the addition of increasing amounts of heme. As mentioned in Chapter 2, heme groups have characteristic absorbance bands that depend on the ligation and conformational state of the chromophore thus allowing detection of heme binding by spectrophotometry. Titration of GXM with heme did not reveal any binding between GXM and heme (Figure 3.12A). ITC was also used to test the interaction between GXM and heme, however, no binding was detected (Figure 3.12B). These preliminary results suggest that GXM does not bind heme, however, the viscous nature of the GXM solution and the approximate and large size of GXM (1,700-7,000 kDa) could possibly have prevented detection of interactions. For example, the concentration of GXM needed for ITC analysis was too viscous and could not be measured. Therefore, a diluted sample had to be used which could have resulted in a weaker interaction that precluded detection. Also, the approximate molecular weight of the polysaccharide led to approximations of the concentrations of the polysaccharide being used which could have resulted in an ineffective ratio of polysaccharides to heme (leading to poor detection of the potential interaction). Exact ratios are particularly important when measuring interactions by ITC or absorbance spectra. Finally, detection of interaction by absorbance spectra has been extensively used for detection of heme-binding proteins but is not commonly used for measuring the interaction between heme and polysaccharides. The parameters may need to be optimized for detection of the interaction. Future work will be needed to confirm whether GXM interacts with heme, and to examine the possible interaction of GalXM or the capsular mannoproteins with heme.

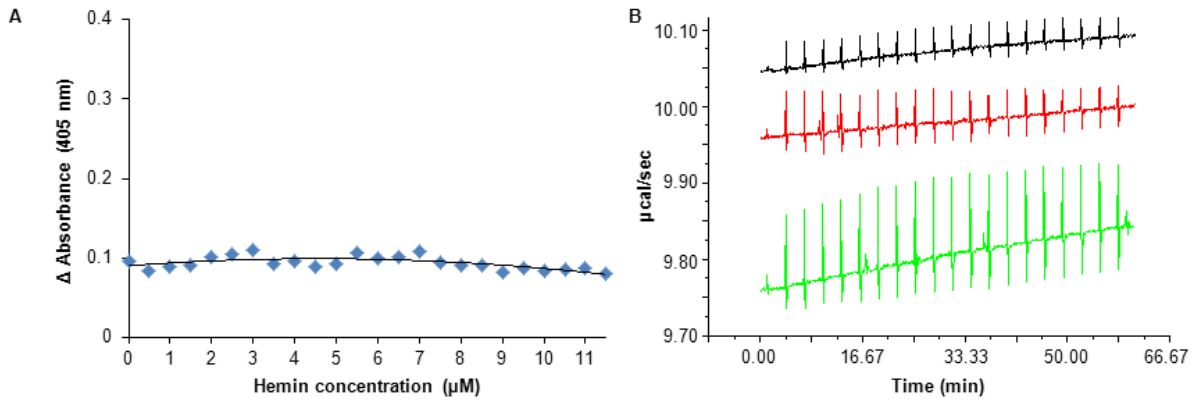

Figure 3.12 GXM does not appear to bind heme. (A) Heme binding curve of GXM isolated from the wild-type strain. The difference between the absorbance of the GXM-heme complex and free heme at 405 nm is plotted against the increasing concentration of heme. (B) Binding of heme to GXM by measuring the isothermal calorimetry of heme alone (black), 0.1 mg/mL GXM plus 1 mM heme (red), or 0.5 mg/mL GXM plus 1 mM heme (green) over the specified period of time. All assays were repeated three times and representative graphs are shown.

3.4. Discussion

Several lines of evidence indicate that additional Cig1-independent mechanisms exist for iron acquisition from heme in *C. neoformans.* First, deletion of *CIG1* resulted in an extended lag phase in LIM supplemented with heme but eventual growth to a density comparable to the wild-type strain. Although heme likely contains some contaminating inorganic iron that could be acquired by the high-affinity iron uptake system (i.e., the permease Cft1 and the ferroxidase Cfo1) (Jung *et al.*, 2008; 2009), the *cig1Δ cfo1Δ* mutant behaved similarly to the *cig1Δ* mutant. This observation rules out a substantial contribution of free iron to the eventual growth of the mutants. An alternate pathway could involve processing of heme by unidentified cell-surface reductases (as discussed in Chapter 2) resulting in free iron to be taken up by a pathway different from the high-affinity iron uptake system. This pathway could possibly mediate heme (or free iron released from heme) uptake via endocytosis. A similar pathway has been described for hemoglobin utilization in *C. albicans*, and Vps23, an important component of the ESCRT involved in endocytosis has been identified as a key player in iron acquisition from heme in *C. neoformans* (Weissman *et al.*, 2008; Hu *et al.*, 2013).

A second piece of evidence for additional heme uptake mechanisms is the absence of a growth defect of the *cig1Δ* mutant and down-regulation of *CIG1* expression at acidic pH. The solubility and bioavailability of iron is highly dependent on pH (Wilkins, 1991; Cotton *et al.*, 1999). It is possible that the pH effect observed is a consequence of an increased bioavailability of heme for *C. neoformans* at acidic pH compared to neutral pH. If the bioavailabilty of heme is increased, the uptake of heme could bypass the Cig1-dependent heme uptake pathway and rely on a different heme uptake pathway, for example a low-affinity heme uptake pathway. Alternatively, the iron state is also dependent on pH, being in its ferric form at neutral/alkaline

pH and ferrous form at acidic pH. The Cig1-dependent heme uptake system may be specific for transportation of ferric iron heme (heme) inside the cell whereas a different heme uptake system would exist to acquire ferrous iron heme. Another possible explanation could be that the activity of the unidentified cell-surface reductases hypothesized to be involved in heme processing are influenced by the pH. Finally, the endocytic pathway described above may also be involved in uptake of heme (or free iron released upon processing of heme). This is supported by unpublished data that indicate a role for the ESCRT components in $FeCl_3$ and heme uptake at acidic pH (Dr. G. Hu, personal communications).

The influence of pH on growth in LIM supplemented with heme implicated the fungal transcription factor Rim101 because of its known regulation of pH-responsive genes and genes encoding functions for iron acquisition (Bensen *et al.*, 2004; Nobile *et al.*, 2008; O'Meara *et al.*, 2010). In the latter case, the expression of *CIG1* was down-regulated in the *rim101Δ* mutant of *C. neoformans* (O'Meara *et al.*, 2010) and deletion of *RIM101* resulted in a growth defect in LIM supplemented with heme similar to that of the *cig1Δ* mutant. Although Rim101 likely influences heme uptake by regulating *CIG1*, it also makes an independent contribution to growth in LIM supplemented with heme as demonstrated by the exacerbated growth defect of a strain lacking both Cig1 and Rim101. This independent contribution could potentially be linked to the ESCRT-mediated endocytic pathway involved in iron acquisition from heme especially since Rim101 is a downstream target of the ESCRT pathway in *C. albicans* (Xu and Mitchell, 2001; Kullas *et al.*, 2004; Xu *et al.*, 2004).

Interestingly, the *rim101Δ* mutant did not have a growth defect when grown in LIM supplemented with heme in presence of galactose, while it had a more severe growth defect when grown in acetate as a carbon source. Furthermore, the transcript levels of *CIG1* were

reduced on galactose versus glucose media and the *cig1Δ* mutant did not grow in LIM supplemented with heme in the presence of acetate. Thus, carbon source appears to influence iron acquisition from heme. A link between carbon source and heme has previously been established in *S. cerevisiae*. Specifically, the Hap 2/3/4/5 complex, which is a heme-regulated transcription factor involved in activation of genes responsible for respiration has been shown to be repressed by glucose and de-repressed by galactose and non-fermentable carbon sources (McNabb and Pinto, 2005; Lai *et al.*, 2006). Also, the expression of the heme oxygenase, the enzyme responsible for catalyzing heme degradation, is regulated by glucose and is induced upon glucose deprivation (Chang *et al.*, 2002).

Further evidence suggests the existence of Cig1-independent heme uptake systems including the correlation between the starting inoculum size and the length of the lag phase of the *cig1Δ* mutant when grown in LIM supplemented with heme. This heme utilization system could rely on QS-like behaviour as indicated by the formation of cell aggregates during lag phase, the ability of the *cig1Δ* mutant to grow as well as the wild-type strain in LIM supplemented with heme at higher inoculum, and finally the partial recovery of the growth defect for the *cig1Δ* mutant when CM or isolated polysaccharides were added to fresh culture. The study of QS in fungi is still in its infancy, and the first evidence of fungal QS was described in *C. albicans* ten years ago. Farnesol, a QS molecule, was observed to control filamentation which is essential for virulence in this pathogenic fungus (Hornby *et al.*, 2001). Since then, only a few other QS molecules have been identified, including tyrosol necessary for controlling growth, morphogenesis and biofilm formation in *C. albicans*, and phenylethanol and tryptophol involved in controlling morphogenesis during nitrogen starvation in *S. cerevisiae* (Chen *et al.*, 2004; Chen and Fink, 2006; Albuquerque and Casadevall, 2012).

Cell density-dependent behaviours have also been described in different fungi, including *C. neoformans*. For example, a cell density-dependent growth phenotype similar to QS was observed in *C. neoformans* var. *neoformans* (serotype D) after deletion of the global repressor *TUP1* (Lee *et al.*, 2007). A small oligopeptide (11 amino acids), Qsp1, encoded by the *CSQ1* genes was identified as an autoregulatory molecule found in CM and was responsible for the cell density-dependent growth phenotype. Another study described the influence of cell density on melanization in both serotypes A and D, in which melanization occurred more rapidly in denser cultures (Eisenman *et al.*, 2011). Finally, growth, secretion of GXM, and biofilm formation were also shown to depend on cell density in *C. neoformans*, although the QS molecule was never confirmed (Albuquerque, 2011).

Additionally, a link between QS and iron uptake has been well documented in many bacteria, notably in *P. aeruginosa*. For example, expression of QS systems were induced under iron starvation conditions in *P. aeruginosa* but repressed under high-iron conditions (Kim *et al.*, 2005; Duan and Surette, 2007; Yang *et al.*, 2007; Hazan *et al.*, 2010). Not surprisingly, some QS regulators of *P. aeruginosa* are also downstream targets of the Fur iron regulator (Ochsner *et al.*, 2002; Oglesby *et al.*, 2008). In contrast, QS regulators also induce many iron responsive genes in *P. aeruginosa*, including the siderophore, pyochelin (Ochsner *et al.*, 2002; Palma *et al.*, 2003; Schuster *et al.*, 2003; Cornelis and Aendekerk, 2004; Juhas *et al.*, 2004; 2005; Deziel *et al.*, 2005; Hazan *et al.*, 2010).

The cell density-dependent heme uptake system is likely distinct from the heme uptake mechanism involved at acidic pH because cell density was not a factor for growth in LIM supplemented with heme at acidic pH. Nevertheless, both pathways may rely on cell-surface reductases involved in heme processing. A higher cell density would result in increased cell-

surface reductase activity which could process heme more rapidly. Consequently, it is possible that different components involved in transport of the heme to the inside of the cell are shared among the two pathways.

Finally, the capsular polysaccharides could potentially be linked with heme uptake. The figures of the aggregates formed during growth in LIM supplemented with heme imply some sort of physical contact between the capsule and heme. Furthermore, addition of exogenous polysaccharides increased the growth of the *cig1Δ* mutant in LIM supplemented with heme suggesting a possible role for the polysaccharides as the QS-like signaling molecule involved in cell to cell communication during growth in LIM supplemented with heme. The capsule is composed of GXM, GalXM, and mannoproteins. Additionally, chitin-like oligomers are found at the cell surface and appear to be involved in linking the capsule to the cell wall by interacting with GXM (Rodrigues *et al.*, 2008b; Ramos *et al.*, 2012). If any of these components could bind heme, they could potentially help trap the heme molecule in the capsule mesh. In fact, the QS molecule, PQS, characterized in *P. aeruginosa* was observed to bind iron and acted as an iron trap molecule (Bredenbruch *et al.*, 2006; Diggle *et al.*, 2007). Although GXM represents approximately 90-95% of the capsular material, it was not shown to bind heme in the conditions tested (Cherniak *et al.*, 1980). Also, studies involving the *cap59Δ* strain, a mutant which cannot produce GXM, indicated that GXM does not appear to be the QS-like molecule. Treatment of the isolated polysaccharide fraction with proteinase K did not reduce the ability of the exogenous polysaccharides to rescue the growth defect of the *cig1Δ* mutant in LIM supplemented with heme suggesting that the QS-like molecule is not a mannoprotein. Other studies will be needed to confirm that GXM does not bind heme but future work should focus on determining whether

GalXM, capsular mannoproteins and/or chitin-like oligomers interact with heme, if this interaction is essential for heme uptake, and if it plays a role in QS-like signaling between cells.

In summary, *C. neoformans* appears to have developed multiple heme uptake systems. In this study, two distinct Cig1-independent heme utilization systems have been identified, including a pathway involved in heme utilization at acidic pH, and another cell density-dependent pathway with similarities to QS. The QS-like molecule was not determined, although secreted polysaccharides could be potential candidates. Further work will be needed to elucidate the receptors and mechanisms involved in heme uptake in both these Cig1-independent pathways.

Chapter 4. Cig1 plays a role in heme utilization, as well as in secretion and maintenance of cell wall integrity in *C. neoformans* var. *neoformans*.

4.1. Introduction

In the work presented in Chapter 2, Cig1 was found to play an important role in heme uptake and utilization in *C. neoformans* var. *grubii*. Although *C. neoformans* var. *neoformans* shares 85-90% similarity with *C. neoformans* var. *grubii* at the genomic level, it cannot be assumed that the one protein will play the same role in both varieties (Kavanaugh *et al.* 2006). In fact, *C. neoformans* var. *grubii* and *C. neoformans* var. *neoformans* diverged approximately 18 million years ago (Fan *et al.*, 1994; Xu *et al.*, 2000). Over that time, genetic diversity has arisen between the two different *C. neoformans* varieties leading to important differences in pathogenicity, virulence, host specificity and geographical distribution. There are multiple reported cases of the same protein playing an important role in one variety while no role could be determined in the other variety (Cruz *et al.*, 2000; Wang *et al.*, 2002; Hicks *et al.*, 2004; Bahn *et al.*, 2005). Therefore, this study focuses on further characterizing the role of Cig1 in *C. neoformans* var. *neoformans* to obtain a broader view of the function of the protein.

Lian *et al.* (2005) characterized a *cig1Δ* mutant in *C. neoformans* var. *neoformans* with regard to iron-related phenotypes. Specifically, the *cig1Δ* mutant in *C. neoformans* var. *neoformans* was reported to have a growth defect in LIM and a change in the capsule response to iron (Lian *et al.*, 2005). Typically, the wild-type strain elaborated a larger capsule when grown in LIM compared to when it was grown in presence of $FeCl_3$. However, the *cig1Δ* mutant appeared to be non-responsive to iron levels and produced a larger capsule than the wild-type strain when grown in LIM supplemented with $FeCl_3$. These preliminary results suggested a possible link between Cig1 and the synthesis of the polysaccharide capsule.

Secretion is an important component for the pathogenesis of *C. neoformans* as many of its known virulence factors are secreted to the cell surface or to the extracellular space, including the polysaccharides required for capsule synthesis. Although little is known about secretion in *C. neoformans*, there is increasing evidence suggesting the existence of more than one secretory pathway, including the conventional and non-conventional pathways (Rodrigues *et al.*, 2007; 2008a; 2008b; 2012; Nosanchuk *et al.*, 2008; Eisenman *et al.*, 2009; Panepinto *et al.*, 2009; Oliveira *et al.*, 2009; 2010; Kmetzsch *et al.*, 2011). Transport through the conventional secretory pathway requires the secreted proteins to have a signal peptide and trafficking of proteins from the endoplasmic reticulum (ER) to the Golgi to subsequently reach the cell periphery in trafficking vesicles. The non-conventional secretory pathway does not require the secreted proteins to have a signal peptide and secretion occurs independently from the ER-Golgi pathway (Rodrigues *et al.*, 2008b; Panepinto *et al.*, 2009; Oliveira *et al.*, 2010; Kmetzsch *et al.*, 2011). Additionally, extracellular vesicles produced by *C. neoformans* can transport cargo material, including proteins, polysaccharides and lipids, across the cell wall (Rodrigues *et al.*, 2007; 2008a; 2008b; Nosanchuk *et al.*, 2008; Eisenman *et al.*, 2009; Oliveira *et al.*, 2009). These different secretory pathways are involved in the secretion of different components to the cell wall, capsule and extracellular space. However, there also appears to be some redundancy between the pathways. For example, there is evidence that GXM, the major polysaccharide of the capsule, can be transported via all of the described secretory pathways (Yoneda and Doering, 2006; 2009; Rodrigues and Djordjevic, 2012).

The link between Cig1 and elaboration of the capsule led to the hypothesis that Cig1 may influence secretion. To test this hypothesis, the role of Cig1 in secretion was assessed by growing the wild-type and *cig1Δ* strains in presence of secretion inhibitors. The susceptibility to

other stresses, including agents that challenge cell wall integrity, as well as osmotic stress and heat stress, were also tested. Additionally, the activity of secreted proteases was compared between the different strains and the concentration of total secreted proteins was also measured. Finally, the relative quantity of secreted extracellular vesicles was compared between the different strains.

4.2. Materials and Methods

4.2.1. Strains and growth conditions

All strains used in this study are listed in Table 4.1. YPD (Fisher), yeast extract peptone galactose (YPG), YNB (Difco), and LIM were used to grow the cells. LIM was prepared as described (Vartivarian *et al.*, 1993) and the pH was adjusted to 7.2. The water used for LIM was treated with Chelex-100 resin (Bio-Rad) to chelate iron. Cells for all assays were pre-grown overnight at 30°C with shaking in YPD, unless specified otherwise.

Table 4.1. Strains used in this study

Strain	Description	Provided/ Prepared by
B3501A	*C. neoformans* var. *neoformans* wild-type strain	Dr. June Kwon-Chung
cig1DΔTL	*cig1* disruption mutant #1	Tian Lian
cig1DΔBC	*cig1* disruption mutant #2	Brigitte Cadieux
cig1DΔdel	*cig1* deletion mutant	Brigitte Cadieux
cig1DΔ +CIG1	*CIG1* complemented strain in *cig1DΔTL*	Tian Lian
cigD1Δstop	Strain with a stop codon after the ATG in the disrupted *CIG1* open reading frame	Brigitte Cadieux
GAL7p::CIG1D	Regulated *CIG1* disruption allele in the B3501A background	Brigitte Cadieux
H99	*C. neoformans* var. *grubii* wild-type strain	Dr. Joseph Heitman
cig1AΔdis	*cig1* disruption mutant	Brigitte Cadieux
cig1AΔdel	*cig1* partial deletion mutant	Carmelo Biondo
cig1AΔ +CIG1	*CIG1* complemented strain	Tian Lian

4.2.2. Construction of strains

Primers used for construction of all strains are listed in Table 4.2 and a schematic of all of the constructs generated is depicted in Figure 4.1A.

Table 4.2. Primers used for strain construction

Allele constructed	Primer identification	Primer sequence
cig1DΔdis	CIG-drup-F	CAAGGGCTTTTCAACCCTGT
	CIG-drup-R	AGTACTTCGGCATCCACTTGAC
cig1D:NEO	CIG1D-1F	AACAATGTACTGACCTTTCCATACC
	CIG1D-3R	AATTCTGCAGATATCCATCACACTGGCGGCGGAA TTAATATTGGAAGTTGTCGTG
	CIG1D-4F	AATTCCAGCACACTGGCGGCCGTTACTAGTCGAT GAGAGTTATTCATTTTCACCT
	CIG1D-6R	GGGATTGCTATTATACCACAGTGAG
	CIG1D-7F	CCCAGTGTTCTGTCCCATCT
	CIG1D-8R	AGGCCAAGGTTCTTGGAAAT
cig1AΔdel	CIG1A-1	TATAGTCATTTTTGAACCAACGACA
	CIG1A-6	ATTCACTGGATCCGTCGGTA
cig1DΔstop	CIG1D-GAL-LA-F	GTCTACTACGGTCTATGTGCTGGAT
	CIG1D-STOP-LA-R2	TGAATGTGAAGCGATTAAAGATTCACATGGTATT CTGTGTGATCGG
	CIG1D-STOP-RA-F2	TACAACGATCACACAGAATACCATGTGAATCTTT AATCGCTTCACATTC
	CIG1D-STOP-R	AGAGTCGATTCAGATCACCAACTT
GAL7p::NAT::CIG1	CIG1D-GAL-LA-R	ACGGCGAGGCGCCGCCAGGCCCCGCCGATCGGT ATTCTGTGTGATCGTTGTAGGC
	CIG1D-GAL-RA-F	AGCTTCACGGCTCAGGCTGAACTTGGATTAATGA TCTTTAATCGCTTCACATTCA
	Nest-CIG1D-STOP-F	GTTTCTTGAAGCTTAACTTGAGGTG
	Nest-CIG1D-STOP-R	TATGAACATATGCCTGATAGTCTCG
GAL7p::NAT	Gal7-CIG1D-F	GCCTACAACGATCACACAGAATACCTAGTGAAGT CGTATTGTCTCTGC
	Gal7-CIG1D-R	TGAATGTGAAGCGATTAAAGATGCATTCTCAGGA GAGAATTGAGTGCTG
NEO	TL2001	ACTAGTAACGGCCGCCAGTGTGCTGGAATT
	TL2002	GCCGCCAGTGTGATGGATATCTGCAGAATT
Transformant screen	colPCR-Rev	GCCACTCGAATCCTGCATGCTTATG

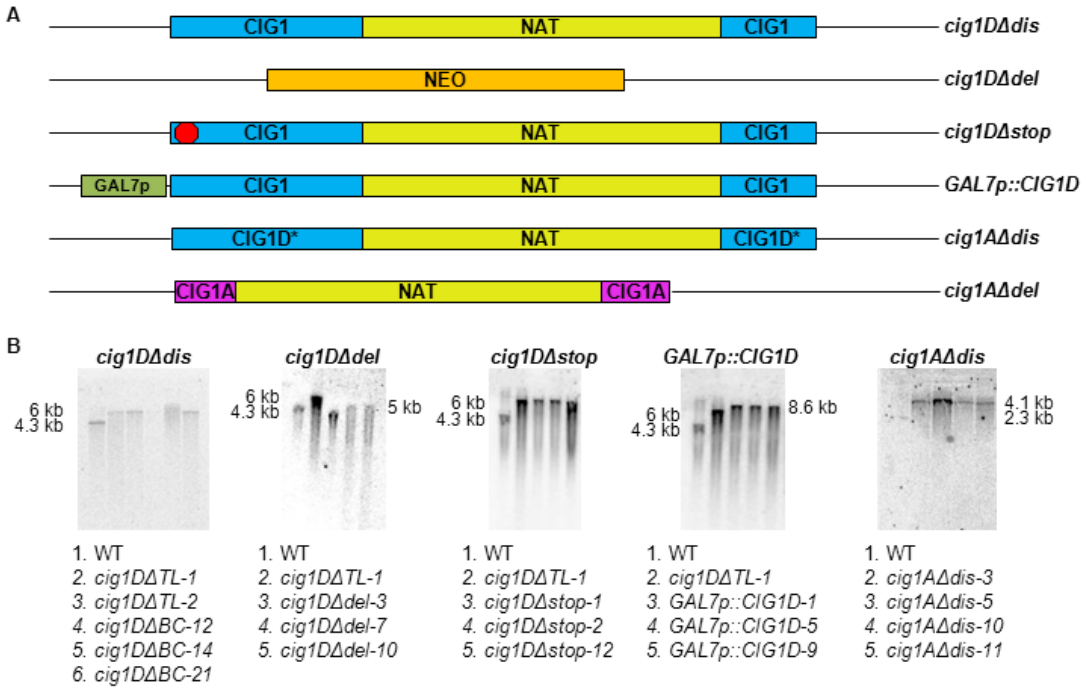

Figure 4.1 Construction and confirmation of mutants. (A) Schematic representation of the constructs generated to create the different mutants used in this study. The coloured boxes represent the indicated open reading frames. NAT and NEO represent the nourseothricin and neomycin resistance cassettes, respectively. The engineered stop codon is represented by the red dot. The galactose-regulated promoter, GAL7p, is in green. Note that the *cig1AΔdis* strain contains the disrupted allele transferred from the *cig1DΔTL* mutant as indicated by the CIG1D* segments. (B) Southern blot analyses were performed to confirm disruption and deletion of *CIG1*, insertion of the engineered stop codon, insertion of the *GAL7* promoter in *C. neoformans* var. *neoformans* and disruption of *CIG1* in *C. neoformans* var. *grubii*. In the first four panels, genomic DNA of the indicated strains was digested with HindIII. In the last panel, genomic DNA from the indicated strains was digested with NcoI. In all cases, the digested DNA was hybridized with a probe amplified from the DNA sequence downstream of the *CIG1* open reading frame.

4.2.2.1. Construction of the *cig1Δ* mutant and complemented strains

The *CIG1* disruption mutant *cig1DΔTL* and the *CIG1* complemented strain *cig1DΔ::CIG1* in *C. neoformans* var. *neoformans* (serotype D) strain B3501A were described by Lian *et al.* (2005). The mutation in the *cig1DΔTL* strain (prepared by Tian Lian) is referred to as a disruption allele because the *NAT* resistance marker was inserted into the gene without deletion of the open reading frame. The *cig1DΔBC* strain (prepared by Brigitte Cadieux) was prepared

by amplifying the *cig1:NAT* disruption allele from the *cig1DΔTL* strain using primer CIG-drup-F and CIG-drup-R. The construct was introduced into strain B3501A by biolistic transformation (Toffaletti *et al.*, 1993) and transformants were screened by colony PCR using primers CIG1D-7F and colPCR-Rev. All transformants in which the wild-type allele was replaced were confirmed by hybridization to genomic DNA blots with a probe amplified using primers CIG1D-1F and CIG1D-3R (Figure 4.1B). The transformant *cig1DΔBC-12* was used for further studies.

To construct the *cig1DΔdel* strain, a *cig1D:NEO* deletion allele was prepared by overlap PCR using the methods described by Davidson *et al.* (2002) and Yu (2004). In the first round of PCR, the 871 bp sequence upstream of the 5' end of the *CIG1* gene was amplified from genomic DNA from strain B3501A with primers CIG1D-4F and CIG1D-6R, and the 941 bp sequence downstream of *CIG1* was amplified with primers CIG1D-1F and CIG1D-3R. The 1,970 bp sequence of the *NEO* gene was amplified from plasmid pJAF1 with primers TL2001 and TL2002. The nested primers CIG1D-7F and CIG1D-8R were then used to overlap the three products to yield the 4,099 bp *cig1:NEO* knock-out construct. The construct was introduced into strain B3501A by biolistic transformation to generate the *cig1DΔBC* strain. The resulting transformants were screened by colony PCR using primers CIG1D-1F and colPCR-Rev. All transformants in which the wild-type allele was replaced were confirmed by hybridization to genomic DNA blots with a probe amplified from genomic B3501A DNA using primers CIG1D-1F and CIG1D-3R (Figure 4.1B). The transformant *cig1DΔdel-7* was used for further studies.

Construction of the *cig1AΔdel* and complemented strains in the H99 background were described in Chapter 2. Construction of the *cig1AΔdis* strain was done by amplifying the *cig1:NAT* disruption allele from the *cig1DΔTL* strain using primer CIG-drup-F and CIG-drup-R and the construct was introduced into strain H99 by biolistic transformation. Transformants

were screened by colony PCR using primers CIG1A-6 and colPCR-Rev. All transformants in which the wild-type allele was replaced were confirmed by hybridization to genomic DNA blots with a probe amplified using primers CIG1A-1 and CIG1D-3R (Figure 4.1B). The transformant *cig1AΔdis-10* was used for further studies.

4.2.2.2. Construction of the *cig1DΔstop* strain

The *cig1DΔstop* allele was prepared by inserting the stop codon, TGA, immediately after the start codon ATG in the *CIG1D* disruption construct using overlap PCR. Specifically, the 892 bp sequence upstream of the *CIG1* gene was amplified from genomic DNA isolated from the *cig1DΔTL* strain with primers CIG1D-GAL-LA-F and CIG1D-STOP-LA-R2. The CIG1D-STOP-LA-R2 primer was designed to include the sequence of the start codon for the *CIG1* gene followed by the stop codon. The 3,378 bp sequence of the *cig1:NAT* disruption allele, including the sequence downstream of the *CIG1* gene, was amplified from genomic DNA from the *cig1DΔTL* strain using primers CIG1D-STOP-RA-F2 and CIG1D-STOP-R. The nested primers were then used to overlap the two products and yield the 4,037 bp construct. The construct was introduced into the B3501A wild-type strain by biolistic transformation and the transformants were screened by colony PCR using primers CIG1D-STOP-R and colPCR-Rev. All transformants in which the wild-type allele was replaced were confirmed by hybridization to genomic DNA blots with a probe amplified from genomic B3501A DNA using primers CIG1D-1F and CIG1D-3R (Figure 4.1B). The transformant *cig1DΔstop-1* was used for further studies.

4.2.2.3. Construction of the galactose-regulated *CIG1D* strain

The *GAL7p::NAT::CIG1* allele was constructed by overlap PCR. The sequence upstream of the 5' end of the *CIG1* gene was amplified from genomic DNA from the *cig1DΔTL* strain using the primers CIG1D-GAL-LA-F and CIG1D-GAL-LA-R, and the *cig1D:NAT* disruption allele was amplified with primers CIG1D-GAL-RA-F and CIG1D-STOP-R. The *NAT::GAL7p* allele was amplified from strain *GAL7p::PKA1* kindly provided by Dr. J. Choi (Choi *et al.*, 2012) with primers Gal7-CIG1D-F and Gal7-CIG1D-R. The nested primers Nest-CIG1D-STOP-F and Nest-CIG1D-STOP-R were then used to overlap the three products to yield the 5.2 kb *GAL7p::NAT::CIG1* allele. The construct was introduced into the *C. neoformans* var. *neoformans* strain B3501A by biolistic transformation to generate the *GAL7p::CIG1D* regulated strains. Transformants were screened by colony PCR using primers CIG1D-STOP-R and colPCR-Rev and confirmed by hybridization to genomic DNA blots with a probe amplified from genomic B3501A DNA using primers CIG1D-1F and CIG1D-3R (Figure 4.1B). The transformant *GAL7p::CIG1D-1* was used for further studies.

4.2.3. Quantitative RT-PCR

To examine gene expression, the cells were grown in LIM (with either glucose or galactose as the carbon source as indicated) for 6 hours at 30°C with shaking. Total RNA was extracted using the RNeasy kit (Qiagen), treated with DNase (Qiagen) and cDNA was synthesized using the SuperScript First Strand System (Invitrogen) following the manufacturers' recommendations. PCR reactions were monitored using the 7500 system (Applied Biosystems) as described previously (Tangen *et al.*, 2007), while the primers used were designed using

Primer Express software 3.0 (Applied Biosystems) and are listed in Table 4.3. The relative gene expression was quantified using the SDS software 1.3.1 (Applied Biosystems), based on the $2^{-\Delta\Delta CT}$ method (Livak and Schmittgen, 2001). The average Ct of 18S rRNA was used for normalization.

Table 4.3. Primers used for quantitative RT-PCR

Primer identification	Primer sequence	Target Gene
CIG1D-RT-F	GCCGTCATCGCTGGCTTA	*CIG1D*
CIG1D-RT-R	TGCTTCTTCTTGCCAAAACGA	*CIG1D*
18S-RT-F	AACAGGTCTGTGATGCCCTTAGA	18S rRNA
18S-RT-R	ACTCGCTGGCTCAGTCAGTGT	18S rRNA

4.2.4. Capsule assay

Cells pre-grown in YPD were washed twice with low iron water, diluted to 4 x 10^6 cells/mL in LIM and grown for 24 hours at 30°C. The cells were then resuspended in $1/10^{th}$ volume of LIM, mixed 1:1 in india ink and visualized by negative staining on a Zeiss Axioplan 2 Imaging microscope.

4.2.5. Growth in LIM supplemented with heme

Cells pre-grown in YPD were washed twice with low iron water, inoculated into LIM at 4 x 10^6 cells/mL and grown at 30°C for two days to starve the cells for iron. After starvation, the cells were harvested, washed and inoculated in LIM supplemented with 10 µM heme (porcine hemin; Sigma) to a final concentration of 5 X 10^4 cells/mL. Cultures were incubated at 30°C and growth was monitored by measuring the optical density at 600 nm using a DU530 Life Science UV/Visible spectrophotometer (Beckman Instruments).

4.2.6. Plate assays

Cells pre-grown in YPD were washed once with water and resuspended at 1 x 10^6 cells/mL in water. Ten-fold serial dilutions were made in water and 5 µL of each dilution were plated on YPD with and without agents that challenge the cell wall integrity: 0.5 mg/mL caffeine (Sigma), 0.0075% sodium dodecyl sulfate (SDS; Sigma) and 0.5% congo red (Sigma), with and without secretion inhibitors: 25 µg/mL brefeldin A (BFA; LC Laboratories), 0.625 µg/µL monensin (Sigma), 625 µM N-ethyl maleimide (NEM; Sigma) and with and without 1.2 M NaCl or 1.2 M sorbitol; 2% agar (Sigma) was added as the solidifying agent. Plates were incubated for three days at 30°C or 37°C as indicated and then photographed.

4.2.7. *In silico* analysis

The predicted *CIG1* DNA sequence (CNC01660) was retrieved from the National Center for Biotechnology Information (http://www.ncbi.nlm.nih.gov/gene/3256784). Genomic DNA was isolated from *C. neoformans* strain B3501A and amplified with the primers listed in Table 4.4. The amplified DNA samples were sent for sequencing at the NAPS Unit at the University of British Columbia. The predicted and confirmed DNA sequences were aligned using Clustal W (http://www.ebi.ac.uk/clustalw/). The Sequence Manipulation Suite was used to predict translation of the DNA sequence (http://bioinformatics.org/sms2/translate.html).

Table 4.4. Primers used for amplifying and sequencing the DNA

Primer identification	Primer sequence
CIG-Adj-3F	ACGTCCTTCGGTTGAGTCAG
CIG-Adj-4R	GCCCCTGACCAAGGTGTT
CIG-Adj-5F	GTACGAGACGACCACGAAGC
CIG-Adj-6R	AGACATGAGGGTTGGTGGAG
CIG-Adj-7F	TTCCGAGCTTGAGATTGCTT
CIG-Adj-8R	CCCAGTGTTCTGTCCCATCT

4.2.8. Total protein secretion assay

Cells pre-grown in YPD were washed twice with water and inoculated in YNB to a final concentration of 5 x 10^5 cells/mL. The cultures were grown for four days at 30°C with shaking and the culture supernatant was harvested by centrifugation (13,500 x g, 1 minute, 25°C). The total amount of proteins secreted in the culture supernatant was measured using the Bio-Rad Protein Assay (Bio-Rad) and normalized to the number of cells in the culture.

4.2.9. Protease assay

Protease activity was monitored by comparing the size of the clearance zones surrounding cells grown on azoalbumin (Choi *et al.*, 2012; Chen *et al.*, 1996). Briefly, cells pre-grown in YPD were harvested by centrifugation (13,500 x g, 1 minute, 25°C), washed once with water and resuspended at 1 x 10^7 cells/mL in water. Five µL were plated on minimal agar media containing 0.1% azoalbumin (Sigma-Aldrich). The plates were incubated for seven days at 30°C and then photographed.

4.2.10. Secretion of extracellular vesicles

Cells pre-grown in YPD were washed in water and inoculated in 500 mL YNB to a final concentration of 5 x 10^5 cells/mL. Cultures were grown for four days at 30°C with shaking. The extracellular vesicles were isolated from the culture supernatant as described by Rodrigues *et al.*, (2007) with minor modifications. Briefly, the culture supernatant was harvested by centrifugation, and the extracellular vesicles were directly isolated by ultracentrifugation (100,000 x g, 1 hour, 4°C). The extracellular vesicles secreted by each strain were compared using thin layer chromatography (TLC; Oliveira *et al.*, 2009). The vesicles were washed once

with water and resuspended in a solution of chloroform/ methanol/water (8:4:3) to extract the lipid fraction. The organic phase was dried at room temperature and resuspended in 50 µL of chloroform/methanol (2:1) solution. The lipid extracts were loaded onto a TLC silica plate and separated using a hexane/ether/acetic acid (20:10:0.5) solvent solution. The plate was then sprayed and developed as described (Oliveira *et al.*, 2009). Densitometric analysis using ImageJ (rsbweb.nih.gov/ij) was performed to quantitate the relative amount of ergosterol in each lane.

4.3. Results

4.3.1. Complementation of the *cig1DΔ* mutation resulted in an enlarged capsule and overexpression of *CIG1*

Previously, Lian *et al.* (2005) had described altered capsule production in response to iron for the *cig1DΔTL* mutant. Typically, *C. neoformans* produces a larger capsule in low iron conditions. Although no significant differences were observed in the capsule size of the *cig1DΔTL* mutant compared to the wild-type strain in LIM, Lian *et al.* (2005) found that the *cig1DΔTL* mutant produced a larger capsule than the wild-type strain in presence of iron. This experiment was repeated to confirm these observations and similar results were obtained (Figure 4.2A). Interestingly, the inclusion of the complemented strain in the experiment revealed that this strain produced an enlarged capsule compared to the wild-type strain in both low iron and iron-replete conditions. Considering the possible link between the role of Cig1 and regulation of capsule size suggested by the results of Lian *et al.* (2005), the expression of *CIG1* in the wild-type and complemented strains was measured by quantitative RT-PCR (Figure 4.2B). Expression of *CIG1* was significantly higher (> 150 times) in the complemented strain compared to the wild-type strain, further supporting a possible link between Cig1 and the control of capsule size. However, upon further investigation, it was found that the transformation event that yielded the complemented strain resulted in ectopic integration of the complementation construct into another gene (*CNBE3170*) leading to its disruption (Dr. G. Hu, personal communications). Specifically, insertion of the transformation construct resulted in deletion of the last 694 bp of the gene. This region represents approximately half of the sequence encoding the protein and corresponds to the C-terminal portion of the protein. Although *CNBE3170* encodes a hypothetical protein of unknown function, it is possible that disruption of this gene also

contributes to the enlarged capsule phenotype and/or overexpression of *CIG1*. Therefore, the phenotypes of the complementation strain must be interpreted cautiously.

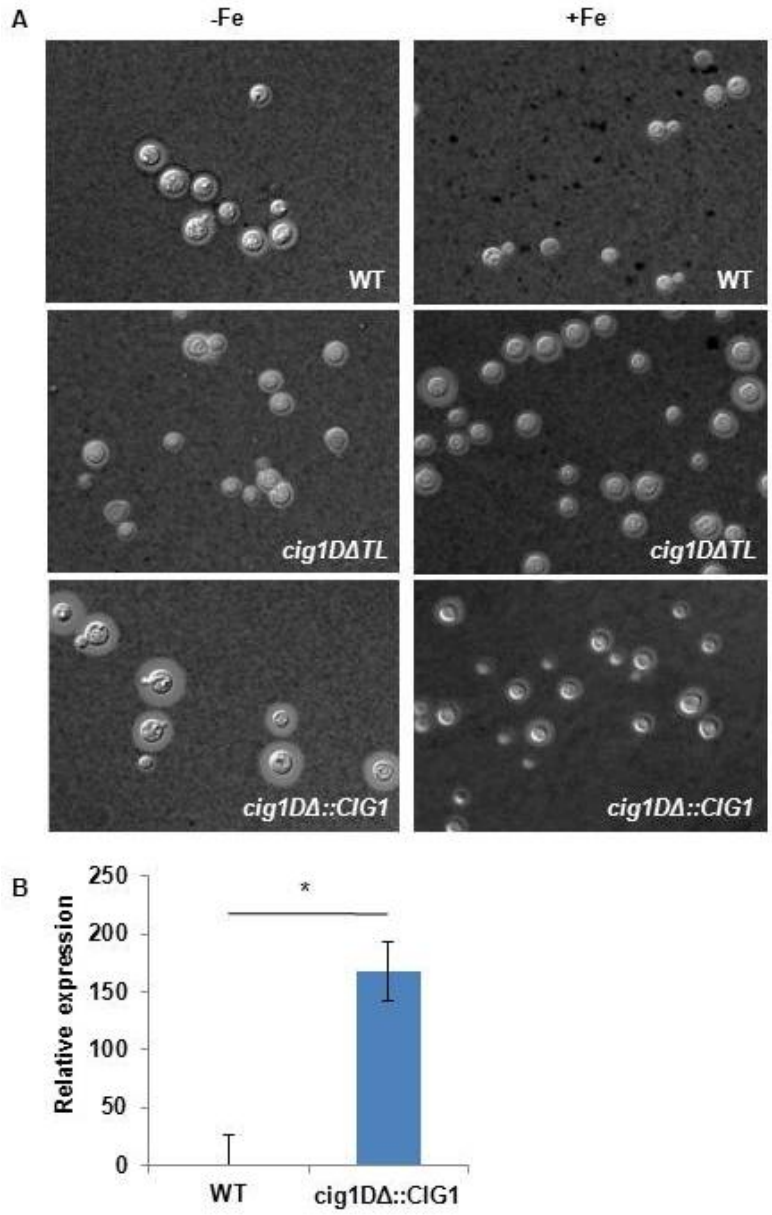

Figure 4.2 Complementation of the *cig1DΔ* mutation results in enlarged capsule and overexpression of *CIG1*. (A) Cells were grown in LIM +/- 100 µM $FeCl_3$, harvested and negatively stained with India ink before visualizing by differential interference contrast microscopy. (B) Expression of *CIG1* in the wild-type and complemented strains grown in LIM. All experiments were repeated three times and the data are plotted as the average ± SD. The * represents a significant difference at $P < 0.0005$.

4.3.2. Construction of additional strains with mutated alleles of *CIG1* in *C. neoformans* var. *neoformans*

As described in the previous section, complementation of the *cig1DΔ* mutant resulted in the unexpected phenotype of an enlarged capsule and, therefore, the strain could not be used as a control to confirm that the phenotypes observed with the mutant resulted from mutation of the *CIG1* gene. Although other complemented strains were generated, none of them reverted the phenotypes to those of the wild-type strain. An accepted alternative is to use independent mutants to confirm that loss of a particular gene causes the observed phenotypes. Therefore, two additional independent mutants were constructed. One of these mutants, *cig1DΔBC*, consisted of a disruption of the *CIG1* gene with the identical construct used for the *cig1DΔTL* mutant, which resulted in partial deletion of the *CIG1* gene. The second mutant, *cig1DΔdel*, was constructed to have a complete deletion of the *CIG1* gene. These three mutants (*cig1DΔTL, cig1DΔBC* and *cig1DΔdel*) were used in all subsequent studies along with the wild-type and complemented strains.

4.3.3. Cig1 also plays a role in heme acquisition in *C. neoformans* var. *neoformans*

Given that Cig1 plays an important role in heme utilization in *C. neoformans* var. *grubii*, the possibility that Cig1 plays a similar role in *C. neoformans* var. *neoformans* was examined. Growth of the *cig1DΔ* mutants in LIM with added heme as a sole iron source was monitored by measuring the optical density and compared to the wild-type and complemented strains (Figure 4.3). Not surprisingly, all of the *cig1DΔ* mutants had a growth defect in LIM supplemented with heme similar to that of the *cig1Δ* mutant in *C. neoformans* var. *grubii*. However, the growth defect of the *cig1DΔTL* and *cig1DΔBC* mutants was more severe because the cells still remained

in lag phase after 96 hours, compared to a lag phase of 60 hours for the *cig1DΔdel* mutant and the *cig1Δ* in *C. neoformans* var. *grubii* (compare Figures 4.3 and 2.6D). The wild-type strain reached stationary phase by 48 hours of growth while the complemented strain partially allowed the cells to recover, remaining in lag phase for 60 hours before starting to grow. An unusual behaviour of the complemented strain was again observed because addition of the wild-type copy of *CIG1* to the mutant *cig1DΔTL* improved growth in LIM supplemented with heme, but growth was not restored to the level of the wild-type strain. Overall, these results indicate that *CIG1* also plays a role in heme acquisition in *C. neoformans* var. *neoformans*.

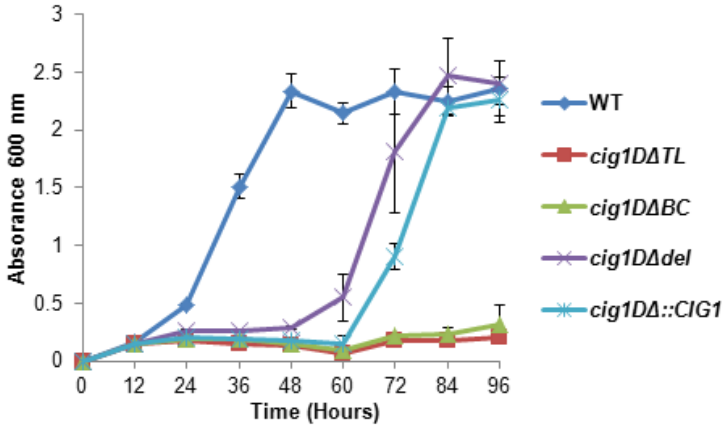

Figure 4.3 Cig1 in *C. neoformans* var. *neoformans* is required for growth in LIM supplemented with heme. Growth of iron-starved cells in LIM + 10 µM heme was monitored by measuring the optical density at 600 nm. The experiment was repeated three times and the data are plotted as the average ± SD.

4.3.4. Disruption of *CIG1* results in increased susceptibility to secretion inhibitors in *C. neoformans* var. *neoformans*, but not in var. *grubii*

The overexpression of *CIG1* and enlarged capsule phenotype of the complemented strain, as well as the larger capsule on the *cig1DΔTL* mutant when grown in iron-replete medium led to the hypothesis that Cig1 may play a role in secretion. For example, it is possible that the

function of one or more secretory pathways is perturbed when changes occur to Cig1 expression levels. To examine whether Cig1 influences secretion, the wild-type strain, the different *cig1DΔ* mutants and the complemented strain in *C. neoformans* var. *neoformans* were serially diluted and plated on media containing different secretion inhibitors (Figure 4.4). The *cig1DΔTL* and *cig1DΔBC* mutants were found to be more susceptible than the wild-type strain to BFA, an agent that arrests the anterograde transport between the ER and Golgi (Misumi *et al.*, 1986; Fujiwara *et al.*, 1988; Orci *et al.*, 1991; Betina, 1992). These mutants were also susceptible to monensin, an agent which blocks intracellular transport in both the trans-Golgi and post-Golgi compartments, thereby preventing glycoprotein secretion (Tartakoff and Vassalli, 1977; Uchida *et al.*, 1979; 1980; Griffiths *et al.*, 1983; Tartakoff, 1983). Finally, the mutants were slightly more susceptible than the wild-type strain to NEM, which inhibits protein transport between successive compartments of the Golgi stack by inactivating the Golgi membranes (Nelson and Taiz, 1989). It is interesting to note that the *cig1DΔBC* mutant was susceptible but consistently less so than the *cig1DΔTL* mutant. Also, the *cig1DΔdel* mutant did not show susceptibility to any of the secretion inhibitors tested suggesting that a complete loss of Cig1 protein eliminated the influence on secretion. Remarkably, the complemented strain, which has been shown to overexpress the *CIG1* transcript, was susceptible to BFA suggesting that overexpression of Cig1 could impact the anterograde transport between the ER and Golgi. However, caution is needed when interpreting the results involving the complemented strain given the possibility of an additional defect in this strain. Overall, these results suggest that perturbations of Cig1 lead to impairment of the secretory pathway as revealed by growth inhibition when the pathway is challenged.

The role of Cig1 in secretion was also evaluated in *C. neoformans* var. *grubii*. In this background, the *cig1AΔdel* and *cig1AΔdis* mutants did not show susceptibility to any of the secretion inhibitors tested suggesting that Cig1 does not influence secretion in this background (Figure 4.4B).

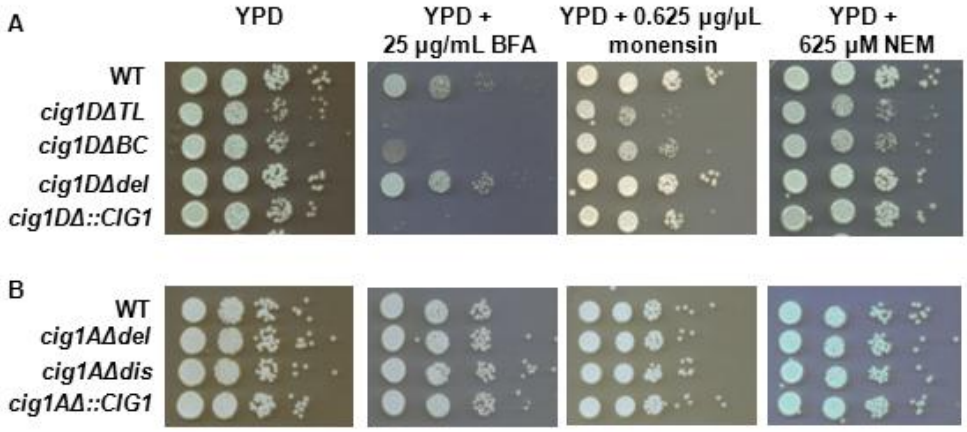

Figure 4.4 Disruption of *CIG1* results in susceptibility to secretion inhibitors in *C. neoformans* var. *neoformans* but not in var. *grubii*. Ten-fold serial dilutions of *C. neoformans* var. *neoformans* strains (A) and *C. neoformans* var. *grubii* strains (B) grown in YPD were spotted onto YPD with and without secretion inhibitors at the concentration indicated. The plates were incubated at 30°C for three days and photographed. The experiments were repeated three times and a representative photograph is shown.

4.3.5. Disruption of *CIG1* results in a defect in cell wall integrity in *C. neoformans* var. *neoformans* but not in var. *grubii*

Defects in the secretory pathway often lead to changes in cell wall integrity due to the improper delivery of proteins, polysaccharides, or lipids involved in cell wall synthesis. The role of Cig1 in cell wall integrity was therefore tested by plating ten-fold serial dilutions of the different strains on media containing agents that challenge the cell wall or agents that cause osmotic stress. In *C. neoformans* var. *neoformans*, the *cig1DΔTL* and *cig1DΔBC* mutants showed a growth defect at 37°C and had slower growth than the wild-type strain in presence of

agents that challenge the cell wall, including caffeine, congo red and SDS (Figure 4.5). Additionally, the mutants grew slower than the wild-type strain in presence of NaCl, which presents a salt and osmotic stress, but not in presence of sorbitol. In a similar manner to growth in presence of secretion inhibitors, the *cig1DΔdel* mutant did not show susceptibility to any of the stresses tested, while the complemented strain was more sensitive than the wild-type strain to growth in presence of congo red, SDS, and NaCl. In terms of complementation of the *cig1DΔTL* mutant, the *cig1DΔ::CIG1* strain showed reduced susceptibility on caffeine, congo red (slight) and at 37°C, but no difference on SDS or NaCl. Overall, these results point to a role for Cig1 in maintaining cell wall integrity, thereby conferring resistance against various stresses, specifically high temperature and osmotic stress. Further investigation will be required to determine whether Cig1 plays a direct role in maintaining cell wall integrity or if susceptibility to the different stresses arose from an influence on the secretory pathway.

The mutants in *C. neoformans* var. *grubii* did not show altered susceptibility to any of the stresses tested (Figure 4.5B) indicating that Cig1 does not play a role in maintaining cell wall integrity in this background.

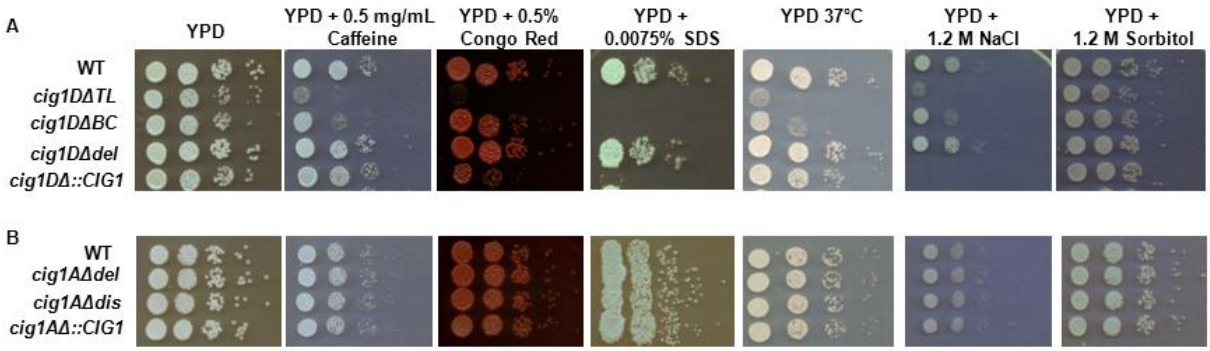

Figure 4.5 Disruption of *CIG1* results in susceptibility to agents that challenge the cell wall in *C. neoformans* var. *neoformans* but not in var. *grubii*. Ten-fold serial dilutions of *C. neoformans* var. *neoformans* strains (A) and *C. neoformans* var. *grubii* strains (B) grown in YPD were spotted onto YPD with and without agents that challenge the cell wall at the concentration indicated. The plates were incubated at 30°C or 37°C for three days and photographed. The experiments were repeated three times and a representative photograph is shown.

4.3.6. Evidence that expression of a truncated Cig1 peptide influenced susceptibility to secretion inhibitors, agents that challenge the cell wall, heat and osmotic stress

The fact that the *cig1DΔTL* and *cig1DΔBC* disruption mutants showed increased susceptibility to secretion inhibitors as well as to agents that challenge the cell wall and different stresses, while the *cig1DΔ* deletion mutant did not, led to the hypothesis that the disruption allele might represent a gain of function mutation. The construct was therefore amplified from the *cig1DΔTL* mutant and sequenced to confirm that the predicted sequence was in fact correct and that no mutation had occurred during cloning and transformation. The construct proved to be correct as predicted except for one amino acid substitution in the 5^{th} codon that changed the predicted arginine to a histidine (Figure 4.6A). In addition, the sequence analysis confirmed that the disruption construct could potentially encode a truncated polypeptide (Figure 4.6B-C). This truncated polypeptide would be 150 amino acids in length and encoded by exons 1, 2, 3, and a small portion of exon 4. Thus, it is possible that the expression of a Cig1 truncated polypeptide

in the *cig1DΔTL* and *cig1DΔBC* disruption mutants, but not in the *cig1DΔ* deletion strain, could explain the phenotypic differences between the mutants.

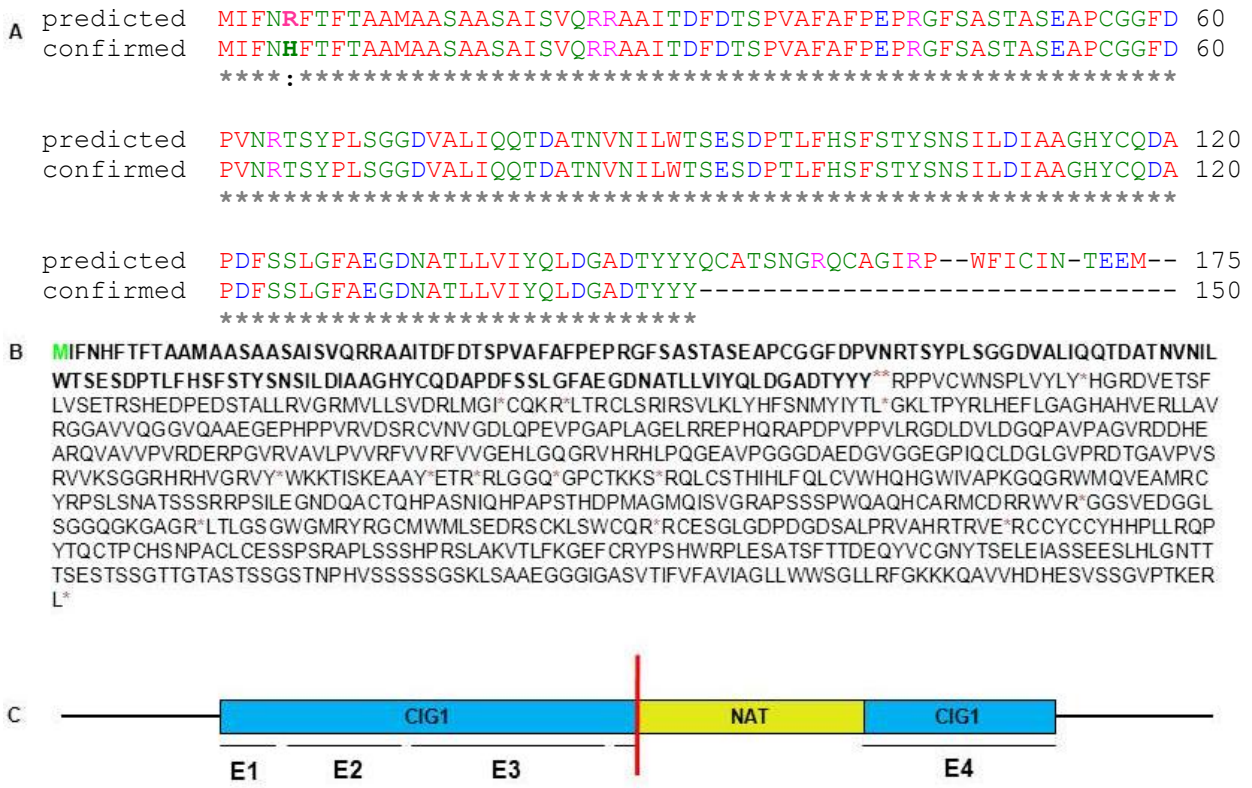

Figure 4.6 The *cig1DΔ* disruption mutants express a truncated polypeptide. (A) Multiple sequence alignment comparing the predicted sequence of the wild-type Cig1 and confirmed sequence encoded by the *cig1DΔTL* construct. The * indicates identical amino acids and : indicates a difference between amino acids. (B) Amino acid sequence of the *cig1DΔTL* construct. The green M is the start codon, while the red * indicates the stop codons. The sequence in bold letters represents the predicted sequence of the expressed truncated polypeptide. (C) Schematic representation of the *cig1DΔTL* construct. The coloured boxes represent the indicated open reading frames. The gray lines under the boxes represent the portions of the exons of the *CIG1* gene. The red line represents the predicted end of the coding region of the truncated polypeptide.

Two additional strains, *GAL7p::CIG1D* and *cig1DΔstop*, were constructed to further investigate the possibility that a truncated polypeptide was expressed and conferred phenotypes on *C. neoformans*. The first strain was constructed to control expression of the disrupted *cig1DΔ*

construct via regulation by the *GAL7* promoter described in Chapter 3. In presence of glucose, the truncated polypeptide should not be expressed and a phenotypic difference might be observed compared with the *cig1DΔTL* and *cig1DΔBC* strains. That is, if the truncated polypeptide is the reason for the detected increased susceptibility to secretion inhibitors, agents that challenge the cell wall, and osmotic stress then no difference in susceptibility should be observed on glucose. However, in the presence of galactose, the truncated polypeptide should be expressed resulting in increased susceptibility to those stresses. Quantitative RT-PCR analysis of *CIG1* expression confirmed the expected carbon source regulation of the *GAL7p::CIG1* construct in the *GAL7p::CIG1D* strain (Figure 4.7A). The second strain, *cig1DΔstop*, was engineered to have a stop codon exactly after the start codon in the disrupted *cig1DΔ* construct thus eliminating translation of the truncated Cig1 polypeptide. This strain would be expected to behave exactly like the *cig1DΔdel* mutant and not have increased susceptibility to any of the chemicals tested.

As in sections 4.3.4. and 4.3.5., all of the strains pre-grown in YPD were serially diluted and plated on media containing different secretion inhibitors, agents that challenge the cell wall, as well as osmotic stressors. As expected, the *GAL7p::CIG1D* strain did not show susceptibility to any of the stresses tested when grown in glucose (Figure 4.7B). Similarly, the *cig1DΔstop* strain did not show susceptibility to any of the agents. Together, these results support the conclusion that expression of the Cig1 truncated polypeptide resulted in the increased susceptibility to secretion inhibitors, agents that challenged cell wall integrity, heat and osmotic stress.

Interestingly, the results were markedly different when the cells were grown in galactose (Figure 4.7C). In these conditions, the *cig1DΔ* disruption mutants (*cig1DΔTL and cig1DΔBC*)

were generally less susceptible to the agents tested, compared to when the cells were grown in glucose, and all strains grew to a similar level as the wild-type strain. However, the complemented strain was still susceptible to BFA and more resistant to SDS. Quantitative RT-PCR analysis of *CIG1* expression in the wild-type strain reveals that growth in galactose reduces expression of *CIG1* relative to growth in glucose (Figure 4.7A), as was seen in *C. neoformans* var. *grubii* described in Chapter 3. Hence, the change in *CIG1* expression in galactose could explain the observed differences in phenotypes.

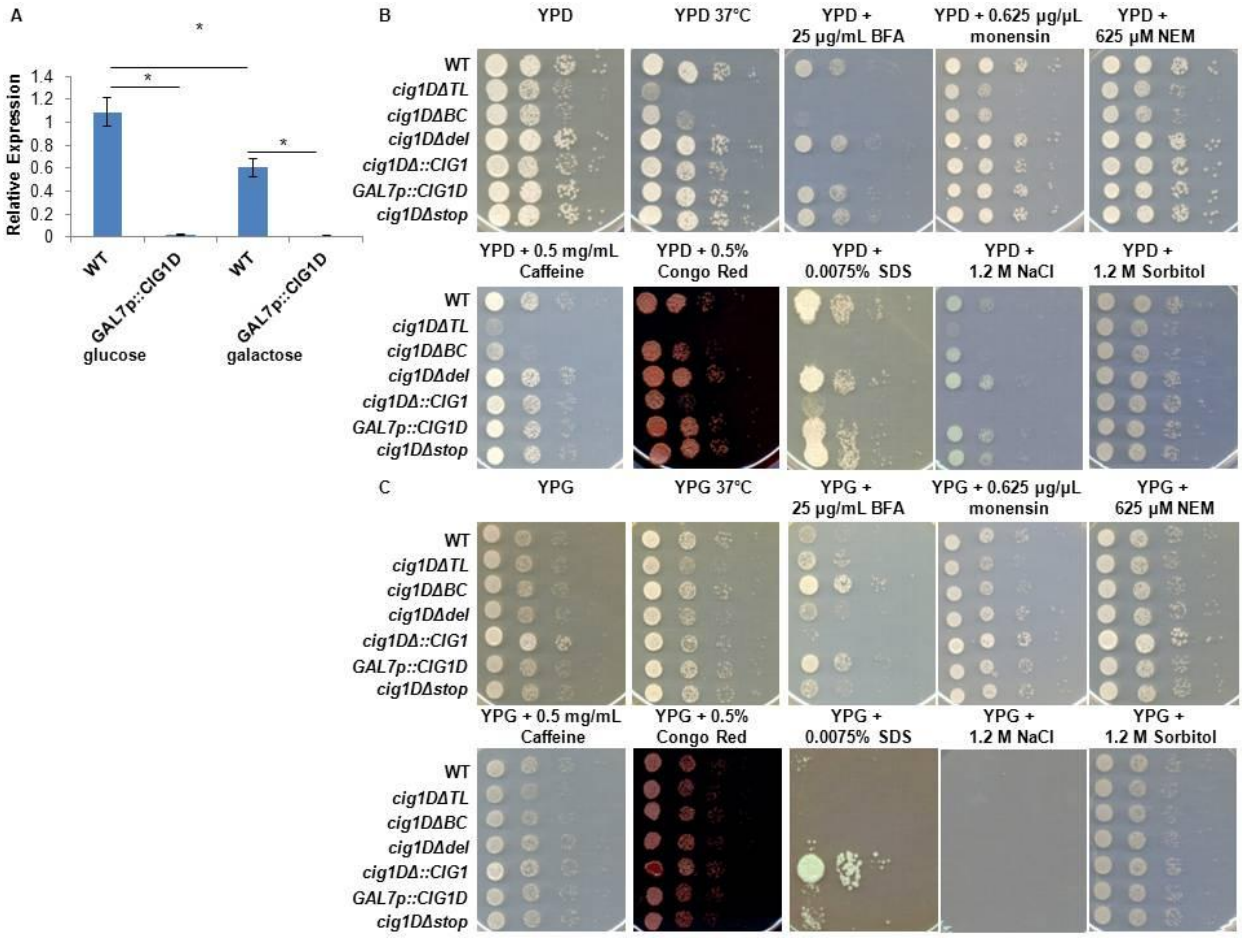

Figure 4.7 Expression of a Cig1 truncated polypeptide results in increased susceptibility to secretion inhibitors, agents that challenge the cell wall, heat and osmotic stress. (A) Expression of *CIG1* in the wild-type and *GAL7p::CIG1D* strains grown in LIM with glucose or galactose as indicated. The experiment was repeated three times and the data are plotted as average ± SD. The * represents significant differences at $P < 0.005$. (B-C) Ten-fold serial dilutions of *C. neoformans* var. *neoformans* strains grown in YPD with glucose (B) or galactose (C) were spotted onto YPD or YPG, respectively with and without secretion inhibitors and agents that challenge the cell wall at the concentration indicated. The plates were incubated at 30°C or 37°C for three days and photographed. The experiments were repeated three times and a representative photograph is shown.

4.3.7. Cig1 may influence the export of total proteins, proteases and extracellular vesicles

The role of Cig1, and the truncated polypeptide, in secretion in *C. neoformans* var. *neoformans* was examined further. Initially, the total amount of protein secreted by the mutants was measured and compared to the amount of protein secreted by the wild-type strain (Figure

4.8A). Approximately 1.5 times more protein was measured in the supernatants of the *cig1DΔTL*, *cig1DΔBC*, *cig1DΔdel*, *GAL7p::CIG1D* and *cig1DΔstop* mutants compared to the wild-type and complemented strains, possibly suggesting increased secretion by the mutants, however the difference is not statistically significant.

The protease activity of the different strains was also evaluated by plating the cells on azoalbumin medium. Once proteases are secreted, they degrade the albumin to create a halo of clearing surrounding the colonies. Therefore, the size of the cleared zone is indicative of the amount of secreted protease activity. A clearing zone was observed around all of the strains tested and appeared to be of similar size, except the one around the *cig1DΔTL* mutant was larger (Figure 4.8B). It is not clear why the *cig1DΔTL* strain would secrete more protease activity than the wild-type strain, and these results indicated that additional, more quantitative assays are needed to examine differences between the strains.

Finally, the relative quantity of extracellular vesicles that accumulated in the culture supernatant of each strain was examined and compared by TLC as another method to evaluate the influence of Cig1 on export (Figure 4.8C). Ergosterol has been shown to be present in the membranes of extracellular vesicles and therefore serves as a marker for determining the relative quantity of vesicles. Similar amounts of ergosterol were detected in the wild-type strain and most of the *cig1DΔ* mutants indicating that similar numbers of extracellular vesicles were secreted by the different strains. However, significantly more ergosterol was detected in the lipid extract isolated from the culture supernatant of the complemented strain suggesting an increased number of extracellular vesicles secreted by this strain.

Overall, these first experiments suggest that Cig1 may influence the export of proteins and lipids to the extracellular environment. However, more quantitative work will be needed to better understand the contribution of Cig1 in secretion and the mechanisms involved.

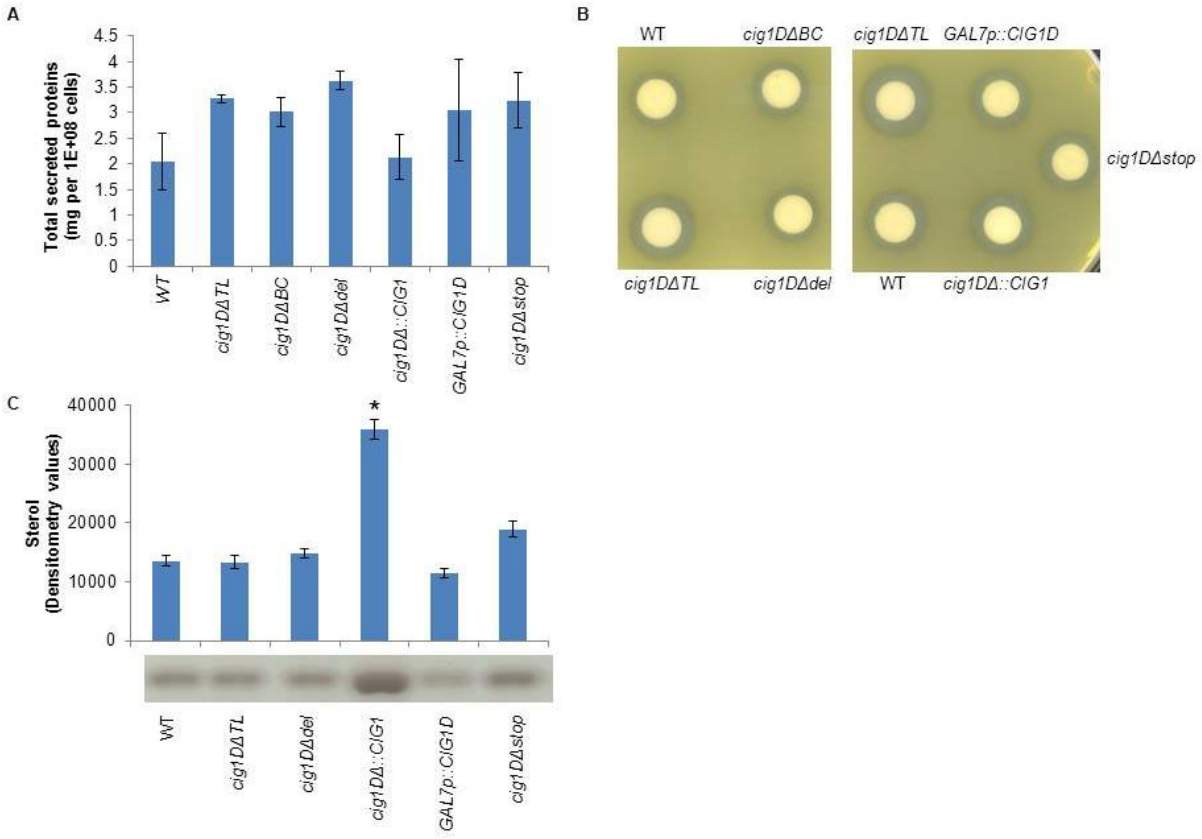

Figure 4.8 Cig1 influences secretion of proteins and extracellular vesicles. (A) Total secreted proteins were measured in the culture supernatant of cells grown for 4 days in YNB. Protein concentrations were determined by Bradford assay and normalized to the total number of cells. The experiment was repeated three times and the data in the graph are plotted as the average ± SD. (B) Protease activity of cells grown in YPD overnight. Cells were spotted onto azoalbumin media and the plates were incubated at 30°C for 7 days and photographed. The experiment was repeated three times and a representative photograph is shown. (C) Relative quantity of extracellular vesicles based on detection of ergosterol by TLC. The densitometry values serve as an index to compare the relative quantity of extracellular vesicles produced by the different strains. The extracellular vesicles were extracted from the culture supernatant of cells grown in YNB for 4 days. The experiment was repeated two times and the data are plotted as the average ± SD and a representative photograph of the TLC plate is shown. The * represents a significant difference at $P < 0.005$.

Additional data showing the capsule response to iron of the *cig1DΔBC* and *cig1DΔdel* strains (absent from Section 4.3.1) are presented in Appendix E, while growth of the *GAL7p::CIG1D* and *cig1DΔstop* mutants in LIM supplemented with heme (absent from Section 4.3.3) can be found in Appendix F. Briefly, the *cig1DΔBC* mutant responded to iron similarly than the *cig1DΔTL* mutant, that is, both mutants produced a capsule larger than the wild-type strain when grown in presence of iron. In contrast, the *cig1DΔdel* mutant behaved like the wild-type strain (i.e., smaller capsule in presence of iron compared to LIM). When growth of the mutants was compared in presence of heme, both the *GAL7p::CIG1D* and *cig1DΔstop* mutants remained in lag phase for 60 hours, but then initiated exponential phase and reached stationary phase at a similar cell density as the wild-type strain. These results closely resemble the data obtained with the *cig1DΔdel* mutant. A summary of all the phenotypes observed throughout this study is presented in Table 4.5.

Table 4.5 Summary of phenotypes observed with the different strains of *C. neoformans* var. *neoformans*

Assay	WT	*cig1DΔTL*	*cig1DΔBC*	*cig1DΔdel*	*GAL7p::CIG1D*	*cig1DΔstop*	*cig1DΔ::CIG1*
Capsule	+ in LIM	Enlarged on $FeCl_3$	Enlarged on $FeCl_3$*	+ in LIM*	n/t	n/t	Enlarged in LIM
Growth in LIM with heme	+	No	No	slow	slow*	slow*	slow
Secretion inhibitors	R	S	S	R	R	R	S to BFA, R to others
Agents that challenge the cell wall	R	S	S	R	R	R	S
NaCl	R	S	S	R	R	R	S
37°C	R	S	S	R	R	R	+/- S
Secretion of total proteins	+	++	++	++	+/-	++	+
Secretion of proteases	+	++	+	+	+	+	+
Secretion of extracellular vesicles	+	+	n/t	+	+	+	++

+: present; R: resistant; S: susceptible; +/- S: slightly more than wild-type; ++: more than wild-type; n/t: not tested; -: less than wild-type; *: data presented in Appendices E-F

4.4. Discussion

Over the course of this study, evidence was accumulated which suggests a role for Cig1 and/or a Cig1 truncated polypeptide in secretion. For example, the strains expressing a Cig1 truncated polypeptide displayed an increased susceptibility to secretion inhibitors and were more susceptible to agents that challenge the cell wall and to different stresses (i.e., osmotic stress and temperature stress) compared to the wild-type strain. It is possible that Cig1 may also play a role in maintaining cell wall integrity and thereby render the cells resistant to osmotic and heat stress. Alternatively, the cell wall defect observed could be a consequence of compromised secretion of the components necessary for cell wall synthesis and repair. Future studies will be needed to examine the contribution of Cig1 in maintaining cell wall integrity.

The link between the Cig1 truncated polypeptide and secretion was reinforced by the observation that the strain expressing the truncated polypeptide had increased protease activity. Considering that these strains were susceptible to BFA, an agent that arrests the anterograde transport between the ER and Golgi, it would imply that the truncated polypeptide plays a role in the conventional secretory pathway (Misumi *et al.*, 1986; Fujiwara *et al.*, 1988; Orci *et al.*, 1991; Betina, 1992). This would also indicate that the proteases measured in this study are secreted via this pathway. Furthermore, the extracellular vesicles are known to transport proteins, enzymes and lipids and have been proposed to be involved in a secretory pathway separate from the conventional pathway (Rodrigues and Djordjevic, 2012). Indeed, the strains expressing the Cig1 truncated polypeptide secreted the same amount of extracellular vesicles than the wild-type strain suggesting that the non-conventional secretory pathway is not affected by the truncated polypeptide. Consequently, it is possible that the Cig1 truncated polypeptide may be poisoning or blocking the conventional secretory pathway. According to the sequence information, the

predicted transmembrane domain would be absent from the Cig1 truncated polypeptide. Without this domain, the protein may not reach its proper destination and may result in accumulation of the protein within the secretory pathway leading to inhibition of secretion. Also, the truncated polypeptide would probably be misfolded which could further interfere with the secretory pathway. For example, altered secretion of proteins involved in heme uptake could explain the exacerbated delay in growth in LIM with added heme of the strains expressing the Cig1 truncated polypeptide compared to the *cig1DΔdel* mutant. Further work involving the examination of the localization of the Cig1 truncated polypeptide could potentially help explain the role and mechanism of the truncated polypeptide in secretion. It is important to consider that an alternative explanation for the increased secretion of proteases by the strains expressing the Cig1 truncated polypeptide could be the result of protein leakage from the damaged cell wall rather than actual secretion according to the observation that the mutants were susceptible to agents that challenge the cell wall and different stresses.

Finally, the phenotypes observed with the complemented strain, which overexpresses the *CIG1* transcript, further support a role for Cig1 in secretion. This strain, which overexpresses *CIG1*, produced a larger capsule than the wild-type strain. Additionally, that same strain appeared to export more extracellular vesicles in the culture supernatant, as judged by ergosterol analysis. This is not surprising as the extracellular vesicles have been linked with capsule synthesis and shown to transport the polysaccharides necessary for capsule formation (Yoneda and Doering, 2006; Rodrigues *et al.*, 2007). In some instances, the complemented strain showed phenotypes similar to that obtained with the strain expressing the Cig1 truncated polypeptide. The combined results of expression of *CIG1* in the complemented strain and the growth of the strain in presence of secretion inhibitors suggest that it could produce both wild-type *CIG1* and

the Cig1 truncated polypeptide. Hence, expression of the truncated peptide in the complemented strain may alter the secretory pathway, as evidenced by the impaired growth of the complemented strain in presence of BFA. Furthermore, the altered secretion of proteins involved in heme uptake could explain delay in growth in LIM supplemented with heme of the complemented strain. It is important to note that the complemented strain also contains a disruption of a different gene, *CNBE3170*, encoding a hypothetical protein of unknown function. The phenotypes associated with this strain could be a consequence of overexpressing *CIG1* alone, or of disrupting the *CNBE3170* gene, either alone or in combination with overexpression of *CIG1*, or of disrupting both *CIG1* and the *CNBE3170* gene in the same strain. Future work, including deletion of *CNBE3170* and/or construction of a new *CIG1* overexpressing strain in the wild-type background, will be needed to confirm that the phenotypes observed with the complemented strain are indeed related to the overexpression of *CIG1*.

Interestingly, susceptibility to secretion inhibitors and agents that challenge the cell wall integrity was observed for the *cig1DΔBC* strain, but it was not as severe as for the *cig1DΔTL* mutant. The two mutants were prepared by different people, with approximately five years in between their construction. It is therefore possible that differences accumulated in the wild-type strain during that time could account for differences in severity of the phenotypes. That is, it is possible that a different stock of the B3501A parental strain was employed for the construction of each mutant. *C. neoformans* is well known for phenotypic plasticity and there are anecdotal and published accounts of changes in laboratory stocks over time (Hu *et al.*, 2008; 2011; Ngamskulrungroj *et al.*, 2012; Sionov *et al.*, 2010; Fries *et al.*, 1996; Okagaki *et al.*, 2010; Zaragoza *et al.*, 2010).

No susceptibility to the secretion inhibitors and agents that challenge the cell wall was observed for the *cig1AΔ* mutants in *C. neoformans* var. *grubii*. The difference in phenotypes between the two *Cryptococcus* varieties is not surprising. Although Cig1 from *C. neoformans* var. *neoformans* shares 97.1% similarity and 87.5% identity at the amino acid level with Cig1 from *C. neoformans* var. *grubii*, there are many cases of the same protein having altered functions in different varieties of *C. neoformans*. For example, the catalytic subunit of protein kinase A, Pka1, is involved in mating, haploid fruiting, melanin synthesis and elaboration of the capsule in *C. neoformans* var. *grubii*, but plays no role in these activities in *C. neoformans* var. *neoformans* (Hicks *et al.*, 2004). However, the second catalytic subunit, Pka2, is required for mating, haploid fruiting, melanin and capsule production in *C. neoformans* var. *neoformans* but not in *C. neoformans* var. *grubii* (Hicks *et al.*, 2004). Nevertheless, it is interesting that the *cig1AΔdis* mutant in *C. neoformans* var. *grubii* did not show any susceptibility to the secretion inhibitors and agents that challenge the cell wall. The *cig1AΔdis* mutant was prepared by transforming the *C. neoformans* var. *grubii* wild-type strain with the *cig1DΔTL* construct amplified from *C. neoformans* var. *neoformans*. Therefore, similar phenotypes would be expected considering that the exact same construct was used. It is possible that the regulation of Cig1 might be different between the two varieties or that differences in other genes modify the influence of Cig1.

In summary, Cig1 plays a role in heme utilization in *C. neoformans* var. *neoformans* as was observed in *C. neoformans* var. *grubii*. A link between Cig1 and secretion was identified, although more work will be needed to fully understand the contribution of Cig1 in secretion as well as the mechanisms involved. Future studies will also be needed to determine whether Cig1 plays a role in maintaining cell wall integrity.

Chapter 5. Discussion

5.1. Heme uptake

The research presented in this thesis makes an important contribution to understanding mechanisms of iron acquisition from heme in *C. neoformans.* Iron is essential for the proliferation of *C. neoformans* and, therefore, iron uptake is an important component of its pathogenesis. The level of free iron in the mammalian host is kept to an extremely low level by sequestration with iron-binding proteins. The control of free iron has the dual purpose of protecting the host cells against the toxicity of iron (i.e., by preventing free radical formation) and also protecting the host against infection by pathogenic microorganisms. *C. neoformans* has developed multiple iron uptake mechanisms to circumvent the problem of iron unavailability (Jacobson *et al.*, 1997; 1998; Tangen *et al.*, 2007; Jung and Kronstad, 2008; Jung *et al.*, 2008; 2009). For example, the reductive high-affinity iron uptake pathway, comprised of the ferroxidase Cfo1 and the iron permease Cft1, is the best characterized system and it appears to be a key iron uptake pathway in *C. neoformans* (Jung *et al.*, 2008; 2009; Jung and Kronstad, 2008). Specifically, deletion of either *CFO1* or *CFT1* results in attenuated virulence and poor accumulation in the central nervous system in a mouse model of infection (Jung *et al.*, 2008; 2009).

One of the most abundant iron sources in the mammalian host is hemoglobin, a tetrameric protein containing one heme molecule per protein subunit. It is unclear whether *C. neoformans* can utilize hemoglobin because the fungus lacks the hemolytic activity required to rupture erythrocytes, the major source of hemoglobin (Drs. W. Jung and G. Hu, personal communications). However, it is possible that the fungal pathogen acquires heme and/or hemoglobin from erythrocytes that have already lysed. Indeed, free hemoglobin has been

detected in various fluids in the human host (Pynnonen *et al.*, 2011; Kipnis *et al.*, 2008). Although *C. neoformans* has been shown to utilize heme as a sole iron source, the mechanism of heme uptake was unknown prior to the work in this thesis (Jung *et al.*, 2008). In fact, when the studies presented in this thesis were started, no proteins involved in heme utilization had yet been identified in *C. neoformans*, and very little was known about heme uptake in other fungi. In *C. albicans*, a family of cell surface proteins (Rbt5 and Rbt51) involved in heme and hemoglobin acquisition had been identified, however the details of the mechanism of heme/hemoglobin uptake were still unknown (Weissman and Kornitzer, 2004). Since then, endocytosis has been proposed as a pathway for hemoglobin acquisition and this pathway depends on the activity of the ESCRT system (Weissman *et al.*, 2008). Recently, Vps23, a protein in the ESCRT-I complex, has been identified as a key player in iron acquisition from heme in *C. neoformans*, suggesting that a similar pathway may be present in this organism (Hu *et al.*, 2013). The research presented in this thesis identified the first protein, Cig1, involved in heme uptake and use in *C. neoformans*. Cig1 may play a role as a hemophore to deliver heme for endocytosis via receptors at the cell surface or to deliver heme to the cell surface for uptake via some unidentified cell surface transporter.

Heme uptake has been well characterized in bacteria and most heme uptake pathways generally consist of specific cell surface heme receptors and transporters to traffic heme molecules from the extracellular environment to the intracellular space (Tong and Guo, 2009; Nobles and Maresso, 2011). Some bacteria have a relay of heme receptors across the cell wall to accommodate the transport of heme to the cell membrane (Hammer and Skaar, 2011; Nobles and Maresso, 2011). Alternatively, other bacteria secrete heme-binding proteins, termed hemophores, in order to sequester heme from the environment and deliver it to the cell surface

receptors (Hanson *et al.*, 1992; Letoffe *et al.*, 1994; 1998; 1999; 2000; Jarosik *et al.*, 1995; Cope *et al.*, 1998; Arnoux *et al.*, 1999; 2000; Wandersman and Stojiljkovic, 2000; Rossi *et al.*, 2001; Maresso *et al.*, 2008; Tong and Guo, 2009; Honsa and Maresso, 2011; Klebba *et al.*, 2012; Wandersman and Delepelaire, 2012). As described below, the characterization of Cig1 suggests that a fungal pathogen of humans also possesses components of a heme uptake system with similar features to the bacterial uptake systems.

5.2. A novel Cig1-dependent heme uptake pathway in *C. neoformans*

In *C. neoformans*, the gene encoding Cig1, a secreted mannoprotein, represented the most abundant transcript in cells grown in LIM and was strongly regulated by iron suggesting an important role for the protein in iron homeostasis (Lian *et al.*, 2005). The study presented in Chapter 2 revealed that Cig1 is a component of a novel heme uptake pathway in *C. neoformans*. A key finding was that growth of a mutant in which *CIG1* had been deleted displayed an extended lag phase compared to the wild-type strain in the presence of heme as a sole iron source. Additionally, the mutant was less sensitive than the wild-type strain to GaPPIX, a toxic heme analog, indicating that Cig1 played a role in heme uptake. A recombinant Cig1 protein was shown to bind to heme, although a K_d could not be determined, possibly because the binding was weak and/or transient. Cig1 was found to be localized at the cell surface and was also secreted to the extracellular space in association with extracellular vesicles produced by *C. neoformans*. Given its extracellular localization, its ability to bind heme, and its role in heme utilization and uptake, it was hypothesized that Cig1 could act as a heme receptor, as illustrated in Figure 5.1A. However, the fact that Cig1 is also secreted to the extracellular space could indicate that it is a fungal hemophore. If this were the case, it would be the first fungal hemophore ever reported. In either scenario, heme uptake could be mediated via unidentified membrane-localized transporters or via endocytosis. Cig1 displayed low affinity for heme in the conditions tested but this finding does not discount its possible role as a heme receptor or hemophore. It is important to keep in mind that the biochemical experiments used to test heme binding were performed with a recombinant Cig1 protein expressed in *E. coli*, a prokaryotic host. Secreted eukaryotic proteins, including Cig1, are subject to post-translational modifications (i.e., glycosylation) that do not generally take place in prokaryotic cells. It is possible that the

glycosylation of Cig1 is important for its interaction with heme. Post-translational modifications of fungal proteins have been shown to influence their stability, their interactions with other proteins, as well as their potential for a contribution to virulence (Leach and Brown, 2012). Additionally, the recombinant Cig1 protein was tagged with *GST* which could interfere with the proper folding of the protein and result in decreased affinity for heme. Interestingly, the study presented in Chapter 2 showed that deletion of *CIG1* in the absence of the reductive high-affinity iron uptake pathway resulted in attenuated virulence in a mouse model of infection for *C. neoformans*. This observation confirms that the high-affinity iron uptake pathway is an important iron uptake pathway in the host, but it also indicates that heme uptake is important in the pathogenesis of *C. neoformans,* thus warranting further studies of this pathway. Cig1 also appears to play a role in heme acquisition in *C. neoformans* var. *neoformans* as presented in Chapter 4.

The MS analysis of secreted cryptococcal proteins capable of binding to heme-agarose beads identified multiple proteins, many of which are involved in carbohydrate metabolism as presented in Chapter 2 (Table 2.4). Cig1 was identified as one of those proteins suggesting that endogenously produced Cig1 binds to heme-agarose and further confirming the extracellular location of the protein. Additionally, a predicted transmembrane receptor protein was also identified as a putative heme-binding protein and was only detected in cells grown in iron-depleted media, just like Cig1. This could be a very interesting candidate for future studies in identifying other key players in the novel heme uptake pathway in *C. neoformans*. Future work will be needed to determine if the transmembrane receptor protein and the other proteins that were detected are involved in heme utilization.

5.3. Multiple heme uptake pathways in *C. neoformans*

The strain in which *CIG1* was deleted had a much longer lag phase than the wild-type strain when grown in LIM supplemented with heme added as a sole iron source. However, the mutant did eventually start to grow and it reached the same final cell density as the wild-type strain. Additionally, prior adaptation of the cells to growth on heme did not shorten the lag phase of the mutant thus suggesting that accumulation of mutations or changes in metabolism could not explain the eventual growth of the *cig1Δ* mutant. Therefore, the eventual growth of the mutant suggested that other heme uptake pathways must exist in *C. neoformans* to allow the cells to utilize iron from heme. Consequently, the *cig1Δ* mutant proved to be an excellent tool to investigate the other heme uptake pathways, as presented in Chapter 3.

Upon further investigation, the requirement of Cig1 for heme uptake appeared to be limited to the condition of physiological pH because the *cig1Δ* mutant grew as well as the wild-type strain in LIM supplemented with heme at lower pH. Additionally, the expression of *CIG1* was down-regulated at acidic pH. Hence, some other mechanism of heme uptake, independent of Cig1, probably plays a more important role at acidic pH. One possible scenario could involve uptake of heme via the ESCRT-mediated endocytic pathway (Hu *et al.*, 2013) as illustrated in Figure 5.1B. This scenario is supported by the defect in growth on heme observed for the mutants of the ESCRT system at acidic pH (Dr. G. Hu, personal communications). Alternatively, proteins (e.g., cell surface reductases) could extract iron from the heme molecule resulting in free iron which could also be transported into the cell via the ESCRT-mediated endocytic pathway, for example, or by another transporter which has not yet been identified (as illustrated in Figure 5.1C). A role for the endocytic pathway in this scenario is also possible as evidenced by the defect in growth in LIM supplemented with $FeCl_3$ observed for the mutants of

the ESCRT system at acidic pH (Dr. G. Hu, personal communications). The iron is probably not taken up by the high-affinity iron uptake pathway because deletion of *CFO1*, the gene encoding an essential component of the pathway, did not result in delayed growth in the presence of heme at low pH. Finally, another pathway for uptake of the entire heme molecule could possibly exist, such as a low-affinity heme transporter for example (Figure 5.1D). The solubility and bioavailability of iron from heme would be increased at lower pH which could support the idea of a functional low-affinity iron or heme uptake pathway at acidic pH (Wilkins, 1991; Cotton *et al.*, 1999).

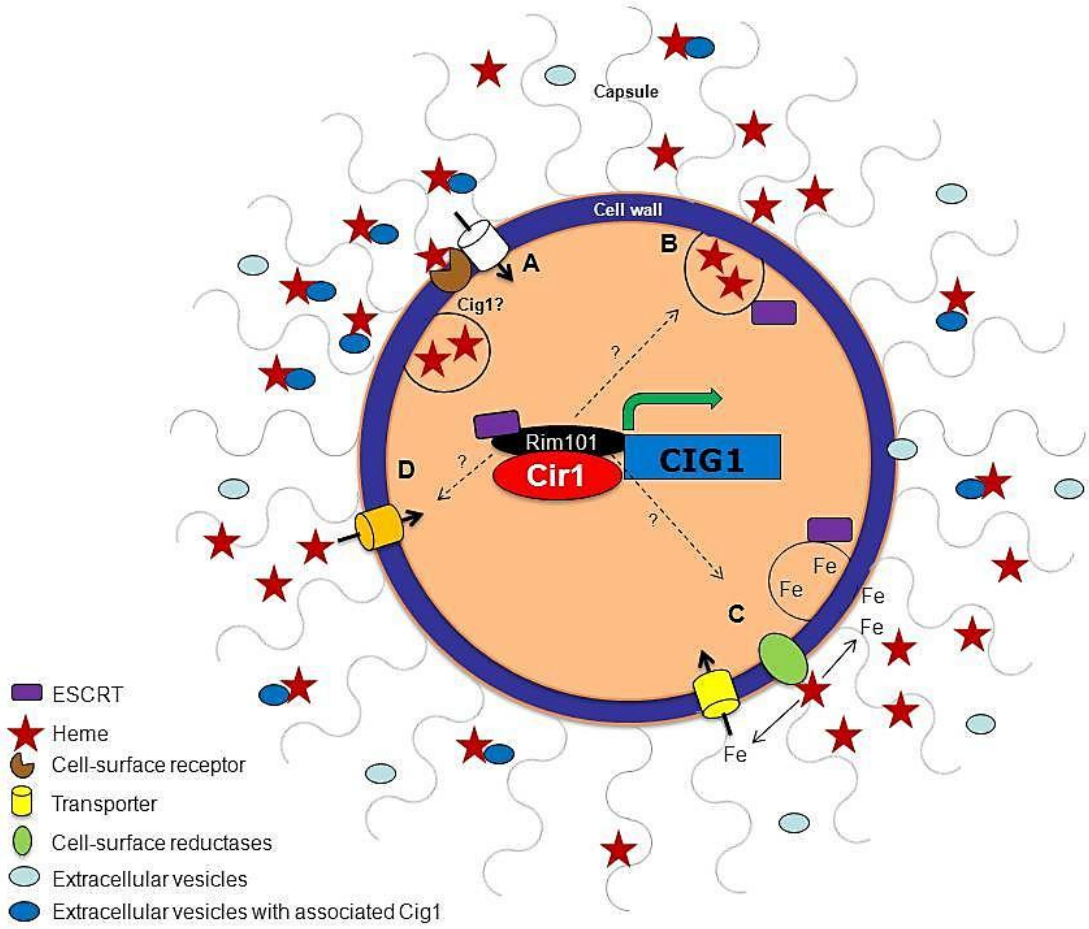

Figure 5.1. Proposed model for different heme uptake pathways in *C. neoformans*. (A) Cig1 heme uptake pathway. Cig1 could be a hemophore which sequesters heme for eventual uptake by a cell-surface receptor. Transport inside the cell could be achieved via endocytosis or via an unidentified transporter. (B) ESCRT-mediated endocytosis for heme. (C) Cell surface reductases may process heme, thereby releasing iron which can be transported to the intracellular space via ESCRT-mediated endocytosis or a predicted iron transporter. (D) Low-affinity heme uptake via an unidentified transporter.

Additional evidence suggests the presence of a third heme uptake pathway which relies on cell density in *C. neoformans*. This heme uptake pathway shares similarities with QS behaviour, including cell aggregation, dependence on cell density and a decreased lag phase for cells grown in LIM supplemented with heme with added CM. QS is a means of cell-cell communication among populations that is common in microorganisms. Signaling molecules are secreted in the environment and when the concentration of signal is high enough, indicating a

sufficient number of cells, the population mounts a coordinated response. This phenomenon is extremely beneficial in order to increase the population's survival by allowing the cells to adapt to low nutrient availability, to organize an attack on the host, or to escape the immune response of the host. QS has been widely studied in bacteria and, in the last decade or so, has also been reported in different fungi including *C. neoformans* (Bassler, 2002; Joint *et al.*, 2007; Lee *et al.*, 2007; Williams, 2007; Albuquerque, 2011; Eisenman *et al.*, 2011; Albuquerque and Casadevall, 2012). It is possible that *C. neoformans* requires QS to induce heme uptake in this specific pathway. Alternatively, QS and heme uptake in *C. neoformans* could share common regulators or the regulators of QS could be downstream of the regulators of heme uptake. A link between iron and QS has previously been established in *P. aeruginosa* (Ochsner *et al.*, 2002; Palma *et al.*, 2003; Schuster *et al.*, 2003; Cornelis and Aendekerk, 2004; Juhas *et al.*, 2004; 2005; Deziel *et al.*, 2005; Kim *et al.*, 2005; Duan and Surette, 2007; Yang *et al.*, 2007; Oglesby *et al.*, 2008; Hazan *et al.*, 2010). It is important to note that the different heme uptake pathways described above (i.e., Cig1, acidic pH, cell density) may not be three completely independent heme uptake pathways and they may share some key players and/or machinery for transportation of heme inside the cell. For example, the cell surface reductases for heme processing (Figure 5.1C) could be involved in both the pathway contributing at acidic pH and the cell density-dependent pathway and could be regulated differently depending on the conditions. That is, at acidic pH, the cell surface reductases could be up-regulated, while the regulation could be dependent on cell density at physiological pH. Alternatively, ESCRT-mediated endocytosis could be involved in all three pathways for heme uptake (Figure 5.1A-C). Further work will be needed to elucidate the receptors, transporters and mechanisms involved in all the heme uptake pathways identified in the studies presented in this thesis.

As mentioned earlier, the *CIG1* transcript is highly abundant in cells grown in low iron medium. The transcription factor Rim101 plays a role in regulating heme uptake along with other transcription factors (Fig. 5.1), and part of this role is most likely due to the regulation of *CIG1* transcript levels (O'Meara *et al.*, 2010). However, part of the role of Rim101 in heme uptake is independent of Cig1 based on the observation that a *rim101Δ* mutant in which the expression of *CIG1* was repressed by a regulated promoter, displayed a longer lag phase than both the *rim101Δ* and the *cig1Δ* mutants when grown in LIM supplemented with heme. Given the role of Rim101 as the master regulator of the pH response, it is possible that Rim101 is linked to the heme uptake pathway that makes a major contribution at acidic pH as illustrated in Figure 5.1 (Tilburn *et al.*, 1995; MacCabe *et al.*, 1996; Ramon *et al.*, 1999; Lamb and Mitchell, 2003). Specifically, Rim101 could be involved in the ESCRT-mediated endocytic pathway given that Rim101 is a downstream target of the ESCRT system. Although the Cig1-dependent heme uptake pathway may be a larger contributor to heme uptake at physiological pH, the proposed ESCRT-mediated endocytic pathway may not be restricted to heme uptake at acidic pH but may also be involved in heme uptake at physiological pH. A growth defect of the mutants of the ESCRT system on heme at physiological pH supports this hypothesis (Hu *et al.*, 2013). Additionally, it is possible that Rim101 regulates the two pathways (i.e., Cig1 and endocytosis) in response to pH. Future work is needed to fully understand the role of Rim101 and the full range of targets that function in heme utilization.

5.4. Expression of the Cig1 truncated polypeptide alters secretion and leads to loss of cell wall integrity

A link between Cig1 and secretion was identified in *C. neoformans* var. *neoformans* but not in *C. neoformans* var. *grubii*. In fact, the expression of a predicted Cig1 truncated polypeptide may alter the function of the conventional secretory pathway as evidenced by the increased susceptibility of the strains to secretion inhibitors, especially BFA. BFA is known to specifically inhibit conventional secretion, which is typically driven by an N-terminal signal sequence and requires traffic between the ER and Golgi, passage through the Golgi apparatus and transport to the cell membrane via intracellular vesicles (Doms *et al.*, 1989; Rodrigues and Djordjevic, 2012). The integrity of the cell wall of the cells expressing the Cig1 truncated polypeptide was affected, possibly as a result of altered secretion, and rendered the cells more sensitive to osmotic and heat stress. Alternatively, Cig1 could play a role in maintaining cell wall integrity and, therefore, loss of *CIG1* would result in loss of cell wall integrity. Furthermore, expression of the Cig1 truncated polypeptide resulted in increased secretion of proteases, although this could be due to loss of cell wall integrity rather than a specific influence on the secretory pathway. The link between Cig1 and secretion was further reinforced by the observation that a strain overexpressing Cig1 elaborated a larger capsule and secreted more extracellular vesicles than the wild-type strain. The extracellular vesicles have previously been shown to contain the capsular polysaccharides and have been linked with capsule biosynthesis (Yoneda and Doering, 2006; Rodrigues *et al.*, 2007). A current working hypothesis is that expression of the Cig1 truncated polypeptide somehow blocks the secretory pathway. It is possible that the expression of the Cig1 polypeptide without the transmembrane domain leads to the protein not reaching its proper destination. Instead, the Cig1 truncated polypeptide could

potentially accumulate somewhere within the secretory pathway and inhibit secretion. More work will be needed to fully understand the contribution of Cig1 to secretion and to determine the mechanism involved.

5.5. Key areas for future work

5.5.1. Cig1 binding to heme

In this study, the K_d of recombinant Cig1 to heme could not be determined. As previously discussed, it is possible that the weak binding observed was due to issues arising because of expression of an eukaryotic protein from a recombinant vector in a prokaryotic system. Attempts were made to express Cig1 in *C. neoformans* but the expression levels achieved were too low to allow further studies. It would be interesting to fuse a stronger constitutive promoter, for example the *TEF1* promoter, to the *CIG1* gene in order to increase the level of expression of Cig1. Additionally, the *GST* tag used to label the recombinant protein may have interfered with proper folding. A *HIS* tag, which is comprised of 6 histidine residues is significantly smaller and could potentially reduce misfolding of the tagged protein. Tagged and endogenously produced Cig1 could be used to further study the interaction with heme and potentially determine the K_d.

5.5.2. Identifying the mechanisms involved in Cig1-dependent heme uptake pathway

Cig1 has been shown to play a role in heme uptake but additional work is needed to define the mechanism. Identifying the structure of the protein by crystallography could provide invaluable information about the role of Cig1 in heme binding. The Cig1 protein expressed in and purified from *C. neoformans* (as described above) could be used to help ensure that the properly folded protein was evaluated. Also, identifying the heme binding domain of Cig1 would be important to understand the mechanism involved in heme uptake. One approach would be to delete different parts of the *CIG1* gene to determine which region of the protein is essential for heme binding activity. The predicted chitin-binding domain would be a good place to start.

Eventually, deletion or substitution of single amino acids by site directed mutagenesis could also be performed to determine the residues needed for Cig1-mediated heme utilization.

A better understanding of the biochemical details of heme uptake could be useful. The work done with the non-iron MP suggested that Cig1 is involved in heme uptake but this method provides an indirect measure of heme uptake. A more direct approach may further confirm the role of Cig1 in uptake of heme. Future work could include examining uptake of radioactive Fe^{55}-heme. The use of Fe^{55}-heme has previously been used in studying heme transport in different organisms (Protchenko *et al.*, 2008; Le Blanc *et al.*, 2012). However, preliminary results using Fe^{55}-heme yielded variable data and no difference was observed between uptake of Fe^{55}-heme by the wild-type strain and the *cig1Δ* mutant. It is possible that the Fe^{55}-heme was contaminated with free iron which could be taken up via the high-affinity iron uptake pathway. A different source of Fe^{55}-heme will be needed to further study heme uptake.

Identifying the heme receptor and/or transporter involved in the Cig1-dependent heme uptake pathway would also be very useful in defining the mechanism involved in heme uptake. Examining the predicted transmembrane receptor identified as a putative heme-binding protein during the MS analysis presented in Chapter 2 would be the easiest approach and could potentially provide a key receptor involved in heme uptake. Another approach would be to perform a pull-down assay of cell membrane/cell wall proteins using heme-agarose beads followed by MS analysis to potentially identify the heme transporters involved in the Cig1-dependent and/or Cig1-independent heme uptake pathways. Following the MS analysis, deletion mutants of the genes encoding the proteins that were identified could be constructed and characterized to assess heme transport function. It is possible that the interaction between some of the proteins identified by MS and the heme-agarose beads may not be specific. Additionally,

some of the identified proteins may be the result of secondary interactions and may not be true direct heme-binding proteins. Nonetheless, this approach would be relatively simple and could yield the missing transporters and/or other cell surface heme receptors. The method for triple peptide formaldehyde labeling could be used to quantify the relative abundance of proteins in each sample but this approach will need to be optimized in order to allow detection of the majority of proteins, as Cig1 was not detected in previous attempts.

5.5.3. Identifying other proteins involved in the Cig1-independent heme uptake pathway(s)

The key players involved in the Cig1-independent heme uptake pathways also need to be identified to fully understand heme uptake in *C. neoformans*. Construction of deletion mutants for the genes encoding the proteins identified as secreted heme-binding proteins in the MS analysis presented in Chapter 2 (specifically the predicted transmembrane receptor), followed by characterization of these mutants would be a logical place to start. Upon construction of the mutants, their role in heme utilization could be confirmed. The interaction between heme and the proteins involved in heme utilization could also be examined. Such analyses could potentially identify other heme receptors and/or hemophores. Alternatively, comparative transcriptome analysis of the wild-type strain and the *cig1Δ* mutant in the presence of heme could also be used to identify candidate functions for subsequent genetic analysis. Different technologies, such as RNA-seq and microarrays, have been extensively used to compare the transcriptomes of *C. neoformans* cells from different growth conditions, and this approach has also been used in many other organisms. It is likely that in the absence of Cig1, the key players involved in the other heme uptake pathways would be more highly expressed to compensate, and this property might facilitate their identification. Again, deletion of the candidate genes and

characterization of the mutants could provide the important additional information about heme uptake. Additionally, further characterization of the role of the other *C. neoformans* putative surface reductases, as predicted by protein homology, in heme utilization are already underway in the laboratory (Dr. S. Saikia, personal communications).

5.5.4. Identifying the QS-like molecule involved in cell density-dependent heme uptake

The cell density-dependent heme uptake pathway described in Chapter 3 has similarities to QS behaviour. Identification of the QS-like molecule is essential in order to further characterize this pathway. Although some crude fractionation of the components found in the culture supernatant has already been done, as presented in Chapter 3, it would be useful to separate the different components further using liquid chromatography. After separation, samples with activity could be analyzed by MS or nuclear magnetic resonance (NMR) to determine the molecules found in these fractions. These molecules in pure form (if available) could be again tested for their ability to decrease the lag phase of the strain in which *CIG1* was deleted, and this approach would hopefully confirm the identity the QS-like molecule.

Preliminary data presented in Chapter 3 indicate that the QS-like molecule could potentially be a polysaccharide (e.g., GXM, GalXM, chitin-like oligomers) secreted into the culture supernatant of *C. neoformans*. It would be interesting to determine if these polysaccharides can bind to heme. Binding of heme to proteins or polysaccharides can be visualized using different chemicals, including 3,3'-dimethoxybenzidine (Mazoy and Lemos, 1996). Additionally, imaging MS of cells grown on agar in the presence of heme could provide invaluable information based on the spatial localization of the QS-like molecule (Watrous and Dorrestein, 2011). For example, this approach could indicate whether more QS-like molecules

are distributed at the surface or within the capsule of the cells. Also, some genes have been found to be essential for elaboration of the capsule, including *CAP10*, *CAP59*, *CAP60*, and *CAP64*, while the *CAS* genes are involved in modification of the capsule (Chang and Kwon-Chung, 1994; 1998; 1999; Chang *et al.*, 1996; Moyrand *et al.*, 2002; 2004). Mutants could be constructed in which both *CIG1* and genes involved in capsule synthesis and/or modification are deleted. Alternatively, mutants expressing only GXM or GalXM could also be constructed in the *cig1Δ* mutant background. Characterization of these mutants could provide insights into the role of capsular polysaccharides in heme uptake.

5.5.5. Further characterization of the link between Cig1 and secretion

Finally, Cig1 has also been linked to secretion through the unusual behaviours of a mutant carrying a disruption allele and of a complemented strain. A key finding was that the complemented strain appeared to overexpresses *CIG1* and produced a larger capsule than the wild-type strain. It was later found that the integration of the complemented construct resulted in disruption of the *CNBE3170* gene. This gene encodes a predicted protein without sequence similarity to other proteins and it is therefore difficult to predict its function. Mutants in which the *CNBE3170* gene was deleted should be constructed to confirm that the phenotypes associated with the complemented strain are in fact related to overexpression of *CIG1* and not to disruption of *CNBE3170*. If the phenotypes are not a result of overexpression of *CIG1* but of disruption of *CNBE3170*, characterization of the mutant would still provide useful information about the secretory pathway involved in capsule production. Alternatively, a strain overexpressing *CIG1* at the endogenous locus could be constructed. For example, the *TEF1* promoter could be inserted upstream of the *CIG1* gene to promote elevated and constitutive expression of *CIG1*.

Based on the data presented in Chapter 4, it is possible that the expression of the Cig1 truncated polypeptide could somehow block the secretory pathway. Creating a GFP-tagged construct for the Cig1 truncated polypeptide would be very useful for future studies. For example, proof for expression of the truncated peptide could be provided by Western blot analysis of the lysates of cells expressing the tagged truncated polypeptide. Also, cells expressing the GFP-tagged truncated polypeptide could allow visualization of the localization of the protein by fluorescence microscopy which could give insight into the mechanism involved in altering secretion. Using dyes (e.g., ER-Tracker, Golgi-Tracker) which stain the different compartments of the secretory pathway and looking for co-localization of the Cig1 truncated polypeptide could help determine whether accumulation of the truncated polypeptide occurs at a specific step within the pathway (as a possible reason for altered secretion). Alternatively, proteins which are known to be found in the specific components of the secretory pathway could be also be used as markers.

5.6. Conclusion

In conclusion, the studies presented in this thesis identified a major role for Cig1 in heme uptake at physiological pH in the fungal pathogens *C. neoformans* var. *grubii* and *C. neoformans* var. *neoformans*. Additionally, it was determined that *C. neoformans* has evolved multiple heme uptake pathways, including a Cig1-independent pathway required for heme uptake at acidic pH and a cell density-dependent heme uptake pathway. The work presented here is novel and important because heme uptake has never been described in *C. neoformans* and very little is generally known about the process in fungi. Although the key players and the mechanism involved in these pathways were not characterized, the data provide the ground work for eventually understanding all of the mechanisms of heme uptake in *C. neoformans* and this could potentially lead to further elucidating heme uptake in other fungi too. Iron is essential for pathogenesis of *C. neoformans* and the majority of iron in the mammalian host is found in heme. Therefore, identifying the key players and the different steps involved in heme uptake could provide new targets for novel drug development in order to offer better treatment to patients with cryptococcosis. There is a pressing need for development of novel treatments as the current antifungal drugs that are available suppress but do not cure cryptococcosis (van der Horst *et al.*, 1997; Bicanic *et al.*, 2005; McCarthy *et al.*, 2006). Finally, the expression of a Cig1 truncated polypeptide in *C. neoformans* var. *neoformans* was linked to secretion and maintenance of cell wall integrity. More work will be needed to fully understand the underlying mechanism of the altered secretion phenomenon and the relationship with cell wall integrity. Given that secretion is also essential for the proliferation of *C. neoformans* and plays a major role in its pathogenesis, further understanding of the process could provide additional strategies to inhibit growth of the pathogen and its pathogenesis in humans.

References

1. Albuquerque,P.C., Nakayasu,E.S., Rodrigues,M.L., Frases,S., Casadevall,A., Zancope-Oliveira,R.M., Almeida,I.C., and Nosanchuk,J.D. (2008). Vesicular transport in *Histoplasma capsulatum*: an effective mechanism for trans-cell wall transfer of proteins and lipids in ascomycetes. Cell Microbiol. *10*, 1695-1710.

2. Albuquerque, P. C. (2011). Cell density-dependent regulation of growth and virulence in *Cryptococcus neoformans*. ProQuest Dissertations & Theses.

3. Albuquerque,P.C. and Casadevall,A. (2012). Quorum sensing in fungi – a review. Med. Mycol. *50*, 337-345.

4. Almeida,R.S., Wilson,D., and Hube,B. (2009). *Candida albicans* iron acquisition within the host. FEMS Yeast Res. *9*, 1000-1012.

5. Andrade,M.A., Ciccarelli,F.D., Perez-Iratxeta,C., and Bork,P. (2002). NEAT: a domain duplicated in genes near the components of a putative Fe3+ siderophore transporter from Gram-positive pathogenic bacteria. Genome Biol. *3*, RESEARCH0047.

6. Ansell,R. and Adler,L. (1999). The effect of iron limitation on glycerol production and expression of the isogenes for NAD(+)-dependent glycerol 3-phosphate dehydrogenase in *Saccharomyces cerevisiae*. FEBS Lett. *461*, 173-177.

7. Aravind,L. (2001). DOMON: an ancient extracellular domain in dopamine beta-monooxygenase and other proteins. Trends Biochem. Sci. *26*, 524-526.

8. Ardon,O., Bussey,H., Philpott,C., Ward,D.M., Kaplan,S., Verroneau,S., Jiang,B., and Kaplan,J. (2001). Identification of a *Candida albicans* ferrichrome transporter and its characterization by expression in *Saccharomyces cerevisiae*. J. Biol. Chem. *276*, 43049-43055.

9. Arnoux,P., Haser,R., Izadi,N., Lecroisey,A., Delepierre,M., Wandersman,C., and Czjzek,M. (1999). The crystal structure of HasA, a hemophore secreted by *Serratia marcescens*. Nat. Struct. Biol. *6*, 516-520.

10. Arnoux,P., Haser,R., Izadi-Pruneyre,N., Lecroisey,A., and Czjzek,M. (2000). Functional aspects of the heme bound hemophore HasA by structural analysis of various crystal forms. Proteins *41*, 202-210.

11. Askwith,C., Eide,D., Van,H.A., Bernard,P.S., Li,L., Kaplan,S., Sipe,D.M., and Kaplan,J. (1994). The FET3 gene of *Saccharomyces cerevisiae* encodes a multicopper oxidase required for ferrous iron uptake. Cell *76*, 403-410.

12. Baek,Y.U., Li,M., and Davis,D.A. (2008). *Candida albicans* ferric reductases are differentially regulated in response to distinct forms of iron limitation by the Rim101 and CBF transcription factors. Eukaryot. Cell *7*, 1168-1179.

13. Bahn,Y.S., Cox,G.M., Perfect,J.R., and Heitman,J. (2005). Carbonic anhydrase and CO2 sensing during *Cryptococcus neoformans* growth, differentiation, and virulence. Curr. Biol. *15*, 2013-2020.

14. Barchiesi,F., Cogliati,M., Esposto,M.C., Spreghini,E., Schimizzi,A.M., Wickes,B.L., Scalise,G., and Viviani,M.A. (2005). Comparative analysis of pathogenicity of *Cryptococcus neoformans* serotypes A, D and AD in murine cryptococcosis. J. Infect. *51*, 10-16.

15. Barluzzi,R., Saleppico,S., Nocentini,A., Boelaert,J.R., Neglia,R., Bistoni,F., and Blasi,E. (2002). Iron overload exacerbates experimental meningoencephalitis by *Cryptococcus neoformans*. J. Neuroimmunol. *132*, 140-146.

16. Bartlett,K.H., Kidd,S.E., and Kronstad,J.W. (2008). The emergence of *Cryptococcus gattii* in British Columbia and the Pacific Northwest. Curr. Infect. Dis. Rep. *10*, 58-65.

17. Bartlett,K.H., Cheng,P.Y., Duncan,C., Galanis,E., Hoang,L., Kidd,S., Lee,M.K., Lester,S., Macdougall,L., Mak,S., Morshed,M., Taylor,M., and Kronstad,J. (2012). A decade of experience: *Cryptococcus gattii* in British Columbia. Mycopathologia *173*, 311-319.

18. Bassler,B.L. (2002). Small talk. Cell-to-cell communication in bacteria. Cell *109*, 421-424.

19. Beasley,F.C., Vines,E.D., Grigg,J.C., Zheng,Q., Liu,S., Lajoie,G.A., Murphy,M.E., and Heinrichs,D.E. (2009). Characterization of staphyloferrin A biosynthetic and transport mutants in *Staphylococcus aureus*. Mol. Microbiol. *72*, 947-963.

20. Bensen,E.S., Martin,S.J., Li,M., Berman,J., and Davis,D.A. (2004). Transcriptional profiling in *Candida albicans* reveals new adaptive responses to extracellular pH and functions for Rim101p. Mol. Microbiol. *54*, 1335-1351.

21. Bernier,G., Girijavallabhan,V., Murray,A., Niyaz,N., Ding,P., Miller,M.J., and Malouin,F. (2005). Desketoneoenactin-siderophore conjugates for *Candida*: evidence of iron transport-dependent species selectivity. Antimicrob. Agents Chemother. *49*, 241-248.

22. Betina,V. (1992). Biological effects of the antibiotic brefeldin A (decumbin, cyanein, ascotoxin, synergisidin): a retrospective. Folia Microbiol. *37*, 3-11.

23. Bhattacharjee,A.K., Bennett,J.E., and Glaudemans,C.P. (1984). Capsular polysaccharides of *Cryptococcus neoformans*. Rev. Infect. Dis. *6*, 619-624.

24. Bicanic,T., Wood,R., Bekker,L.G., Darder,M., Meintjes,G., and Harrison,T.S. (2005). Antiretroviral roll-out, antifungal roll-back: access to treatment for cryptococcal meningitis. Lancet Infect. Dis. *5*, 530-531.

25. Biondo,C., Beninati,C., Delfino,D., Oggioni,M., Mancuso,G., Midiri,A., Bombaci,M., Tomaselli,G., and Teti,G. (2002). Identification and cloning of a cryptococcal deacetylase that produces protective immune responses. Infect. Immun. *70*, 2383-2391.

26. Biondo,C., Messina,L., Bombaci,M., Mancuso,G., Midiri,A., Beninati,C., Cusumano,V., Gerace,E., Papasergi,S., and Teti,G. (2005). Characterization of two novel cryptococcal mannoproteins recognized by immune sera. Infect. Immun. *73*, 7348-7355.

27. Biondo,C., Mancuso,G., Midiri,A., Bombaci,M., Messina,L., Beninati,C., and Teti,G. (2006). Identification of major proteins secreted by *Cryptococcus neoformans*. FEMS Yeast Res. *6*, 645-651.

28. Blasi,E., Barluzzi,R., Mazzolla,R., Tancini,B., Saleppico,S., Puliti,M., Pitzurra,L., and Bistoni,F. (1995). Role of nitric oxide and melanogenesis in the accomplishment of anticryptococcal activity by the BV-2 microglial cell line. J. Neuroimmunol. *58*, 111-116.

29. Bose,I., Reese,A.J., Ory,J.J., Janbon,G., and Doering,T.L. (2003). A yeast under cover: the capsule of *Cryptococcus neoformans*. Eukaryot. Cell *2*, 655-663.

30. Braun,V., Braun,M., and Killmann,H. (2000). Iron transport in *Escherichia coli*. Crystal structure of FhuA, an outer membrane iron and antibiotic transporter. Adv. Exp. Med. Biol. *485*, 33-43.

31. Braun,V. (2001). Iron uptake mechanisms and their regulation in pathogenic bacteria. Int. J. Med. Microbiol. *291*, 67-79.

32. Braun,V. and Endriss,F. (2007). Energy-coupled outer membrane transport proteins and regulatory proteins. Biometals *20*, 219-231.

33. Bredenbruch,F., Geffers,R., Nimtz,M., Buer,J., and Haussler,S. (2006). The *Pseudomonas aeruginosa* quinolone signal (PQS) has an iron-chelating activity. Environ. Microbiol. *8*, 1318-1329.

34. Buchanan,K.L. and Murphy,J.W. (1998). What makes *Cryptococcus neoformans* a pathogen? Emerg. Infect. Dis. *4*, 71-83.

35. Bullen,J.J., Rogers,H.J., and Griffiths,E. (1978). Role of iron in bacterial infection. Curr. Top. Microbiol. Immunol. *80*, 1-35.

36. Cadieux,B., Lian,T., Hu,G., Wang,J., Biondo,C., Teti,G., Liu,V., Murphy,M.E., Creagh,A.L., and Kronstad,J.W. (2013). The mannoprotein Cig1 supports iron acquisition from heme and virulence in the pathogenic fungus *Cryptococcus neoformans*. J. Infect. Dis. [Epub ahead of print].

37. Candiano,G., Bruschi,M., Musante,L., Santucci,L., Ghiggeri,G.M., Carnemolla,B., Orecchia,P., Zardi,L., and Righetti,P.G. (2004). Blue silver: a very sensitive colloidal Coomassie G-250 staining for proteome analysis. Electrophoresis *25*, 1327-1333.

38. Cartron,M.L., Maddocks,S., Gillingham,P., Craven,C.J., and Andrews,S.C. (2006). Feo-transport of ferrous iron into bacteria. Biometals *19*, 143-157.

39. Centers for Disease Control and Prevention (2010). Emergence of *Cryptococcus gattii*-Pacific Northwest, 2004-2010. MMWR Morb. Mortal. Wkly. Rep. *59*, 865-868.

40. Cescau,S., Cwerman,H., Letoffe,S., Delepelaire,P., Wandersman,C., and Biville,F. (2007). Heme acquisition by hemophores. Biometals *20*, 603-613.

41. Chang,S.H., Barbosa-Tessmann,I., Chen,C., Kilberg,M.S., and Agarwal,A. (2002). Glucose deprivation induces heme oxygenase-1 gene expression by a pathway independent of the unfolded protein response. J. Biol. Chem. *277*, 1933-1940.

42. Chang,Y.C. and Kwon-Chung,K.J. (1994). Complementation of a capsule-deficient mutation of *Cryptococcus neoformans* restores its virulence. Mol. Cell Biol. *14*, 4912-4919.

43. Chang,Y.C., Wickes,B.L., and Kwon-Chung,K.J. (1995). Further analysis of the CAP59 locus of *Cryptococcus neoformans*: structure defined by forced expression and description of a new ribosomal protein-encoding gene. Gene *167*, 179-183.

44. Chang,Y.C., Penoyer,L.A., and Kwon-Chung,K.J. (1996). The second capsule gene of *Cryptococcus neoformans*, CAP64, is essential for virulence. Infect. Immun. *64*, 1977-1983.

45. Chang,Y.C. and Kwon-Chung,K.J. (1998). Isolation of the third capsule-associated gene, CAP60, required for virulence in *Cryptococcus neoformans*. Infect. Immun. *66*, 2230-2236.

46. Chang,Y.C. and Kwon-Chung,K.J. (1999). Isolation, characterization, and localization of a capsule-associated gene, CAP10, of *Cryptococcus neoformans*. J. Bacteriol. *181*, 5636-5643.

47. Chaturvedi,V., Flynn,T., Niehaus,W.G., and Wong,B. (1996). Stress tolerance and pathogenic potential of a mannitol mutant of *Cryptococcus neoformans*. Microbiology *142*, 937-943.

48. Chaturvedi,V., Fan,J., Stein,B., Behr,M.J., Samsonoff,W.A., Wickes,B.L., and Chaturvedi,S. (2002). Molecular genetic analyses of mating pheromones reveal intervariety mating or hybridization in *Cryptococcus neoformans*. Infect. Immun. *70*, 5225-5235.

49. Chen,L.C. Blank,E.S. and Casadevall,A. (1996). Extracellular proteinase activity of *Cryptococcus neoformans*. Clin. Diagn. Lab. Immunol. *3*, 570-574.

50. Chen,H., Fujita,M., Feng,Q., Clardy,J., and Fink,G.R. (2004). Tyrosol is a quorum-sensing molecule in *Candida albicans*. Proc. Natl. Acad. Sci. U. S. A *101*, 5048-5052.

51. Chen,H. and Fink,G.R. (2006). Feedback control of morphogenesis in fungi by aromatic alcohols. Genes Dev. *20*, 1150-1161.

52. Chen,L.C., Goldman,D.L., Doering,T.L., Pirofski,L., and Casadevall,A. (1999). Antibody response to *Cryptococcus neoformans* proteins in rodents and humans. Infect. Immun. *67*, 2218-2224.

53. Cherniak,R., Reiss,E., Slodki,M.E., Plattner,R.D., and Blumer,S.O. (1980). Structure and antigenic activity of the capsular polysaccharide of *Cryptococcus neoformans* serotype A. Mol. Immunol. *17*, 1025-1032.

54. Cherniak,R. (1988). Soluble polysaccharides of *Cryptococcus neoformans*. Curr. Top. Med. Mycol. *2*, 40-54.

55. Choi,J., Vogl,A.W., and Kronstad,J.W. (2012). Regulated expression of cyclic AMP-dependent protein kinase A reveals an influence on cell size and the secretion of virulence factors in *Cryptococcus neoformans*. Mol. Microbiol. *85*, 700-715.

56. Clarke,T.E., Ku,S.Y., Dougan,D.R., Vogel,H.J., and Tari,L.W. (2000). The structure of the ferric siderophore binding protein FhuD complexed with gallichrome. Nat. Struct. Biol. *7*, 287-291.

57. Cohen,A., Nelson,H., and Nelson,N. (2000). The family of SMF metal ion transporters in yeast cells. J. Biol. Chem. *275*, 33388-33394.

58. Collopy-Junior,I., Esteves,F.F., Nimrichter,L., Rodrigues,M.L., Alviano,C.S., and Meyer-Fernandes,J.R. (2006). An ectophosphatase activity in *Cryptococcus neoformans*. FEMS Yeast Res. *6*, 1010-1017.

59. Conconi,A., Zucca,E., Roggero,E., Bertoni,F., Bernasconi,A., Mingrone,W., Pedrinis,E., and Cavalli,F. (2000). Prognostic models for diffuse large B-cell lymphoma. Hematol. Oncol. *18*, 61-73.

60. Cope,L.D., Thomas,S.E., Hrkal,Z., and Hansen,E.J. (1998). Binding of heme-hemopexin complexes by soluble HxuA protein allows utilization of this complexed heme by *Haemophilus influenzae*. Infect. Immun. *66*, 4511-4516.

61. Cornelis,P. and Aendekerk,S. (2004). A new regulator linking quorum sensing and iron uptake in *Pseudomonas aeruginosa*. Microbiology *150*, 752-756.

62. Cotton, F. A., Wilkinson, G., Murillo, C. A., and Bochmann, M. (1999). Advanced inorganic chemistry. [6th edition]. New York, NY, John Wiley and Sons.

63. Cox,G.M., Mukherjee,J., Cole,G.T., Casadevall,A., and Perfect,J.R. (2000). Urease as a virulence factor in experimental cryptococcosis. Infect. Immun. *68*, 443-448.

64. Cox,G.M., McDade,H.C., Chen,S.C., Tucker,S.C., Gottfredsson,M., Wright,L.C., Sorrell,T.C., Leidich,S.D., Casadevall,A., Ghannoum,M.A., and Perfect,J.R. (2001). Extracellular phospholipase activity is a virulence factor for *Cryptococcus neoformans*. Mol. Microbiol. *39*, 166-175.

65. Crowe,J.H. (2007). Trehalose as a "chemical chaperone": fact and fantasy. Adv. Exp. Med. Biol. *594*, 143-158.

66. Cruz,M.C., Del,P.M., Wang,P., Wenger,R., Zenke,G., Quesniaux,V.F., Movva,N.R., Perfect,J.R., Cardenas,M.E., and Heitman,J. (2000). Immunosuppressive and nonimmunosuppressive cyclosporine analogs are toxic to the opportunistic fungal pathogen *Cryptococcus neoformans* via cyclophilin-dependent inhibition of calcineurin. Antimicrob. Agents Chemother. *44*, 143-149.

67. Culotta,V.C., Yang,M., and Hall,M.D. (2005). Manganese transport and trafficking: lessons learned from *Saccharomyces cerevisiae*. Eukaryot. Cell *4*, 1159-1165.

68. Currie,B.P. and Casadevall,A. (1994). Estimation of the prevalence of cryptococcal infection among patients infected with the human immunodeficiency virus in New York City. Clin. Infect. Dis. *19*, 1029-1033.

69. Dale,S.E., Sebulsky,M.T., and Heinrichs,D.E. (2004). Involvement of SirABC in iron-siderophore import in *Staphylococcus aureus*. J. Bacteriol. *186*, 8356-8362.

70. Daou,N., Buisson,C., Gohar,M., Vidic,J., Bierne,H., Kallassy,M., Lereclus,D., and Nielsen-LeRoux,C. (2009). IlsA, a unique surface protein of *Bacillus cereus* required for iron acquisition from heme, hemoglobin and ferritin. PLoS. Pathog. *5*, e1000675.

71. Davidson,R.C., Blankenship,J.R., Kraus,P.R., de Jesus,B.M., Hull,C.M., D'Souza,C., Wang,P., and Heitman,J. (2002). A PCR-based strategy to generate integrative targeting alleles with large regions of homology. Microbiology *148*, 2607-2615.

72. De Silva,D.M., Askwith,C.C., Eide,D., and Kaplan,J. (1995). The FET3 gene product required for high affinity iron transport in yeast is a cell surface ferroxidase. J. Biol. Chem. *270*, 1098-1101.

73. De Silva,D.M., Kaplan,S., Fergestad,J., and Kaplan,J. (1997). Purification and characterization of Fet3 protein, a yeast homologue of ceruloplasmin. J. Biol. Chem. *272*, 14208-14213.

74. Deziel,E., Gopalan,S., Tampakaki,A.P., Lepine,F., Padfield,K.E., Saucier,M., Xiao,G., and Rahme,L.G. (2005). The contribution of MvfR to *Pseudomonas aeruginosa* pathogenesis and quorum sensing circuitry regulation: multiple quorum sensing-regulated genes are modulated without affecting lasRI, rhlRI or the production of N-acyl-L-homoserine lactones. Mol. Microbiol. *55*, 998-1014.

75. Diggle,S.P., Matthijs,S., Wright,V.J., Fletcher,M.P., Chhabra,S.R., Lamont,I.L., Kong,X., Hider,R.C., Cornelis,P., Camara,M., and Williams,P. (2007). The *Pseudomonas aeruginosa* 4-quinolone signal molecules HHQ and PQS play multifunctional roles in quorum sensing and iron entrapment. Chem. Biol. *14*, 87-96.

76. Dix,D., Bridgham,J., Broderius,M., and Eide,D. (1997). Characterization of the FET4 protein of yeast. Evidence for a direct role in the transport of iron. J. Biol. Chem. *272*, 11770-11777.

77. Dix,D.R., Bridgham,J.T., Broderius,M.A., Byersdorfer,C.A., and Eide,D.J. (1994). The FET4 gene encodes the low affinity Fe(II) transport protein of *Saccharomyces cerevisiae*. J. Biol. Chem. *269*, 26092-26099.

78. Djordjevic,J.T., Del,P.M., Sorrell,T.C., Turner,K.M., and Wright,L.C. (2005). Secretion of cryptococcal phospholipase B1 (PLB1) is regulated by a glycosylphosphatidylinositol (GPI) anchor. Biochem. J. *389*, 803-812.

79. Djordjevic,J.T. (2010). Role of phospholipases in fungal fitness, pathogenicity, and drug development - lessons from *Cryptococcus neoformans*. Front Microbiol. *1*, 125.

80. Doering,T.L. (2009). How sweet it is! Cell wall biogenesis and polysaccharide capsule formation in *Cryptococcus neoformans*. Annu. Rev. Microbiol. *63*, 223-247.

81. Doms,R.W., Russ,G., and Yewdell,J.W. (1989). Brefeldin A redistributes resident and itinerant Golgi proteins to the endoplasmic reticulum. J. Cell Biol. *109*, 61-72.

82. Dromer, F. and Levitz, S. M. (2011). Invasion of *Cryptococcus* into the central nervous system. In Heitman, J., Kozel, T. R., Kwon-Chung, K. J., Perfect, J., and Casadevall, A., eds, *Cryptococcus* from human pathogen to model yeast. ASM Press, Washington, DC, 465-472.

83. Duan,K. and Surette,M.G. (2007). Environmental regulation of *Pseudomonas aeruginosa* PAO1 Las and Rhl quorum-sensing systems. J. Bacteriol. *189*, 4827-4836.

84. Dubois,M., Gilles,K., Hamilton,J.K., Rebers,P.A., and Smith,F. (1951). A colorimetric method for the determination of sugars. Nature *168*, 167.

85. Eck,R., Hundt,S., Hartl,A., Roemer,E., and Kunkel,W. (1999). A multicopper oxidase gene from *Candida albicans*: cloning, characterization and disruption. Microbiology *145*, 2415-2422.

86. Eigenheer,R.A., Jin,L.Y., Blumwald,E., Phinney,B.S., and Gelli,A. (2007). Extracellular glycosylphosphatidylinositol-anchored mannoproteins and proteases of *Cryptococcus neoformans*. FEMS Yeast Res. *7*, 499-510.

87. Eisenman,H.C., Nosanchuk,J.D., Webber,J.B., Emerson,R.J., Camesano,T.A., and Casadevall,A. (2005). Microstructure of cell wall-associated melanin in the human pathogenic fungus *Cryptococcus neoformans*. Biochemistry *44*, 3683-3693.

88. Eisenman,H.C., Frases,S., Nicola,A.M., Rodrigues,M.L., and Casadevall,A. (2009). Vesicle-associated melanization in *Cryptococcus neoformans*. Microbiology *155*, 3860-3867.

89. Eisenman,H.C., Chow,S.K., Tse,K.K., McClelland,E.E., and Casadevall,A. (2011). The effect of L-DOPA on *Cryptococcus neoformans* growth and gene expression. Virulence. *2*, 329-336.

90. Eisenman,H.C. and Casadevall,A. (2012). Synthesis and assembly of fungal melanin. Appl. Microbiol. Biotechnol. *93*, 931-940.

91. Fan,M., Currie,B.P., Gutell,R.R., Ragan,M.A., and Casadevall,A. (1994). The 16S-like, 5.8S and 23S-like rRNAs of the two varieties of *Cryptococcus neoformans*: sequence, secondary structure, phylogenetic analysis and restriction fragment polymorphisms. J. Med. Vet. Mycol. *32*, 163-180.

92. Ferguson,A.D., Hofmann,E., Coulton,J.W., Diederichs,K., and Welte,W. (1998). Siderophore-mediated iron transport: crystal structure of FhuA with bound lipopolysaccharide. Science *282*, 2215-2220.

93. Ferguson,A.D., Braun,V., Fiedler,H.P., Coulton,J.W., Diederichs,K., and Welte,W. (2000). Crystal structure of the antibiotic albomycin in complex with the outer membrane transporter FhuA. Protein Sci. *9*, 956-963.

94. Foster,L.A. (2002). Utilization and cell-surface binding of hemin by *Histoplasma capsulatum*. Can. J. Microbiol. *48*, 437-442.

95. Fox,D.S., Cruz,M.C., Sia,R.A., Ke,H., Cox,G.M., Cardenas,M.E., and Heitman,J. (2001). Calcineurin regulatory subunit is essential for virulence and mediates interactions with FKBP12-FK506 in *Cryptococcus neoformans*. Mol. Microbiol. *39*, 835-849.

96. Franzot,S.P., Hamdan,J.S., Currie,B.P., and Casadevall,A. (1997). Molecular epidemiology of *Cryptococcus neoformans* in Brazil and the United States: evidence for both local genetic differences and a global clonal population structure. J. Clin. Microbiol. *35*, 2243-2251.

97. Fries,B.C., Chen,F., Currie,B.P., and Casadevall,A. (1996). Karyotype instability in *Cryptococcus neoformans* infection. J. Clin. Microbiol. *34*, 1531-1534.

98. Fujiwara,T., Oda,K., Yokota,S., Takatsuki,A., and Ikehara,Y. (1988). Brefeldin A causes disassembly of the Golgi complex and accumulation of secretory proteins in the endoplasmic reticulum. J. Biol. Chem. *263*, 18545-18552.

99. Ganendren,R., Carter,E., Sorrell,T., Widmer,F., and Wright,L. (2006). Phospholipase B activity enhances adhesion of *Cryptococcus neoformans* to a human lung epithelial cell line. Microbes. Infect. *8*, 1006-1015.

100. Garcia-Rivera,J., Chang,Y.C., Kwon-Chung,K.J., and Casadevall,A. (2004). *Cryptococcus neoformans* CAP59 (or Cap59p) is involved in the extracellular trafficking of capsular glucuronoxylomannan. Eukaryot. Cell *3*, 385-392.

101. Garcia-Rodas,R. and Zaragoza,O. (2012). Catch me if you can: phagocytosis and killing avoidance by *Cryptococcus neoformans*. FEMS Immunol. Med. Microbiol. *64*, 147-161.

102. Gaudin,C.F., Grigg,J.C., Arrieta,A.L., and Murphy,M.E. (2011). Unique heme-iron coordination by the hemoglobin receptor IsdB of *Staphylococcus aureus*. Biochemistry *50*, 5443-5452.

103. Giles,S.S., Batinic-Haberle,I., Perfect,J.R., and Cox,G.M. (2005). *Cryptococcus neoformans* mitochondrial superoxide dismutase: an essential link between antioxidant function and high-temperature growth. Eukaryot. Cell *4*, 46-54.

104. Gomez,B.L. and Nosanchuk,J.D. (2003). Melanin and fungi. Curr. Opin. Infect. Dis. *16*, 91-96.

105. Govender, N. P., Mitchell, T. G., Litvintseva, A. P., and Miglia, K. J. (2011). Cryptococcosis in Africa. In Heitman, J., Kozel, T. R., Kwon-Chung, K. J., Perfect, J., and Casadevall, A., eds, *Cryptococcus* from human pathogen to model yeast. ASM Press, Washington, DC, 269-286.

106. Granger,D.L., Perfect,J.R., and Durack,D.T. (1985). Virulence of *Cryptococcus neoformans*. Regulation of capsule synthesis by carbon dioxide. J. Clin. Invest *76*, 508-516.

107. Griffiths,G., Quinn,P., and Warren,G. (1983). Dissection of the Golgi complex. I. Monensin inhibits the transport of viral membrane proteins from medial to trans Golgi cisternae in baby hamster kidney cells infected with Semliki Forest virus. J. Cell Biol. *96*, 835-850.

108. Grigg,J.C., Ukpabi,G., Gaudin,C.F., and Murphy,M.E. (2010). Structural biology of heme binding in the *Staphylococcus aureus* Isd system. J. Inorg. Biochem. *104*, 341-348.

109. Grigg,J.C., Vermeiren,C.L., Heinrichs,D.E., and Murphy,M.E. (2007). Haem recognition by a *Staphylococcus aureus* NEAT domain. Mol. Microbiol. *63*, 139-149.

110. Haas,H., Schoeser,M., Lesuisse,E., Ernst,J.F., Parson,W., Abt,B., Winkelmann,G., and Oberegger,H. (2003). Characterization of the *Aspergillus nidulans* transporters for the siderophores enterobactin and triacetylfusarinine C. Biochem. J. *371*, 505-513.

111. Haas,H., Eisendle,M., and Turgeon,B.G. (2008). Siderophores in fungal physiology and virulence. Annu. Rev. Phytopathol. *46*, 149-187.

112. Haas,H. (2012). Iron - A key nexus in the virulence of *Aspergillus fumigatus*. Front Microbiol. *3*, 28.

113. Hammer,N.D. and Skaar,E.P. (2011). Molecular mechanisms of *Staphylococcus aureus* iron acquisition. Annu. Rev. Microbiol. *65*, 129-147.

114. Hanson,M.S., Slaughter,C., and Hansen,E.J. (1992). The hbpA gene of *Haemophilus influenzae* type b encodes a heme-binding lipoprotein conserved among heme-dependent *Haemophilus* species. Infect. Immun. *60*, 2257-2266.

115. Hantke,K. (2001). Iron and metal regulation in bacteria. Curr. Opin. Microbiol. *4*, 172-177.

116. Harding,A.E., Diengdoh,J.V., and Lees,A.J. (1984). Autosomal recessive late onset multisystem disorder with cerebellar cortical atrophy at necropsy: report of a family. J. Neurol. Neurosurg. Psychiatry *47*, 853-856.

117. Hassett,R., Dix,D.R., Eide,D.J., and Kosman,D.J. (2000). The Fe(II) permease Fet4p functions as a low affinity copper transporter and supports normal copper trafficking in *Saccharomyces cerevisiae*. Biochem. J. *351*, 477-484.

118. Hassett,R.F., Yuan,D.S., and Kosman,D.J. (1998). Spectral and kinetic properties of the Fet3 protein from *Saccharomyces cerevisiae*, a multinuclear copper ferroxidase enzyme. J. Biol. Chem. *273*, 23274-23282.

119. Hazan,R., He,J., Xiao,G., Dekimpe,V., Apidianakis,Y., Lesic,B., Astrakas,C., Deziel,E., Lepine,F., and Rahme,L.G. (2010). Homeostatic interplay between bacterial cell-cell signaling and iron in virulence. PLoS. Pathog. *6*, e1000810.

120. Hemenway,C.S. and Heitman,J. (1999). Calcineurin. Structure, function, and inhibition. Cell Biochem. Biophys. *30*, 115-151.

121. Heymann,P., Gerads,M., Schaller,M., Dromer,F., Winkelmann,G., and Ernst,J.F. (2002). The siderophore iron transporter of *Candida albicans* (Sit1p/Arn1p) mediates uptake of ferrichrome-type siderophores and is required for epithelial invasion. Infect. Immun. *70*, 5246-5255.

122. Hicks,J.K., D'Souza,C.A., Cox,G.M., and Heitman,J. (2004). Cyclic AMP-dependent protein kinase catalytic subunits have divergent roles in virulence factor production in two varieties of the fungal pathogen *Cryptococcus neoformans*. Eukaryot. Cell *3*, 14-26.

123. Hissen,A.H., Wan,A.N., Warwas,M.L., Pinto,L.J., and Moore,M.M. (2005). The *Aspergillus fumigatus* siderophore biosynthetic gene sidA, encoding L-ornithine N5-oxygenase, is required for virulence. Infect. Immun. *73*, 5493-5503.

124. Honsa,E.S. and Maresso,A.W. (2011). Mechanisms of iron import in anthrax. Biometals. *24*, 533-545.

125. Hornby,J.M., Jensen,E.C., Lisec,A.D., Tasto,J.J., Jahnke,B., Shoemaker,R., Dussault,P., and Nickerson,K.W. (2001). Quorum sensing in the dimorphic fungus *Candida albicans* is mediated by farnesol. Appl. Environ. Microbiol. *67*, 2982-2992.

126. Hortschansky,P., Eisendle,M., Al-Abdallah,Q., Schmidt,A.D., Bergmann,S., Thon,M., Kniemeyer,O., Abt,B., Seeber,B., Werner,E.R., Kato,M., Brakhage,A.A., and Haas,H. (2007). Interaction of HapX with the CCAAT-binding complex--a novel mechanism of gene regulation by iron. EMBO J. *26*, 3157-3168.

127. Hu,C.J., Bai,C., Zheng,X.D., Wang,Y.M., and Wang,Y. (2002). Characterization and functional analysis of the siderophore-iron transporter CaArn1p in *Candida albicans*. J. Biol. Chem. *277*, 30598-30605.

128. Hu,G., Liu,I., Sham,A., Stajich,J.E., Dietrich,F.S., and Kronstad,J.W. (2008). Comparative hybridization reveals extensive genome variation in the AIDS-associated pathogen *Cryptococcus neoformans*. Genome Biol. *9*, R41.

129. Hu,G., Wang,J., Choi,J., Jung,W.H., Liu,I., Litvintseva,A.P., Bicanic,T., Aurora,R., Mitchell,T.G., Perfect,J.R., and Kronstad,J.W. (2011). Variation in chromosome copy number influences the virulence of *Cryptococcus neoformans* and occurs in isolates from AIDS patients. BMC. Genomics *12*, 526.

130. Hu,G., Caza,M., Cadieux,B., Chan,V., Liu,V., and Kronstad,J. (2013). *Cryptococcus neoformans* requires the ESCRT protein Vps23 for iron acquisition from heme, for capsule formation, and for virulence. Infect. Immun. *81*, 292-302.

131. Hua,J., Meyer,J.D., and Lodge,J.K. (2000). Development of positive selectable markers for the fungal pathogen *Cryptococcus neoformans*. Clin. Diagn. Lab Immunol. *7*, 125-128.

132. Huang,C., Nong,S.H., Mansour,M.K., Specht,C.A., and Levitz,S.M. (2002). Purification and characterization of a second immunoreactive mannoprotein from *Cryptococcus neoformans* that stimulates T-Cell responses. Infect. Immun. *70*, 5485-5493.

133. Hurley,J.H. (2010). The ESCRT complexes. Crit Rev. Biochem. Mol. Biol. *45*, 463-487.

134. Jacobson,E.S. and Hong,J.D. (1997). Redox buffering by melanin and Fe(II) in *Cryptococcus neoformans*. J. Bacteriol. *179*, 5340-5346.

135. Jacobson,E.S., Goodner,A.P., and Nyhus,K.J. (1998). Ferrous iron uptake in *Cryptococcus neoformans*. Infect. Immun. *66*, 4169-4175.

136. Janbon,G., Himmelreich,U., Moyrand,F., Improvisi,L., and Dromer,F. (2001). Cas1p is a membrane protein necessary for the O-acetylation of the *Cryptococcus neoformans* capsular polysaccharide. Mol. Microbiol. *42*, 453-467.

137. Janbon, G. and Doering, T. L. (2011). Biosynthesis and genetics of the *Cryptococcus* capsule. In Heitman, J., Kozel, T. R., Kwon-Chung, K. J., Perfect, J., and Casadevall, A., eds., *Cryptococcus* from human pathogen to model yeast. ASM Press, Washington, DC, 27-42.

138. Jansen,H.J., Grenier,D., and Van der Hoeven,J.S. (1995). Characterization of immunoglobulin G-degrading proteases of *Prevotella intermedia* and *Prevotella nigrescens*. Oral Microbiol. Immunol. *10*, 138-145.

139. Jarosik,G.P., Maciver,I., and Hansen,E.J. (1995). Utilization of transferrin-bound iron by *Haemophilus influenzae* requires an intact tonB gene. Infect. Immun. *63*, 710-713.

140. Jarvis, J. N., Bicanic, T., and Harrison, T. S. (2011). Management of cryptococcal meningoencephalitis in both developed and developing countries. In Heitman, J., Kozel, T. R., Kwon-Chung, K. J., Perfect, J., and Casadevall, A., eds., *Cryptococcus* from human pathogen to model yeast. ASM Press, Washington, DC, 565-584.

141. Johnstone,R.M. (2005). Revisiting the road to the discovery of exosomes. Blood Cells Mol. Dis. *34*, 214-219.

142. Joint,I., Allan,D.J., and Williams,P. (2007). Bacterial conversations: talking, listening and eavesdropping. An introduction. Philos. Trans. R. Soc. Lond B Biol. Sci. *362*, 1115-1117.

143. Juhas,M., Wiehlmann,L., Huber,B., Jordan,D., Lauber,J., Salunkhe,P., Limpert,A.S., von,G.F., Steinmetz,I., Eberl,L., and Tummler,B. (2004). Global regulation of quorum sensing and virulence by VqsR in *Pseudomonas aeruginosa*. Microbiology *150*, 831-841.

144. Juhas,M., Wiehlmann,L., Salunkhe,P., Lauber,J., Buer,J., and Tummler,B. (2005). GeneChip expression analysis of the VqsR regulon of *Pseudomonas aeruginosa* TB. FEMS Microbiol. Lett. *242*, 287-295.

145. Jung,W.H., Sham,A., White,R., and Kronstad,J.W. (2006). Iron regulation of the major virulence factors in the AIDS-associated pathogen *Cryptococcus neoformans*. PLoS. Biol. *4*, e410.

146. Jung,W.H., Sham,A., Lian,T., Singh,A., Kosman,D.J., and Kronstad,J.W. (2008). Iron source preference and regulation of iron uptake in *Cryptococcus neoformans*. PLoS. Pathog. *4*, e45.

147. Jung,W.H. and Kronstad,J.W. (2008). Iron and fungal pathogenesis: a case study with *Cryptococcus neoformans*. Cell Microbiol. *10*, 277-284.

148. Jung,W.H., Hu,G., Kuo,W., and Kronstad,J.W. (2009). Role of ferroxidases in iron uptake and virulence of *Cryptococcus neoformans*. Eukaryot. Cell *8*, 1511-1520.

149. Jung,W.H., Saikia,S., Hu,G., Wang,J., Fung,C.K., D'Souza,C., White,R., and Kronstad,J.W. (2010). HapX positively and negatively regulates the transcriptional response to iron deprivation in *Cryptococcus neoformans*. PLoS. Pathog. *6*, e1001209.

150. Kaminishi,H., Miyaguchi,H., Tamaki,T., Suenaga,N., Hisamatsu,M., Mihashi,I., Matsumoto,H., Maeda,H., and Hagihara,Y. (1995). Degradation of humoral host defense by *Candida albicans* proteinase. Infect. Immun. *63*, 984-988.

151. Kammler,M., Schon,C., and Hantke,K. (1993). Characterization of the ferrous iron uptake system of *Escherichia coli*. J. Bacteriol. *175*, 6212-6219.

152. Kaplan,C.D. and Kaplan,J. (2009). Iron acquisition and transcriptional regulation. Chem. Rev. *109*, 4536-4552.

153. Karkowska-Kuleta,J., Rapala-Kozik,M., and Kozik,A. (2009). Fungi pathogenic to humans: molecular bases of virulence of *Candida albicans*, *Cryptococcus neoformans* and *Aspergillus fumigatus*. Acta Biochim. Pol. *56*, 211-224.

154. Kavanaugh,L.A., Fraser,J.A., and Dietrich,F.S. (2006). Recent evolution of the human pathogen *Cryptococcus neoformans* by intervarietal transfer of a 14-gene fragment. Mol. Biol. Evol. *23*, 1879-1890.

155. Kidd,S.E., Hagen,F., Tscharke,R.L., Huynh,M., Bartlett,K.H., Fyfe,M., Macdougall,L., Boekhout,T., Kwon-Chung,K.J., and Meyer,W. (2004). A rare genotype of *Cryptococcus gattii* caused the cryptococcosis outbreak on Vancouver Island (British Columbia, Canada). Proc. Natl. Acad. Sci. U. S. A *101*, 17258-17263.

156. Kim,E.J., Wang,W., Deckwer,W.D., and Zeng,A.P. (2005). Expression of the quorum-sensing regulatory protein LasR is strongly affected by iron and oxygen concentrations in cultures of *Pseudomonas aeruginosa* irrespective of cell density. Microbiology *151*, 1127-1138.

157. Kipnis,E., Hansen,K., Sawa,T., Moriyama,K., Zurawel,A., Ishizaka,A., and Wiener-Kronish,J. (2008). Proteomic analysis of undiluted lung epithelial lining fluid. Chest *134*, 338-345.

158. Klebba,P.E., Charbit,A., Xiao,Q., Jiang,X., and Newton,S.M. (2012). Mechanisms of iron and haem transport by *Listeria monocytogenes*. Mol. Membr. Biol. *29*, 69-86.

159. Kmetzsch,L., Joffe,L.S., Staats,C.C., de Oliveira,D.L., Fonseca,F.L., Cordero,R.J., Casadevall,A., Nimrichter,L., Schrank,A., Vainstein,M.H., and Rodrigues,M.L. (2011). Role for Golgi reassembly and stacking protein (GRASP) in polysaccharide secretion and fungal virulence. Mol. Microbiol. *81*, 206-218.

160. Kornitzer,D. (2009). Fungal mechanisms for host iron acquisition. Curr. Opin. Microbiol. *12*, 377-383.

161. Kosman,D.J. (2003). Molecular mechanisms of iron uptake in fungi. Mol. Microbiol. *47*, 1185-1197.

162. Kremer,S.M. and Wood,P.M. (1992). Evidence that cellobiose oxidase from *Phanerochaete chrysosporium* is primarily an Fe(III) reductase. Kinetic comparison with neutrophil NADPH oxidase and yeast flavocytochrome b2. Eur. J. Biochem. *205*, 133-138.

163. Kronstad,J.W., Attarian,R., Cadieux,B., Choi,J., D'Souza,C.A., Griffiths,E.J., Geddes,J.M., Hu,G., Jung,W.H., Kretschmer,M., Saikia,S., and Wang,J. (2011). Expanding fungal pathogenesis: *Cryptococcus* breaks out of the opportunistic box. Nat. Rev. Microbiol. *9*, 193-203.

164. Kuehn,M.J. and Kesty,N.C. (2005). Bacterial outer membrane vesicles and the host-pathogen interaction. Genes Dev. *19*, 2645-2655.

165. Kulkarni,R.D., Kelkar,H.S., and Dean,R.A. (2003). An eight-cysteine-containing CFEM domain unique to a group of fungal membrane proteins. Trends Biochem. Sci. *28*, 118-121.

166. Kullas,A.L., Li,M., and Davis,D.A. (2004). Snf7p, a component of the ESCRT-III protein complex, is an upstream member of the RIM101 pathway in *Candida albicans*. Eukaryot. Cell *3*, 1609-1618.

167. Kwon-Chung,K.J., Polacheck,I., and Bennett,J.E. (1982). Improved diagnostic medium for separation of *Cryptococcus neoformans* var. *neoformans* (serotypes A and D) and *Cryptococcus neoformans* var. *gattii* (serotypes B and C). J. Clin. Microbiol. *15*, 535-537.

168. Kwon-Chung,K.J. and Rhodes,J.C. (1986). Encapsulation and melanin formation as indicators of virulence in *Cryptococcus neoformans*. Infect. Immun. *51*, 218-223.

169. Kwon-Chung, K. J., Boekhout, T., Wickes, B. L., and Fell, J. W. Systematics of the genus *Cryptococcus* and its type species *C. neoformans*. (2011). In Heitman, J., Kozel, T. R., Kwon-Chung, K. J., Perfect, J., and Casadevall, A., eds., *Cryptococcus* from human pathogen to model yeast. ASM Press, Washington, DC, 3-16.

170. Laemmli,U.K., Beguin,F., and Gujer-Kellenberger,G. (1970). A factor preventing the major head protein of bacteriophage T4 from random aggregation. J. Mol. Biol. *47*, 69-85.

171. Lai,L.C., Kosorukoff,A.L., Burke,P.V., and Kwast,K.E. (2006). Metabolic-state-dependent remodeling of the transcriptome in response to anoxia and subsequent reoxygenation in *Saccharomyces cerevisiae*. Eukaryot. Cell *5*, 1468-1489.

172. Lakshminarayan,K., Anderson,D.C., Borbas,C., Duval,S., and Luepker,R.V. (2007). Blood pressure management in acute ischemic stroke. J. Clin. Hypertens. *9*, 444-453.

173. Lamb,T.M. and Mitchell,A.P. (2003). The transcription factor Rim101p governs ion tolerance and cell differentiation by direct repression of the regulatory genes NRG1 and SMP1 in *Saccharomyces cerevisiae*. Mol. Cell Biol. *23*, 677-686.

174. Lan,C.Y., Rodarte,G., Murillo,L.A., Jones,T., Davis,R.W., Dungan,J., Newport,G., and Agabian,N. (2004). Regulatory networks affected by iron availability in *Candida albicans*. Mol. Microbiol. *53*, 1451-1469.

175. Le Blanc,S., Garrick,M.D., and Arredondo,M. (2012). Heme carrier protein 1 transports heme and is involved in heme-Fe metabolism. Am. J. Physiol Cell Physiol *302*, C1780-C1785.

176. Leach,M.D. and Brown,A.J. (2012). Posttranslational modifications of proteins in the pathobiology of medically relevant fungi. Eukaryot. Cell *11*, 98-108.

177. Lee,E.Y., Choi,D.Y., Kim,D.K., Kim,J.W., Park,J.O., Kim,S., Kim,S.H., Desiderio,D.M., Kim,Y.K., Kim,K.P., and Gho,Y.S. (2009). Gram-positive bacteria produce membrane vesicles: proteomics-based characterization of *Staphylococcus aureus*-derived membrane vesicles. Proteomics. *9*, 5425-5436.

178. Lee,H., Chang,Y.C., Nardone,G., and Kwon-Chung,K.J. (2007). TUP1 disruption in *Cryptococcus neoformans* uncovers a peptide-mediated density-dependent growth phenomenon that mimics quorum sensing. Mol. Microbiol. *64*, 591-601.

179. Lee,J.H., Wang,T., Ault,K., Liu,J., Schmitt,M.P., and Holmes,R.K. (1997). Identification and characterization of three new promoter/operators from *Corynebacterium diphtheriae* that are regulated by the diphtheria toxin repressor (DtxR) and iron. Infect. Immun. *65*, 4273-4280.

180. Lesuisse,E., Raguzzi,F., and Crichton,R.R. (1987). Iron uptake by the yeast *Saccharomyces cerevisiae*: involvement of a reduction step. J. Gen. Microbiol. *133*, 3229-3236.

181. Lesuisse,E., Simon-Casteras,M., and Labbe,P. (1998). Siderophore-mediated iron uptake in *Saccharomyces cerevisiae*: the SIT1 gene encodes a ferrioxamine B permease that belongs to the major facilitator superfamily. Microbiology *144*, 3455-3462.

182. Lesuisse,E., Knight,S.A., Camadro,J.M., and Dancis,A. (2002). Siderophore uptake by *Candida albicans*: effect of serum treatment and comparison with *Saccharomyces cerevisiae*. Yeast *19*, 329-340.

183. Letoffe,S., Ghigo,J.M., and Wandersman,C. (1994). Secretion of the *Serratia marcescens* HasA protein by an ABC transporter. J. Bacteriol. *176*, 5372-5377.

184. Letoffe,S., Redeker,V., and Wandersman,C. (1998). Isolation and characterization of an extracellular haem-binding protein from *Pseudomonas aeruginosa* that shares function and sequence similarities with the *Serratia marcescens* HasA haemophore. Mol. Microbiol. *28*, 1223-1234.

185. Letoffe,S., Nato,F., Goldberg,M.E., and Wandersman,C. (1999). Interactions of HasA, a bacterial haemophore, with haemoglobin and with its outer membrane receptor HasR. Mol. Microbiol. *33*, 546-555.

186. Letoffe,S., Omori,K., and Wandersman,C. (2000). Functional characterization of the HasA(PF) hemophore and its truncated and chimeric variants: determination of a region involved in binding to the hemophore receptor. J. Bacteriol. *182*, 4401-4405.

187. Levitz,S.M., Nong,S., Mansour,M.K., Huang,C., and Specht,C.A. (2001). Molecular characterization of a mannoprotein with homology to chitin deacetylases that stimulates T cell responses to *Cryptococcus neoformans*. Proc. Natl. Acad. Sci. U. S. A *98*, 10422-10427.

188. Levitz,S.M. and Specht,C.A. (2006). The molecular basis for the immunogenicity of *Cryptococcus neoformans* mannoproteins. FEMS Yeast Res. *6*, 513-524.

189. Lian,T., Simmer,M.I., D'Souza,C.A., Steen,B.R., Zuyderduyn,S.D., Jones,S.J., Marra,M.A., and Kronstad,J.W. (2005). Iron-regulated transcription and capsule formation in the fungal pathogen *Cryptococcus neoformans*. Mol. Microbiol. *55*, 1452-1472.

190. Liang,Y., Gui,L., Wei,D.S., Zheng,W., Xing,L.J., and Li,M.C. (2009). *Candida albicans* ferric reductase FRP1 is regulated by direct interaction with Rim101p transcription factor. FEMS Yeast Res. *9*, 270-277.

191. Lige,B., Ma,S., and van Huystee,R.B. (2001). The effects of the site-directed removal of N-glycosylation from cationic peanut peroxidase on its function. Arch. Biochem. Biophys. *386*, 17-24.

192. Lin,X., Litvintseva,A.P., Nielsen,K., Patel,S., Floyd,A., Mitchell,T.G., and Heitman,J. (2007). alpha AD alpha hybrids of *Cryptococcus neoformans*: evidence of same-sex mating in nature and hybrid fitness. PLoS. Genet. *3*, 1975-1990.

193. Livak,K.J. and Schmittgen,T.D. (2001). Analysis of relative gene expression data using real-time quantitative PCR and the 2(-Delta Delta C(T)) Method. Methods *25*, 402-408.

194. Locher,K.P., Rees,B., Koebnik,R., Mitschler,A., Moulinier,L., Rosenbusch,J.P., and Moras,D. (1998). Transmembrane signaling across the ligand-gated FhuA receptor: crystal structures of free and ferrichrome-bound states reveal allosteric changes. Cell *95*, 771-778.

195. Loomes,L.M., Kerr,M.A., and Senior,B.W. (1993). The cleavage of immunoglobulin G *in vitro* and *in vivo* by a proteinase secreted by the urinary tract pathogen *Proteus mirabilis*. J. Med. Microbiol. *39*, 225-232.

196. MacCabe,A.P., van den Hombergh,J.P., Tilburn,J., Arst,H.N., Jr., and Visser,J. (1996). Identification, cloning and analysis of the *Aspergillus niger* gene pacC, a wide domain regulatory gene responsive to ambient pH. Mol. Gen. Genet. *250*, 367-374.

197. MacDougall,L., Kidd,S.E., Galanis,E., Mak,S., Leslie,M.J., Cieslak,P.R., Kronstad,J.W., Morshed,M.G., and Bartlett,K.H. (2007). Spread of *Cryptococcus gattii* in British Columbia, Canada, and detection in the Pacific Northwest, USA. Emerg. Infect. Dis. *13*, 42-50.

198. Manns,J.M., Mosser,D.M., and Buckley,H.R. (1994). Production of a hemolytic factor by *Candida albicans*. Infect. Immun. *62*, 5154-5156.

199. Mansour,M.K., Schlesinger,L.S., and Levitz,S.M. (2002). Optimal T cell responses to *Cryptococcus neoformans* mannoprotein are dependent on recognition of conjugated carbohydrates by mannose receptors. J. Immunol. *168*, 2872-2879.

200. Mansour, M. K. and Levitz, S. M. (2003). Fungal mannoproteins: the sweet path to immunodominance. ASM News *69*, 595-600.

.

201. Maresso,A.W., Garufi,G., and Schneewind,O. (2008). *Bacillus anthracis* secretes proteins that mediate heme acquisition from hemoglobin. PLoS. Pathog. *4*, e1000132.

202. Margraf-Schonfeld,S., Bohm,C., and Watzl,C. (2011). Glycosylation affects ligand binding and function of the activating natural killer cell receptor 2B4 (CD244) protein. J. Biol. Chem. *286*, 24142-24149.

203. Mazoy,R. and Lemos,M.L. (1996). Identification of heme-binding proteins in the cell membranes of *Vibrio anguillarum*. FEMS Microbiol. Lett. *135*, 265-270.

204. McCarthy,K.M., Morgan,J., Wannemuehler,K.A., Mirza,S.A., Gould,S.M., Mhlongo,N., Moeng,P., Maloba,B.R., Crewe-Brown,H.H., Brandt,M.E., and Hajjeh,R.A. (2006). Population-based surveillance for cryptococcosis in an antiretroviral-naive South African province with a high HIV seroprevalence. AIDS *20*, 2199-2206.

205. McFadden,D., Zaragoza,O., and Casadevall,A. (2006). The capsular dynamics of *Cryptococcus neoformans*. Trends Microbiol. *14*, 497-505.

206. McNabb,D.S. and Pinto,I. (2005). Assembly of the Hap2p/Hap3p/Hap4p/Hap5p-DNA complex in *Saccharomyces cerevisiae*. Eukaryot. Cell *4*, 1829-1839.

207. Mednick,A.J., Nosanchuk,J.D., and Casadevall,A. (2005). Melanization of *Cryptococcus neoformans* affects lung inflammatory responses during cryptococcal infection. Infect. Immun. *73*, 2012-2019.

208. Mey,A.R., Wyckoff,E.E., Hoover,L.A., Fisher,C.R., and Payne,S.M. (2008). *Vibrio cholerae* VciB promotes iron uptake via ferrous iron transporters. J. Bacteriol. *190*, 5953-5962.

209. Missall,T.A., Pusateri,M.E., and Lodge,J.K. (2004). Thiol peroxidase is critical for virulence and resistance to nitric oxide and peroxide in the fungal pathogen, *Cryptococcus neoformans*. Mol. Microbiol. *51*, 1447-1458.

210. Misumi,Y., Misumi,Y., Miki,K., Takatsuki,A., Tamura,G., and Ikehara,Y. (1986). Novel blockade by brefeldin A of intracellular transport of secretory proteins in cultured rat hepatocytes. J. Biol. Chem. *261*, 11398-11403.

211. Modun,B., Evans,R.W., Joannou,C.L., and Williams,P. (1998). Receptor-mediated recognition and uptake of iron from human transferrin by *Staphylococcus aureus* and *Staphylococcus epidermidis*. Infect. Immun. *66*, 3591-3596.

212. Moyrand,F., Klaproth,B., Himmelreich,U., Dromer,F., and Janbon,G. (2002). Isolation and characterization of capsule structure mutant strains of *Cryptococcus neoformans*. Mol. Microbiol. *45*, 837-849.

213. Moyrand,F., Chang,Y.C., Himmelreich,U., Kwon-Chung,K.J., and Janbon,G. (2004). Cas3p belongs to a seven-member family of capsule structure designer proteins. Eukaryot. Cell *3*, 1513-1524.

214. Murphy,J.W., Mosley,R.L., Cherniak,R., Reyes,G.H., Kozel,T.R., and Reiss,E. (1988). Serological, electrophoretic, and biological properties of *Cryptococcus neoformans* antigens. Infect. Immun. *56*, 424-431.

215. Murphy,J.W. (1988). Influence of cryptococcal antigens on cell-mediated immunity. Rev. Infect. Dis. *10*, S432-S435.

216. Murphy,J.W. (1993). Cytokine profiles associated with induction of the anticryptococcal cell-mediated immune response. Infect. Immun. *61*, 4750-4759.

217. Narasipura,S.D., Ault,J.G., Behr,M.J., Chaturvedi,V., and Chaturvedi,S. (2003). Characterization of Cu, Zn superoxide dismutase (SOD1) gene knock-out mutant of *Cryptococcus neoformans* var. *gattii*: role in biology and virulence. Mol. Microbiol. *47*, 1681-1694.

218. Nelson,N. and Taiz,L. (1989). The evolution of H+-ATPases. Trends Biochem. Sci. *14*, 113-116.

219. Ngamskulrungroj,P., Chang,Y., Hansen,B., Bugge,C., Fischer,E., and Kwon-Chung,K.J. (2012). Characterization of the chromosome 4 genes that affect fluconazole-induced disomy formation in *Cryptococcus neoformans*. PLoS. One. *7*, e33022.

220. Nimrichter,L., Frases,S., Cinelli,L.P., Viana,N.B., Nakouzi,A., Travassos,L.R., Casadevall,A., and Rodrigues,M.L. (2007). Self-aggregation of *Cryptococcus neoformans* capsular glucuronoxylomannan is dependent on divalent cations. Eukaryot. Cell *6*, 1400-1410.

221. Nobile,C.J., Solis,N., Myers,C.L., Fay,A.J., Deneault,J.S., Nantel,A., Mitchell,A.P., and Filler,S.G. (2008). *Candida albicans* transcription factor Rim101 mediates pathogenic interactions through cell wall functions. Cell Microbiol. *10*, 2180-2196.

222. Nobles,C.L. and Maresso,A.W. (2011). The theft of host heme by Gram-positive pathogenic bacteria. Metallomics. *3*, 788-796.

223. Nosanchuk,J.D. and Casadevall,A. (1997). Cellular charge of *Cryptococcus neoformans*: contributions from the capsular polysaccharide, melanin, and monoclonal antibody binding. Infect. Immun. *65*, 1836-1841.

224. Nosanchuk,J.D., Rosas,A.L., Lee,S.C., and Casadevall,A. (2000). Melanisation of *Cryptococcus neoformans* in human brain tissue. Lancet *355*, 2049-2050.

225. Nosanchuk,J.D., Nimrichter,L., Casadevall,A., and Rodrigues,M.L. (2008). A role for vesicular transport of macromolecules across cell walls in fungal pathogenesis. Commun. Integr. Biol. *1*, 37-39.

226. Noverr,M.C., Cox,G.M., Perfect,J.R., and Huffnagle,G.B. (2003). Role of PLB1 in pulmonary inflammation and cryptococcal eicosanoid production. Infect. Immun. *71*, 1538-1547.

227. Noverr,M.C., Williamson,P.R., Fajardo,R.S., and Huffnagle,G.B. (2004). CNLAC1 is required for extrapulmonary dissemination of *Cryptococcus neoformans* but not pulmonary persistence. Infect. Immun. *72*, 1693-1699.

228. Nurudeen,T.A. and Ahearn,D.G. (1979). Regulation of melanin production by *Cryptococcus neoformans*. J. Clin. Microbiol. *10*, 724-729.

229. O'Meara,T.R., Norton,D., Price,M.S., Hay,C., Clements,M.F., Nichols,C.B., and Alspaugh,J.A. (2010). Interaction of *Cryptococcus neoformans* Rim101 and protein kinase A regulates capsule. PLoS. Pathog. *6*, e1000776.

230. Ochsner,U.A., Johnson,Z., and Vasil,M.L. (2000). Genetics and regulation of two distinct haem-uptake systems, phu and has, in *Pseudomonas aeruginosa*. Microbiology *146*, 185-198.

231. Ochsner,U.A., Wilderman,P.J., Vasil,A.I., and Vasil,M.L. (2002). GeneChip expression analysis of the iron starvation response in *Pseudomonas aeruginosa*: identification of novel pyoverdine biosynthesis genes. Mol. Microbiol. *45*, 1277-1287.

232. Odom,A., Muir,S., Lim,E., Toffaletti,D.L., Perfect,J., and Heitman,J. (1997). Calcineurin is required for virulence of *Cryptococcus neoformans*. EMBO J. *16*, 2576-2589.

233. Oglesby,A.G., Farrow,J.M., III, Lee,J.H., Tomaras,A.P., Greenberg,E.P., Pesci,E.C., and Vasil,M.L. (2008). The influence of iron on *Pseudomonas aeruginosa* physiology: a regulatory link between iron and quorum sensing. J. Biol. Chem. *283*, 15558-15567.

234. Okagaki,L.H., Strain,A.K., Nielsen,J.N., Charlier,C., Baltes,N.J., Chretien,F., Heitman,J., Dromer,F., and Nielsen,K. (2010). Cryptococcal cell morphology affects host cell interactions and pathogenicity. PLoS. Pathog. *6*, e1000953.

235. Oliveira,D.L., Nimrichter,L., Miranda,K., Frases,S., Faull,K.F., Casadevall,A., and Rodrigues,M.L. (2009). *Cryptococcus neoformans* cryoultramicrotomy and vesicle fractionation reveals an intimate association between membrane lipids and glucuronoxylomannan. Fungal. Genet. Biol. *46*, 956-963.

236. Oliveira,D.L., Freire-de-Lima,C.G., Nosanchuk,J.D., Casadevall,A., Rodrigues,M.L., and Nimrichter,L. (2010). Extracellular vesicles from *Cryptococcus neoformans* modulate macrophage functions. Infect. Immun. *78*, 1601-1609.

237. Olszewski,M.A., Noverr,M.C., Chen,G.H., Toews,G.B., Cox,G.M., Perfect,J.R., and Huffnagle,G.B. (2004). Urease expression by *Cryptococcus neoformans* promotes microvascular sequestration, thereby enhancing central nervous system invasion. Am. J. Pathol. *164*, 1761-1771.

238. Orci,L., Tagaya,M., Amherdt,M., Perrelet,A., Donaldson,J.G., Lippincott-Schwartz,J., Klausner,R.D., and Rothman,J.E. (1991). Brefeldin A, a drug that blocks secretion, prevents the assembly of non-clathrin-coated buds on Golgi cisternae. Cell *64*, 1183-1195.

239. Palma,M., Worgall,S., and Quadri,L.E. (2003). Transcriptome analysis of the *Pseudomonas aeruginosa* response to iron. Arch. Microbiol. *180*, 374-379.

240. Pan,B.T., Teng,K., Wu,C., Adam,M., and Johnstone,R.M. (1985). Electron microscopic evidence for externalization of the transferrin receptor in vesicular form in sheep reticulocytes. J. Cell Biol. *101*, 942-948.

241. Panepinto,J., Komperda,K., Frases,S., Park,Y.D., Djordjevic,J.T., Casadevall,A., and Williamson,P.R. (2009). Sec6-dependent sorting of fungal extracellular exosomes and laccase of *Cryptococcus neoformans*. Mol. Microbiol. *71*, 1165-1176.

242. Park,B.J., Wannemuehler,K.A., Marston,B.J., Govender,N., Pappas,P.G., and Chiller,T.M. (2009). Estimation of the current global burden of cryptococcal meningitis among persons living with HIV/AIDS. AIDS *23*, 525-530.

243. Park, B. J., Lockhart, S. R., Brandt, M. E., and Chiller, T. M. Public health importance of cryptococcal disease: epidemiology, burden, and control. (2011). In Heitman, J., Kozel, T. R., Kwon-Chung, K. J., Perfect, J., and Casadevall, A., eds., *Cryptococcus* from human pathogen to model yeast. ASM Press, Washington, DC, 585-594.

244. Penalva,M.A. and Arst,H.N., Jr. (2002). Regulation of gene expression by ambient pH in filamentous fungi and yeasts. Microbiol. Mol. Biol. Rev. *66*, 426-46.

245. Penalva,M.A. and Arst,H.N., Jr. (2004). Recent advances in the characterization of ambient pH regulation of gene expression in filamentous fungi and yeasts. Annu. Rev. Microbiol. *58*, 425-451.

246. Pendrak,M.L., Krutzsch,H.C., and Roberts,D.D. (2000). Structural requirements for hemoglobin to induce fibronectin receptor expression in *Candida albicans*. Biochemistry *39*, 16110-16118.

247. Perfect, J. and Casadevall, A. (2011). The history of *Cryptococcus* and cryptococcosis. In Heitman, J., Kozel, T. R., Kwon-Chung, K. J., Perfect, J., and Casadevall, A., eds., *Cryptococcus* from human pathogen to model yeast. ASM Press, Washington, DC, 17-26.

248. Perfect,J.R., Rude,T.H., Wong,B., Flynn,T., Chaturvedi,V., and Niehaus,W. (1996). Identification of a *Cryptococcus neoformans* gene that directs expression of the cryptic *Saccharomyces cerevisiae* mannitol dehydrogenase gene. J. Bacteriol. *178*, 5257-5262.

249. Perfect,J.R. (2006). *Cryptococcus neoformans*: the yeast that likes it hot. FEMS Yeast Res. *6*, 463-468.

250. Petzold,E.W., Himmelreich,U., Mylonakis,E., Rude,T., Toffaletti,D., Cox,G.M., Miller,J.L., and Perfect,J.R. (2006). Characterization and regulation of the trehalose synthesis pathway and its importance in the pathogenicity of *Cryptococcus neoformans*. Infect. Immun. *74*, 5877-5887.

251. Philpott,C.C. (2006). Iron uptake in fungi: a system for every source. Biochim. Biophys. Acta *1763*, 636-645.

252. Polacheck,I., Hearing,V.J., and Kwon-Chung,K.J. (1982). Biochemical studies of phenoloxidase and utilization of catecholamines in *Cryptococcus neoformans*. J. Bacteriol. *150*, 1212-1220.

253. Polacheck,I. and Kwon-Chung,K.J. (1988). Melanogenesis in *Cryptococcus neoformans*. J. Gen. Microbiol. *134*, 1037-1041.

254. Polacheck,I. (1991). The discovery of melanin production in *Cryptococcus neoformans* and its impact on diagnosis and the study of virulence. Zentralbl. Bakteriol. *276*, 120-123.

255. Ponting,C.P. (2001). Domain homologues of dopamine beta-hydroxylase and ferric reductase: roles for iron metabolism in neurodegenerative disorders? Hum. Mol. Genet. *10*, 1853-1858.

256. Portnoy,M.E., Liu,X.F., and Culotta,V.C. (2000). *Saccharomyces cerevisiae* expresses three functionally distinct homologues of the nramp family of metal transporters. Mol. Cell Biol. *20*, 7893-7902.

257. Protchenko,O., Ferea,T., Rashford,J., Tiedeman,J., Brown,P.O., Botstein,D., and Philpott,C.C. (2001). Three cell wall mannoproteins facilitate the uptake of iron in *Saccharomyces cerevisiae*. J. Biol. Chem. *276*, 49244-49250.

258. Protchenko,O., Shakoury-Elizeh,M., Keane,P., Storey,J., Androphy,R., and Philpott,C.C. (2008). Role of PUG1 in inducible porphyrin and heme transport in *Saccharomyces cerevisiae*. Eukaryot. Cell *7*, 859-871.

259. Pynnonen,M., Stephenson,R.E., Schwartz,K., Hernandez,M., and Boles,B.R. (2011). Hemoglobin promotes *Staphylococcus aureus* nasal colonization. PLoS. Pathog. *7*, e1002104.

260. Ramanan,N. and Wang,Y. (2000). A high-affinity iron permease essential for *Candida albicans* virulence. Science *288*, 1062-1064.

261. Ramon,A.M., Porta,A., and Fonzi,W.A. (1999). Effect of environmental pH on morphological development of *Candida albicans* is mediated via the PacC-related transcription factor encoded by PRR2. J. Bacteriol. *181*, 7524-7530.

262. Ramos,C.L., Fonseca,F.L., Rodrigues,J., Guimaraes,A.J., Cinelli,L.P., Miranda,K., Nimrichter,L., Casadevall,A., Travassos,L.R., and Rodrigues,M.L. (2012). Chitin-like molecules associate with *Cryptococcus neoformans* glucuronoxylomannan to form a glycan complex with previously unknown properties. Eukaryot. Cell *11*, 1086-1094.

263. Rappsilber,J., Ishihama,Y., and Mann,M. (2003). Stop and go extraction tips for matrix-assisted laser desorption/ionization, nanoelectrospray, and LC/MS sample pretreatment in proteomics. Anal. Chem. *75*, 663-670.

264. Reiss,E., Huppert,M., and Cherniak,R. (1985). Characterization of protein and mannan polysaccharide antigens of yeasts, moulds, and actinomycetes. Curr. Top. Med. Mycol. *1*, 172-207.

265. Reniere,M.L., Ukpabi,G.N., Harry,S.R., Stec,D.F., Krull,R., Wright,D.W., Bachmann,B.O., Murphy,M.E., and Skaar,E.P. (2010). The IsdG-family of haem oxygenases degrades haem to a novel chromophore. Mol. Microbiol. *75*, 1529-1538.

266. Rhodes,J.C., Polacheck,I., and Kwon-Chung,K.J. (1982). Phenoloxidase activity and virulence in isogenic strains of *Cryptococcus neoformans*. Infect. Immun. *36*, 1175-1184.

267. Rodrigues,M.L., Nimrichter,L., Oliveira,D.L., Frases,S., Miranda,K., Zaragoza,O., Alvarez,M., Nakouzi,A., Feldmesser,M., and Casadevall,A. (2007). Vesicular polysaccharide export in *Cryptococcus neoformans* is a eukaryotic solution to the problem of fungal trans-cell wall transport. Eukaryot. Cell *6*, 48-59.

268. Rodrigues,M.L., Nakayasu,E.S., Oliveira,D.L., Nimrichter,L., Nosanchuk,J.D., Almeida,I.C., and Casadevall,A. (2008a). Extracellular vesicles produced by *Cryptococcus neoformans* contain protein components associated with virulence. Eukaryot. Cell *7*, 58-67.

269. Rodrigues,M.L., Nimrichter,L., Oliveira,D.L., Nosanchuk,J.D., and Casadevall,A. (2008b). Vesicular trans-cell wall transport in fungi: A mechanism for the delivery of virulence-associated macromolecules? Lipid Insights. *2*, 27-40.

270. Rodrigues,M.L. and Djordjevic,J.T. (2012). Unravelling secretion in *Cryptococcus neoformans*: more than one way to skin a cat. Mycopathologia *173*, 407-418.

271. Rohrbach,M.R., Braun,V., and Köster,W. (1995). Ferrichrome transport in *Escherichia coli* K-12: altered substrate specificity of mutated periplasmic FhuD and interaction of FhuD with the integral membrane protein FhuB. J. Bacteriol. *177*, 7186-7193.

272. Rosas,A.L., MacGill,R.S., Nosanchuk,J.D., Kozel,T.R., and Casadevall,A. (2002). Activation of the alternative complement pathway by fungal melanins. Clin. Diagn. Lab Immunol. *9*, 144-148.

273. Rossi,M.S., Fetherston,J.D., Letoffe,S., Carniel,E., Perry,R.D., and Ghigo,J.M. (2001). Identification and characterization of the hemophore-dependent heme acquisition system of *Yersinia pestis*. Infect. Immun. *69*, 6707-6717.

274. Salas,S.D., Bennett,J.E., Kwon-Chung,K.J., Perfect,J.R., and Williamson,P.R. (1996). Effect of the laccase gene CNLAC1, on virulence of *Cryptococcus neoformans*. J. Exp. Med. *184*, 377-386.

275. Santangelo,R., Zoellner,H., Sorrell,T., Wilson,C., Donald,C., Djordjevic,J., Shounan,Y., and Wright,L. (2004). Role of extracellular phospholipases and mononuclear phagocytes in dissemination of cryptococcosis in a murine model. Infect. Immun. *72*, 2229-2239.

276. Santangelo,R.T., Nouri-Sorkhabi,M.H., Sorrell,T.C., Cagney,M., Chen,S.C., Kuchel,P.W., and Wright,L.C. (1999). Biochemical and functional characterisation of secreted phospholipase activities from *Cryptococcus neoformans* in their naturally occurring state. J. Med. Microbiol. *48*, 731-740.

277. Santos,R., Buisson,N., Knight,S., Dancis,A., Camadro,J.M., and Lesuisse,E. (2003). Haemin uptake and use as an iron source by *Candida albicans*: role of CaHMX1-encoded haem oxygenase. Microbiology *149*, 579-588.

278. Schmitt,M.P. (1997). Transcription of the *Corynebacterium diphtheriae* hmuO gene is regulated by iron and heme. Infect. Immun. *65*, 4634-4641.

279. Schneider,R. and Hantke,K. (1993). Iron-hydroxamate uptake systems in *Bacillus subtilis*: identification of a lipoprotein as part of a binding protein-dependent transport system. Mol. Microbiol. *8*, 111-121.

280. Schrettl,M., Bignell,E., Kragl,C., Joechl,C., Rogers,T., Arst,H.N., Jr., Haynes,K., and Haas,H. (2004). Siderophore biosynthesis but not reductive iron assimilation is essential for *Aspergillus fumigatus* virulence. J. Exp. Med. *200*, 1213-1219.

281. Schrettl,M., Kim,H.S., Eisendle,M., Kragl,C., Nierman,W.C., Heinekamp,T., Werner,E.R., Jacobsen,I., Illmer,P., Yi,H., Brakhage,A.A., and Haas,H. (2008). SreA-mediated iron regulation in *Aspergillus fumigatus*. Mol. Microbiol. *70*, 27-43.

282. Schuster,M., Lostroh,C.P., Ogi,T., and Greenberg,E.P. (2003). Identification, timing, and signal specificity of *Pseudomonas aeruginosa* quorum-controlled genes: a transcriptome analysis. J. Bacteriol. *185*, 2066-2079.

283. Sebulsky,M.T., Hohnstein,D., Hunter,M.D., and Heinrichs,D.E. (2000). Identification and characterization of a membrane permease involved in iron-hydroxamate transport in *Staphylococcus aureus*. J. Bacteriol. *182*, 4394-4400.

284. Sebulsky,M.T., Shilton,B.H., Speziali,C.D., and Heinrichs,D.E. (2003). The role of FhuD2 in iron(III)-hydroxamate transport in *Staphylococcus aureus*. Demonstration that FhuD2 binds iron(III)-hydroxamates but with minimal conformational change and implication of mutations on transport. J. Biol. Chem. *278*, 49890-49900.

285. Sebulsky,M.T., Speziali,C.D., Shilton,B.H., Edgell,D.R., and Heinrichs,D.E. (2004). FhuD1, a ferric hydroxamate-binding lipoprotein in *Staphylococcus aureus*: a case of gene duplication and lateral transfer. J. Biol. Chem. *279*, 53152-53159.

286. Sharp,K.H., Schneider,S., Cockayne,A., and Paoli,M. (2007). Crystal structure of the heme-IsdC complex, the central conduit of the Isd iron/heme uptake system in *Staphylococcus aureus*. J. Biol. Chem. *282*, 10625-10631.

287. Shevchenko,A., Wilm,M., Vorm,O., and Mann,M. (1996). Mass spectrometric sequencing of proteins silver-stained polyacrylamide gels. Anal. Chem. *68*, 850-858.

288. Sionov,E., Lee,H., Chang,Y.C., and Kwon-Chung,K.J. (2010). *Cryptococcus neoformans* overcomes stress of azole drugs by formation of disomy in specific multiple chromosomes. PLoS. Pathog. *6*, e1000848.

289. Skaar,E.P., Gaspar,A.H., and Schneewind,O. (2004). IsdG and IsdI, heme-degrading enzymes in the cytoplasm of *Staphylococcus aureus*. J. Biol. Chem. *279*, 436-443.

290. Skaar,E.P., Gaspar,A.H., and Schneewind,O. (2006). *Bacillus anthracis* IsdG, a heme-degrading monooxygenase. J. Bacteriol. *188*, 1071-1080.

291. Specht,C.A., Nong,S., Dan,J.M., Lee,C.K., and Levitz,S.M. (2007). Contribution of glycosylation to T cell responses stimulated by recombinant *Cryptococcus neoformans* mannoprotein. J. Infect. Dis. *196*, 796-800.

292. Speziali,C.D., Dale,S.E., Henderson,J.A., Vines,E.D., and Heinrichs,D.E. (2006). Requirement of *Staphylococcus aureus* ATP-binding cassette-ATPase FhuC for iron-restricted growth and evidence that it functions with more than one iron transporter. J. Bacteriol. *188*, 2048-2055.

293. Stearman,R., Yuan,D.S., Yamaguchi-Iwai,Y., Klausner,R.D., and Dancis,A. (1996). A permease-oxidase complex involved in high-affinity iron uptake in yeast. Science *271*, 1552-1557.

294. Stephen,C., Lester,S., Black,W., Fyfe,M., and Raverty,S. (2002). Multispecies outbreak of cryptococcosis on southern Vancouver Island, British Columbia. Can. Vet. J. *43*, 792-794.

295. Stojiljkovic,I., Kumar,V., and Srinivasan,N. (1999). Non-iron metalloporphyrins: potent antibacterial compounds that exploit haem/Hb uptake systems of pathogenic bacteria. Mol. Microbiol. *31*, 429-442.

296. Sutak,R., Lesuisse,E., Tachezy,J., and Richardson,D.R. (2008). Crusade for iron: iron uptake in unicellular eukaryotes and its significance for virulence. Trends Microbiol. *16*, 261-268.

297. Tai,S.P., Krafft,A.E., Nootheti,P., and Holmes,R.K. (1990). Coordinate regulation of siderophore and diphtheria toxin production by iron in *Corynebacterium diphtheriae*. Microb. Pathog. *9*, 267-273.

298. Tangen,K.L., Jung,W.H., Sham,A.P., Lian,T., and Kronstad,J.W. (2007). The iron- and cAMP-regulated gene SIT1 influences ferrioxamine B utilization, melanization and cell wall structure in *Cryptococcus neoformans*. Microbiology *153*, 29-41.

299. Tartakoff,A.M. and Vassalli,P. (1977). Plasma cell immunoglobulin secretion: arrest is accompanied by alterations of the Golgi complex. J. Exp. Med. *146*, 1332-1345.

300. Tartakoff,A.M. (1983). Perturbation of vesicular traffic with the carboxylic ionophore monensin. Cell *32*, 1026-1028.

301. Thewes,S., Kretschmar,M., Park,H., Schaller,M., Filler,S.G., and Hube,B. (2007). *In vivo* and *ex vivo* comparative transcriptional profiling of invasive and non-invasive *Candida albicans* isolates identifies genes associated with tissue invasion. Mol. Microbiol. *63*, 1606-1628.

302. Tilburn,J., Sarkar,S., Widdick,D.A., Espeso,E.A., Orejas,M., Mungroo,J., Penalva,M.A., and Arst,H.N., Jr. (1995). The *Aspergillus* PacC zinc finger transcription factor mediates regulation of both acid- and alkaline-expressed genes by ambient pH. EMBO J. *14*, 779-790.

303. Toffaletti,D.L., Rude,T.H., Johnston,S.A., Durack,D.T., and Perfect,J.R. (1993). Gene transfer in *Cryptococcus neoformans* by use of biolistic delivery of DNA. J. Bacteriol. *175*, 1405-1411.

304. Toffaletti,D.L., Nielsen,K., Dietrich,F., Heitman,J., and Perfect,J.R. (2004). *Cryptococcus neoformans* mitochondrial genomes from serotype A and D strains do not influence virulence. Curr. Genet. *46*, 193-204.

305. Tong,Y. and Guo,M. (2009). Bacterial heme-transport proteins and their heme-coordination modes. Arch. Biochem. Biophys. *481*, 1-15.

306. Trofa, D., Casadevall, A., and Nosanchuk, J. D. (2011). Melanin: structure, function, and biosynthesis in *Cryptococcus*. In Heitman, J., Kozel, T. R., Kwon-Chung, K. J., Perfect, J., and Casadevall, A., eds., *Cryptococcus* from human pathogen to model yeast. ASM Press, Washington, DC, 55-66. 2011.

307. Tsolis,R.M., Baumler,A.J., Stojiljkovic,I., and Heffron,F. (1995). Fur regulon of *Salmonella typhimurium*: identification of new iron-regulated genes. J. Bacteriol. *177*, 4628-4637.

308. Tsutsui,K. and Mueller,G.C. (1982a). Affinity chromatography of heme-binding proteins: an improved method for the synthesis of hemin-agarose. Anal. Biochem. *121*, 244-250.

309. Tsutsui,K. and Mueller,G.C. (1982b). A protein with multiple heme-binding sites from rabbit serum. J. Biol. Chem. *257*, 3925-3931.

310. Tucker,S.C. and Casadevall,A. (2002). Replication of *Cryptococcus neoformans* in macrophages is accompanied by phagosomal permeabilization and accumulation of vesicles containing polysaccharide in the cytoplasm. Proc. Natl. Acad. Sci. U. S. A *99*, 3165-3170.

311. Tullius,M.V., Harmston,C.A., Owens,C.P., Chim,N., Morse,R.P., McMath,L.M., Iniguez,A., Kimmey,J.M., Sawaya,M.R., Whitelegge,J.P., Horwitz,M.A., and Goulding,C.W. (2011). Discovery and characterization of a unique mycobacterial heme acquisition system. Proc. Natl. Acad. Sci. U. S. A *108*, 5051-5056.

312. Uchida,N., Smilowitz,H., and Tanzer,M.L. (1979). Monovalent ionophores inhibit secretion of procollagen and fibronectin from cultured human fibroblasts. Proc. Natl. Acad. Sci. U. S. A *76*, 1868-1872.

313. Uchida,N., Smilowitz,H., Ledger,P.W., and Tanzer,M.L. (1980). Kinetic studies of the intracellular transport of procollagen and fibronectin in human fibroblasts. Effects of the monovalent ionophore, monensin. J. Biol. Chem. *255*, 8638-8644.

314. van der Horst,C.M., Saag,M.S., Cloud,G.A., Hamill,R.J., Graybill,J.R., Sobel,J.D., Johnson,P.C., Tuazon,C.U., Kerkering,T., Moskovitz,B.L., Powderly,W.G., and Dismukes,W.E. (1997). Treatment of cryptococcal meningitis associated with the acquired immunodeficiency syndrome. National Institute of Allergy and Infectious Diseases Mycoses Study Group and AIDS Clinical Trials Group. N. Engl. J. Med. *337*, 15-21.

315. Vartivarian,S.E., Anaissie,E.J., Cowart,R.E., Sprigg,H.A., Tingler,M.J., and Jacobson,E.S. (1993). Regulation of cryptococcal capsular polysaccharide by iron. J. Infect. Dis. *167*, 186-190.

316. Vecchiarelli,A. (2000). Immunoregulation by capsular components of *Cryptococcus neoformans*. Med. Mycol. *38*, 407-417.

317. Vecchiarelli,A., Pericolini,E., Gabrielli,E., Chow,S.K., Bistoni,F., Cenci,E., and Casadevall,A. (2011). *Cryptococcus neoformans* galactoxylomannan is a potent negative immunomodulator, inspiring new approaches in anti-inflammatory immunotherapy. Immunotherapy. *3*, 997-1005.

318. Velayudhan,J., Hughes,N.J., McColm,A.A., Bagshaw,J., Clayton,C.L., Andrews,S.C., and Kelly,D.J. (2000). Iron acquisition and virulence in *Helicobacter pylori*: a major role for FeoB, a high-affinity ferrous iron transporter. Mol. Microbiol. *37*, 274-286.

319. Viviani,M.A., Cogliati,M., Esposto,M.C., Lemmer,K., Tintelnot,K., Colom Valiente,M.F., Swinne,D., Velegraki,A., and Velho,R. (2006). Molecular analysis of 311 *Cryptococcus neoformans* isolates from a 30-month ECMM survey of cryptococcosis in Europe. FEMS Yeast Res. *6*, 614-619.

320. Wai,S.N., Lindmark,B., Soderblom,T., Takade,A., Westermark,M., Oscarsson,J., Jass,J., Richter-Dahlfors,A., Mizunoe,Y., and Uhlin,B.E. (2003). Vesicle-mediated export and assembly of pore-forming oligomers of the enterobacterial ClyA cytotoxin. Cell *115*, 25-35.

321. Wandersman,C. and Stojiljkovic,I. (2000). Bacterial heme sources: the role of heme, hemoprotein receptors and hemophores. Curr. Opin. Microbiol. *3*, 215-220.

322. Wandersman,C. and Delepelaire,P. (2012). Haemophore functions revisited. Mol. Microbiol. *85*, 618-631.

323. Wang,P., Nichols,C.B., Lengeler,K.B., Cardenas,M.E., Cox,G.M., Perfect,J.R., and Heitman,J. (2002). Mating-type-specific and nonspecific PAK kinases play shared and divergent roles in *Cryptococcus neoformans*. Eukaryot. Cell *1*, 257-272.

324. Wang,T.P., Quintanar,L., Severance,S., Solomon,E.I., and Kosman,D.J. (2003). Targeted suppression of the ferroxidase and iron trafficking activities of the multicopper oxidase Fet3p from *Saccharomyces cerevisiae*. J. Biol. Inorg. Chem. *8*, 611-620.

325. Wang,Y., Aisen,P., and Casadevall,A. (1995). *Cryptococcus neoformans* melanin and virulence: mechanism of action. Infect. Immun. *63*, 3131-3136.

326. Warkentien,T. and Crum-Cianflone,N.F. (2010). An update on *Cryptococcus* among HIV-infected patients. Int. J. STD AIDS *21*, 679-684.

327. Watanabe,M., Tanaka,Y., Suenaga,A., Kuroda,M., Yao,M., Watanabe,N., Arisaka,F., Ohta,T., Tanaka,I., and Tsumoto,K. (2008). Structural basis for multimeric heme complexation through a specific protein-heme interaction: the case of the third neat domain of IsdH from *Staphylococcus aureus*. J. Biol. Chem. *283*, 28649-28659.

328. Waterman,S.R., Hacham,M., Panepinto,J., Hu,G., Shin,S., and Williamson,P.R. (2007). Cell wall targeting of laccase of *Cryptococcus neoformans* during infection of mice. Infect. Immun. *75*, 714-722.

329. Watrous,J.D. and Dorrestein,P.C. (2011). Imaging mass spectrometry in microbiology. Nat. Rev. Microbiol. *9*, 683-694.

330. Weissman,Z. and Kornitzer,D. (2004). A family of *Candida* cell surface haem-binding proteins involved in haemin and haemoglobin-iron utilization. Mol. Microbiol. *53*, 1209-1220.

331. Weissman,Z., Shemer,R., Conibear,E., and Kornitzer,D. (2008). An endocytic mechanism for haemoglobin-iron acquisition in *Candida albicans*. Mol. Microbiol. *69*, 201-217.

332. Wilkins, R. G. (1991). Kinetics and mechanism of reactions of transition metal complexes. [2nd ed.]. New York, NY, VCH Publishers.

333. Wilks,A. (2002). Heme oxygenase: evolution, structure, and mechanism. Antioxid. Redox. Signal. *4*, 603-614.

334. Williams, K. L., Wormley, F. L. Jr., Geunes-Boyer, S., Wright, J. R., and Huffnagle, G. B. (2011). Pulmonary innate and adaptive defenses against *Cryptococcus*. In Heitman, J., Kozel, T. R., Kwon-Chung, K. J., Perfect, J., and Casadevall, A., eds., *Cryptococcus* from human pathogen to model yeast. ASM Press, Washington, DC, 451-464. 2011.

335. Williams,P. (2007). Quorum sensing, communication and cross-kingdom signalling in the bacterial world. Microbiology *153*, 3923-3938.

336. Wolf,J.M., Rivera,J., and Casadevall,A. (2012). Serum albumin disrupts *Cryptococcus neoformans* and *Bacillus anthracis* extracellular vesicles. Cell Microbiol. *14*, 762-773.

337. Wozniak,K.L. and Levitz,S.M. (2008). *Cryptococcus neoformans* enters the endolysosomal pathway of dendritic cells and is killed by lysosomal components. Infect. Immun. *76*, 4764-4771.

338. Wu,R., Skaar,E.P., Zhang,R., Joachimiak,G., Gornicki,P., Schneewind,O., and Joachimiak,A. (2005). *Staphylococcus aureus* IsdG and IsdI, heme-degrading enzymes with structural similarity to monooxygenases. J. Biol. Chem. *280*, 2840-2846.

339. Wyckoff,E.E., Mey,A.R., Leimbach,A., Fisher,C.F., and Payne,S.M. (2006). Characterization of ferric and ferrous iron transport systems in *Vibrio cholerae*. J. Bacteriol. *188*, 6515-6523.

340. Xiong,A., Singh,V.K., Cabrera,G., and Jayaswal,R.K. (2000). Molecular characterization of the ferric-uptake regulator, fur, from *Staphylococcus aureus*. Microbiology *146*, 659-668.

341. Xu,J., Vilgalys,R., and Mitchell,T.G. (2000). Multiple gene genealogies reveal recent dispersion and hybridization in the human pathogenic fungus *Cryptococcus neoformans*. Mol. Ecol. *9*, 1471-1481.

342. Xu,W. and Mitchell,A.P. (2001). Yeast PalA/AIP1/Alix homolog Rim20p associates with a PEST-like region and is required for its proteolytic cleavage. J. Bacteriol. *183*, 6917-6923.

343. Xu,W., Smith,F.J., Jr., Subaran,R., and Mitchell,A.P. (2004). Multivesicular body-ESCRT components function in pH response regulation in *Saccharomyces cerevisiae* and *Candida albicans*. Mol. Biol. Cell *15*, 5528-5537.

344. Yamaguchi-Iwai,Y., Dancis,A., and Klausner,R.D. (1995). AFT1: a mediator of iron regulated transcriptional control in *Saccharomyces cerevisiae*. EMBO J. *14*, 1231-1239.

345. Yamaguchi-Iwai,Y., Stearman,R., Dancis,A., and Klausner,R.D. (1996). Iron-regulated DNA binding by the AFT1 protein controls the iron regulon in yeast. EMBO J. *15*, 3377-3384.

346. Yang,L., Barken,K.B., Skindersoe,M.E., Christensen,A.B., Givskov,M., and Tolker-Nielsen,T. (2007). Effects of iron on DNA release and biofilm development by *Pseudomonas aeruginosa*. Microbiology *153*, 1318-1328.

347. Yoneda,A. and Doering,T.L. (2006). A eukaryotic capsular polysaccharide is synthesized intracellularly and secreted via exocytosis. Mol. Biol. Cell *17*, 5131-5140.

348. Yoneda,A. and Doering,T.L. (2009). An unusual organelle in *Cryptococcus neoformans* links luminal pH and capsule biosynthesis. Fungal. Genet. Biol. *46*, 682-687.

349. Yu,J.H., Hamari,Z., Han,K.H., Seo,J.A., Reyes-Dominguez,Y., and Scazzocchio,C. (2004). Double-joint PCR: a PCR-based molecular tool for gene manipulations in filamentous fungi. Fungal. Genet. Biol. *41*, 973-981.

350. Zaragoza,O., Fries,B.C., and Casadevall,A. (2003). Induction of capsule growth in *Cryptococcus neoformans* by mammalian serum and CO_2. Infect. Immun. *71*, 6155-6164.

351. Zaragoza,O., Chrisman,C.J., Castelli,M.V., Frases,S., Cuenca-Estrella,M., Rodriguez-Tudela,J.L., and Casadevall,A. (2008). Capsule enlargement in *Cryptococcus neoformans* confers resistance to oxidative stress suggesting a mechanism for intracellular survival. Cell Microbiol. *10*, 2043-2057.

352. Zaragoza,O., Rodrigues,M.L., De,J.M., Frases,S., Dadachova,E., and Casadevall,A. (2009). The capsule of the fungal pathogen *Cryptococcus neoformans*. Adv. Appl. Microbiol. *68*, 133-216.

353. Zaragoza,O., Garcia-Rodas,R., Nosanchuk,J.D., Cuenca-Estrella,M., Rodriguez-Tudela,J.L., and Casadevall,A. (2010). Fungal cell gigantism during mammalian infection. PLoS. Pathog. *6*, e1000945.

354. Zhu,X., Gibbons,J., Garcia-Rivera,J., Casadevall,A., and Williamson,P.R. (2001). Laccase of *Cryptococcus neoformans* is a cell wall-associated virulence factor. Infect. Immun. *69*, 5589-5596.

355. Zhu,X. and Williamson,P.R. (2004). Role of laccase in the biology and virulence of *Cryptococcus neoformans*. FEMS Yeast Res. *5*, 1-10.

Appendices

Appendix A

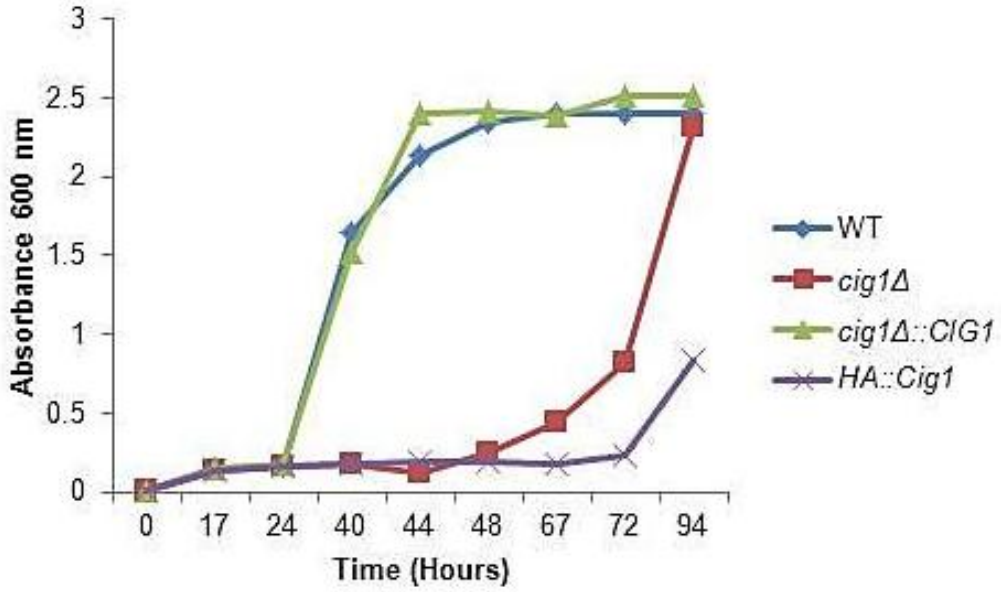

Figure A.1. The *HA::Cig1* strain has a growth defect when grown in LIM supplemented with heme. Growth of iron-starved cells in LIM + 10 µM heme was monitored by measuring the optical density at 600 nm.

Appendix B

Polysaccharide binding assays

A 100 µg/ml solution of *Cig1::GST* protein in 50 mM sodium phosphate, pH 7 was mixed one to one with a 1 mg/ml polysaccharides solution, including different forms of cellulose and chitin, in the same buffer. The mixture was incubated at room temperature with shaking for 4 hours. The insoluble polysaccharides were precipitated by centrifugation and the residual unbound protein in the supernatant was measured by absorbance spectrophotometry at 280 nm. *Cig1::GST* protein in buffer without insoluble polysaccharides served as a reference.

Binding to polysaccharides was also monitored by ITC, as described in Chapter 2, using a solution of 50 µM *Cig1::GST* in 50 mM sodium phosphate, pH 7 and injection of consecutive 2 µL aliquots of 500 µM glucose, mannose, galactose, xylose, or glucosamine prepared in the same buffer. ITC experiments were performed by Dr. Louise Creagh.

Although not conclusive, these preliminary results suggest that Cig1 does not bind sugars or the tested polysaccharides.

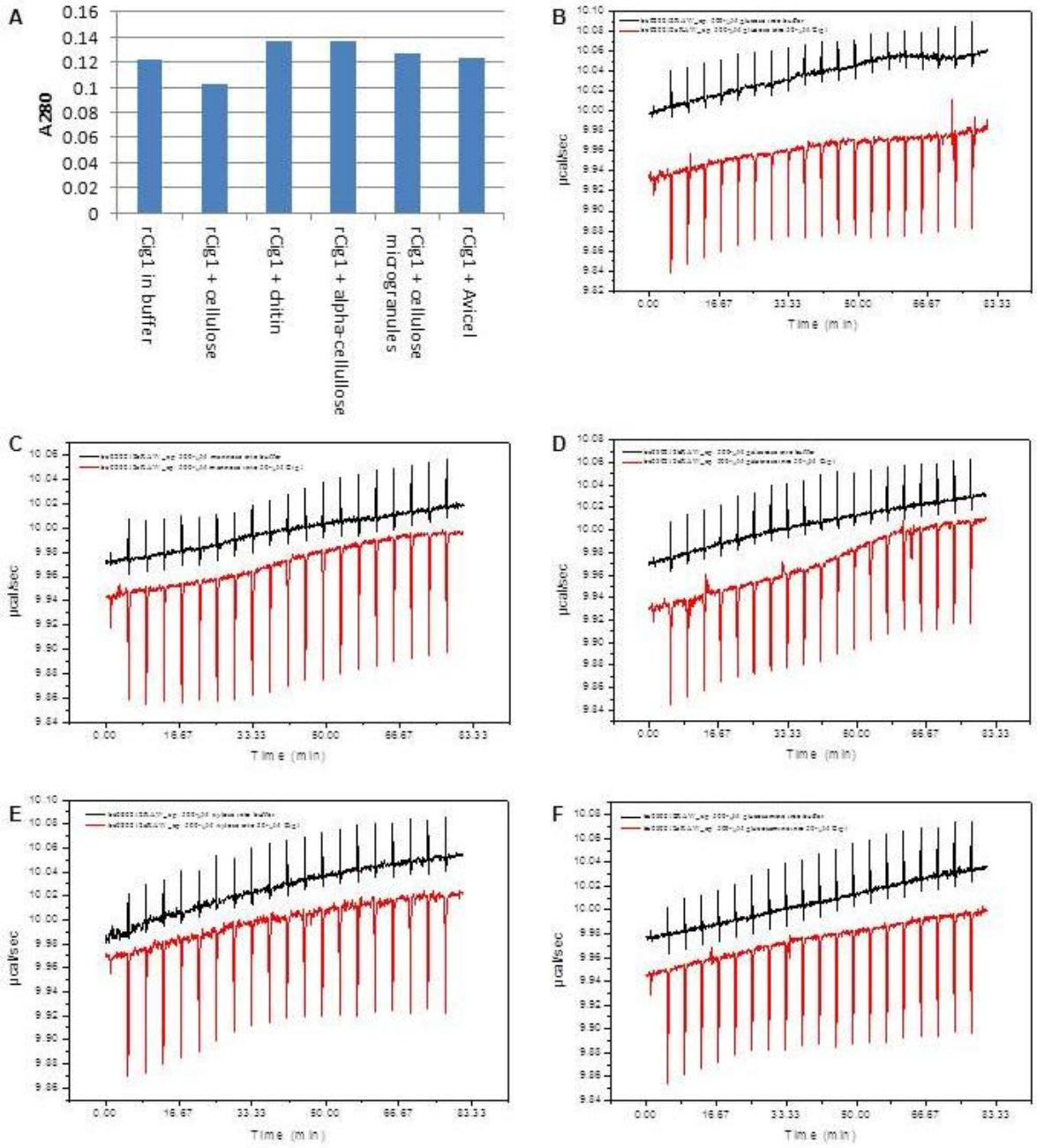

Figure B.1. Cig1 does not appear to bind polysaccharides. (A) *Cig::GST* was mixed with cellulose, chitin, α-cellulose and microgranules of cellulose. Binding was determined by comparing the spectral absorbance at 280 nm of the supernatant of *Cig1::GST* protein in buffer alone or in presence of the insoluble polysaccharide after 4 hours of incubation at room temperature. ITC of glucose (B), galactose (C), mannose (D), xylose (E), and glucosamine (F) alone (red) or *Cig1::GST* plus sugars (black) over the specified period of time. All assays were repeated three times and representative graphs are shown.

Appendix C

Table C.1. Potential heme-binding proteins identified in the culture supernatants of cells grown in LI-YNB

Accession	# AAs	Description	Coverage	# PSMs	# Peptides	Score	Times Detected (n = 2)
CNAG_01239	412	chitin deacetylase	10.44	29	3	1004.92	2
CNAG_02030	677	glyoxal oxidase	26.14	47	11	773.78	2
CNAG_00407	664	glyoxal oxidase	14.16	21	6	575.23	2
CNAG_01854	835	heparinase II/III family protein	12.57	16	6	574.18	2
CNAG_06501	564	1,3-beta-glucanosyltransferase	7.62	17	3	510.53	2
CNAG_03465	624	laccase	15.87	22	7	497.78	2
CNAG_02860	452	endo-1,3(4)-beta-glucanase	7.30	32	2	379.03	2
CNAG_06081	867	glucose oxidase	8.77	12	5	315.21	2
CNAG_04373	499	alginate lyase	15.63	15	6	305.52	2
CNAG_06291	249	deacetylase	12.45	19	2	302.52	2
CNAG_01653	281	cytokine inducing-glycoprotein	18.15	8	3	298.55	2
CNAG_00588	171	conserved hypothetical protein	30.99	12	2	285.88	1
CNAG_06835	588	glucosidase	8.16	6	3	243.33	2
CNAG_02966	395	carboxypeptidase D	11.90	9	4	224.07	2
CNAG_05138	785	exo-beta-1,3-glucanase	8.92	10	5	212.26	2
CNAG_03525	728	trehalase	3.57	7	2	199.52	2
CNAG_00799	789	cellulase	3.42	5	3	181.56	1
CNAG_00919	548	carboxypeptidase D	6.39	8	3	179.72	1
CNAG_00150	931	peptidase	7.52	5	4	178.36	2
CNAG_05799	470	chitin deacetylase	7.87	6	3	177.47	2
CNAG_02189	532	alpha-amylase	5.64	5	3	171.95	2
CNAG_02225	431	cellulase	9.98	5	4	151.97	2
CNAG_06085	637	secreted phospholipase B	4.55	5	3	120.49	2
CNAG_04524	862	zinc metalloprotease	2.67	2	2	120.28	2
CNAG_00250	422	conserved hypothetical protein	7.58	2	2	119.81	1
CNAG_01405	700	conserved hypothetical protein	6.00	3	3	108.08	1
CNAG_02850	896	glucan endo-1,3-alpha-glucosidase agn1	2.46	2	2	107.75	2
CNAG_03120	2430	alpha-1,3-glucan synthase	2.55	5	5	106.72	2
CNAG_05471	972	alpha-glucosidase	5.14	3	3	98.04	1
CNAG_00581	438	endopeptidase	5.25	4	2	91.59	1
CNAG_03524	1717	transmembrane receptor	1.51	2	2	90.30	2
CNAG_01562	299	conserved hypothetical protein	10.37	3	2	89.51	1
CNAG_01019	154	Cu/Zn superoxide dismutase	22.08	4	3	85.96	2
CNAG_05918	547	F0F1 ATP synthase subunit beta	8.78	3	3	85.07	1
CNAG_01984	323	transaldolase	14.24	3	3	83.53	1
CNAG_04869	620	carboxylesterases	7.58	4	3	79.03	1

Accession	# AAs	Description	Coverage	# PSMs	# Peptides	Score	Times Detected (n = 2)
CNAG_07445	687	transketolase	7.28	4	4	75.18	1
CNAG_04601	499	glycine hydroxymethyltransferase	6.21	2	2	71.14	1
CNAG_05731	631	glyoxal oxidase	4.44	3	3	67.96	1
CNAG_04753	467	lactonohydrolase	5.14	2	2	67.49	2
CNAG_02944	551	acid phosphatase	5.08	2	2	65.07	2
CNAG_01577	451	glutamate dehydrogenase	6.21	2	2	63.67	2
CNAG_01040	543	carboxypeptidase D	6.08	4	3	62.85	1
CNAG_07736	715	glucan endo-1,3-alpha-glucosidase agn1	2.94	2	2	59.11	1
CNAG_03072	444	phosphopyruvate hydratase	4.95	2	2	56.47	1
CNAG_04944	422	conserved hypothetical protein	5.92	2	2	46.68	1
CNAG_01890	763	5-methyltetrahydropteroyltriglutamate-homocysteine S-methyltransferase	2.75	2	2	45.89	1

AAs: amino acids, PSMs: peptide spectrum match, n: number of replicates.

Table C.2. Proteins binding to agarose beads identified in the culture supernatants of cells grown in LI-YNB

Accession	# AAs	Description	Coverage	# PSMs	# Peptides	Score	Times detected (n = 2)
CNAG_00588	171	conserved hypothetical protein	33.33	7	2	97.52	1

AAs: amino acids, PSMs: peptide spectrum match, n: number of replicates.

Table C.3. Potential heme-binding proteins identified in the culture supernatants of cells grown in LI-YNB + $FeCl_3$

Accession	# AAs	Description	Coverage	# PSMs	# Peptides	Score	Times detected (n = 2)
CNAG_04373	499	alginate lyase	11.62	13	4	365.71	1
CNAG_02030	677	glyoxal oxidase	9.16	12	4	353.30	1
CNAG_02860	452	endo-1,3(4)-beta-glucanase	8.41	18	2	297.55	1
CNAG_00799	789	cellulase	4.56	10	4	295.58	1
CNAG_00407	664	glyoxal oxidase	10.39	12	5	265.02	1
CNAG_06501	564	1,3-beta-glucanosyltransferase	6.03	7	2	264.51	2
CNAG_06081	867	glucose oxidase	5.07	6	3	200.99	1
CNAG_02850	896	glucan endo-1,3-alpha-glucosidase agn1	3.13	3	2	166.85	1
CNAG_00587	185	conserved hypothetical protein	15.14	5	2	152.94	1
CNAG_01984	323	transaldolase	8.98	3	2	143.51	1
CNAG_02225	431	cellulase	4.64	6	2	131.57	1
CNAG_05799	470	chitin deacetylase	3.62	3	2	124.55	1
CNAG_02189	532	alpha-amylase	6.77	5	3	118.76	1
CNAG_01890	763	5-methyltetrahydropteroyltriglutamate-homocysteine S-methyltransferase	5.37	5	3	110.50	1
CNAG_06085	637	secreted phospholipase B	4.24	3	2	102.60	1
CNAG_01854	835	heparinase II/III family protein	3.83	5	2	88.01	1
CNAG_03525	728	trehalase	3.57	2	2	86.19	1
CNAG_00581	438	endopeptidase	5.25	2	2	48.88	1

AAs: amino acids, PSMs: peptide spectrum match, n: number of replicates.

Table C.4. Proteins binding to agarose beads identified in the culture supernatants of cells grown in LI-YNB + $FeCl_3$

Accession	# AAs	Description	Coverage	# PSMs	# Peptides	Score	Times detected (n = 2)
CNAG_05918	547	F0F1 ATP synthase subunit beta	10.60	4	4	175.90	1
CNAG_01984	323	transaldolase	18.27	4	4	118.34	1
CNAG_03072	444	phosphopyruvate hydratase	7.88	2	2	78.43	1
CNAG_00588	171	conserved hypothetical protein	33.33	9	2	74.01	1
CNAG_06699	339	glyceraldehyde-3-phosphate dehydrogenase	6.49	2	2	71.15	1
CNAG_03225	338	malate dehydrogenase	7.99	2	2	66.82	1
CNAG_01890	763	5-methyltetrahydropteroyltriglutamate-homocysteine S-methyltransferase	3.01	2	2	44.03	1
CNAG_02225	431	cellulase	4.64	2	2	41.62	2

AAs: amino acids, PSMs: peptide spectrum match, n: number of replicates.

Appendix D

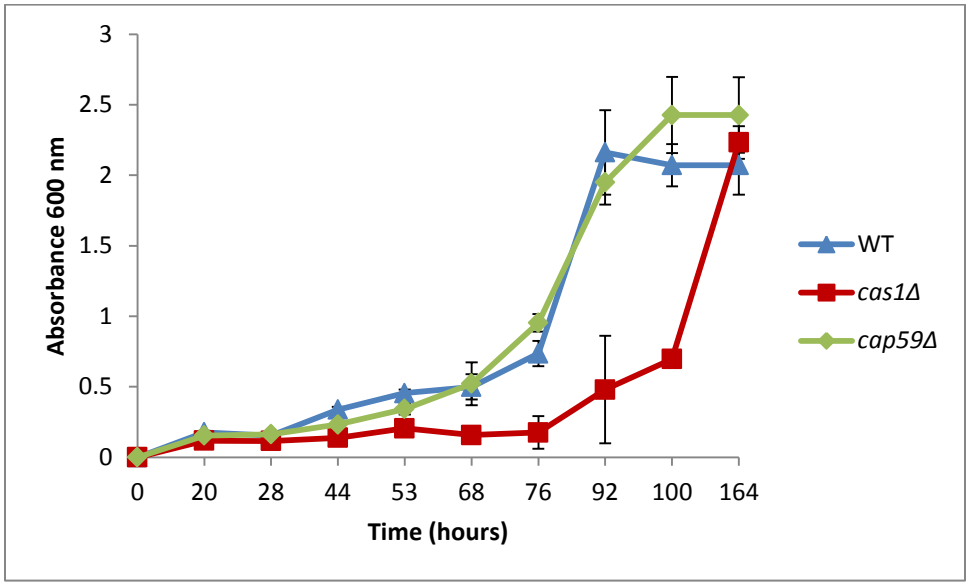

Figure D.1. Cas1 may be involved in iron acquisition. Growth of iron-starved cells in LIM + 100 µM $FeCl_3$ was monitored by measuring the optical density at 600 nm. The experiment was repeated three times and the data are plotted as the average ± SD.

Appendix E

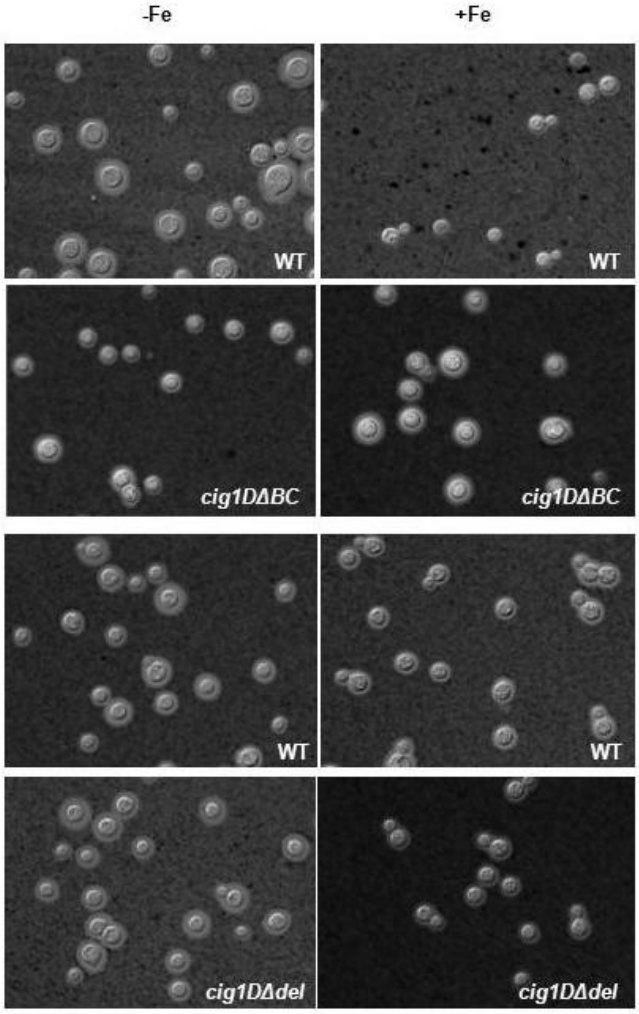

Figure E.1. Elaboration of the capsule by additional *cig1DΔ* mutants in *C. neoformans* var. *neoformans*. Cells were grown in LIM +/- 100 µM $FeCl_3$, harvested and negatively stained with India ink before visualizing by differential interference contrast microscopy.

Appendix F

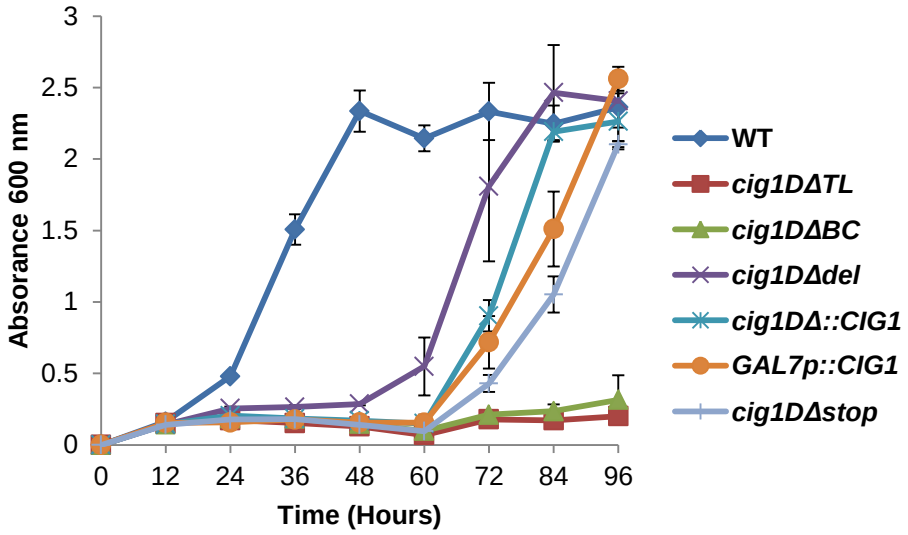

Figure F.1. All *cig1DΔ* mutants in *C. neoformans* var. *neoformans* grow more slowly than wild-type in LIM supplemented with heme. Growth of iron-starved cells in LIM + 10 µM heme was monitored by measuring the optical density at 600 nm. The experiment was repeated three times and the data are plotted as the average ± SD.